Title	Carbon and oxygen isotopic paleoceanography of the Indian and South Atlantic Oceans: Paleoclimate and paleo-ocean circulation
Author(s)	SETO, Koji
Citation	Journal of science of the Hiroshima University. Series C, Earth and planetary sciences , 10 (3) : 393 - 485
Issue Date	1995-08-07
DOI	
Self DOI	10.15027/53150
URL	https://ir.lib.hiroshima-u.ac.jp/00053150
Right	
Relation	

Jour. Sci. Hiroshima Univ., Ser. C, Vol. 10, No. 3, 393-485 (1995)

Carbon and oxygen isotopic paleoceanography of the Indian and South Atlantic Oceans – Paleoclimate and paleo-ocean circulation –

By

Koji SETO

With 7 Tables, 69 Text-figures and 1 Appendix

(Received, May 31, 1995)

Abstract: Ocean circulation is intimately associated with continental arrangement and global climate. The purposes of this study are to reconstruct the water mass structure and the deep ocean circulation in the Indian and South Atlantic Oceans during the Cenozoic.

Oxygen and carbon isotopes were studied in Cenozoic sediments at six sites (Sites 752, 754, 756, 757, 758, and 762) in ODP (Ocean Drilling Program) Legs 121 and 122 in the northeastern Indian Ocean. These isotopic records are related to global events occurring in middle Miocene, the Eocene / Oligocene boundary, middle to late Eocene, and the Paleocene / Eocene boundary. To compile those records along with a number of published isotopic data from the Indian and South Atlantic Oceans, adjustments to isotopic ratios have been calculated for different foraminiferal species, and benthic and planktonic foraminiferal isotopic data converted into δ values of dissolved inorganic carbon (DIC) of marine water. The general trends of oxygen and carbon isotopic values show an increase to the south.

Averaged values in one million year intervals of oxygen and carbon isotopes were calculated for each ODP and DSDP (Deep Sea Drilling Project) site, and the time and spatial distributions of the oxygen and carbon isotopic values were examined from the estimated paleodepth. In the Paleocene ocean, the vertical distribution of isotopic ratios is uniform. However, notable negative shift in oxygen isotopic the remarkable in the Miocene are recognized at about 1500m paleodepth in the northeastern Indian Ocean. The source of the water masses are assumed to be as follows: AABW (Antarctic Bottom Water) or proto-AABW formed in the Southern Ocean (Atlantic sector) throughout the Cenozoic. In the Paleocene, another water mass may have formed at low latitudes including the Tethyan Sea, and this water may could have been warm and highly saline, judging from oxygen isotopic ratios. This water mass corresponds to WSDW (Warm Saline Deep Water), which have encounterd Proto-AABW at mid latitudes during the early Paleogene. This water mass rapidly reduced in size with the closing of the Tethyan Sea at the Paleocene / Eocene boundary, but still continued to 50 Ma in the Indian Ocean and to 40 Ma in the South Atlantic Ocean. AAIW (Antarctic Intermediate Water) developed from the Oligocene (30 Ma) in the Indian Ocean. Proto-NADW (Proto-North Atlantic Deep Water) distinctly developed from the late Pliocene (3 Ma).

Contents

I. Introduction

It is generally believed that ocean circulation is intimately associated with global climate and continental arrangement. In order to reconstruct of paleoclimate and paleoceanography, oxygen and carbon isotopic analyses have been measured in deep sea sediments, as those isotopes are can be used to estimate paleotemperature and tracer of ocean circulation. Urey (1947) first pointed out that the oxygen isotopic composition of fossils can be used to determination paleotemperature, and the first paleotemperature determinations were published from belemnite shells of the Peedee Formation (Urey et al., 1951). Epstein et al. (1951) empirically determined the relationship between the oxygen isotopic composition of mollusk-shells and growth temperature as a temperature scale. This scale was adjusted by Craig (1965) and Horibe and Oba (1969). Woodruff and Savin (1989) showed that the distribution pattern of fossil foraminiferal $\delta^{13}C$ values during the Holocene is similar to the $\delta^{13}C$ pattern of dissolved inorganic carbon (DIC) in the modern ocean which is related to deep water formation (Kroopnick, 1985). Based on this evidence, they proposed the existence of Tethyan Indian Saline Water (TISW), which flowed from the Tethys into the northern Indian Ocean.

Cenozoic oxygen and carbon isotopic records at many DSDP (Deep Sea Drilling Project) and ODP (Ocean Drilling Program) sites have been published (Shackleton et al., 1984; Oberhansli et al., 1984; Poore and Matthews, 1984; Vincent et al., 1985; Oberhansli, 1986; Miller et al., 1989; Stott at al., 1990; Kennett and Stott, 1990; Stott and Kennett, 1990; Barrera and Huber, 1990; 1991; Katz and Miller, 1991; Woodruff et al., 1990; Boersma and Mikkelsen, 1990; Woodruff and Chamber, 1991; Vincent et al., 1991; Zachos et al., 1992a; 1992b; Rea et al., 1991).

A continuous record of post late Maastrichtian sediments were also recovered from various water depths in the Broken and Ninetyeast Ridge (Leg 121) and the Exmouth Plateau (Leg 122) in the northeastern Indian Ocean. In this area, the isotopic studied using foraminiferal tests have been made by Vincent et al. (1985), Oberhansli (1986), Rea et al. (1991), Seto et al. (1991), and Nomura et al. (1992).

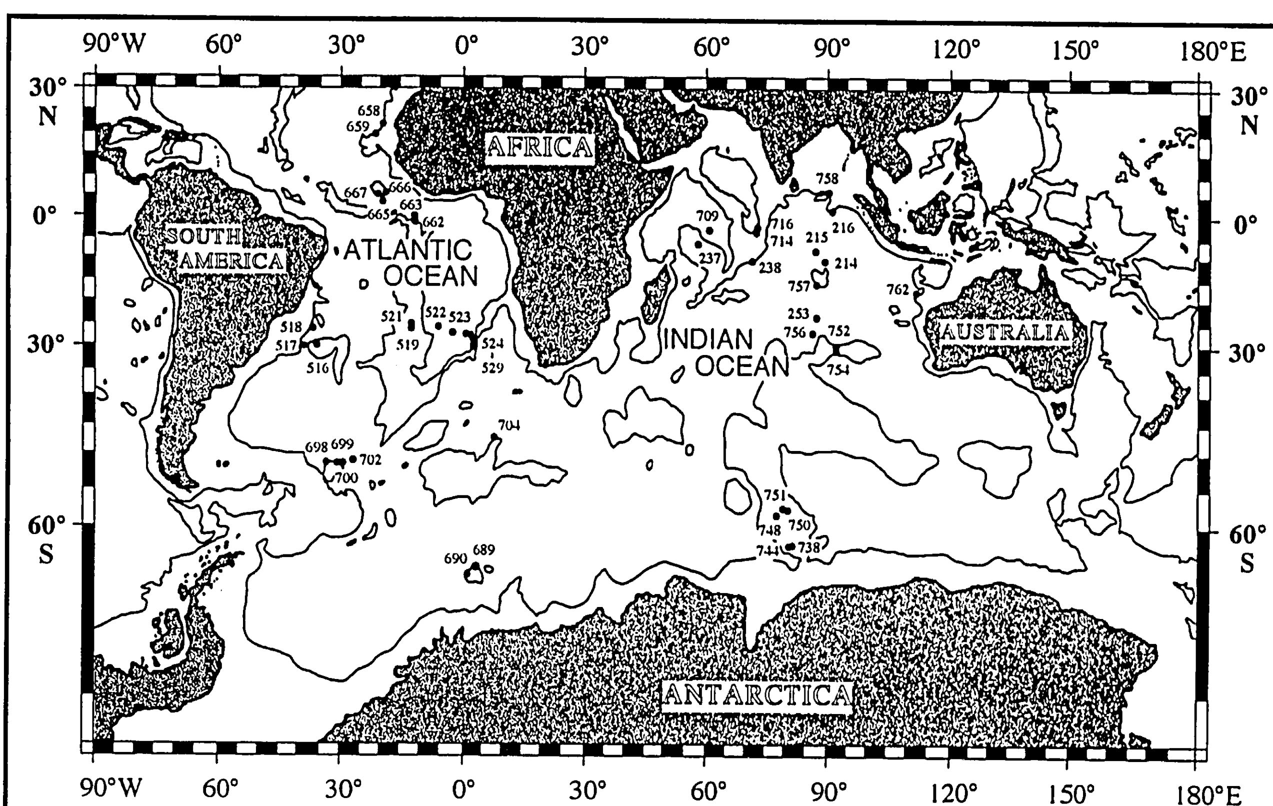

Fig. 1. Location of DSDP and ODP sites examined in this study.

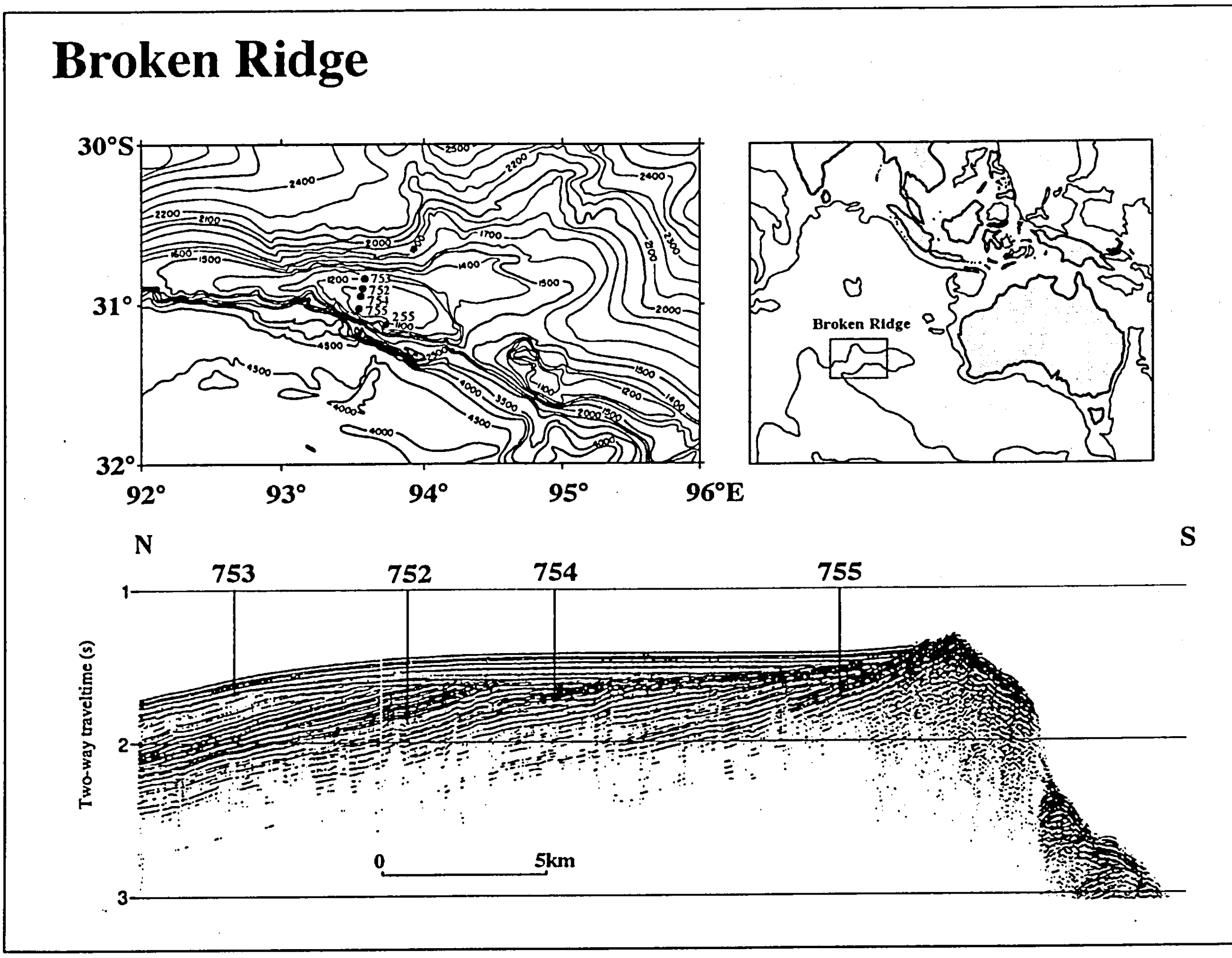

Fig. 2. Bathymetric map and single-channel seismic-reflection profile (RC2708 line 20) across Broken Ridge showing locations of ODP Leg 121 sites at Broken Ridge.

However, these studies mainly focused on the Neogene, and few Paleogene isotope data have been published. Therefore, In this study, oxygen and carbon isotope changes after the late Maastrichtian at six sites (Sites 752, 754, 756, 757, 758, and 762) within Legs 121 and 122 have been examined. These records record global events such as the sharp increase in $\delta^{18}O$ values near the middle Miocene and the Eocene / Oligocene boundary, the increase of $\delta^{18}O$ values in the Eocene (Miller et al., 1987), the chron-6 shift and the chron-16 shift of $\delta^{13}C$ values (Vincent et al., 1980; 1985), and the drastic change of $\delta^{13}C$ values across the Paleocene / Eocene boundary. These events resulted from climate change and/or changes in ocean circulation.

The purposes of this study are to reconstruct the water-mass structure and the ocean circulation of the deep sea during the Cenozoic in the Indian and South Atlantic Oceans, including the Southern Ocean which should be the main source region of deep water during the Cenozoic.

II. The isotopic record in ODP Legs 121 and 122

A. Samples

Sediment samples for isotope analysis were obtained from ODP Sites 752 and 754 (Broken Ridge), Sites 756, 757, and 758 (Ninetyeast Ridge), and Site 762 (Exmouth Plateau), in the northeast Indian Ocean (Fig. 1). Initial description of these sites have been made by Peirce, Weissel, et al. (1989) and Haq, B. U., von Rad, U., et al. (1990).

Site 752 (30° 53.475' S, 93°34.652' E) is located near the northern edge of Broken Ridge with a present water depth of 1086 m (Fig 2). A 436-m-long section of sediments from the Pleistocene through to the upper Maastrichtian was recovered. Hole 752A was cored with an advanced hydraulic piston corer (APC) and an extended core barrel (XCB), until refusal at 308 m below seafloor (mbsf). Average core recovery of all core was 70.6%, but recovery for Cores 121-752-1H to 121-752A-11H and Cores 121-752A-26X to 121-752A-33X were 95.8% and 82.2%, respectively. Hole 752B was cored using a rotary core barrel (RCB) to a total depth of 436 mbsf, with an average recovery of 71% over the cored interval. Neogene and late Oligocene sediments were composed of foraminiferal ooze and nannofossil - foraminiferal or foraminiferal - nannofossil ooze. The Paleogene and late Maastrichtian sediments are light green or gray nannofossil calcareous chalk with fine laminations and bioturbation (Fig. 3). The lithology above the Cretaceous / Tertiary boundary at 358.75 mbsf is dark green volcanic ash

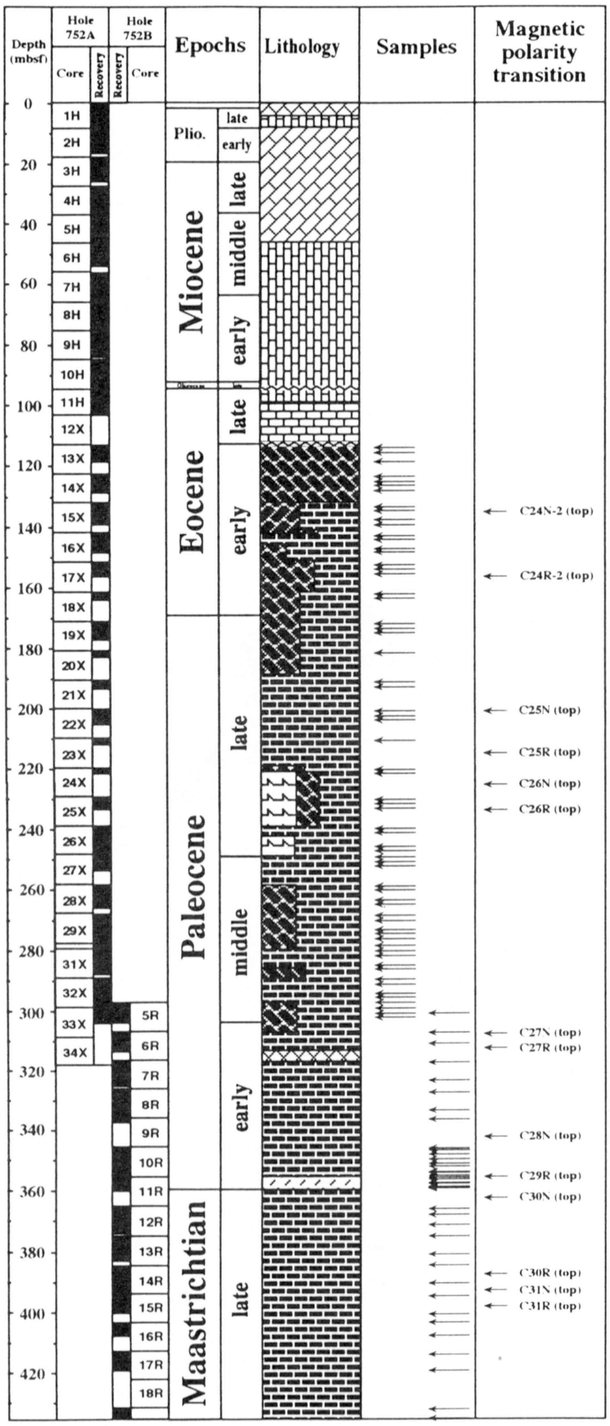

Fig. 3. Lithostratigraphy and Sample horizons at Site 752. See legend of Fig. 4.

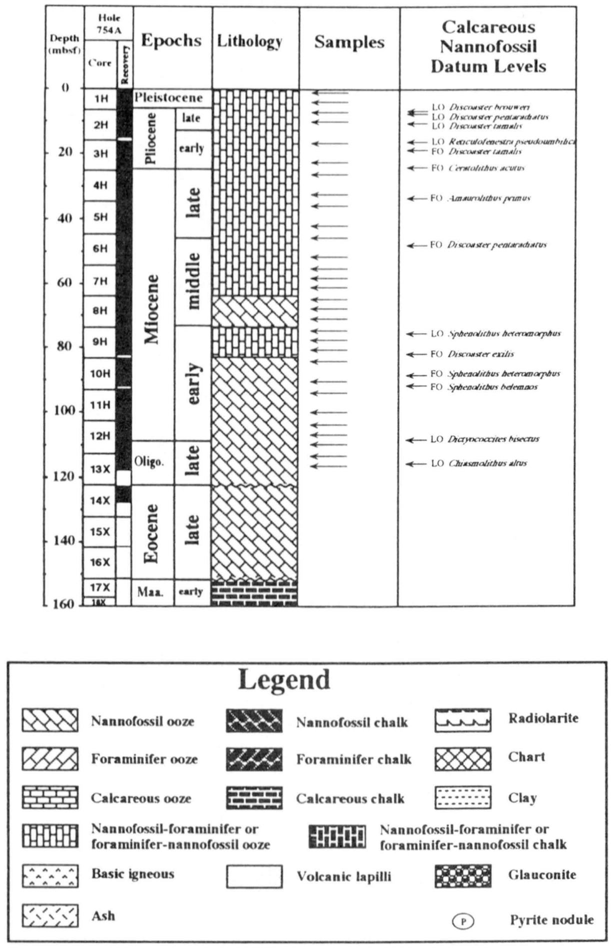

Fig. 4. Lithostratigraphy and Sample horizons at Site 754.

layers (Rea et al., 1990). A middle Eocene angular unconformity is marked by coarse-grained sediments with molluscan shell fragments (Peirce, Weissel, et al., 1989; Rea et al., 1990) and foraminifer including small numbers of inner neritic species such as *Amphistegina* (Peirce, Weissel, et al., 1989). An unconformity within the nannofossil - foraminiferal or foraminiferal - nannofossil ooze was recognized during the late Eocene to late Oligocene. Sediment samples examined in this study include Samples 121-752A-13X-1 through 121-752A-33X-3 (113.6-301.97; 63 samples) from the early Eocene to middle Paleocene in Hole 752A, Samples 121-752A-5R-3 through 121-752A-19R-3 (300.5-435.09 mbsf; 38 samples) from the early Paleocene to late Maastrichtian sediments (including the Cretaceous / Tertiary boundary) in Hole 752C. The location of these samples is shown in Fig 3.

Site 754 (30°56.439'S, 93°33.991' E) is located on the central part of Broken Ridge at a present water depth of 1075m, which is the shallowest among the sites of this study (Fig. 2). Hole 754A was cored using the APC, XCB, and Navidrill (NCB) systems to a depth of 172 mbsf. Although average core recovery was 75.5%, Cores 121-754A-1H through 121-754A-13X were almost completely recovered. Pleistocene through late Oligocene and late Eocene sediments consist of white nannofossil - foraminiferal or foraminiferal - nannofossil ooze and white - yellowish brown nannofossil ooze, which are unconformably underlain by early Maastrichtian light gray to greenish gray calcareous chalk with planar and cross-bedded laminae (Fig. 4). An angular unconformity caused by uplift during the middle Eocene was recorded (Fig. 2). A late Eocene to late Oligocene unconformity was recognized in the nannofossil-foraminiferal or foraminiferal - nannofossil ooze. At Site 754, sediment samples used in this study were Samples 121-754A-1H-1

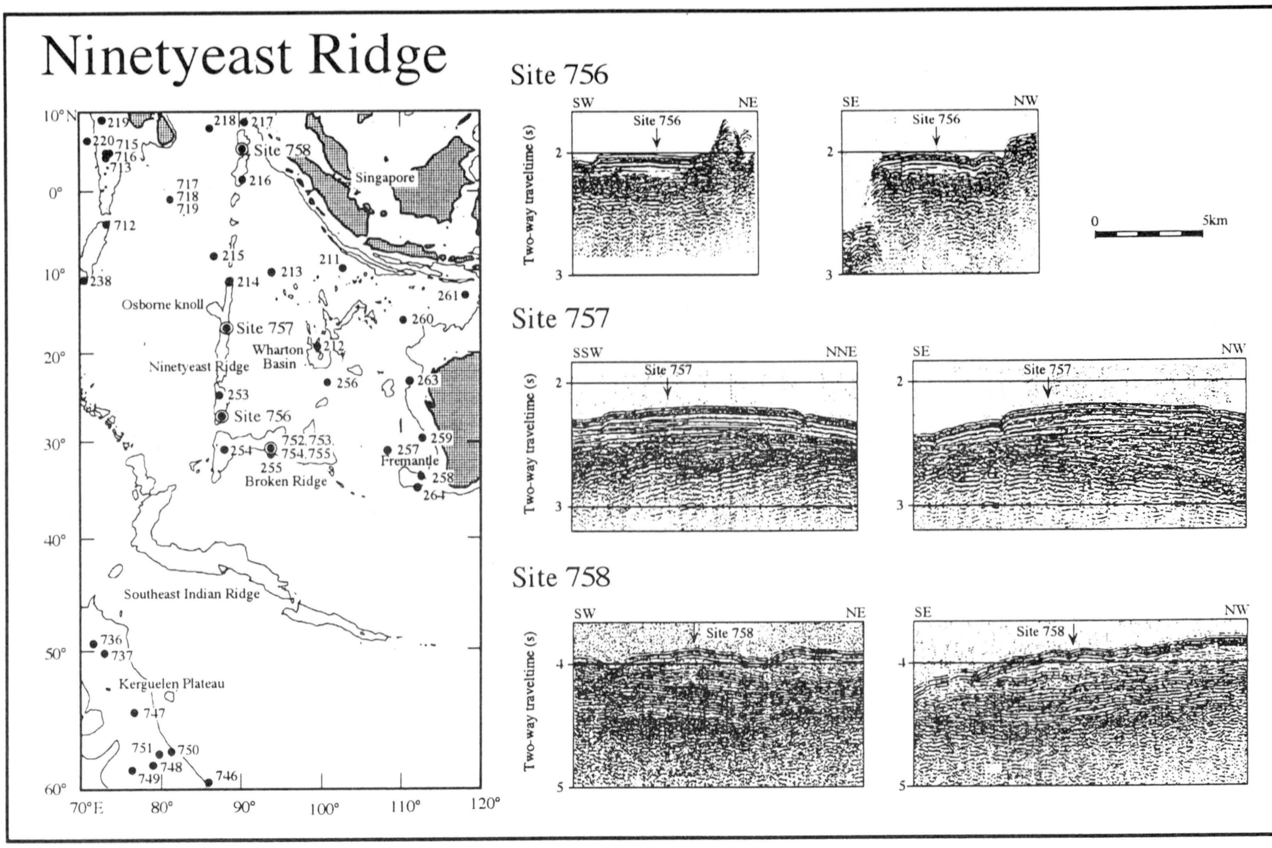

Fig. 5. Bathymetric map and seismic-reflection profile across Sites 756, 757, and 758 at Ninetyeast Ridge.

through 121-754A-13X-3 (0.7-116 mbsf; 29 samples) spanning the Neogene to Late Oligocene (Fig. 4).

Site 756 (27°21.330'S, 87°35.805' E) is located near the crest of southern end of Ninetyeast Ridge at a present water depth of 1518m (Fig. 5). Pleistocene through late Eocene sediments (228-m-thick) were recovered at this site 756. Hole 756B was cored with the APC to 104 mbsf. Hole 756C was washed to 101 mbsf with the XCB system to 150 mbsf (80.7% recovery). Pleistocene to late Eocene sediments consist of nannofossil ooze with foraminifer overlying basaltic basement. At Site 756, 33 sediment samples were analyzed comprising Samples 121-756B-1H-1 through 121-756B-11H-1 (0.7-101.3 mbsf) from the Neogene and Oligocene at Hole 756B, and Sample 121-756C-4X-1 through 121-756C-7X-5 from the early Oligocene and late Eocene at Hole 756C (Fig. 6).

Site 757 (27°21.330'S, 87°35.805' E) is near the crest of central part of Ninetyeast Ridge at a present water depth of 1652m (Fig. 5). Hole 757B was drilled to a depth of 375 m by the APC and XCB systems and recovered a section ranging from Pleistocene to late Paleocene, including the basement, with an average recovery, of 72.6%. Pleistocene through middle Eocene sediments consist of mainly nannofossil ooze, and early Eocene calcareous ooze and chalk overlying pre-Eocene volcanic ash and basement (Fig. 7). At Site 757, 55 Pleistocene to late Paleocene sediment samples were analyzed comprising Samples 121-757B-1H-2 through 121-757B-24X-4 (2.03-216.78 mbsf), (Fig. 7).

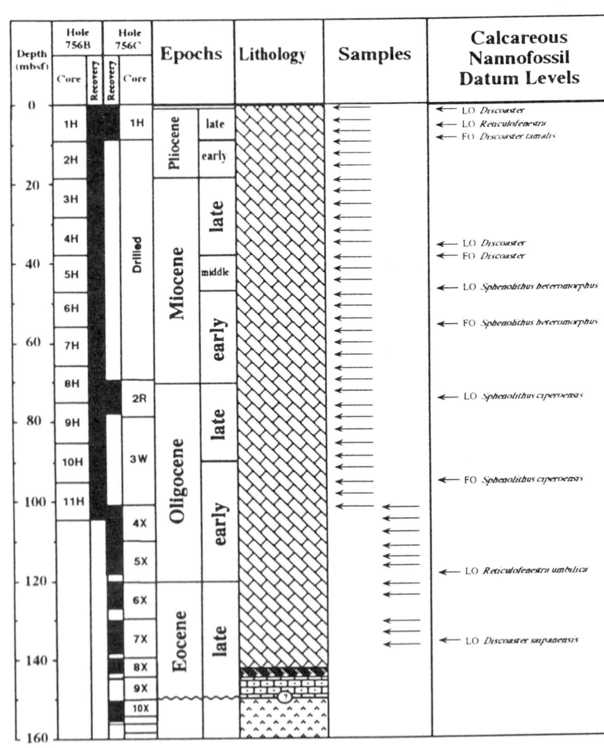

Fig. 6. Lithostratigraphy and Sample horizons at Site 756. See legend of Fig. 4.

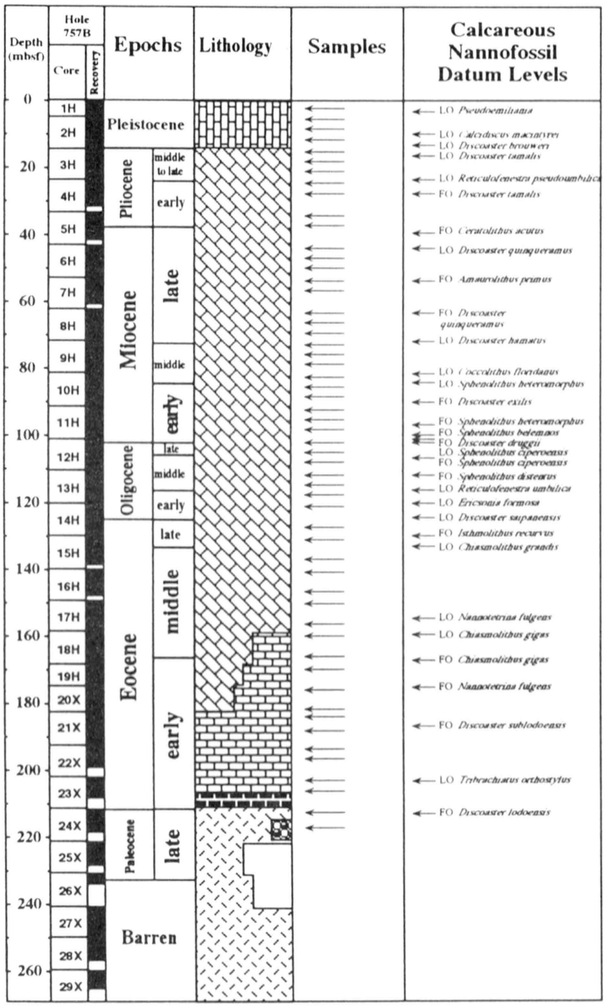

Fig. 7. Lithostratigraphy and Sample horizons at Site 757. See legend of Fig. 4.

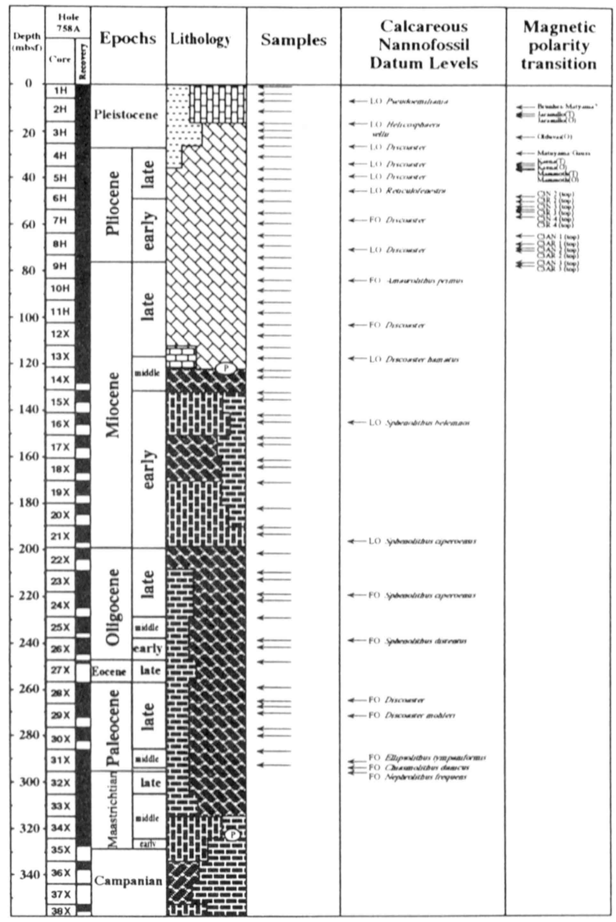

Fig. 8. Lithostratigraphy and Sample horizons at Site 758. See legend of Fig. 4.

Site 758 (5°23.049'S, 90°21.673' E) is located on the southeast side of Ninetyeast Ridge at a present water depth of 2922 m (Fig. 5), which is the deepest among Leg 121 sites. Hole 758A was cored with the APC and XCB systems to refusal at 422 mbsf, and with the RCB to a total depth of 677 mbsf. Average core recovery is 67.1%, but Cores 121-758A-1H through 121-758A-13X were completely recovered. Holocene to middle Miocene sediments are composed of nannofossil ooze with foraminifer, and the upper sediment units include terrigenous clay. Middle Miocene to Campanian sediments are mainly nannofossil and calcareous chalk, and occur across the unconformity that spans nearly the entire Eocene (Fig. 8). At Site 758, 58 sediment samples were analyzed (Samples 121-758A-1H-1 through 121-758A-31X-3, 0.75-292.65 mbsf) from the Pleistocene to late Eocene and Paleocene (Fig. 8).

Site 762 (19°53.23'S, 112°15.24' E) is located on the western part of the central Exmouth Plateau at a present water depth of 1371 m (Fig. 9). Hole 762C was drilled to a total depth of 940m by the XCB system, and recovered sediments from the Berriasian to Pleistocene (average recovery of 69.4%). The upper 182 m of foraminiferal-nannofossil and nannofossil ooze of late Oligocene and Neogene age is underlain by nannofossil ooze and chalk of early Santonian to late Oligocene age (Fig. 10). At Site 762, 31 sediment samples were analyzed (Samples 122-762C-23X-1 through 122-762C-35X-1, 370.19-479.18 mbsf) from the early Eocene and late Paleocene (Fig. 10).

B. Methods

The sediment samples were processed by two methods. Loose sediments were washed with 63 μm sieve, whereas slightly consolidated sediments were treated with <3% hydrogen peroxide solution, and then washed on a 63 μm sieve (Nomura, 1991a; 1991b).

For stable isotope analysis, the benthic genus *Cibicidoides* has been measured in many oceanographic studies (Miller et al., 1989; Woodruff et al., 1990; Hodell et al., 1991; Barrera and Huber, 1991, amongst others). $\delta^{13}C$ values of *Cibicidoides* are closely correlated with those of dissolved HCO_3^- in sea water at the sediment-water interface (Duplessy et al., 1984; Shackleton et al., 1984; Berger and Vincent, 1986; Savin and Woodruff, 1990). Because of microhabitat effects, infaunal taxa such as a *Oridorsalis* and

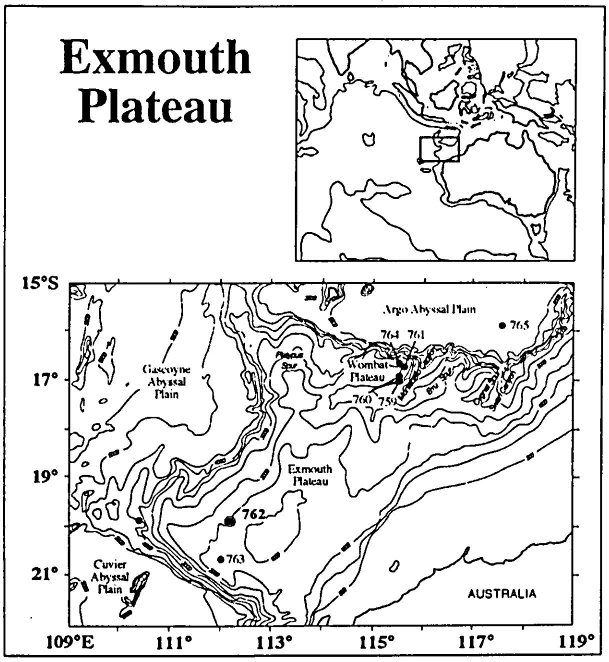

Fig. 9. Bathymetric map and seismic-reflection profile showing locations of ODP Leg 122 sites at Exmouth Plateau.

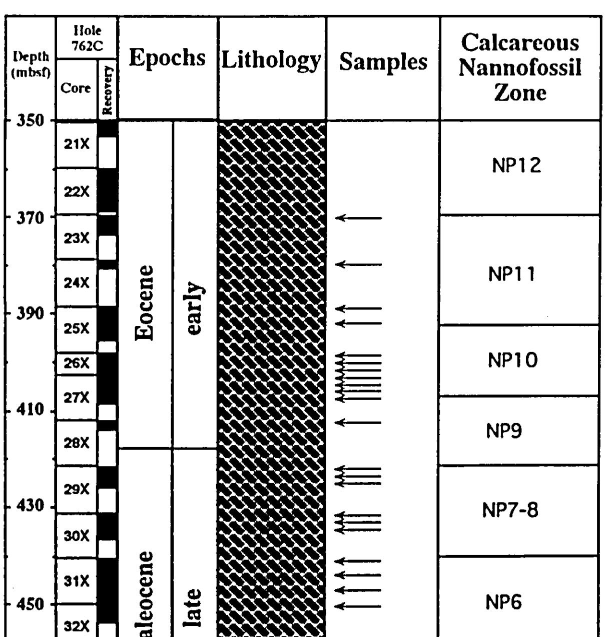

Fig. 10. Lithostratigraphy and Sample horizons at Site 762. See legend of Fig. 4.

Uvigerina are less well correlated with $\delta^{13}C$ values of dissolved HCO_3^- than epifaunal taxa such as a *Cibicidoides* (Belanger et al., 1981; Ganssen and Sarthein, 1983; Zahn et al., 1986; Savin and Woodruff, 1990; Woodruff and Savin, 1989). The species of *Cibicidoides*, however, are not common over a long stratigraphic range. For isotopic measurements, several species of the genus *Cibicidoides* were have been analyzed (e.g., Miller et al., 1989) or various species (e.g., Woodruff et al., 1990) at one examination. For example, the interspecific difference between *Cibicidoides kullenbergi* and *C. lamontdohertyi* is -0.22±0.12‰ according to Woodruff et al. (1990). Therefore monospecies such as *Oridorsalis umbonatus* (which show consistent occurrence over a long range) are more useful for an isotopic study than the genus *Cibicidoides*. In this study, benthic foraminifer *Oridorsalis umbonatus* (Pleistocene to middle Eocene), *Anomalinoides danicus* (middle Eocene to middle Paleocene), *Nuttallides truempyi* (early Eocene to late Paleocene), and *Stensioina beccariiformis* (Paleocene to Maastrichtian) were mainly selected for stable isotopic analysis. They have been used in many other isotopic study by Vincent et al. (1985), Kennett and Stott (1990), Katz and Miller (1991), and others. To compare the isotopic values of these epifaunal species, *Cibicidoides wuellerstorfi*, *C. mundulus*, and *C. velascoensis* were measured. *Groidinoides soldanii* was also measured to correlate with data of Rea et al. (1991). Planktonic foraminifera *Subbotina* spp. (*S. triangularis*, *S. triloculinoides* and/or *S. linaperta*) were mainly used for stable isotope analysis from the Paleocene to Eocene. *Globorotalia pseudobulloides* and *Rugoglobigerna pennyi* were used for the Cretaceous / Tertiary boundary.

Benthic foraminifera for analysis were >380 μm in this study, and three isotopic measurements were made on a single specimen in each sample. When there were few specimens >380 μm in size, approximately 5-10 specimens in the 150-380 μm size fraction were analyzed. The differences between the averaged values of a single specimen per sample and values of 5-10 specimens were -0.041±0.182 for $\delta^{18}O$ and -0.019±0.129 for $\delta^{13}C$ (N=27) in *Stensioina beccariiformis*, -0.115±0.194 for $\delta^{18}O$ and 0.014±0.143 (N=22) in *Nuttallides truempyi*. Approximately 5 specimens (180-350 μm size fraction) of the planktonic foraminifera *Subbotina* spp. and approximately 8 specimens (127-228 μm size fraction) of *Globorotalia pseudobulloides* and *Rugoglobigerna pennyi* were used for isotopic analysis. Other planktonic foraminifera were used according to various size fractions (Appendix A).

Specimens were put in a stainless-steel thimble and immersed in methyl alcohol. After the tests were disaggregated with a thin needle. They were ultrasonically cleaned. Stable isotope analyses were made using a Finnigan-MAT 250 mass spectrometer modified for ultra-small sample analysis, at the Shizuoka University. Oxygen and carbon isotope measurements were performed using the procedure of Wada et al. (1984; 1991). Carbonate specimens were reacted in saturated phosphoric acid, mixed solution of pyrophosphoric acid and few metaphosphoric acid (Wada et al., 1982), at 60.00°C. After the resulting CO_2 gas was purified in a glass-line, it was analyzed. The value thus obtained was converted into a value against a PDB standard by using NBS 20. The converted values are -4.18‰ for

$\delta^{18}O$ and -1.07‰ for $\delta^{13}C$, which is Craig's value of NBS 20 (in Blattner and Hulston, 1978). The precision for the isotope analysis is 0.02‰ for $\delta^{13}C$ and 0.05‰ for $\delta^{18}O$. Minimum volume of CO_2 gas for isotopic analysis is 2μl.

C. Results

Results of isotopic analysis of benthic and planktonic foraminifera from Sites 752, 754, 756, 757, 758, and 762 are presented in Appendix A.

1. Site 752

At Site 752, oxygen and carbon isotopes were analyzed for five species; *Oridorsalis umbonatus*, *Anomalinoides danicus*, *Nuttallides truempyi*, *Stensioina beccariiformis*, and *Cibicidoides velascoensis*, and five planktonic foraminiferal species; *Acarinina primitiva*, *Morozovella marginodentata*, *Subbotina* spp., *Globorotalia pseudobulloides*, and *Rugoglobigerina penny*. However, analysis of *O. umbonatus* could only be made in Sample 121-752A-21X-1, 70-75cm (191.10 mbsf) from the late Paleocene, and values -0.221‰ (oxygen isotope) and 1.613‰ (carbon isotope).

Anomalinoides danicus

Isotopes were analyzed for Samples 121-752A-13X-1,70-75cm to 121-752A-32X-5,70-75cm (113.60-295.40 mbsf) from the late Paleocene to early Eocene. Rare occurrences of *A. danicus* from Samples 121-752A-23X-1, 54-56cm to 121-752A-27X-3, 70-75cm (210.34-252.10 mbsf) from the upper Paleocene provide a few isotope data in this section. The isotopic records of *A. danicus* are plotted as a function of depth (mbsf) in Fig. 11.

Oxygen isotopes: Averaged $\delta^{18}O$ values of *A. danicus* between 295.40 and 252.1 mbsf gradually increase by 0.64‰, from -1.011 to -0.390‰. Between 239.77 and 192.60 mbsf in the upper Paleocene, $\delta^{18}O$ values are constant at about -0.6‰. Near the Paleocene/Eocene boundary, two oxygen isotopic ratios of 191.1 mbsf and 181.4 mbsf exhibit relatively high values of -0.389 and -0.189‰, respectively. $\delta^{18}O$ values from 174.85 to 113.60 mbsf in the lower Eocene show wide fluctuations, but gradually decrease by about 0.4‰ from -0.6 to -1.0‰. During this period, the difference between the maximum (-0.561‰) and minimum (-1.420‰) values of $\delta^{18}O$ reaches 0.86‰. $\delta^{18}O$ values at 152.40 mbsf and 123.30 mbsf are remarkably low (-1.420 and -1.371‰, respectively).

Carbon isotopes: Averaged $\delta^{13}C$ values between 295.40 and 200.8 mbsf in the Paleocene gradually increase by 0.85‰, from 1.433 to 2.315‰. The $\delta^{13}C$ value at 200.8 mbsf is highest among the values of *A. danicus* at Site 752. $\delta^{13}C$ values at 289.40 and 252.10 mbsf are distinctively low. $\delta^{13}C$ values decrease by about 1.9‰ in the section between 200.80 and 155.40 mbsf, across the Paleocene / Eocene boundary. In the lower part of this section, $\delta^{13}C$ values dramatically decrease until a level slightly below the Paleocene / Eocene boundary. From 155.40 to 113.60 mbsf in the lower Eocene, $\delta^{13}C$ values are constant (about 0.2‰), with slight fluctuations value (max. 0.395 and min. -0.746‰). The pattern of fluctuation in $\delta^{13}C$ is similar to that of the oxygen isotopic record. $\delta^{13}C$ values at 152.40 mbsf and 123.30 mbsf are extremely low (-0.746 and -0.648‰, respectively), similar to $\delta^{18}O$ values.

Nuttallides truempyi

Two to five individuals were examined, because a single individual is too small (153-380μm diameter) for isotopic analysis. However, measurements using a single individual were possible for the interval from 200.80 to 203.80 mbsf. However the difference in values between the measured individuals is small, and thus the results of both methods (using an individual and a few individuals) are almost the same. At this site, isotopic records were obtained from Samples 121-752A-13X-1, 70-75cm to 121-752A-26X-1, 97-100cm (113.60-239.77 mbsf) covering the upper Paleocene and lower Eocene. The isotopic records of *N. truempyi* are shown in Fig. 12.

Oxygen isotopes: *N. truempyi* $\delta^{18}O$ values decrease

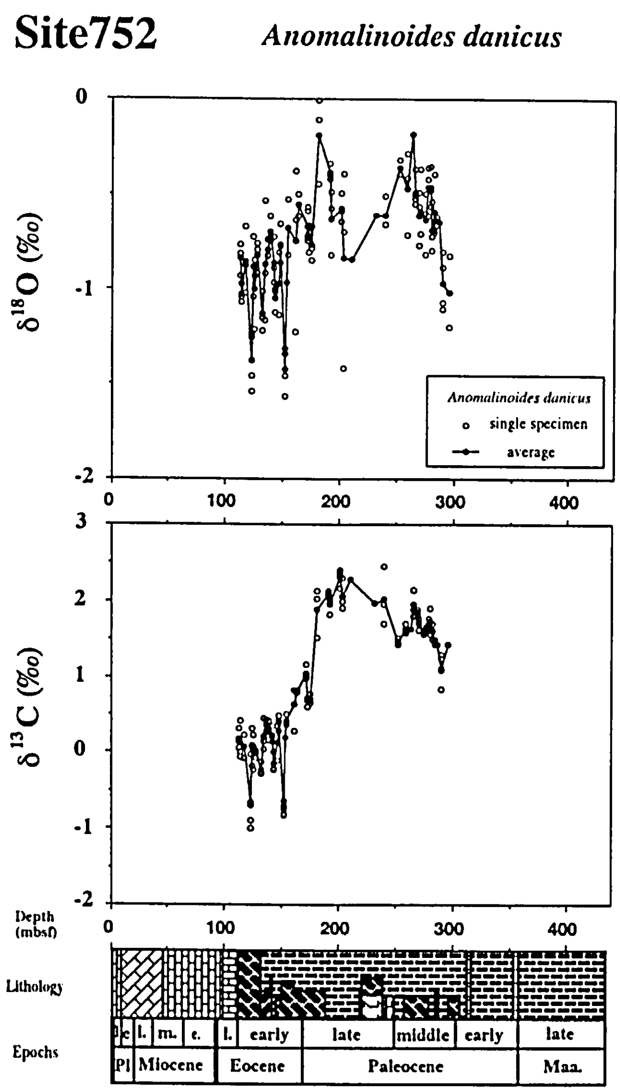

Fig. 11. Oxygen and carbon isotope records of benthic foraminifer *Anomalinoides danicus* at Site 752.

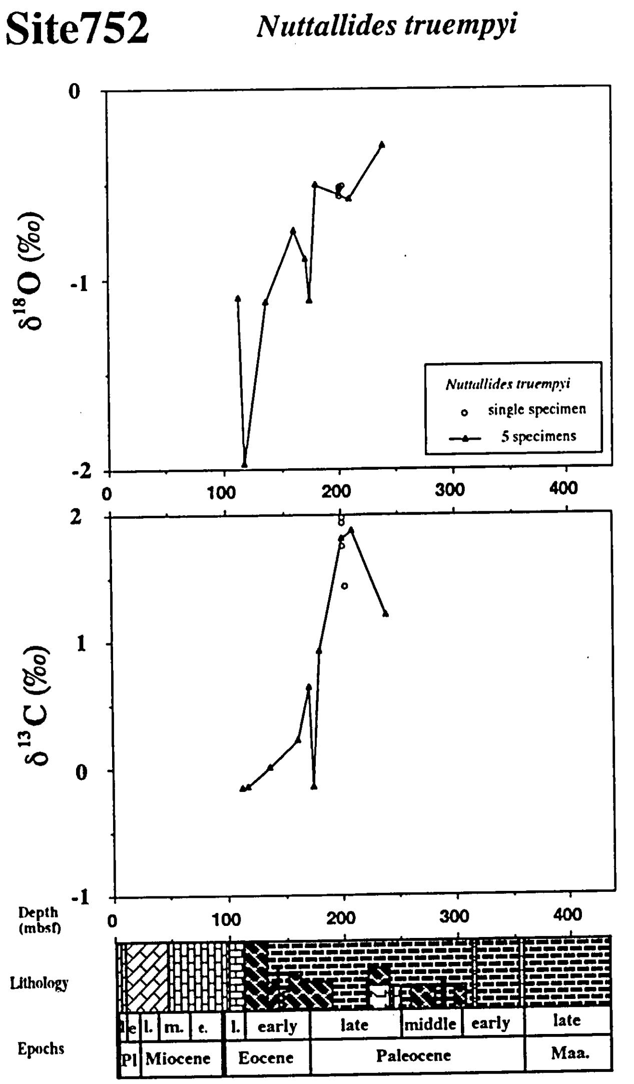

Fig. 12. Oxygen and carbon isotope records of benthic foraminifer *Nuttallides truempyi* at Site 752.

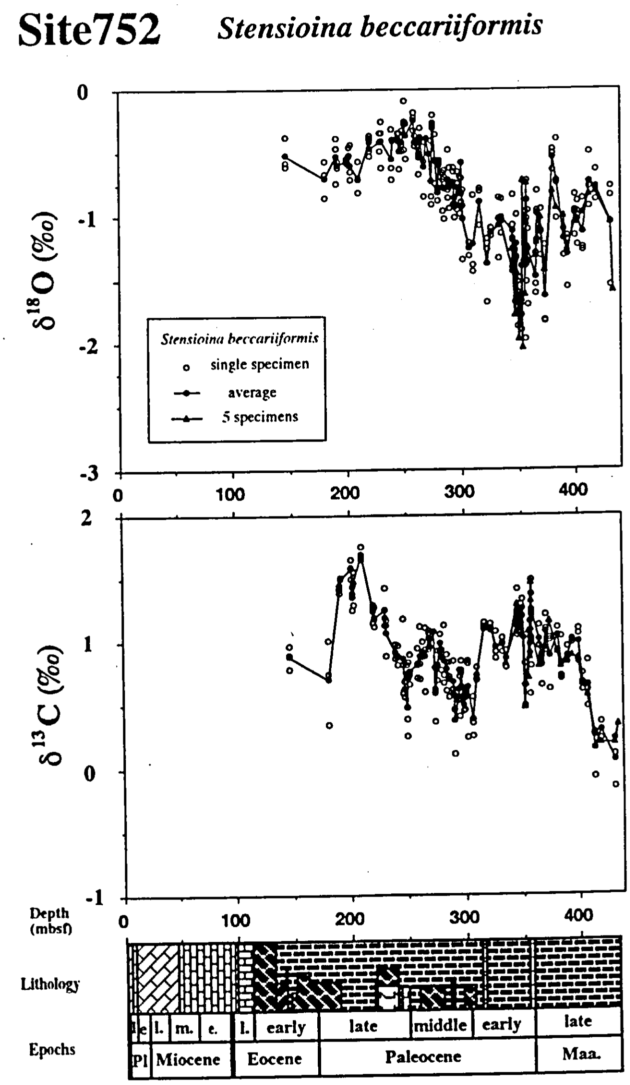

Fig. 13. Oxygen and carbon isotope records of benthic foraminifer *Stensioina beccariiformis* at Site 752.

gradually by 0.2‰ from 239.77 to 181.40 mbsf in the upper Paleocene, and decrease more rapidly by 0.6‰ (-0.506 to -1.094‰) from 181.4 to 113.60 mbsf. $\delta^{18}O$ values of 174.85 mbsf (below the Paleocene / Eocene boundary) and 118.02 mbsf (above the P/E boundary) show remarkably little deviating from the general decreasing trend. The latter, in particular, records the lowest values (-1.971 ‰) among the *N. truempyi*data.

Carbon isotopes: $\delta^{13}C$ values increase from 239.77 to 210.34 mbsf in the upper Paleocene, peaking at 210.34 mbsf (1.873‰). From 210.34 to 113.60 mbsf across the Paleocene / Eocene boundary, $\delta^{13}C$ values decrease by about 2.0‰ from 1.873 to -0.149‰. $\delta^{13}C$ values decrease rapidly below the Paleocene / Eocene boundary (200.80 to 174.85 mbsf). $\delta^{13}C$ values at 174.85 mbsf are remarkably low (-0.143‰), and related to the "benthic extinction event".

Stensioina beccariiformis

Isotope analyses were performed for material from Samples 121-752A-16X-4, 59-65cm to 121-752A-33X-3, 57-60cm (147.09-301.97 mbsf) and from Samples 121-752B-5R-3, 50-53cm to 121-752B-19R-3, 49-52cm (300.50-435.09 mbsf) from the upper Maastrichtian to lower Eocene. The isotopes of *S. beccariiformis* below 335.82 mbsf were analyzed using five to ten individuals, or a single individual. No occurrence of *S. beccariiformis* slightly above Sample 121-752A-20X-1, 70-75cm (181.40 mbsf) before the Paleocene / Eocene boundary indicates that this species became extinct by the late Paleocene Benthic Event (e,g., Nomura, 1991a). However, reworked *S. beccariiformis* was found in Sample 121-752A-16X-4, 59-65cm (147.09 mbsf) above the event. The oxygen and carbon isotopic values of this sample are similar to those of 181.40 mbsf located before the "extinction event", and are high in comparison with those of *A. danicus* from the same sample. Therefore, *S. beccariiformis* at 174.85 mbsf supports the intercalation of reworked sediment. The isotopic records of *S. beccariiformis* are shown in Fig. 13.

Oxygen isotopes: Fluctuations in $\delta^{18}O$ with a general decreasing trend of 0.3‰, from -0.8 to -1.1‰, is shown from 435.09 to 326.85 mbsf (late Maastrichtian to early Paleocene). Above the Cretaceous / Tertiary boundary, $\delta^{18}O$ values show the largest amplitude from a maximum of -0.746‰ at 358.18 mbsf, to a minimum of -1.969‰ at 351.60 mbsf. From 326.85 to 252.10 mbsf in the Paleocene section, $\delta^{18}O$ values increase from -1.120 to -0.244‰. From a maximum value of 258.80 mbsf, $\delta^{18}O$ values gradually decrease to -0.699‰ at 181.40 mbsf, located below the Paleocene / Eocene boundary near the extinction event.

Carbon isotopes: Four $\delta^{13}C$ values between 435.09 and 413.63 mbsf in the upper Maastrichtian are constant at ~0.2‰, showing the lowest $\delta^{13}C$ values at Site 752. $\delta^{13}C$ values rapidly increase by 0.6-0.8‰ up to 400.42 mbsf in the upper Maastrichtian. The section across the Cretaceous / Tertiary boundary (400.42 to 345.6 mbsf) shows a slight increase with a small oscillation of carbon isotopic records. However, the values just above the Cretaceous / Tertiary boundary show a large variation from 1.486‰ (358.18 mbsf) to 0.475‰ (353.10 mbsf). Averaged $\delta^{13}C$ values tend to decrease by 0.75‰ from 345.6 to 307.04 mbsf in the lower Paleocene. In this section, averaged $\delta^{13}C$ values increase from 335.82 mbsf to 316.92 mbsf, and rapidly decrease to 307.04 mbsf (0.392‰), which is the lowest value among the Paleocene $\delta^{13}C$ values. In the late early and late Paleocene, averaged $\delta^{13}C$ values tend to increase by about 1.3‰, up to a peak value of 1.689‰ at 210.34 mbsf. However, averaged $\delta^{13}C$ values decrease between 272.92 and 247.12 mbsf in the late Paleocene. A rapid decrease of $\delta^{13}C$ value is shown from 210.34 to 181.40 mbsf, where *S. beccariiformis* became extinct below the Paleocene / Eocene boundary.

Cibicidoides velascoensis

Isotopic records were obtained from Samples 121-752A-20X-1, 70-75cm to 121-752A-33X-3, 57-60cm (181.40-301.99 mbsf) and from Samples 121-752B-5R-3, 50-53cm to 121-752B-19R-3, 49-52cm (300.50-435.09 mbsf) from the lower Maastrichtian and Paleocene. No occurrence of *C. velascoensis* above Sample 121-752A-20X-1, 70-75cm (181.40 mbsf) before the Paleocene / Eocene boundary may result from the late Paleocene Benthic Event. The rare occurrence of *C. velascoensis* through Samples 121-752A-25X-3, 79-84cm to 121-752A-30X-1, 73-76cm (232.89-278.13 mbsf) in the Paleocene provides some isotope data in this section. The isotopic record of *C. velascoensis* is shown in Fig. 14.

Oxygen isotopes: $\delta^{18}O$ values repeatedly fluctuate from 435.09 to 310.59 mbsf in the upper Maastrichtian and lower Paleocene. In this section, $\delta^{18}O$ values increase by ~ 0.2‰ from 435.09 to 358.18 mbsf, shift down about 0.4‰ around 360 mbsf immediately above the Cretaceous / Tertiary boundary, then show a general increasing trend of ~0.1‰ up to 310.59 mbsf. From 310.59 to 284.65 mbsf in the late early Paleocene, $\delta^{18}O$ values rapidly increase by ~ 0.7‰ from -1.044 to -0.345‰. In the late Paleocene, $\delta^{18}O$ values are relatively constant (~ -0.4‰).

Carbon isotopes: $\delta^{13}C$ values slightly decrease from 435.09 to 413.63 mbsf in the upper Maastrichtian, then show the lowest value among Site 752. From 413.63 to 400.32 mbsf in upper Maastrichtian, $\delta^{13}C$ values increase from 0.531 to 1.289‰. $\delta^{13}C$ values gradually decrease up to 367.50 mbsf. In the section from 367.50 to 347.60 mbsf just across the Cretaceous / Tertiary boundary, $\delta^{13}C$ values show a large fluctuation with a maximum of 1.719‰ (358.44 mbsf) and a minimum of 0.880‰ (353.10 mbsf). In the interval from 347.60 to 307.04 mbsf, $\delta^{13}C$ values increase by 0.3‰ between 326.85 and 322.86 mbsf; however the values decrease by 0.45‰ between 316.92 and 310.59 mbsf. $\delta^{13}C$ value at 307.04 mbsf is the lowest among the early Paleocene. In the late early and late Paleocene, $\delta^{13}C$ values tend to increase by 1.5‰ up to a peak value of 2.375‰ at 210.34 mbsf. In this section, $\delta^{13}C$ values of 245.77 mbsf are relatively low. In the latest late Paleocene, $\delta^{13}C$ values decrease rapidly by 0.9‰ from 210.34 to 181.40 mbsf and then *C. velascoensis* disappears in the section.

Subbotina spp.

Isotopic analysis is analyzed for Samples 121-752A-17X-3, 70-75cm to 121-752A-33X-3, 57-60cm (155.40-

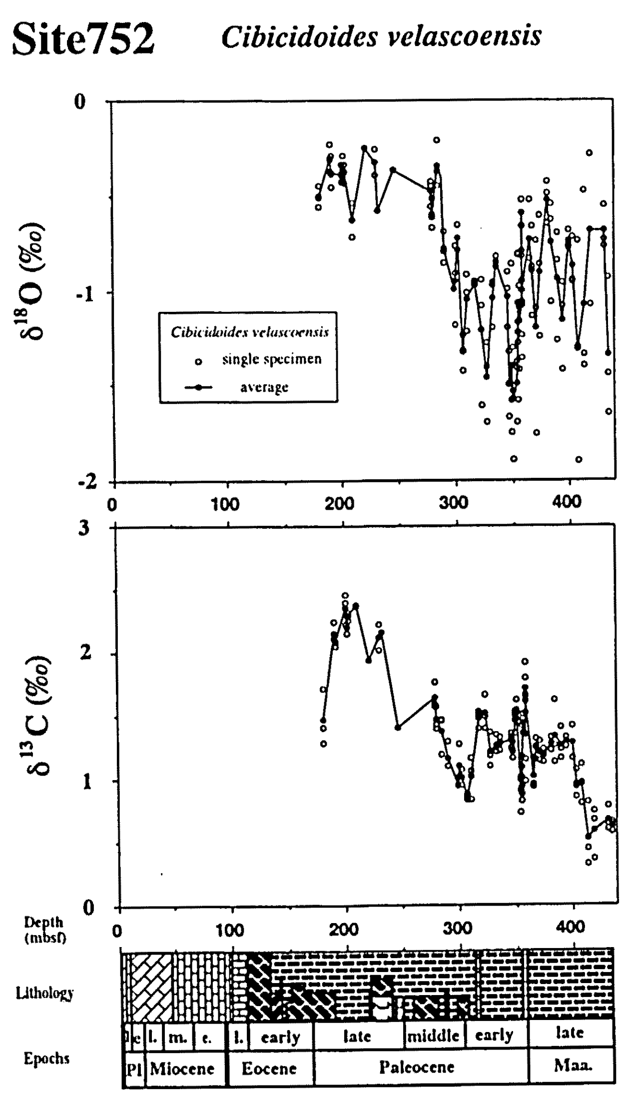

Fig. 14. Oxygen and carbon isotope records of benthic foraminifer *Cibicidoides velascoensis* at Site 752.

301.97 mbsf) were made, from the lower and upper Paleocene. The isotopic records of *Subbotina* spp. are shown in Fig 15..

Oxygen isotopes: $\delta^{18}O$ values increase by about 0.6‰ from 301.97 to 258.80 mbsf. In this section, $\delta^{18}O$ values show a distinct decrease just above lower / upper Paleocene boundary with a minimum value of -1.870‰ at 274.40 mbsf. From 258.8 to 155.40 mbsf (upper Paleocene and lowermost early Eocene), $\delta^{18}O$ values fluctuate although generally decrease. $\delta^{18}O$ values increase from -1.873 to -1.324‰ in the section between 174.85 and 163.75 mbsf just across the Paleocene / Eocene boundary.

Carbon isotopes: $\delta^{13}C$ values from 301.97 to 220.20 mbsf in the lower Paleocene increase by about 1.3‰ (1.640 to 2.917‰), then decrease by 0.55‰ between 268.40 and 249.10 mbsf in the upper Paleocene section. From 220.20 to 155.40 mbsf (upper Paleocene and lowermost Eocene), $\delta^{13}C$ values decrease by about 2.2‰. The dramatic decrease in this section occurs slightly below the Paleocene / Eocene boundary.

Other planktonic foraminifera

Less common planktonic foraminiferal species, *Acarinina primitiva*, *Morozovella marginodentata*, *Globorotalia pseudobulloides*, and *Rugoglobigerina penny*, were analyzed for Samples 121-752A-13X-1, 70-75cm to 121-752A-17X-3, 70-75cm (113.60-155.40 mbsf, lower Eocene), Samples 121-752A-15X-1, 70-75cm to 121-752A-20X-3, 70-75cm (133.00-181.40 mbsf, lower Eocene to the uppermost Paleocene), Samples 121-752B-10R-2, 100-102cm to 121-752B-10R-7, 41-43cm (347.60-354.51 mbsf, above the Cretaceous / Tertiary boundary), and Samples 121-752B-11R-1, 112-114cm to 121-752B-12R-5, 54-57cm (358.92-370.94 mbsf, below the Cretaceous / Tertiary boundary), respectively. Two to eight individuals analyzed at

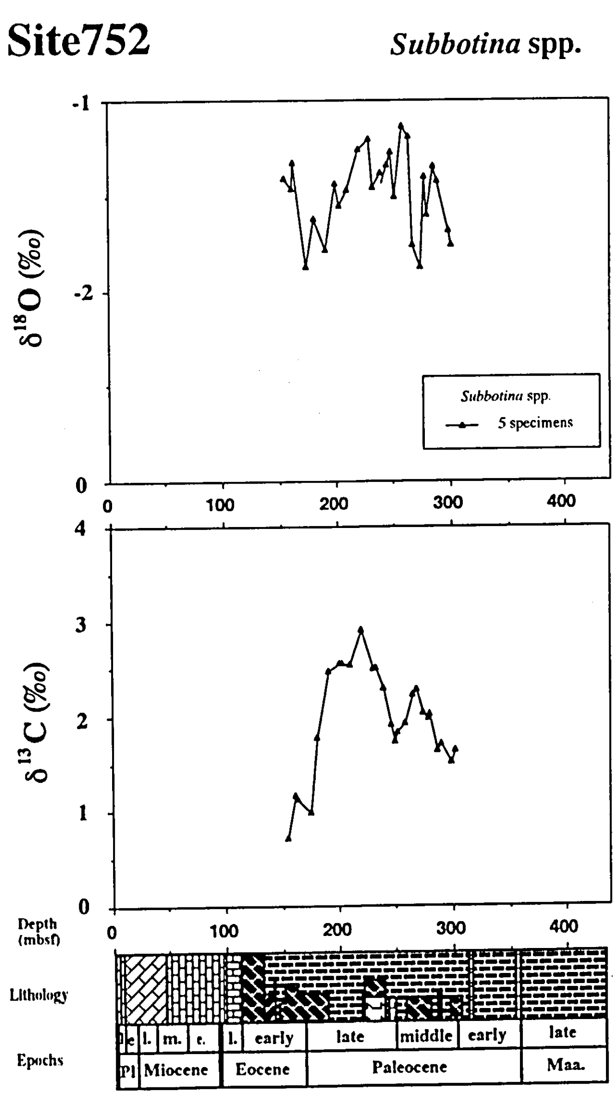

Fig. 15. Oxygen and carbon isotope records of planktonic foraminifer *Subbotina* spp. at Site 752.

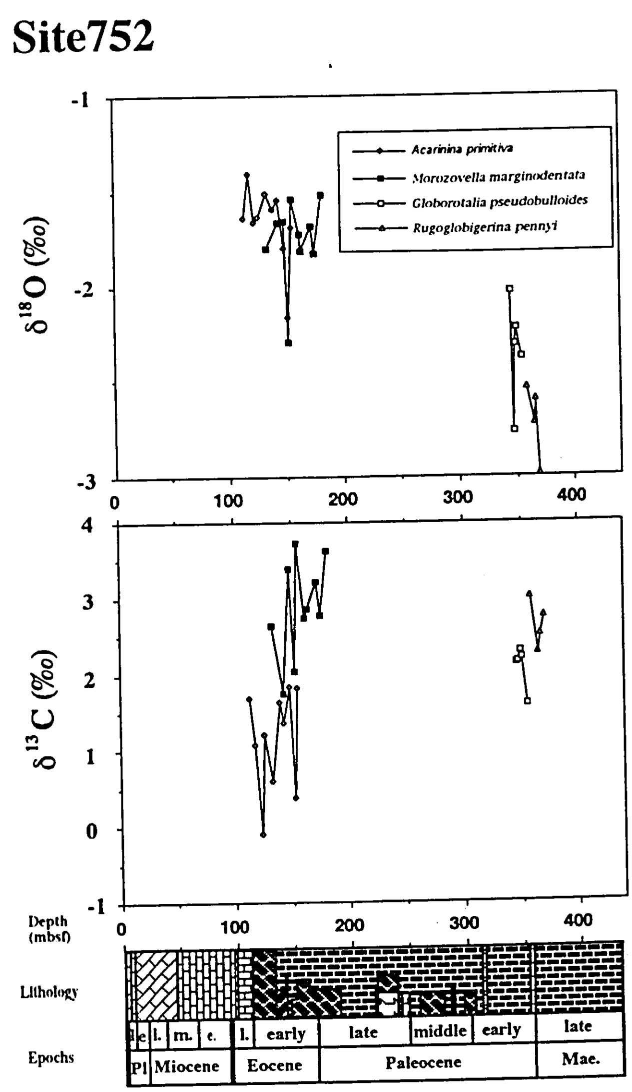

Fig. 16. Oxygen and carbon isotope records of other planktonic foraminifers at Site 752.

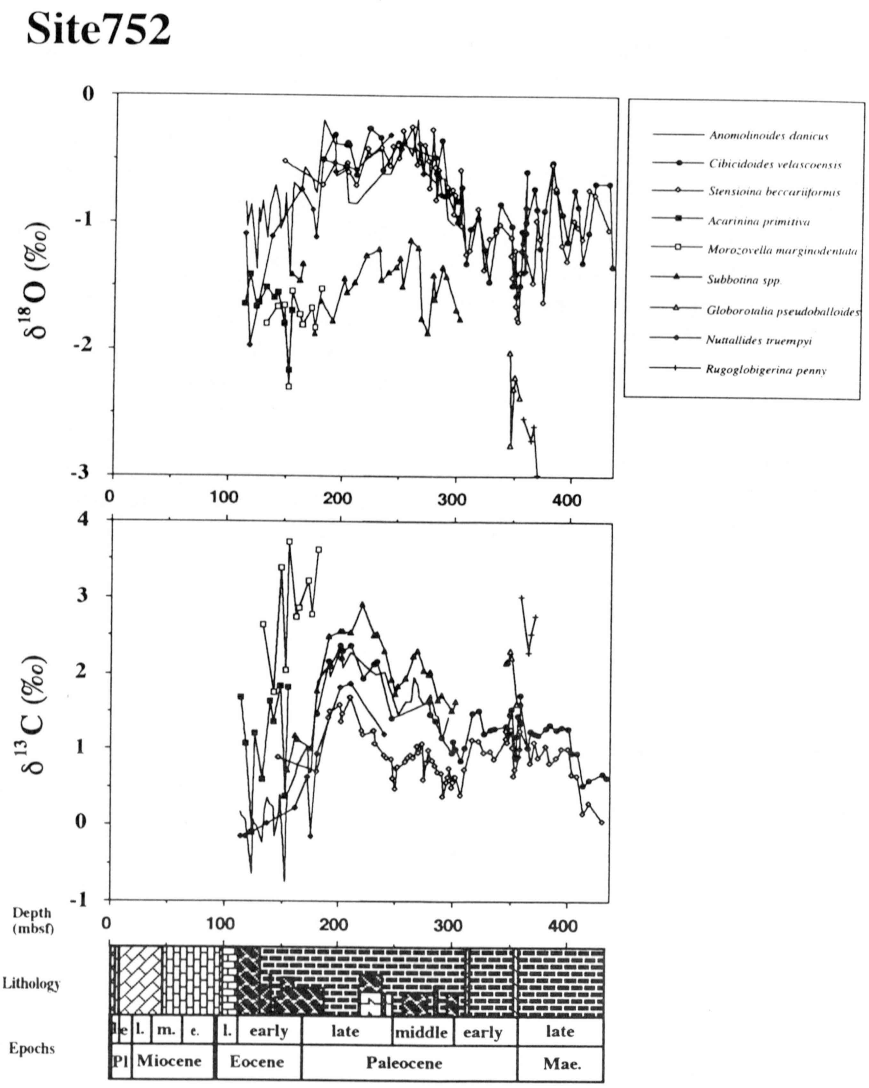

Fig. 17. Summary of oxygen and carbon isotope records at Site 752.

Site 752. *Globorotalia pseudobulloides* and *R. penny* do not overlap. The isotopic records of those species are shown in Fig. 16.

Oxygen isotopes: $\delta^{18}O$ values of *R. penny* below the Cretaceous / Tertiary boundary increase from -2.988 to -2.538‰. $\delta^{18}O$ values of *G. pseudobulloides* above the Cretaceous / Tertiary boundary also show a general increase, from -2.377 to -2.020‰. However, $\delta^{18}O$ of *G. pseudobulloides* shows remarkably low values at 347.60 mbsf. In the latest late Paleocene and early Eocene, $\delta^{18}O$ values of *M. marginodentata* are constant (~ -1.7‰). In the early Eocene, $\delta^{18}O$ values of *A. primitiva* tend to increase. No significant change of *M. marginodentata* is observed across the Paleocene / Eocene boundary, which differs from the oxygen isotopic records of *Subbotina* spp. In *A. primitiva* and *M. marginodentata*, $\delta^{18}O$ values at 152.4 mbsf exhibit remarkably low values of -2.160 and -2.291‰, respectively.

Carbon isotopes: $\delta^{13}C$ values of *R. penny* below the Cretaceous / Tertiary boundary are constant at ~2.6‰. Above the Cretaceous / Tertiary boundary, $\delta^{13}C$ values of *G. pseudobulloides* are about 2.2 ‰, except for a slightly low value at 354.51 mbsf. In *M. marginodentata*, $\delta^{18}O$ values are constant at ~3‰ from 181.4 to 155.4 mbsf across the Paleocene / Eocene boundary, and tend to decrease from 155.40 to 133.00 mbsf in the lower Eocene. $\delta^{13}C$ values of *A. primitiva* in the lower Eocene are constant at ~1‰. However, $\delta^{13}C$ values of *M. marginodentata* and *A. primitiva* fluctuate. At 152.40 mbsf and 123.30 mbsf, $\delta^{13}C$ values are remarkably low.

Isotopic values obtained from Site 752 are summarized in Fig. 17.

2. Site 754

At Site 754, only the benthic foraminifer *Oridorsalis umbonatus* was analyzed for oxygen and carbon isotopes. Isotope analyses were made on material from Samples 121-754A-1H-1, 70-75cm to 121-754A-13X-3, 70-75cm (0.70-

116.00 mbsf) from the Pleistocene to late Oligocene. The isotopic records of *Oridorsalis umbonatus* at Site 754 are shown in Fig. 18.

Oxygen isotopes: The oxygen isotopic records of *Oridorsalis umbonatus* are constant at ~1.2‰ from 116.00 mbsf to 89.90 mbsf in the upper Oligocene and the lower Miocene. $\delta^{18}O$ values decrease by ~0.4‰ across the early / middle Miocene boundary. $\delta^{18}O$ values are relatively low from 83.90 to 77.20 mbsf (nannofossil Zones CN3-4). In this interval, $\delta^{18}O$ values at 83.90 mbsf display the lowest value (0.933‰) among the Neogene samples. In the middle Miocene, $\delta^{18}O$ values from 77.20 to 60.80 mbsf increase significantly by 0.85‰ from 1.077‰ to 1.924‰. $\delta^{18}O$ values are constant about 2.0‰ from 60.80 to 32.00 mbsf through the upper

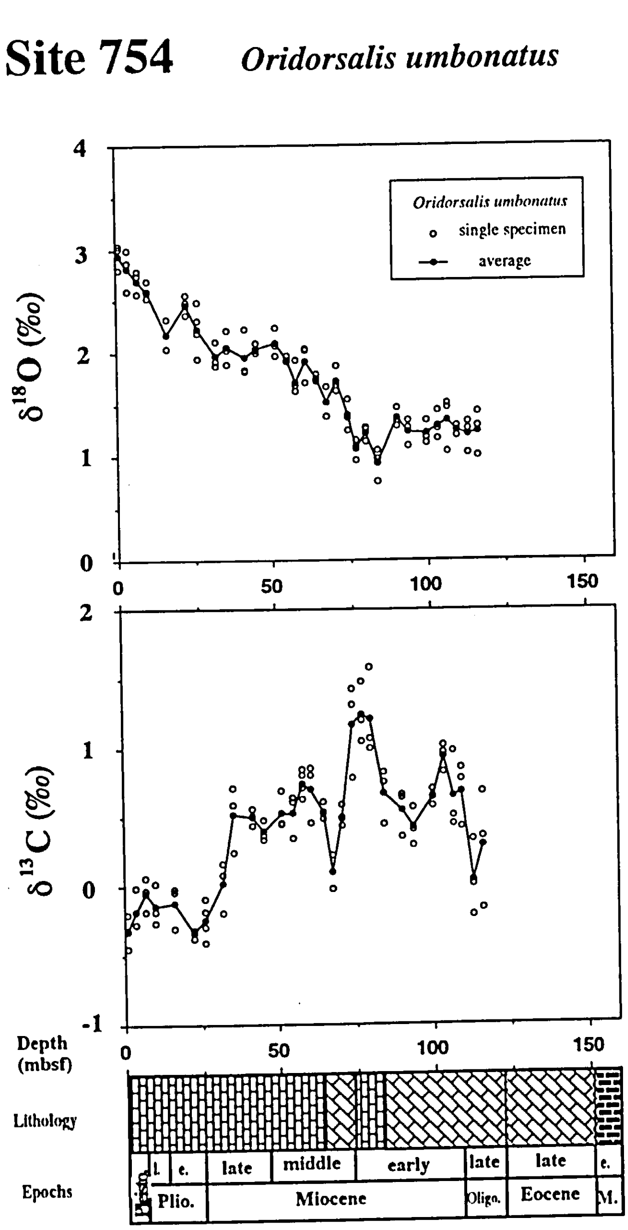

Fig. 18. Oxygen and carbon isotope records of benthic foraminifer *Oridorsalis umbonatus* at Site 754.

middle and upper Miocene. In the early Pliocene, $\delta^{18}O$ values increase by 0.5‰ up to a small peak at 22.40 mbsf (2.467‰), and decrease by ~0.3‰. A shift of $\delta^{18}O$ (of ~0.4‰) is observed across the early / late Pliocene boundary. During the late Pliocene and Pleistocene, $\delta^{18}O$ values increase up to 2.945‰ at 0.70 mbsf near to the present.

Carbon isotopes: The carbon isotopic records show a notable increase from 113.00 to 103.30 mbsf across the Oligocene / Miocene boundary, and then attain the highest (0.938‰) among lower Miocene samples. The magnitude of this increase is 0.9‰. $\delta^{13}C$ values decease by 0.5‰ up to 93.60 mbsf in nannofossil Zone CN1, then begin to increase again. This increase is gradual up to 83.90 mbsf, then changes up to 80.20 mbsf within Zones CN3-4. From 80.20 to 74.20 mbsf across the Zone CN4/5 boundary in the middle Miocene, $\delta^{13}C$ values are distinctly high (~1.2‰). During the middle Miocene, $\delta^{13}C$ values drastically decrease by about 1.1‰ from 1.2 to 0.1‰ at 67.50 mbsf, and then rapidly increase by 0.65‰ up to a weak peak at 57.80 mbsf (0.749‰). $\delta^{13}C$ values are constant at ~0.5‰ from 54.80 to 35.60 mbsf (middle and upper Miocene). $\delta^{13}C$ values display a distinct shift to lower values (decreasing by ~0.5‰) between 35.60 and 32.00 mbsf (uppermost Miocene), and show a decreasing trend up to minimum value at 22.40 mbsf (-0.341‰) in the early Pliocene (Zones CN11a-10b). This shift is correlated with the Chron-6 Carbon Shift in the latest Miocene (Vincent et al., 1980; 1985). The carbon isotopic records exhibit a slight increase up to a weak peak at 6.80 mbsf (Zone CN12d) just below the Pleistocene / Pliocene boundary, and then show a decreasing trend up to 0.70 mbsf near to the present.

3. Site 756

At Site 756, only the benthic foraminifer *Oridorsalis umbonatus* was analyzed for oxygen and carbon isotopes. The analyzed material was obtained from Samples 121-756A-1H-1, 70-75cm to 121-756A-11H-5, 70-75cm (0.70-101.30 mbsf), and from Samples 121-756A-4X-1, 70-75cm to 121-756A-7X-5, 70-75cm (101.60-136.50 mbsf), from the Pleistocene to the uppermost Eocene. Fig. 19 shows the oxygen and carbon isotopic records for *Oridorsalis umbonatus* at Site 756.

Oxygen isotopes: The oxygen isotopic records show an increasing trend up to 120.90 mbsf within nannofossil Zone CP16 in the earliest Oligocene. The magnitude of this increase is 0.95‰. During the late early Oligocene to early Miocene, $\delta^{18}O$ values show a slight increase with fluctuations of amplitude of ~0.5‰. In this interval, weak peaks in $\delta^{18}O$ value are observed at 101.60 mbsf (Zones CP17-18), 81.90 mbsf (Zone CP19), and 56.90 mbsf (Zones CN1-2) (1.622, 1.715, and 1.643‰, respectively). The value of 53.60 mbsf (Zone CN3-4 just below the early / middle Miocene boundary) is the lowest among the Neogene samples. During the middle Miocene, $\delta^{18}O$ values rapidly increase by about 1.4‰ up to 2.590‰ at 41.0 mbsf (Zones CN5-6). A constant value of ~2.5‰ is observed from 41.00 to 9.20 mbsf (middle Miocene to lower Pliocene). Across the late / early Pliocene boundary, $\delta^{18}O$ values rapidly increase by about 0.8‰ from 2.335‰ (9.20 mbsf) to 3.169‰ (3.70

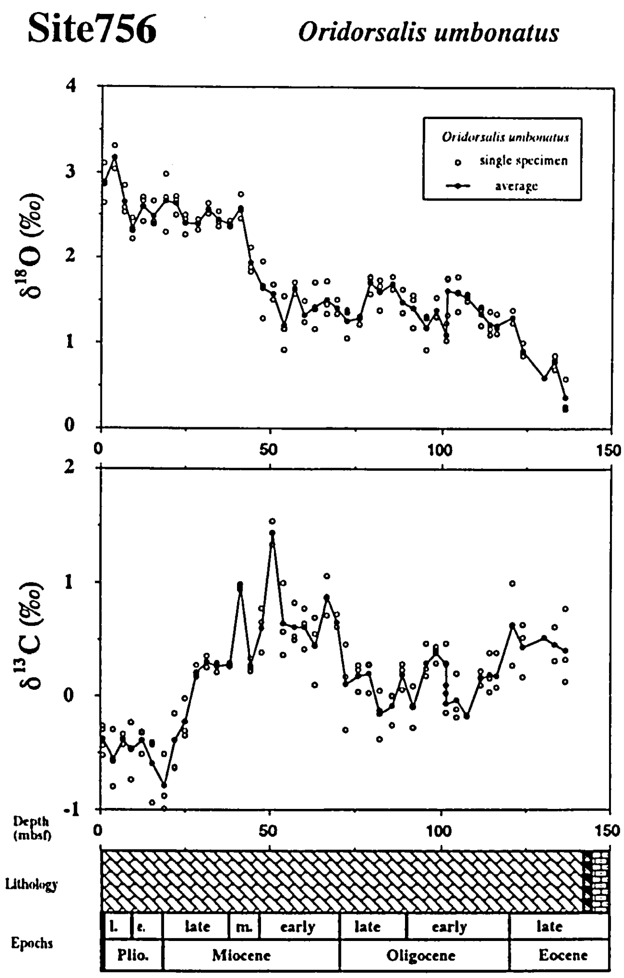

Fig. 19. Oxygen and carbon isotope records of benthic foraminifer *Oridorsalis umbonatus* at Site 756.

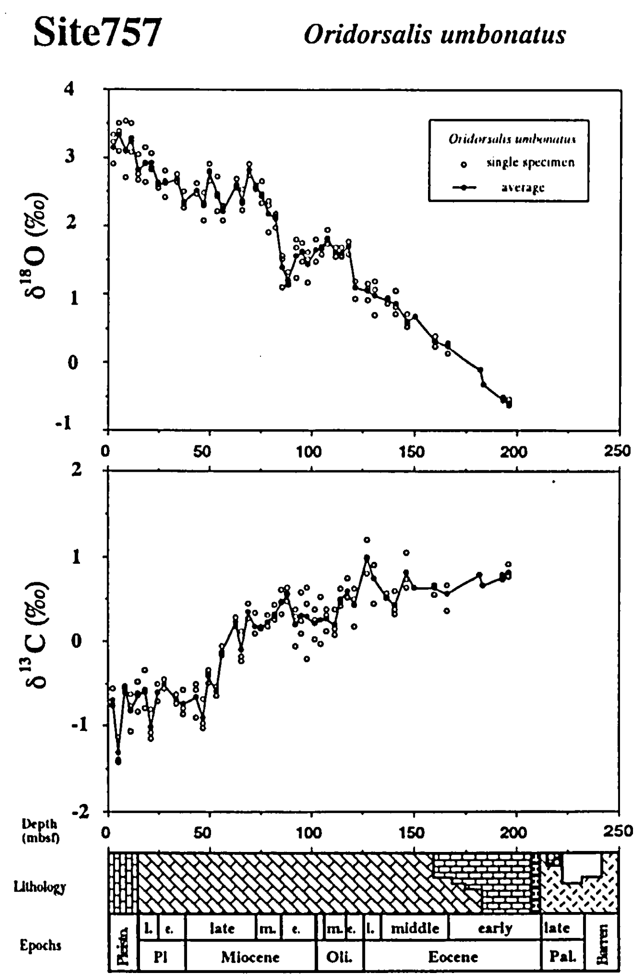

Fig. 20. Oxygen and carbon isotope records of benthic foraminifer *Oridorsalis umbonatus* at Site 757.

mbsf). Limited data from the late Pliocene and Pleistocene shows ~3.0‰.

Carbon isotopes: The carbon isotopic record shows a gradual increase up to 0.636‰ at 120.90 mbsf (Zones CP16 in the early Oligocene). In the lower Oligocene, $\delta^{13}C$ values from 120.90 to 107.60 mbsf decrease by 0.8‰. $\delta^{13}C$ values increase from -0.173‰ (107.60 mbsf) to 0.383‰ (98.30 mbsf) in the late early Oligocene and then reverse at the early / late Oligocene boundary, decreasing to -0.148‰ at 81.90 mbsf (Zone CP19). Across the Oligocene / Miocene boundary, $\delta^{13}C$ values rapidly increase by 1.0‰ up to the peak at 66.30 mbsf (Zones CN2-1). From 62.90 to 50.60 mbsf, $\delta^{13}C$ values increase by ~1.0‰ from 0.449 to 1.439‰. In this section, a notable shift is observed between 53.60 and 50.60 mbsf. During the middle Miocene, $\delta^{13}C$ values significantly decrease by ~1.2‰ up to 44.00 mbsf in Zones CN5-6, and then rapidly increase by 0.7‰ up to a distinct peak at 41.00 mbsf (0.967‰), and again decrease up to 38.0 mbsf in Zone CN7. From 38.00 to 28.40 mbsf, $\delta^{13}C$ values are constant (~0.25‰). In the uppermost Miocene, the carbon isotopic records between 28.40 and 18.80 mbsf exhibit a remarkable negative shift that correlates with the Chron-6 Carbon Shift in the latest Miocene (Vincent et al., 1980; 1985). During the Pliocene and Pleistocene, $\delta^{13}C$ increases to 0.4‰ up to 12.2 mbsf. Those values are constant at ~-0.4‰.

4. Site 757

At Site 757, oxygen and carbon isotopes were analyzed for 2 species of benthic foraminifers; *Oridorsalis umbonatus* and *Anomalinoides danicus*, and for planktonic foraminifera *Subbotina* spp. The isotopic values *A. danicus* overlap with that of *Oridorsalis umbonatus* from Samples 121-757B-15H-5, 70-75cm to 121-757B-22X-3, 70-75cm (136.5-196.10 mbsf) , and with that of *Subbotina* spp. from Samples 121-757B-15H-5, 70-75cm to 121-757B-24X-4, 48-61cm (136.5-216.78 mbsf).

Oridorsalis umbonatus

Isotopes were analyzed for Samples 121-757B-1H-2, 70-75cm to 121-757B-22X-3, 70-75cm (2.03-196.1 mbsf) from the lower Eocene to Pleistocene. Insufficient isotopic data were obtained below the middle Eocene, because *Oridorsalis umbonatus* are rare. The isotopic records of *Oridorsalis umbonatus* are shown in Fig 20.

Oxygen isotopes: $\delta^{18}O$ values increase gradually through the Eocene, and up to 120.80 mbsf within the nannofossil Zones CP16a-b in the lowermost Oligocene. In this section, they increase up to 1.6‰. Furthermore, $\delta^{18}O$ values show a remarkable positive shift of 0.6‰ (from 1.104 to 1.710) between 120.80 and 117.20 mbsf across the Zone CP16b/c boundary. From the early Oligocene to early Miocene, $\delta^{18}O$ values decrease with small fluctuations. In this section, weak peaks are observed at 107.50 and 94.90 mbsf. In the early middle Miocene, in Zones CN3-4, $\delta^{18}O$ values decrease to the minimum value of 1.217‰ at 88.29 mbsf throughout the Neogene . From 88.20 to 68.90 mbsf, $\delta^{18}O$ values rapidly increase by ~1.6‰ from 1.217 to 2.825‰ in the middle Miocene. From the late Miocene to early Pliocene, $\delta^{18}O$ values are constant at around 2.6‰, despite a relatively large fluctuation (~0.6‰ amplitude). In this section, the peak $\delta^{18}O$ value of 2.793‰ is observed at 49.50 mbsf within Zone CN9b. In the late Pliocene and Pleistocene, $\delta^{18}O$ values increase up to ~3.3‰ near to the present. In this section, two small positive shifts are recognized; a shift of 0.30‰ between 24.30 and 20.70 mbsf across the Zone CN11b/12a boundary, and a shift of 0.45‰ between 11.20 and 14.70 mbsf across the CN12/13 boundary.

Carbon isotopes: The carbon isotopic record in the Eocene shows a trend of slight decrease up to 0.436‰ at 140.20 mbsf, then an increase up to a peak value at 126.80 mbsf (0.991‰) just below the Eocene / Oligocene boundary. The magnitude of this increase is about 0.6‰. From 126.80 to 112.20 mbsf in the lower Oligocene, $\delta^{13}C$ values decrease by ~0.8‰. From the late early Oligocene to early Miocene, $\delta^{13}C$ values are rather stable at 0.25‰. Above the early / middle Miocene boundary, a small positive shift of 0.35‰ is recognized between 91.90 and 88.20 mbsf, and then $\delta^{13}C$ values decrease to a maximum value of 0.56‰ throughout the Neogene. During the middle Miocene, $\delta^{13}C$ values gradually decrease by 0.4‰. Within Zones CN9a-8 in the late Miocene, $\delta^{13}C$ values increase up to slight peak at 68.90 mbsf (0.375‰), then immediately decrease to a lower value at 65.90 mbsf (-0.094‰), and again increase up to 62.90 mbsf. The notable decrease of $\delta^{13}C$ value from 62.90 to 46.50 mbsf in the uppermost Miocene reaches ~1.1‰, from 0.233 to -0.892‰. This decrease is correlated with the Chron-6 Carbon Shift in the latest Miocene (Vincent et al., 1980; 1985). During the Pliocene and Pleistocene, $\delta^{13}C$ values are constant at ~-0.7‰. However, lower values are observed at 20.70 mbsf (-1.005‰) and 5.20 mbsf (-1.310‰).

Anomalinoides danicus

Isotope analyses were performed on material from Samples 121-757B-15H-5, 70-75cm to 121-757B-24X-4, 58-61cm (136.50-216.78 mbsf) in lower and middle Eocene. The isotopic records of *A. danicus* are shown in Fig. 21.

Oxygen isotopes: The oxygen isotopic record displays a gradual increase up to 0.420‰ at 159.50 mbsf (nannofossil Zone CP13b). The magnitude of this increase reaches 1.74‰. In Zones CP13c and 14 in the upper middle Eocene, $\delta^{18}O$ values are constant at ~0.4‰.

Carbon isotopes: $\delta^{13}C$ values notably increase by about 1.0‰ from 0.302‰ (212.28 mbsf) to 1.340‰ (183.90 mbsf) through Zones CP10 and 11 in the lower Eocene. In the middle Eocene, $\delta^{13}C$ values exhibit a decrease of 0.4‰ up to 169.20 mbsf (0.934‰) within Zone CP13a, an increase of 0.3‰ up to a peak value at 146.20 mbsf (Zones CP14), and a decrease of 0.35‰.

Subbotina spp.

Isotope analyses were performed on five small sized tests. The oxygen and carbon isotopic values were obtained from Samples 121-757B-14H-1, 70-75cm to 121-757B-24X-4, 58-61cm (120.80-216.78 mbsf) in middle and lower Eocene. The isotopic records of *Subbotina* spp. are shown in Fig. 22.

Oxygen isotopes: $\delta^{18}O$ values increase gradually throughout the Eocene, except for a lower value at 193.10 mbsf (within nannofossil Zone CP11). The magnitude of this increase reaches 2.35‰ (from -1.323 to 1.012‰).

Carbon isotopes: $\delta^{13}C$ values increase about 0.9‰ from 212.28 to 202.70 mbsf across the Zone 10/11 boundary in the

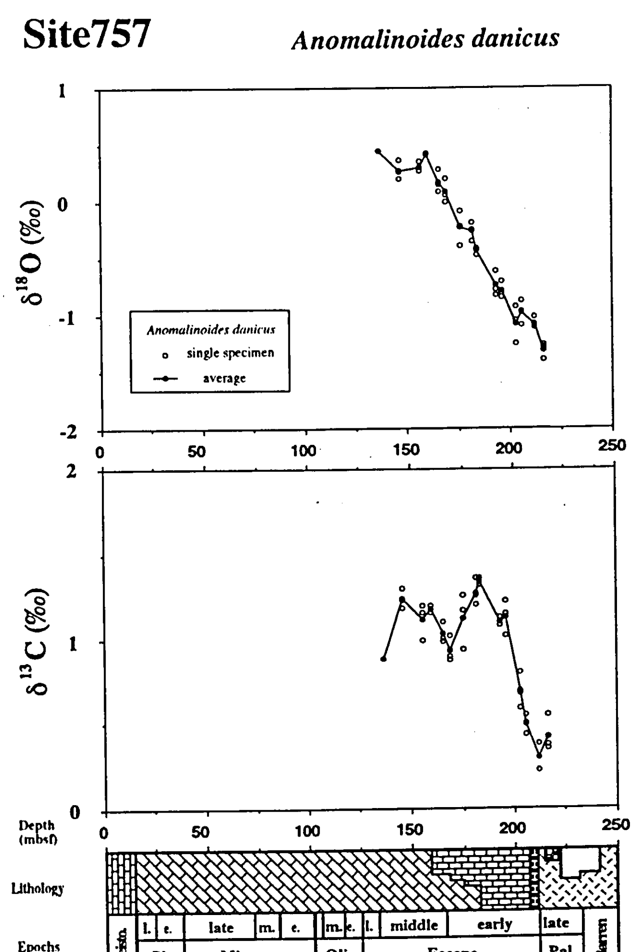

Fig. 21. Oxygen and carbon isotope records of benthic foraminifer *Anomalinoides danicus* at Site 757.

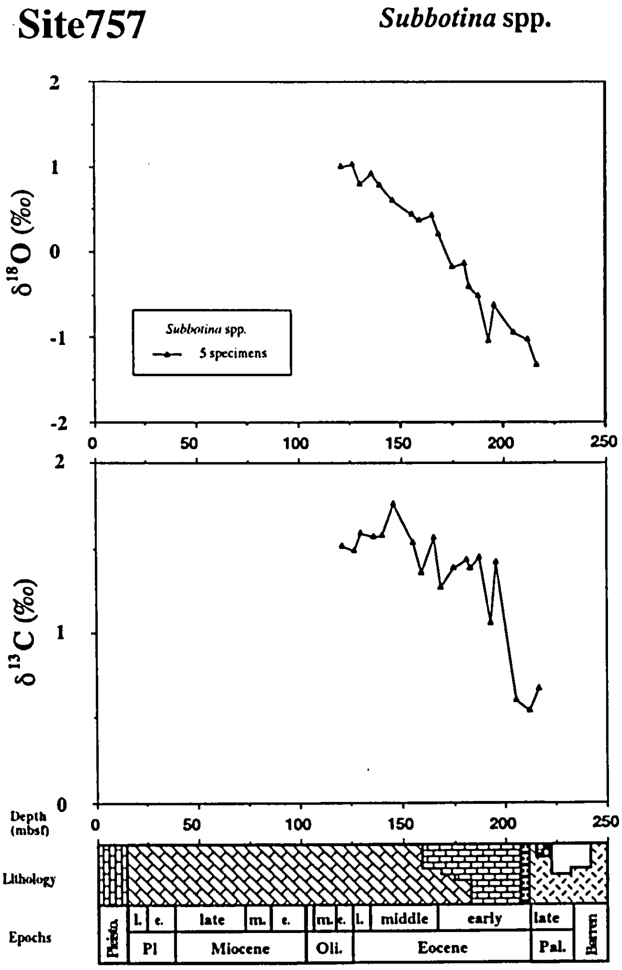

Fig. 22. Oxygen and carbon isotope records of planktonic foraminifer *Subbotina* spp. at Site 757.

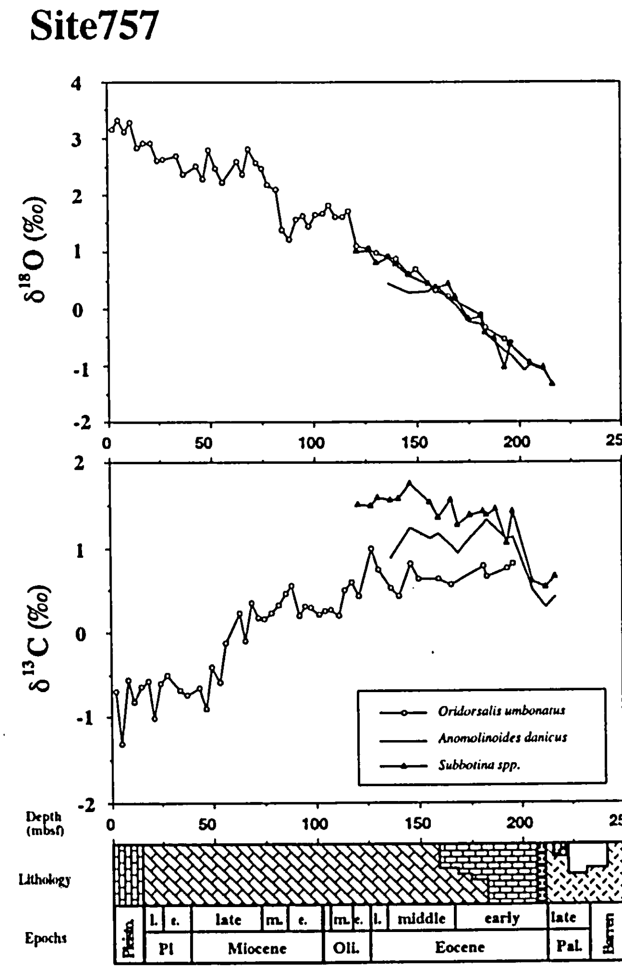

Fig. 23. Summary of oxygen and carbon isotope records at Site 757.

lower Eocene, and are constant (~1.4‰) up to 155.80 mbsf in Zone CP13b of the middle Eocene. The carbon isotopic record shows an increase up to a peak at 146.20 mbsf within Zone CP14 in the upper middle Eocene, and a gradual decrease up to 120.80 mbsf within Zones CP16a-b of the earliest Oligocene.

Isotopic values obtained from Site 757 are summarized in Fig. 23.

5. Site 758

At Site 758, oxygen and carbon isotopes were analyzed for seven benthic foraminiferal taxa, *Oridorsalis umbonatus, Anomalinoides danicus, Nuttallides truempyi, Stensioina beccariiformis, Cibicidoides wuellerstorfi, Cibicidoides mundulus*, and *Groidinoides soldanii*, and for seven planktonic foraminiferal taxa, *Acarinina primitiva, A. praecursoria, Morozovella velascoensis, Subbotina pseudoeocaena, S. eocaena, S.* sp.1, and *S.* spp. At this site, an unconformity has been recognized at ~250 mbsf, which lacks almost all of Eocene sequence (Peirce, Weissel, et al., 1989).

Oridorsalis umbonatus

Isotope analyses were performed for material from Samples 121-758A-1H-1, 75-80cm to 121-758A-27X-1, 75-80cm (0.75-248.05 mbsf) from the uppermost Eocene to Pleistocene. The isotopic records of *O. umbonatus* are shown in Fig. 24.

Oxygen isotopes: The oxygen isotopic records are constant at ~1.8‰, with a fluctuation from 248.05 to 135.15 mbsf through the uppermost Eocene to lower Miocene. In this interval, the amplitude of the fluctuation is ~0.4‰, and a significant negative peak (1.265‰) is observed at 190.05 mbsf above the Oligocene / Miocene boundary. $\delta^{18}O$ values at 135.15 and 122.45 mbsf just above the early / middle Miocene boundary are relatively low (1.669 and 1.660‰, respectively). In the middle and early late Miocene, the oxygen isotopic records display a remarkable positive shift of 1.3‰ up to a weak peak at 112.85 mbsf (2.911‰). From 112.85 to 35.55 mbsf, $\delta^{18}O$ values are constant at ~2.8‰ with smaller fluctuations (amplitude of ~0.3‰). In this section, two minor peaks are observed at 78.65 mbsf (nannofossil Zone CN9b) and 64.45 mbsf (Zones CN10-

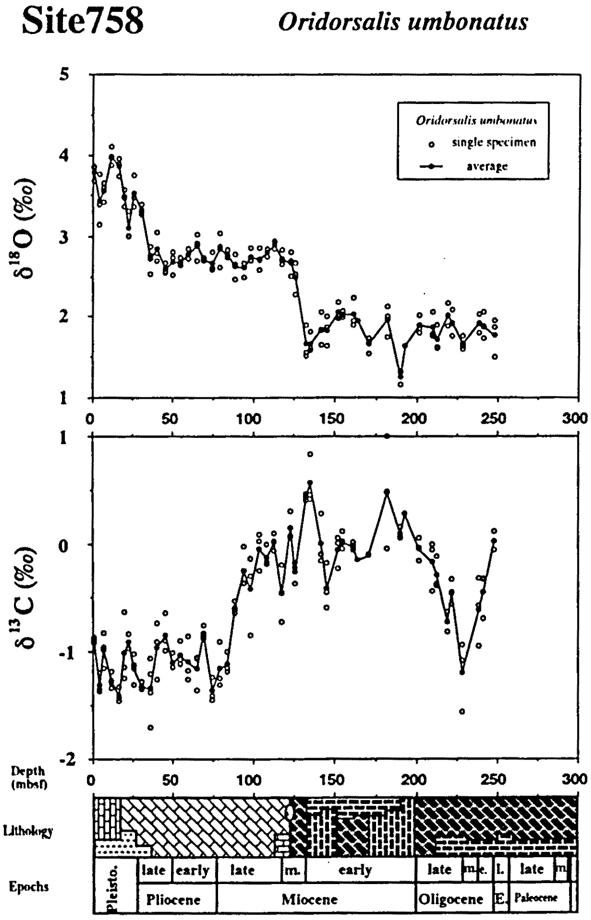

Fig. 24. Oxygen and carbon isotope records of benthic foraminifer *Oridorsalis umbonatus* at Site 758.

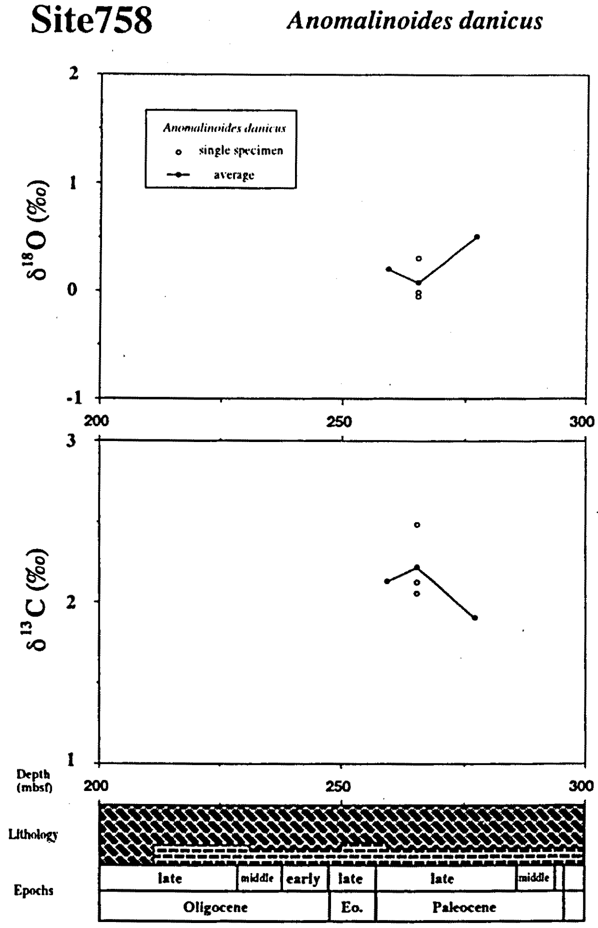

Fig. 25. Oxygen and carbon isotope records of benthic foraminifer *Anomalinoides danicus* at Site 758.

11a), with values of 2.850 and 2.845‰, respectively. Just across the Zone CN12 c/d boundary, a positive shift of 0.6‰ (from 2.731 to 3.322‰) in $\delta^{18}O$ value is recognized in the interval between 35.55 and 30.45 mbsf. From 30.45 to 0.75 mbsf, $\delta^{18}O$ values show increase with relatively large fluctuations. The amplitude of these fluctuations reaches ~0.6‰. An $\delta^{18}O$ peak value is observed at 11.25 mbsf just below the Zone CN14b/a boundary.

Carbon isotopes: $\delta^{13}C$ values decrease by 1.2‰ up to -1.196‰ at 228.76 mbsf (within Zone CP18), and immediately increase up to a peak value at 181.95 mbsf (0.480‰). The magnitude of this increase reaches 1.7‰. From 181.95 to 144.75 mbsf in the lower Miocene, $\delta^{13}C$ values decrease. In this section, a minor peak is observed at 154.45 mbsf (0.030‰). Across the early / middle Miocene boundary, a remarkable positive shift of ~1.0‰ occurred between 144.75 (-0.409‰) and 135.15 mbsf (0.569‰), and then $\delta^{13}C$ values are the highest among Neogene samples. In the middle Miocene, $\delta^{13}C$ values rapidly decrease by 0.9‰ from 0.569 to -0.255‰, and increase by 0.4‰ up to a peak at 122.45 mbsf (0.151‰). From 117.35 to 93.55 mbsf in the lower upper Miocene, the carbon isotopic ratios are constant (with fluctuation) at ~-0.2‰. The amplitude of fluctuation reaches to 0.5‰. A distinct negative shift of 1.15‰ is recognized from 93.55 (-0.247‰) to 74.15 (-1.362‰) mbsf in the uppermost Miocene. This shift is correlated with the Chron-6 Carbon Shift of the latest Miocene (Vincent et al., 1980; 1985). Throughout the Pliocene and Pleistocene, $\delta^{13}C$ values (about -1.1‰) fluctuate by 0.5‰. In this section, four minor peaks are observed at 68.95 mbsf within Zones 10-11a, 45.15 mbsf (within Zones 12a-c), 25.35 mbsf (within 13), and 6.75 mbsf (within Zones 14b-15), with values of -0.828, -0.844, -0.905, and -0.981‰, respectively.

Anomalinoides danicus

Isotopes were analyzed for three samples from Samples 121-758A-28X-2, 75-80cm to 121-758A-30X-1, 75-80cm (265.15-277.05 mbsf) in the upper Paleocene, because of the rare occurrence of *A. danicus*. The isotopic records of *A. danicus* are shown in Fig. 25.

Oxygen and Carbon isotopes: $\delta^{18}O$ values tend to decrease, whereas $\delta^{13}C$ values tend to increase. The minimum $\delta^{18}O$ value and the maximum $\delta^{13}C$ value are 0.085 and 2.220‰, respectively.

Nuttallides truempyi

Isotope analyses were performed for two to five individuals and single specimen in each sample. The difference in values between the measured individuals is relatively small. No significant difference in the two measuring methods is recognized, except for Sample 121-758A-28X-6, 75-80 cm. At this site, the isotopic records were obtained from Samples 121-758A-28X-2, 75-80 cm to 121-758A-31X-5, 75-80 cm (259.15-292.65 mbsf) in the Paleocene. The isotopic records of *N. truempyi* are shown in Fig. 26.

Oxygen isotopes: *Nuttallides truempyi* $\delta^{18}O$ values increase up to a peak of 277.05 mbsf, and decrease with a small fluctuations.

Carbon isotopes: The carbon isotopic record shows an increase from 0.77 to 1.82‰. The magnitude of the increase is 1.1‰ in the studied section.

Stensioina beccariiformis

Isotopes were analyzed for Samples 121-758A-28X-2, 75-80cm to 121-758A-31X-5, 75-80cm (259.15-292.65 mbsf) in the Paleocene. The isotopic records of *S. beccariiformis* are shown in Fig. 27.

Oxygen isotopes: $\delta^{18}O$ values increase up to a peak at 277.05 mbsf (0.526‰) within the nannofossil Zones CP6-7 of the upper Paleocene, and decrease from 277.05 mbsf (0.526 ‰) to 265.15 mbsf (-0.140‰).

Carbon isotopes: $\delta^{13}C$ values increase up to a maximum value at 267.35 mbsf (2.071‰) within Zones CP6-7 in the upper Paleocene. The magnitude of this increase reaches 1.2‰.

Other Benthic foraminifers

Isotope analyses were performed for specimens from Samples 121-758A-9H-4, 75-80cm to 121-758A-27X-1, 75-80cm (78.65-248.05 mbsf) for *Groidinoides soldanii*, from Samples 121-758A-10H-1, 75-80cm to 121-758A-27X-1, 75-80cm (81.85-248.05 mbsf) for *Cibicidoides mundulus*, and from Samples 121-758A-12X-1, 75-80cm to 121-758A-14X-3, 75-80cm (103.15-125.45 mbsf) for *Cibicidoides wuellerstorfi* in the Miocene and Oligocene. The isotopic records of those species are shown in Fig. 28.

Oxygen isotopes: The trend of isotopic records of those species resembles those of *Oridorsalis umbonatus*. $\delta^{18}O$ values show a general increase. The $\delta^{13}C$ values for *Groidinoides soldanii* decrease by 0.75‰ from 248.05 to 228.76 mbsf in the lower Eocene, and are constant at ~0.4‰ up to 122.45 mbsf in the middle Miocene. During the late

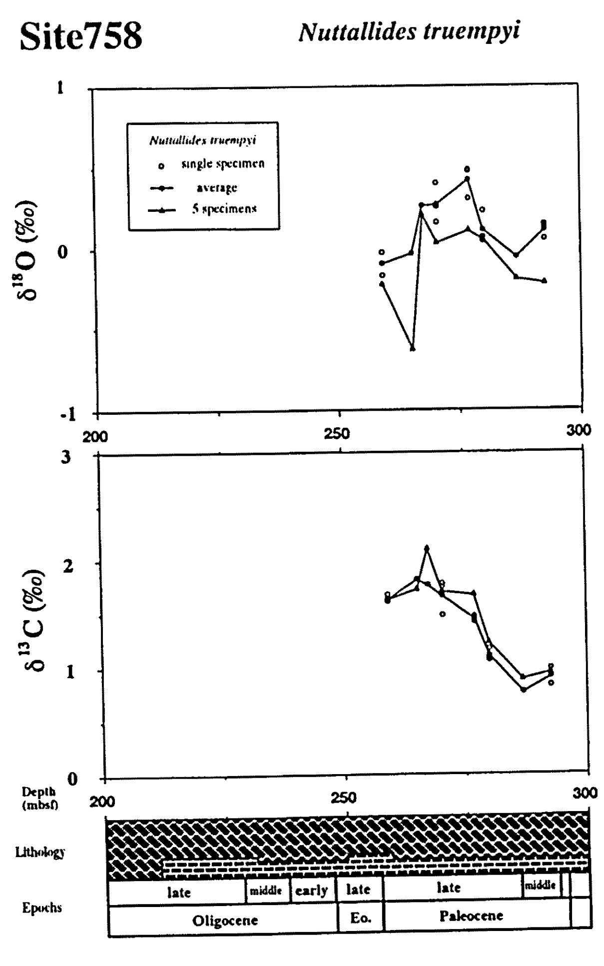

Fig. 26. Oxygen and carbon isotope records of benthic foraminifer *Nuttallides truempyi* at Site 758.

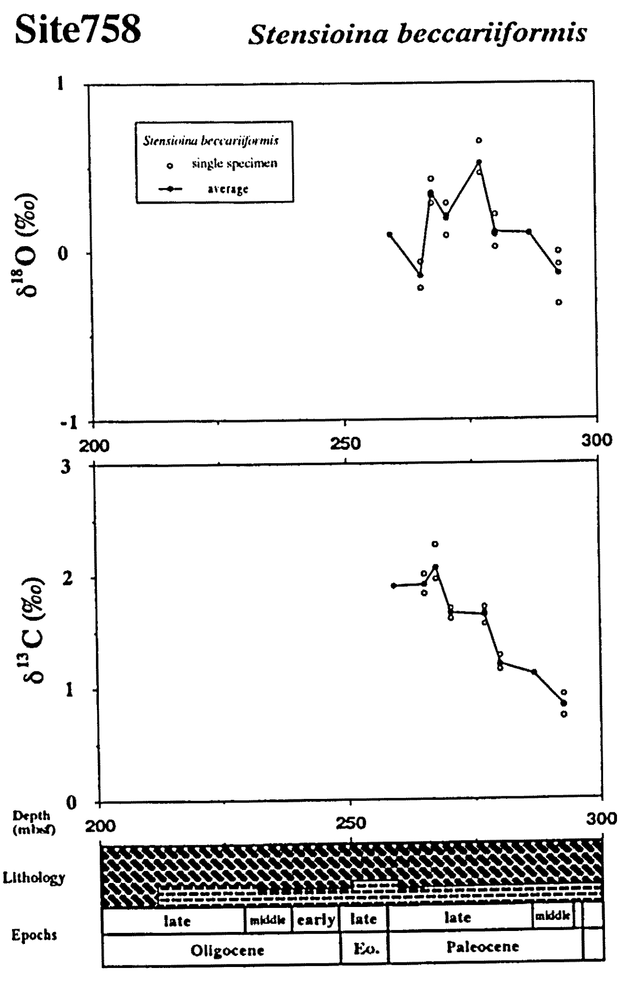

Fig. 27. Oxygen and carbon isotope records of benthic foraminifer *Stensioina beccariiformis* at Site 758.

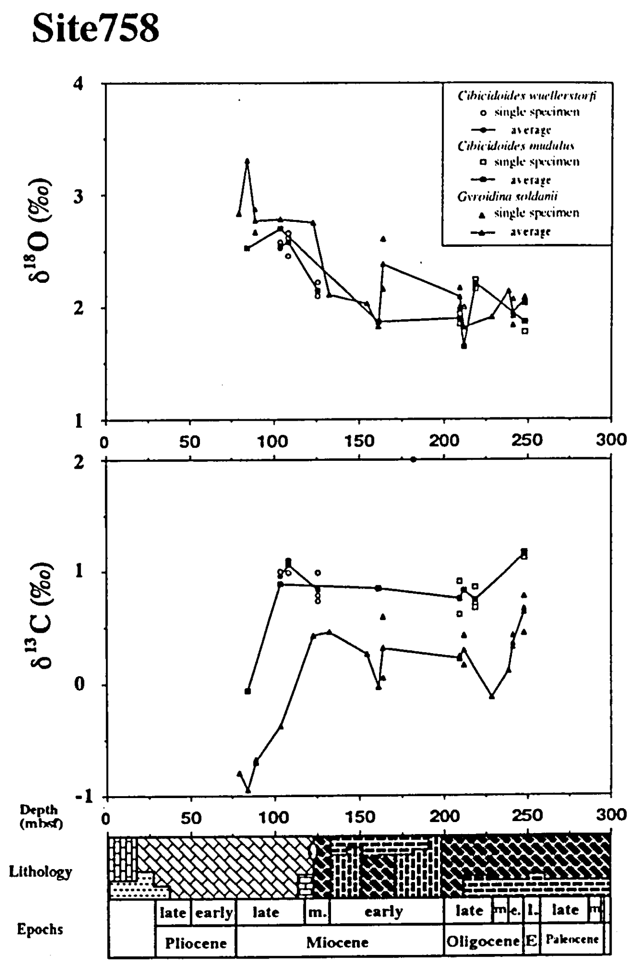

Fig. 28. Oxygen and carbon isotope records of other benthic foraminifers at Site 758.

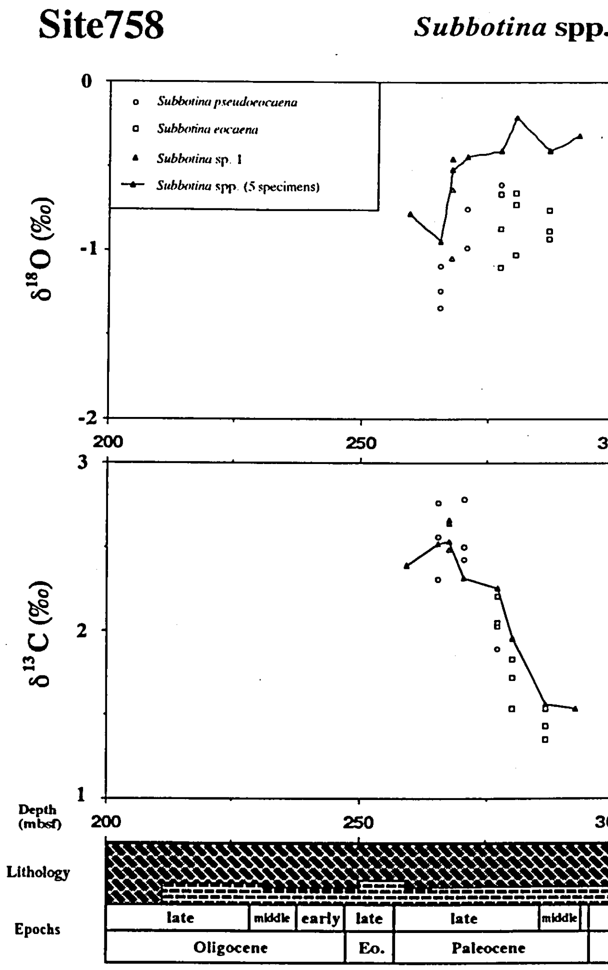

Fig. 29. Oxygen and carbon isotope records of planktonic foraminifer *Subbotina* group at Site 758.

Miocene, the *Groidinoides soldanii* $\delta^{13}C$ values decrease. The $\delta^{13}C$ values of *Cibicidoides mundulus* are constant (~0.8‰) up to 103.15 mbsf within Zones CN8-9a in the upper Miocene, and exhibit a decreasing trend. The distribution of $\delta^{13}C$ in *Cibicidoides wuellerstorfi* resembles that of *Cibicidoides mundulus*.

Subbotina group

At Site 758, isotopes of the *Subbotina* group were analyzed for four taxa. Isotope analyses of *Subbotina* spp. were performed for five individuals (253-367μm in diameter). The isotope analyses of other taxa were made on a single individual (>380μm in diameter). The isotopic records of *Subbotina* group were obtained from Samples 121-758A-28X-2, 75-80cm to 121-758A-31X-5, 75-80cm (259.15-292.65 mbsf) in the Paleocene. The isotopic records of *Subbotina* group are shown in Fig. 29.

The oxygen isotopic record of *Subbotina* spp. shows a general decrease from 280.05 mbsf to 265.15 mbsf in the late Paleocene. $\delta^{18}O$ values at 280.05 mbsf are relatively high, and are the maximum values among the Paleocene samples. Between 367.35 and 265.15 mbsf, $\delta^{18}O$ values show a negative shift of 0.4‰. The same trend of $\delta^{18}O$ values are recognized, but the identified taxa such as *Subbotina* spp. show an offset of *Subbotina* spp. toward low values by 0.3-0.5‰.

Carbon isotopes: $\delta^{13}C$ values of *Subbotina* spp. show an increase with stratigraphic height up to 267.35 mbsf (within Zones CP6-7), then decrease. The magnitude of this increase reaches 1.0‰, and the peak of this increase exhibits the maximum value (2.529‰) among the Paleocene samples. The carbon isotopic signals of other *Subbotina* show the same trend as *Subbotina* spp.

Other Planktonic foraminifers

The isotopes of *Morozovella velascoensis* were analyzed for Samples 121-758A-28X-2, 75-80cm to 121-758A-31X-1, 75-80cm (259.15-286.65 mbsf) from the upper Paleocene. *Acarinina primitiva* and *A. praecursoria* were used in Sample 121-758A-28X-2, 75-80cm (259.15) in the upper Paleocene and Sample 121-758A-31X-5, 75-80cm (292.65 mbsf) from the lower Paleocene, respectively. The isotopic records of those species are shown in Fig. 30.

Oxygen and Carbon isotopes: The oxygen isotopic records of *M. velascoensis* show a constant trend (about -1.5‰). In this section, $\delta^{18}O$ values at 265.15 mbsf are relatively low.

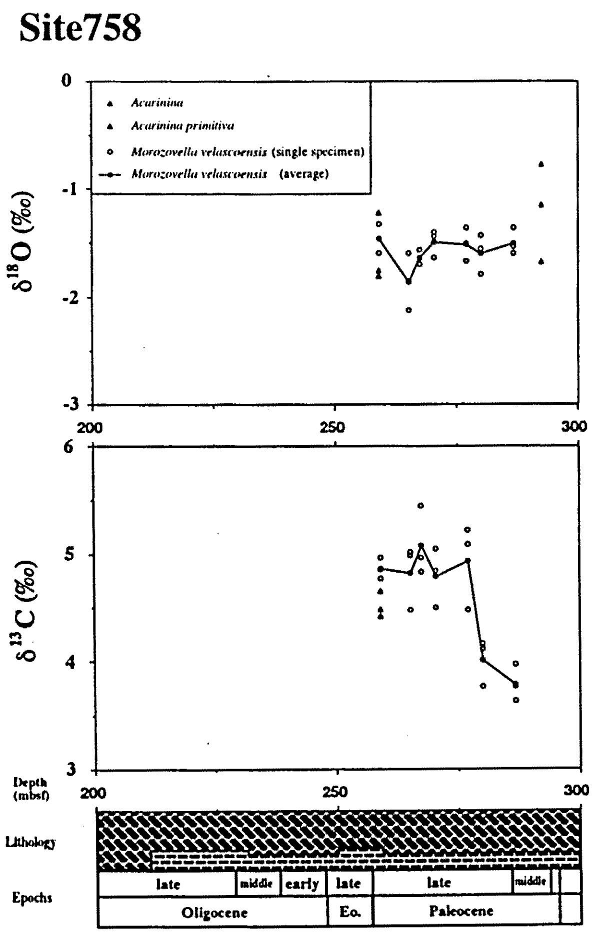

Fig. 30. Oxygen and carbon isotope records of other planktonic foraminifers at Site 758.

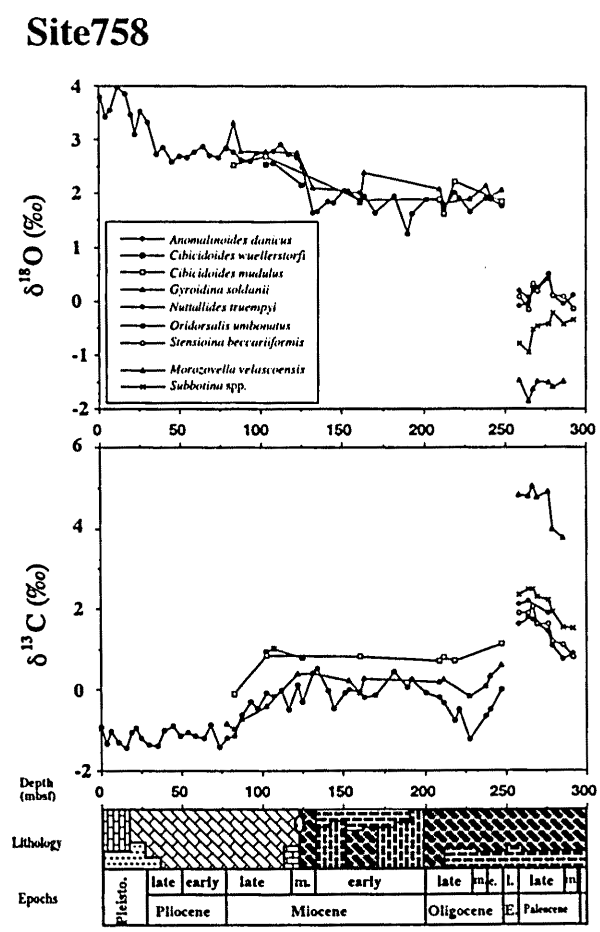

Fig. 31. Summary of oxygen and carbon isotope records at Site 758.

$\delta^{13}C$ values of *M. velascoensis* rapidly increase by ~1.0‰ up to 277.05 mbsf, and then are constant at ~4.8‰. A minor peak is observed at 267.35 mbsf (5.084), with the maximum value for the Paleocene. $\delta^{18}O$ of *Acarinina primitiva* values are close to those of *M. velascoensis*, whereas their $\delta^{18}O$ values are slightly lower than *M. velascoensis*. The isotopic ratios of *A. praecursoria* are similar to those of *Subbotina* group rather than *M. velascoensis*.

Isotopic values obtained from Site 758 are summarized in Fig. 31.

6. Site 762

At Site 762, oxygen and carbon isotopes were analyzed for four benthic foraminiferal taxa: *Anomalinoides danicus, Nuttallides truempyi, Oridorsalis umbonatus,* and *Stensioina beccariiformis*. At this site, isotope analyses were limited to the lower Eocene and upper Paleocene (370-490 mbsf). The analysis of *O. umbonatus* was only available in Sample 122-762A-24X-2, 77-82cm (379.77 mbsf) from the earliest Eocene, and values -0.628‰ for oxygen isotopes and -0.547‰ for carbon isotopes.

Anomalinoides danicus

Isotopes were determined for Samples 122-762C-26X-1, 70-73cm to 122-762C-32X-1, 65-69cm (398.70-450.65 mbsf). The occurrence of *A. danicus* is rare in all samples. The isotopic records of *A. danicus* are shown in Fig. 32.

Oxygen isotopes: $\delta^{18}O$ values tend to increase up to 434.69 mbsf, and reaching a maximum value (0.325‰). $\delta^{18}O$ values decrease by ~1.0‰ from 434.69 to 398.16 mbsf.

Carbon isotopes: The carbon isotopic records show an increase up to 425.19 mbsf, with small fluctuations, and the maximum value of $\delta^{13}C$ is 2.623‰. $\delta^{13}C$ values drastically decrease from 425.19-404.70 mbsf across the Paleocene / Eocene boundary. The magnitude of this decrease reaches ~2.2‰. Above 404.70 mbsf, $\delta^{13}C$ values are constant at ~0.4‰. However, a weak negative peak is observed at 400.21 mbsf (0.120‰).

Nuttallides truempyi

Isotope analyses were performed for two to five individuals and single specimen in each sample. No significant differences were recognized for the different analyses. At this site, isotopic records were obtained from

Samples 122-762C-23X-1, 69-74cm to 122-762A-35X-1, 68-73cm (370.19-497.18 mbsf). The isotopic records of *N. truempyi* are shown in Fig. 33.

Oxygen isotopes: The records of *N. truempyi* $\delta^{18}O$ show an increase, with small fluctuations up to 450.65 mbsf in the upper Paleocene. $\delta^{18}O$ values decrease by 0.9‰ (-0.138 to -1.055‰) up to 379.77 mbsf across the Paleocene / Eocene boundary. Above this, oxygen isotopic records exhibit an increasing trend.

Carbon isotopes: Carbon isotope record increase, with fluctuations up to 431.69 mbsf. The magnitude of increase is 1.0‰. In this section, A ^{13}C maximum is recognized at 447.18 mbsf (1.748‰). $\delta^{13}C$ values drastically decrease by 1.9‰ from 1.812‰ (431.69 mbsf) to -0.088‰ (406.18 mbsf) across the benthic event. From 406.18 to 379.77 mbsf, $\delta^{13}C$ records are a constant with small fluctuations at ~0.1‰. A ^{13}C minimum is observed at 400.21 mbsf (-0.487‰). The carbon isotopic records tend to increase above this level.

Stensioina beccariiformis

Isotope analyses were performed for Samples 122-762C-29X-1, 76-80cm to 122-762C-35X-1, 68-73cm (422.26-479.18 mbsf) in the upper Eocene. *S. beccariiformis* does not occur above Sample 122-762C-29X-1, 76-80cm (422.26 mbsf) below the Paleocene / Eocene boundary. The isotopic records of *S. beccariiformis* are shown in Fig. 34.

Oxygen isotopes: The oxygen isotopic record of *S. beccariiformis* shows an increasing trend, with fluctuations, up to a maximum value (0.165‰) at 434.69 mbsf, with an increasing trend of 0.65‰. In this section, a notable peak is observed at 469. 61 mbsf. From a maximum value at 434.69 mbsf, $\delta^{18}O$ values decrease to -0.525‰ at 422.26 mbsf.

Carbon isotopes: In the late Paleocene, averaged $\delta^{13}C$ values increase by ~1.1‰ with relatively large fluctuations up to a maximum value (1.946‰) at 423.69 mbsf. In this section, two remarkable peaks are recognized at 469.61 and 447.18 mbsf. $\delta^{13}C$ values rapidly decrease by 0.6‰ up to 422.26 mbsf, located just below the level of the benthic event, where *S. beccariiformis* disappears.

Isotopic values obtained from Site 762 are summarized in Fig. 35.

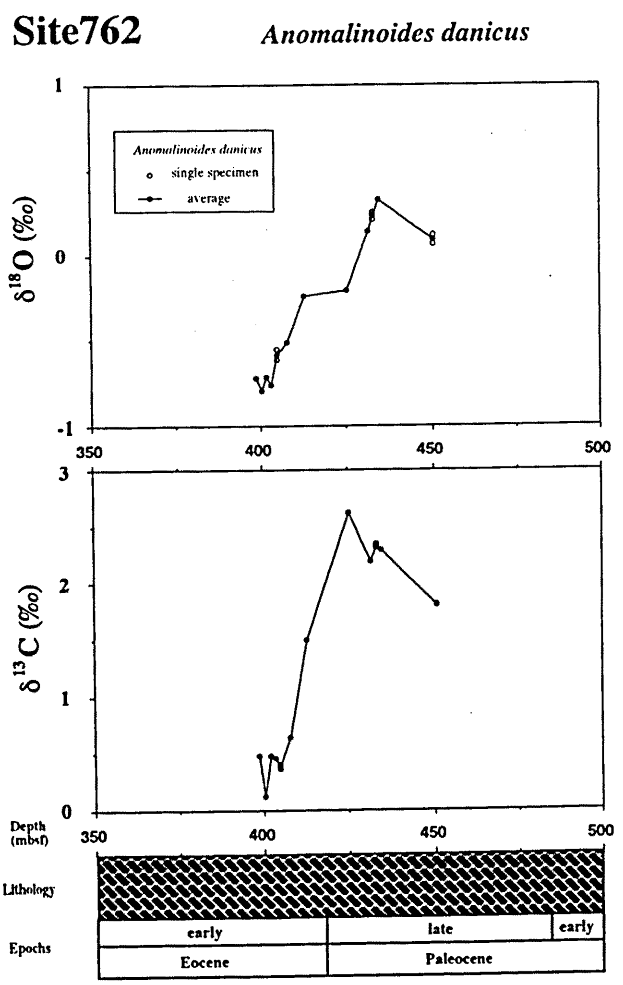

Fig. 32. Oxygen and carbon isotope records of benthic foraminifer *Anomalinoides danicus* at Site 762.

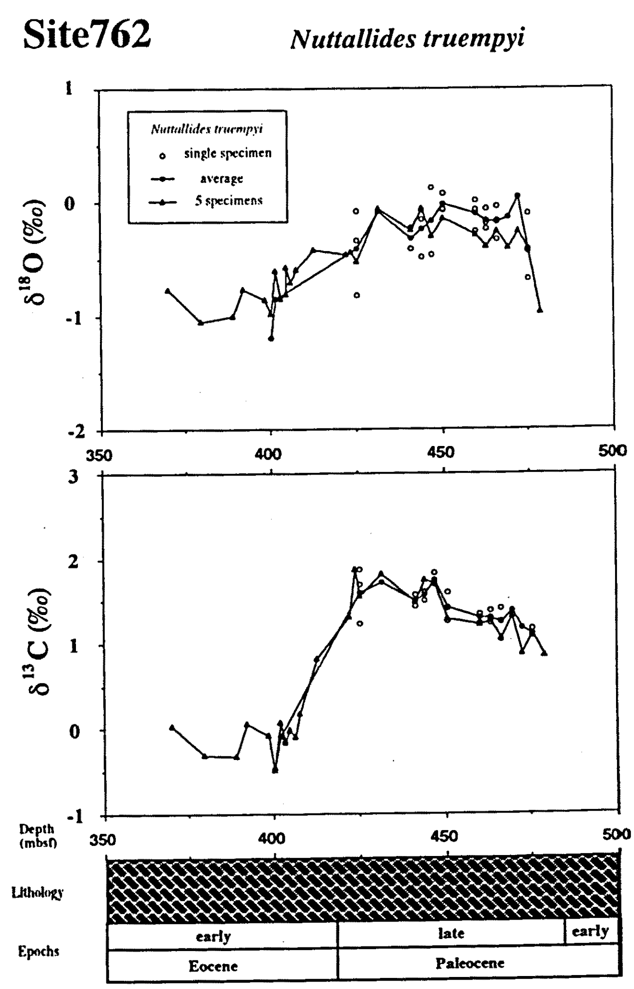

Fig. 33. Oxygen and carbon isotope records of benthic foraminifer *Nuttallides truempyi* at Site 762.

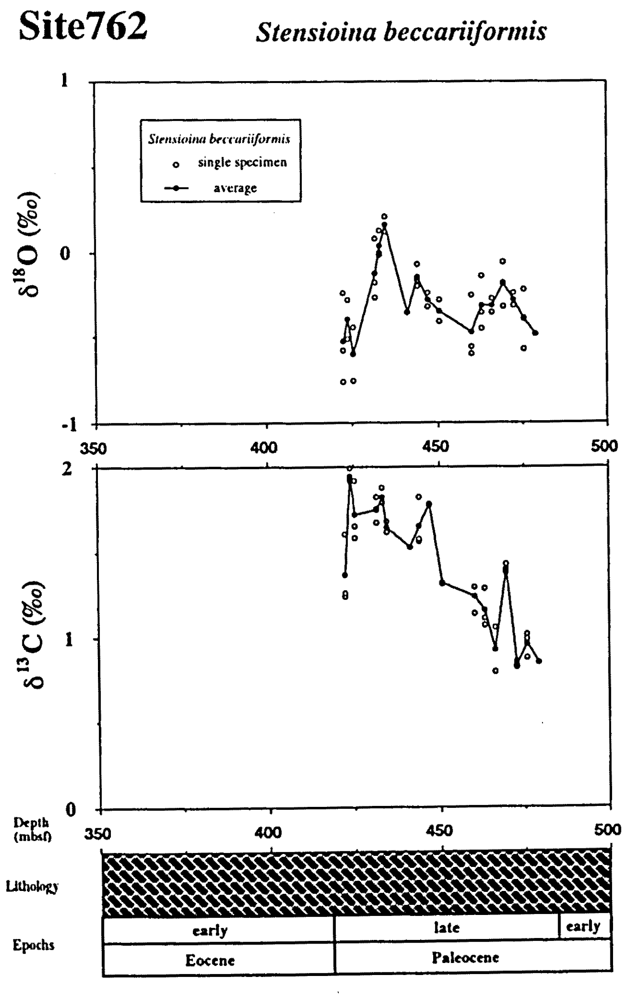

Fig. 34. Oxygen and carbon isotope records of benthic foraminifer *Stensioina beccariiformis* at Site 762.

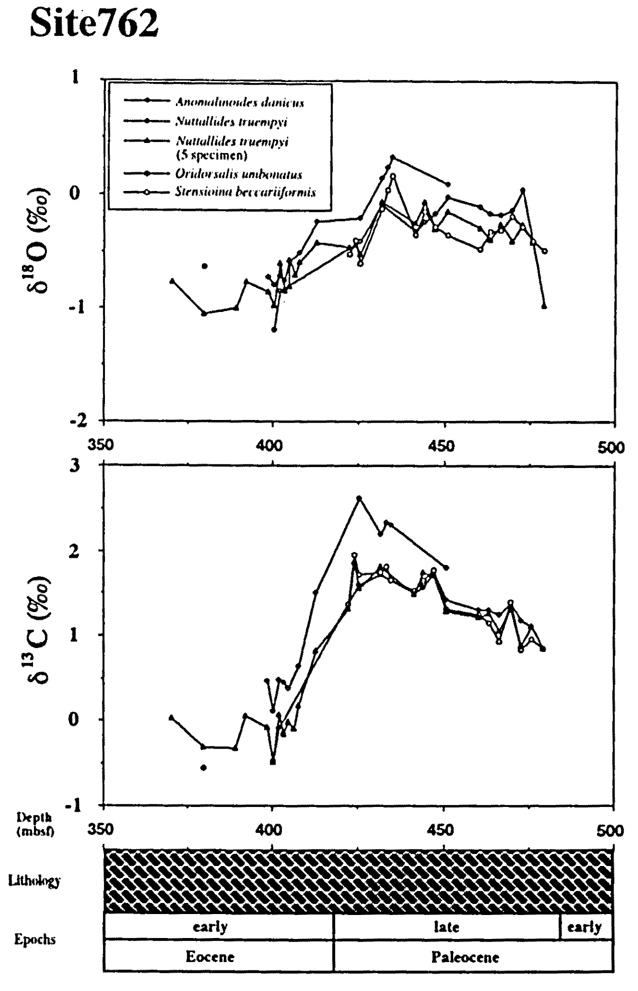

Fig. 35. Summary of oxygen and carbon isotope records at Site 762.

III. Stable isotopic paleoceanography in the South Atlantic and Indian Oceans

A. Compiled data

In and around the Indian and South Atlantic Oceans, oxygen and carbon isotopic data of Cenozoic foraminifera have been obtained at many DSDP and ODP sites. Information from these sites, including this study, is shown in Table 1. The Indian and South Atlantic Oceans are divided into six areas: the northeastern Indian Ocean (Sites 214, 215, 216, 253, 752, 754, 756, 757, 758, and 762), northwestern Indian Ocean (Sites 237, 238, 709, 714, and 716), southern Indian Ocean (Sites 538, 744, 748, 750, and 751), Central Atlantic Ocean (Sites 366, 658, 659, 665, and 667), South Atlantic Ocean (Sites 516, 517, 518, 519, 521, 522, 523, 525, 526, 527, 528, and 529), and Southern Ocean of the Atlantic (Sites 658, 689,690, 699, 700, 702, and 704). The oxygen and carbon isotopic data of these areas are compiled in order to compare the Cenozoic paleoceanography of the Indian and South Atlantic Oceans. However, there are limited resources to compile part of the section, such as the Paleogene section of the northwestern Indian Ocean, Neogene of the Southern Ocean (Atlantic sector), and deep sea sections below 3000 m.

1. Adjustment of data

Although oxygen and carbon isotopes have been measured from foraminiferal tests at many sites, these comprise different foraminiferal species. In the studied area, the benthic foraminifer *Oridorsalis umbonatus* has been commonly measured, and *Nuttallides truempyi, Cibicidoides* spp., *Cibicidoides wuellerstorfi* have also been measured. For the purpose of this study, the isotopic values of sea water should be indicated by the values of different species. However, benthic species may draw in pore water and overlying water as carbon dioxide pools (Shackleton *et al.*, 1984; Woodruff *et al.*, 1990; Zachos *et al.*, 1992a; 1992c; and other), and thus different species record different values according to their paleoecology. Therefore, the oxygen and carbon isotopic data cannot be directly compared, because of interspecific variation in the isotopic values. Most workers use the adjusted values obtained by Shackleton *et al.* (1984). Barrera and Huber (1990; 1991), however, pointed out that the magnitudes of departure in the Maastrichtian and Paleogene differ from those of Shackleton *et al.* (1984). Interspecific difference vary according to region and age. Therefore, adjustment should be made at each site based on

Table 1. Sources for foraminiferal oxygen and carbon isotopic data in the studied area.

Site	Latitude	Longitude	Geographical area	Water depth (m)	Species	Range		Reference
						mbsf	Age (Ma)	
Site 214	11°20.21' S	88°43.08' E	Indian Ocean	1655	*Globigerinoides sacculifer*	86.34-200.48	5~18	Vincent et al., 1985
					Dentoglobigerina altispira	123.92-200.48	7~18	Vincent et al., 1985
					Globoquadrina venezuelana	86.34-217.95	5~23	Vincent et al., 1985
					Oridorsalis umbonatus	86.34-224.33	5~24	Vincent et al., 1985
Site 216	1°27.73' N	90°12.48' E	Indian Ocean	2247	*Globigerinoides sacculifer*	109.32-188.10	8~23	Vincent et al., 1985
					Dentoglobigerina altispira	109.32-174.39	8~21	Vincent et al., 1985
					Globoquadrina venezuelana	109.32-199.78	8~23	Vincent et al., 1985
					Oridorsalis umbonatus	109.32-199.78	8~23	Vincent et al., 1985
Site 237	7°04.99' S	58°07.48' E	Indian Ocean	1640	*Globigerinoides sacculifer*	109.82-175.42	8~20	Vincent et al., 1985
					Dentoglobigerina altispira	83.32-184.24	5~23	Vincent et al., 1985
					Globoquadrina venezuelana	83.32-200.32	5~24	Vincent et al., 1985
					Oridorsalis umbonatus	83.32-200.32	5~24	Vincent et al., 1985
Site 238	11°09.20' S	70°31.56' E	Indian Ocean	2844	*Globigerinoides sacculifer*	132.66-439.03	5~24	Vincent et al., 1985
					Dentoglobigerina altispira	132.66-398.86	5~24	Vincent et al., 1985
					Globoquadrina venezuelana	132.66-455.83	5~24	Vincent et al., 1985
					Oridorsalis umbonatus	132.66-455.83	5~24	Vincent et al., 1985
Site 253	24°52.65' S	87°21.97' E	Indian Ocean	1962	various species (Planktonic)	19.31-132.48	4~37	Oberhansli, 1986
					various species (Benthic)	19.31-132.48	4~37	Oberhansli, 1986
Site 366	5°40.7' N	19°51.1' W	Eastern Tropical Atlantic	2853	*Cibicides* spp.	114.68-433.46	8~38	Miller et al., 1989
Site 516	30°16.6' S	35°37.1' W	western South Atlantic	1313	*Globigerinoides sacculifer*	8.80-37.50	2~4	Leonard et al., 1983
					Cibicidoides wuellerstorfi	8.90-37.50	2~4	Leonard et al., 1983
Site 517	30°56.8' S	38°02.5' W	western South Atlantic	2963	*Globigerinoides sacculifer*	24.70-50.70	1~3	Leonard et al., 1983
					Cibicidoides wuellerstorfi	36.50-50.70	2~3	Hodell et al., 1983
Site 518	29°58.4' S	38°08.1' W	western South Atlantic	3944	*Orbulina universa*	28.0-43.70	2~4	Hodell et al., 1983
					Cibicidoides wuellerstorfi	28.0-44.0	2~4	Hodell et al., 1983
Site 519	26°08.20' S	11°39.97' W	South Atlantic	3779	*Globigerinoides sacculifer*	33.15-95.15	0~4	Weissert et al., 1984
					Dentoglobigerina altispira	64.25-101.00	3~4	Weissert et al., 1984
					Orbulina universa	101.40-112.50	4~5	Weissert et al., 1984
					Cibicidoides wuellerstorfi	31.65-112.50	0~5	Weissert et al., 1984
					Nuttallides umbonifera	31.65-101.00	0~4	Weissert et al., 1984
					Orbulina universa	97.20-146.80	0~9	McKenzie et al., 1984
					Cibicidoides wuellerstorfi	31.60-144.6	0~6	McKenzie et al., 1984
					Nuttallides umbonifera	31.60-121.0	5~6	McKenzie et al., 1984
					Oridorsalis umbonatus	115.60-122.2	4~9	McKenzie et al., 1984
Site 521	26°04.43' S	10°15.87' W	South Atlantic	4141	*Globigerinoides sacculifer*	13.24-37.37	1~4	Weissert et al., 1984
					Oridorsalis umbonatus	31.33-41.60	3~5	Weissert et al., 1984
					Cibicidoides wuellerstorfi	12.40-45.31	1~6	Weissert et al., 1984
					Nuttallides umbonifera	13.92-45.31	1~6	Weissert et al., 1984
Site 522	26°06.84' S	05°06.78' W	South Atlantic	4457	*Globigerinoides conglobatus*	11.11-16.03	1~2	Weissert et al., 1984
					Oridorsalis umbonatus	16.58-30.15	2~6	Weissert et al., 1984
					Cibicidoides wuellerstorfi	16.58-30.15	2~6	Weissert et al., 1984
					Nuttallides umbonifera	11.11-30.15	1~6	Weissert et al., 1984
					various species (Planktonic)	66.45-145.52	26~36	Poore and Matthews, 1984
					various species (Benthic)	66.45-145.52	26~36	Poore and Matthews, 1984
					Globoquadrina venezuelana	130.7-145.4	35~36	Oberhansli et al., 1984
					Catapsydrax dissimilis	130.20-146.80	35~36	Oberhansli et al., 1984
					Stilostomella spp.	130.20-146.80	35~36	Oberhansli et al., 1984
					Oridorsalis umbonatus	119.20-140.40	34~36	Oberhansli et al., 1984
Site 523	28°33.13' S	02°15.08' W	South Atlantic	4572	*Globigerinoides ruber*	5.75-25.45	1~3	Weissert et al., 1984
					Oridorsalis umbonatus	9.63-24.70	1~3	Weissert et al., 1984
					Cibicidoides wuellerstorfi	5.75-25.45	1~3	Weissert et al., 1984
					Nuttallides umbonifera	9.63-24.70	1~3	Weissert et al., 1984
					various species (Planktonic)	85.90-184.00	34~48	Oberhansli et al., 1984
					various species (Benthic)	85.90-184.00	34~48	Oberhansli et al., 1984
Site 524	29°29.05' S	03°30.74' E	South Atlantic	4806	various species (Planktonic)	9.50-117.30	55~56	Oberhansli et al., 1984
					Stensioina beccariiformis	98.3	61	Oberhansli et al., 1984
					Nuttallides truempyi	9.50-28.10	55~56	Oberhansli et al., 1984
					Oridorsalis umbonatus	9.50-18.90	55~56	Oberhansli et al., 1984
					Stensioina beccariiformis	164.57-230.19	61~67	He et al., 1984
Site 525	29°04.24' S	02°59.12' E	South Atlantic	2467	various species (Benthic)	0.8-470.91	0~68	Shackleton et al., 1984
					various species (Planktonic)	99.37-433.72	8~62	Shackleton et al., 1984
Site 526	29°07.36' S	03°08.28' E	South Atlantic	1054	various species (Benthic)	6.71-217.53	1~37	Shackleton et al., 1984
					various species (Planktonic)	30.80-214.71	4~37	Shackleton et al., 1984
Site 527	28°02.49' S	01°45.80' E	South Atlantic	4428	various species (Benthic)	40.94-282.20	4~67	Shackleton et al., 1984
					various species (Planktonic)	146.77-283.14	50~67	Shackleton et al., 1984
Site 528	28°31.49' S	02°19.44' E	South Atlantic	3800	various species (Benthic)	8.87-315.99	1~58	Shackleton et al., 1984
					various species (Planktonic)	8.87-315.99	1~58	Shackleton et al., 1984
Site 529	28°55.83' S	02°46.08' E	South Atlantic	3035	various species (Benthic)	0.11-268.84	0~58	Shackleton et al., 1984
					various speci spp. anktonic)	0.11-268.84	0~58	Shackleton et al., 1984

Table 1. (continued).

Site	Latitude	Longitude	Geographical area	Water depth (m)	Species	Range mbsf	Range Age (Ma)	Reference
Site 658	20°44.95' N	18°34.87' W	Eastern Tropical Atlantic	2263	*Globorotalia inflata*	0.24-136.07	0~2	Sarnthein and Tiedemann,1989
					Cibicidoides wuellerstorfi	0.24-293.01	0~4	Sarnthein and Tiedemann,1989
					Uvigerina auberiana	151.73-293.01	2~4	Sarnthein and Tiedemann,1989
					Uvigerina peregrina	151.73-293.01	2~4	Sarnthein and Tiedemann,1989
Site 659	18°04.63' N	21°01.57' W	Eastern Tropical Atlantic	3071	*Globorotalia inflata*	0.47-32.59	0~1	Sarnthein and Tiedemann,1989
					Cibicidoides wuellerstorfi	0.47-32.92	0~1	Sarnthein and Tiedemann,1989
Site 662	1°23.41' S	11°44.35' W	Eastern Tropical Atlantic	3824	*Globigerinoides ruber*	117.39-136.09	1~2	Karlin et al., 1989
Site 663	1°11.87' S	11°52.71' W	Eastern Tropical Atlantic	3708	*Globigerinoides ruber*	4.81-32.21	0~1	Ruddiman and Janecek, 1989
Site 665	2°57.07' N	19°40.07' W	Eastern Tropical Atlantic	4752	*Cibicidoides* spp.	41.06-57.93	2	Curry and Miller, 1989
Site 667	4°34.15' N	21°54.68' W	Eastern Tropical Atlantic	3529	*Cibicidoides* spp.	220.16-375.16	19~31	Miller et al., 1989
Site 689	64°31' S	03°06' E	Weddell Sea	2080	various species (Planktonic)	102.10-233.10	31~66	Stott at al., 1990
					various species (Planktonic)	227.51-261.8	64~68	Stott and Kennett, 1990
					Archaeoglobigerina australis	246.87-291.30	68~76	Barrera and Huber, 1990
					Globigerinelloides multispinatus	246.87-294.50	68~77	Barrera and Huber, 1990
					Abathomphalus mayaroensis	246.87-256.38	68~69	Barrera and Huber, 1990
					Nuttallides spp.	165.90-236.47	18~67	Kennett and Stott, 1990
					Cibicidoides spp.	93.15-233.54	18~66	Kennett and Stott, 1990
					Nuttallides truempyi	246.87-256.38	68~69	Barrera and Huber, 1990
					Stensioina beccariiformis	246.87-294.50	68~77	Barrera and Huber, 1990
					Coryphostoma incrassata	246.87-269.50	66~71	Barrera and Huber, 1990
Site 690	65°10' S	01°12' E	Weddell Sea	2914	various species (Planktonic)	93.95-247.76	38~66	Stott at al., 1990
					various species (Planktonic)	224.74-242.94	63~65	Stott and Kennett, 1990
					Archaeoglobigerina australis	263.01-314.52	68~72	Barrera and Huber, 1990
					Globigerinelloides multispinatus	258.00-316.62	67~72	Barrera and Huber, 1990
					Abathomphalus mayaroensis	258.00-277.87	67~70	Barrera and Huber, 1990
					Nuttallides truempyi	53.00-206.06	26~59	Kennett and Stott, 1990
					Cibicidoides spp.	50.75-212.82	20~60	Kennett and Stott, 1990
					Nuttallides truempyi	258.00-283.81	68~71	Barrera and Huber, 1990
					Stensioina beccariiformis	263.01-316.62	68~72	Barrera and Huber, 1990
					Coryphostoma incrassata	258.00-300.40	67~71	Barrera and Huber, 1990
Site 698	51°27.51' S	33°05.96' W	South Atlantic	2128	*Nuttallides truempyi*	45.20-73.40	55~58	Katz and Miller, 1991
					Cibicidoides spp.	4.86-81.71	52~59	Katz and Miller, 1991
Site 699	51°32.537' S	30°40.619' W	South Atlantic	3708	*Nuttallides truempyi*	442.94-498.32	52~57	Katz and Miller, 1991
Site 700	51°31.977' S	30°16.688' W	South Atlantic	3598	*Nuttallides truempyi*	131.20-329.18	50~65	Katz and Miller, 1991
					Cibicidoides spp.	67-290.49	46~61	Katz and Miller, 1991
Site 702	50°56.786' S	26°22.117' W	South Atlantic	3083	*Nuttallides truempyi*	32.23-274.10	39~59	Katz and Miller, 1991
					Cibicidoides spp.	21.23-287.60	38~60	Katz and Miller, 1991
Site 704	46°52.8' S	7°25.3' E	South Atlantic	2532	*Neogloboquadrina pachyderma*	0.41-233.41	0~5	Hodell and Ciesielski, 1991
					Cibicidoides spp.	2.28-53.90	0~1	Hodell and Ciesielski, 1991
					various species (Benthic)	214.21-384.71	4~9	Muller et al., 1991
Site 709	03°54.9 S	60°33.1' E	Mascarene Plateau	3041	*Globigerinoides sacculifer*	13.35-36.50	1~4	Shackleton and Hall, 1990
					Globigerinoides ruber	26.30-53.96	3~5	Shackleton and Hall, 1990
					Globigerinoides sacculifer	25.70-103.40	2~5	Vincent et al., 1991
					Dentoglobigerina altispira	30.20-171.00	3~19	Vincent et al., 1991
					Globoquadrina venezuelana	133.80-215.45	13~26	Vincent et al., 1991
					various species (Benthic)	54.2-200.5	5~24	Woodruff et al., 1990
Site 714	05°03.6 S	73°47.2' E	Mascarene Plateau	2038	*Globigerinoides sacculifer*	0.15-19.48	0~5	Droxler et al., 1990
					Globigerinoides sacculifer	26.5-70.3	7~12	Boersma and Mikkelsen, 1990
					various species (Benthic)	26.5-205.0	7~24	Boersma and Mikkelsen, 1990
Site 716	04°56.0' S	73°17.0' E	Mascarene Plateau	544	*Globigerinoides sacculifer*	0.20-40.90	0~1	Droxler et al., 1990
Site 738	62°42.54' S	82°47.25' E	Kerguelen Plateau	2253	various species (Planktonic)	23.00-377.23	35~65	Barrera and Huber, 1991
					Cibicidoides spp.	18.42-33.86	35~37	Barrera and Huber, 1991
					Nuttallides truempyi	61.00-380.70	39~66	Barrera and Huber, 1991
					Stilostomella subspinosa	23.00-80.00	35~40	Barrera and Huber, 1991
					Stensioina beccariiformis	286.02-377.80	57~65	Barrera and Huber, 1991
Site 744	61°34.66' S	80°35.46' E	Kerguelen Plateau	2317	*Globigerinita juvenilis*	100.17-109.67	26~27	Barrera and Huber, 1991
					Chiloguembelina cubensis	118.2-175.07	31~39	Barrera and Huber, 1991
					Globorotaloides suteri	82.63-175.07	19~39	Barrera and Huber, 1991
					Cibicidoides spp.	28.11-175.07	9~39	Barrera and Huber, 1991
					Nuttallides spp.	27.11-77.09	9~18	Barrera and Huber, 1991
					Stilostomella subspinosa	81.13-175.07	18~39	Barrera and Huber, 1991
					Cibicidoides spp.	38.05-63.55	10~15	Woodruff and Chamber, 1991
					Cibicidoides wuellerstorfi	55.24-57.75	13~14	Woodruff and Chamber, 1991
					Cibicidoides kullenbergi	51.20-77.75	11~18	Woodruff and Chamber, 1991
					Cibicidoides spp.B	50.23-52.70	10~11	Woodruff and Chamber, 1991
Site 747	54°48.68' S	76°47.64' E	Central Kerguelen Plateau	1695	*Cibicidoides* spp.	33.50-141.90	8~26	Wright and Miller, 1992
Site 748	58°26.45' S	78°58.89' E	Central Kerguelen Plateau	1290	*Subbotina angiporoides*	104.28-127.00	33~37	Zachos et al., 1992a
					Subbotina lin spp. a	171.90-147.90	40~44	Zachos et al., 1992a

Table 1. (continued).

Site	Latitude	Longitude	Geographical area	Water depth (m)	Species	Range		Reference
						mbsf	Age (Ma)	
Site 748	58°26.45' S	78°58.89' E	Central Kerguelen Plateau	1290	*Chiloguembelina cubensis*	104.50-176.00	33~45	Zachos et al., 1992a
					Chiloguembelina spp.	154.28-389.22	42~59	Zachos et al., 1992a
					Cibicidoides	67.57-350.80	22~58	Zachos et al., 1992a
					Gyroidina spp.	67.57-389.22	22~59	Zachos et al., 1992a
					Stensioina beccariiformis	379.26-388.53	59	Zachos et al., 1992a
					Nuttallides umbonifera	77.10-96.10	25~30	Zachos et al., 1992a
Site 750	57°35.54' S	81°14.42' E	Kerguelen Plateau	2031	*Heterohelix globulosa*	349.73-356.28	66	Zachos et al., 1992b
					Eoblobigerina eobulloides	349.73-349.93	66	Zachos et al., 1992b
					Globigerinelloides spp.	349.73-350.25	66	Zachos et al., 1992b
					Nuttallides truempyi	348.08-356.06	65~66	Zachos et al., 1992b
					Stensioina beccariiformis	350.11-356.60	66	Zachos et al., 1992b
Site 751	57°43.56' S	79°48.89' E	Kerguelen Plateau	1634	various species (Benthic)	40.28-165.2	4~19	Mackensen et al., in press
Site 752	30°53.48' S	93°34.65' E	Broken Ridge	1086	*Cibicidoides* spp.	0.80-102.05	0~35	Rea et al., 1991
Site 754	30°56.44' S	93°33.99' E	Broken Ridge	1064	*Cibicidoides* spp.	0.78-125.78	0~28	Rea et al., 1991
Site 756	27°21.33' S	87°35.80' E	Ninetyeast Ridge	1518	*Gyroidinoides* spp.	18.90-136.60	5~36	Rea et al., 1991
					Uvigerina spp.	0.80-140.20	0~37	Rea et al., 1991
Site 757	17°01.46' S	88°10.90' E	Ninetyeast Ridge	1652	*Gyroidinoides* spp.	8.30-161.1	1~47	Rea et al., 1991
					Uvigerina spp.	2.13-123.90	0~37	Rea et al., 1991
Site 758	05°23.05' S	90°21.67' E	Ninetyeast Ridge	2935	*Globigerinoides sacculifer*	30.25-110.45	2~7	Vincent et al., 1991
					Dentoglobigerina altispira	39.85-146.02	2~18	Vincent et al., 1991
					Globoquadrina venezuelana	63.55-146.02	4~18	Vincent et al., 1991
					Globigerinoides sacculifer	0.01-34.91	0~2	Farrell and Janecek, 1991

data of interspecific differences previously compiled by many workers as well as in the present study.

In this study, the isotopic composition of various foraminiferal species is adjusted to that of *O. umbonatus*. This species was measured in the largest number of studied sites, occurs over a long time range, and has a stable magnitude of departure from the isotopic composition of the *Cibicidoides* group. The original δ values of *O. umbonatus* are converted into the δ values of dissolved CO_2 of bottom water by 0 ‰ for $\delta^{18}O$ and by +1.0 ‰ for $\delta^{13}C$ (Shackleton *et al.*, 1984). For the Early to middle Paleogene, the isotopic composition is adjusted to that of *N. truempyi* and the δ values of *N. truempyi* are converted into the δ values of dissolved CO_2 of bottom water by +0.330 ‰ for $\delta^{18}O$ and by +1.082 ‰ for $\delta^{13}C$. If no measurements are given for *O. umbonatus*, the isotopic compositions of various species are adjusted to those of one taxon (*Cibicidoides* group, such as *C. wuellerstorfi*), and the data are converted to the δ values of dissolved CO_2 of bottom water. Adjusted values used in this study are shown in Table 2.

The δ values of planktonic foraminifers are adjusted to those of *Globigerinoides sacculifer* because this species has been measured at many sites and the ecology of this species is well known. An ecological investigation by plankton net reveals that *G. sacculifer* mostly inhabits water shallower than 50m (Be, 1977). Therefore, this study assumes the isotopic composition of *G. sacculifer* as an indication of the δ values of dissolved CO_2 of surface water shallower than 50 m depth. The adjustments of planktonic foraminifera are established by the same method as benthic foraminifera, and most of the adjustments are calculated based on the data of Shackleton *et al.* (1984). Some of the adjustments, however, are established by indirect differences, because the range of planktonic foraminifer is often short. The isotopic compositions of Paleogene planktonic foraminifera are adjusted to those of *Subbotina* spp., which has been measured in many studies. In the *Subbotina* group, the intergeneric difference and the isotopic fluctuation according test size is relatively small (Shackleton *et al.*, 1985; Stott *et al.*, 1990). The δ values of *Subbotina* spp. in the Paleogene are converted into the δ values of *G. sacculifer* by -0.610 ‰ for $\delta^{18}O$ and by +0.850 ‰ for $\delta^{13}C$, which are indirectly obtained from the interspecific difference studied by Shackleton *et al.* (1984). The δ values adjusted from *Subbotina* spp., however, may not indicate that of dissolved CO_2 of surface water (50 m depth), because the δ values adjusted from *Subbotina* spp are >1‰ lower than those of the *Morozovella* group and the *Acarinina* group. The adjusted values of planktonic foraminifers are shown in Table 2.

2. Chronology of the samples

The ages of the studied section are defined by geomagnetic polarity events and the biostratigraphy of calcareous nannofossils. The numerical ages of nannofossil events have been originally determined by correlation with the geomagnetic polarity time scale.

The magnetic polarity time scale used in this study is based on Berggren *et al.* (1985a, 1985b, 1985c). The time scale of nannofossil species events has been proposed in many studies (Thiersten *et al.*, 1977; Backman and Shackleton, 1983; Backman and Pestiaux, 1986; Berggren *et al.*, 1985a; 1985b; 1985c; Backman, 1987; Gartner, 1977; Zijdeveld *et al.*, 1986; Poore *et al.*, 1983; Lohman, 1986; Barton and Bloemendal, 1986; Baldauf *et al.*, 1987; Clement and Robinson, 1987; Takayama and Sato, 1987; Rahman and Roth, 1989; Rio *et al.*, 1990; Gartner, 1990; Okada, 1990;

Table 2. Values to adjust to d value of the bottom or surface (about 50m) DIC in the studied area.

Site / Species	Site 752 Site 758 Site 754 Site 762 Site 756		Site 214 Site 238 Site 216 Site 237		Site 253		Site 516 Site 517 Site 518		Site 521 Site 519 Site 522 Site 523		Site 527 Site 525 Site 528 Site 526 Site 529		Site 667 Site 662 Site 658 Site 665 Site 659	
	$\delta^{18}O$	$\delta^{13}C$	$\delta^{18}O$	$\delta^{13}C$	$\delta^{18}O$	$\delta^{13}C$	$\delta^{18}O$	$\delta^{13}C$	$\delta^{18}O$	$\delta^{13}C$	$\delta^{18}O$	$\delta^{13}C$	$\delta^{18}O$	$\delta^{13}C$
Benthic foraminifera (bottom water)														
Anomalinoides danicus	0.178	0.547												
Bulimina jarvisi											-0.080	0.460		
Bulimina spp.											-0.140	0.445		
Cassidulina cornuta														
Cibicidoides kullenbergi									0.336	0.036	0.615	0.070		
Cibicidoides lamontdohertyi														
Cibicidoides mundulus														
Cibicidoides sp.B														
Cibicidoides sp.C														
Cibicidoides spp.					0.396	0.210					0.280	0.290	0.280	0.290
Cibicidoides wuellerstorfi					0.490	0.240	0.208	-0.437	0.208	-0.437	0.795	-0.105	0.795	-0.105
Gavelinella spp.											0.167	0.737		
Globocassidulina spp.											-0.230	0.441		
Globocassidulina subglobosa									-0.094	0.616				
Gyroidina spp.											0.110	0.280		
Nuttallides spp.											0.418	0.548		
Nuttallides truempyi	0.330	1.082												
Nuttallides umbonifera									0.147	-0.222				
Oridorsalis umbonatus	0.000	1.000	0.000	1.000	0.000	1.000			0.000	1.000	0.000	1.000		
Planulina bradyi														
Planulina renzi											0.870	-0.085		
Rectuvigerina spinea														
Stensioina beccariiformis	0.214	1.203												
Stilostomella spp.											0.035	0.515		
Uvigerina spp.											-0.036	0.498		
Planktonic foraminifera (surface water)														
Acarinina nitida											-0.449	0.239		
Acarinina primitiva	-0.511	0.367												
Acarinina spp.											-0.580	0.052		
Catapsydrax echinatus											-0.110	-0.133		
Catapsydrax spp.											-0.649	0.999		
Catapsydrax unicavus											-0.822	1.244		
Chiloguembelina spp.														
Chiloguembelina wilcoxensis											-0.439	1.317		
Dentoglobigerina altispira	-0.184	0.140	0.102	-0.060							-0.290	0.600		
Globigerina angulisuturalis											-0.229	0.849		
Globigerina apertura											0.080	0.285		
Globigerina barbemoensis											-0.569	1.219		
Globigerina corpulenta											-0.540	0.580		
Globigerina euaperta											-0.729	0.679		
Globigerina globularis											-0.689	1.159		
Globigerina gortanii											-1.220	0.696		
Globigerina nepenthes											-0.221	0.349		
Globigerina obesa											-0.811	0.879		
Globigerina ouachitensis											-0.649	0.689		
Globigerina pseudoampliapertura											-0.754	0.944		
Globigerina selli											-0.719	0.579		
Globigerina tripartita											-0.529	0.859		
Globigerina venezuelana	-1.759	1.065	-1.115	1.027	-1.115	1.027								
Globigerina winkleri											-0.540	0.430		
Globigerinoides ruber									0.264	-0.011	-0.285	0.095	0.264	
Globigerinoides sacculifer	0.000	0.000			0.000	0.000					0.000	0.000		
Globigerinoides seiglei											-0.110	1.230		
Globigerinoides subquadratus											0.140	0.230		
Globigerinoides trilobus					-0.550	0.415								
Globogerinatheka index											-0.490	0.380		
Globogerinatheka mexicana											-0.309	0.266		
Globogerinatheka spp.											-0.355	0.450		
Globoquadrina dehiscens					-0.100	0.785					-0.100	0.785		
Globoquadrina pradehiscens											-0.679	0.579		
Globoquadrina spp.											-0.639	0.869		
Globoquadrina transdehiscens											-0.779	0.564		
Globorotalia cerroazulensis											-0.530	0.952		
Globorotalia conoidea											-0.571	0.679		
Globorotalia inflata											-1.465	0.198	-1.465	0.198
Globorotalia peripheroronda											-0.340	0.655		
Globorotalia siakensis											-0.659	0.999		
Globorotalia truncatulinoides											-1.335	0.285		
Globorotaloides miozea											-0.401	0.869		
Globorotaloides suteri														
Hantkenina spp.											-0.466	0.840		
Morozovella acuta											0.408	-0.263		
Morozovella aragonensis											0.296	-0.860		
Morozovella formosa											-0.249	-0.331		
Morozovella lehneri											-0.059	-0.221		
Morozovella marginodentata	-0.464	-1.139												
Morozovella pseudomenardii											-0.652	1.485		
Morozovella rex											-0.034	-0.221		
Morozovella subbotinae											-0.371	0.251		
Morozovella velascoensis											-0.294	0.330		
Planoglobulina spp.											-0.234	-0.064		
Subbotina spp.	-0.610	0.850									-0.610	0.850		
Turborotalia increbescens											-0.463	0.759		
Turborotalia spp.											-0.594	0.899		

Table 2. (continued).

Site / Species	Site 689, Site 690		Site 700, Site 698, Site 702, Site 699, Site 704		Site 709		Site 714		Site 738, Site 744		Site 748, Site 750		Site 751	
	$\delta^{13}C$	$\delta^{18}O$	$\delta^{18}O$	$\delta^{13}C$	$\delta^{18}O$	$\delta^{13}C$	$\delta^{18}O$	$\delta^{13}C$	$\delta^{18}O$	$\delta^{13}C$	$\delta^{18}O$	$\delta^{13}C$	$\delta^{18}O$	$\delta^{13}C$
Benthic foraminifera (bottom water)														
Anomalinoides danicus														
Bulimina jarvisi														
Bulimina spp.														
Cassidulina cornuta							-0.360	0.720						
Cibicidoides kullenbergi			0.358	0.340	0.358	0.340			0.358	0.340				
Cibicidoides lamontdohertyi					0.305	0.417								
Cibicidoides mundulus													0.587	0.512
Cibicidoides sp.B					0.400	-0.250			0.400	-0.250				
Cibicidoides sp.C					0.428	0.300								
Cibicidoides spp.	0.134	0.794	0.396	0.210					0.297	0.783	0.490	0.210	0.507	0.192
Cibicidoides wuellerstorfi					0.490	0.240			0.490	0.240			0.490	0.240
Gavelinella spp.														
Globocassidulina spp.														
Globocassidulina subglobosa							-0.147	0.868						
Gyroidina spp.											-0.146	0.519	0.099	0.694
Nuttallides spp.	0.330	1.082												
Nuttallides truempyi			0.330	1.082					0.330	1.082	0.330	1.082		
Nuttallides umbonifera			0.183	0.803									0.728	0.689
Oridorsalis umbonatus														
Planulina bradyi					0.178	0.700								
Planulina renzi					0.343	0.140	0.662	0.230						
Rectuvigerina spinea							0.013	1.260						
Stensioina beccariiformis											0.214	1.203		
Stilostomella spp.														
Uvigerina spp.							0.038	0.982						
Planktonic foraminifera (surface water)														
Acarinina nitida														
Acarinina primitiva									-0.108	-0.081				
Acarinina spp.														
Catapsydrax echinatus														
Catapsydrax spp.														
Catapsydrax unicavus														
Chiloguembelina spp.											-0.166	0.291		
Chiloguembelina wilcoxensis														
Dentoglobigerina altispira					-0.184	0.140								
Globigerina angulisuturalis														
Globigerina apertura														
Globigerina barbemoensis														
Globigerina corpulenta														
Globigerina euaperta														
Globigerina globularis														
Globigerina gortanii														
Globigerina nepenthes														
Globigerina obesa														
Globigerina ouachitensis														
Globigerina pseudoampliapertura														
Globigerina selli														
Globigerina tripartita														
Globigerina venezuelana					-1.759	1.065								
Globigerina winkleri														
Globigerinoides ruber					0.264	-0.011								
Globigerinoides sacculifer					0.000	0.000								
Globigerinoides seiglei														
Globigerinoides subquadratus														
Globigerinoides trilobus														
Globogerinatheka index														
Globogerinatheka mexicana														
Globogerinatheka spp.														
Globoquadrina dehiscens														
Globoquadrina pradehiscens														
Globoquadrina spp.														
Globoquadrina transdehiscens														
Globorotalia cerroazulensis														
Globorotalia conoidea														
Globorotalia inflata														
Globorotalia peripheroronda														
Globorotalia siakensis														
Globorotalia truncatulinoides														
Globorotaloides miozea														
Globorotaloides suteri									-0.884	1.079				
Hantkenina spp.														
Morozovella acuta														
Morozovella aragonensis														
Morozovella formosa														
Morozovella lehneri														
Morozovella marginodentata														
Morozovella pseudomenardii														
Morozovella rex														
Morozovella subbotinae														
Morozovella velascoensis														
Planoglobulina spp.														
Subbotina spp.	-0.610	0.850							-0.610	0.850	-0.610	0.850		
Turborotalia cerrebescens														
Turborotalia spp.														

Backman *et al.*, 1990; and others). Among them, the biostratigraphic time scale proposed by Berggren *et al.* (1985a, 1985b) has been accepted as the standard time scale (e.g., Peirce, Weissel, *et al.*, 1989). Backman *et al.* (1990), however, pointed out that low-latitude nannofossil biochronology differs from the standard of mid-latitude biostratigraphy established by Berggren *et al.* (1985a, 1985b).

Based on their information the biochronology of nannofossil species events is constructed as follows; a) the basic biostratigraphic time scale follows that of Berggren *et al.* (1985a), b) nannofossil species events near the studied area are included if they are not contradictory in order, and c) species events described since Berggren *et al.* (1985a, 1985b) are considered. Thus, the biochronology applied in the time interval are: Pleistocene (Takayama and Sato, 1987), late Pliocene (Backman and Shackleton, 1983), early Pliocene to late Miocene (Rio *et al.*, 1990), middle Miocene to early Miocene (Backman *et al.*, 1990), Oligocene to middle Eocene (Okada, 1990), and the early Eocene to Paleocene (Berggren *et al.*, 1985a; 1985b; 1985c). In addition to the species events proposed by Martini (1971) and Okada and Bukry (1980), zonal schemes (Backman, J., Duncan, R. A., *et al.*, 1988; Peirce, Weissel, *et al.*, 1989; Rio *et al.*, 1990) are also considered. These compiled nannofossil events are shown in Table 3.

The numerical age of a sampled horizon is calculated by assuming a constant sedimentation rate between the two stratigraphic levels. The geomagnetic polarity events and nannofossil event levels at each site used in this study are shown in Tables 4 and 5, respectively.

3. Paleodepth

Paleodepths in this study were reconstructed by published data based on a "backtrack method" (Sites 214, 215, 216, 237, 238, 709, 752, 754, 756, and 758: Zachos *et al.*, 1992c; Sites 738 and 744: Barrera and Huber, 1991; Site 253: Kidd and Davies, 1978; Site 519: Finger, 1984; Sites 521, 522, and 523: Hsü *et al.*, 1984; Sites 525, 526, 527, 528, and 529: Moore, Jr. *et al.*, 1984; Sites 366 and 667: Miller *et al.*, 1989; Sites 698, 699, 700, and 702: Katz and Miller, 1991). The paleodepth at Site 748 through the Paleogene was upper bathyal (water depth: ~1000 m; Mackensen and Berggren, 1991). The paleodepth at Site 748 was calculated by a assuming linear change from this depth to the present depth (1290 m). In case of an unknown subsidence curve, the present depth was used for the paleodepth for relatively young ages.

4. Paleolatitude and Paleolongitude

Paleolatitude and paleolongitude of the Indian Ocean site are estimated from migration velocity calculated from backtracked paleocoordinate (Zachos *et al.*, 1992c). Paleolatitude and paleolongitude of the South Atlantic Ocean site are estimated from migration velocity given by Scotese *et al.* (1988), and based on sea-floor spreading isochrons (Larson *et al.*, 1985). The paleolatitude and paleolongitude at each site are shown in Table 6.

B. General trend of isotopic records in the northern Indian Ocean

In the northern Indian Ocean, distribution pattern of carbon and oxygen isotopic ratios in surface (~50 m in depth) and bottom waters throughout the Cenozoic are illustrated in Figs. 36-39.

The oxygen isotopic records of bottom water around the Cretaceous / Tertiary boundary show a negative shift of 0.4‰ from -0.8 to -1.2‰. During the Paleocene, $\delta^{18}O$ values increase by 1.3‰ (66-61 Ma), and decrease down to a minimum value (-0.6‰) in the earliest Eocene (56 Ma). $\delta^{18}O$ values throughout the Eocene gradually increase by 1.6‰ from the minimum value in the earliest Eocene. From the Oligocene, distinct positive shifts are recognized three times. These shifts are observed immediately above epoch or subepoch boundaries, and accompanied by decreasing $\delta^{18}O$ values before the shifts. The first shift is recognized around the Eocene / Oligocene boundary, and the second shift in the middle Miocene. The net magnitudes of the first and second shifts are 0.7‰, 0.8‰, respectively. In the interval between the first and second shifts, the oxygen isotopic ratios vary from 1.0 to 2.5 ‰, with a gradual increase. Although a discontinuity is found near the Oligocene / Miocene boundary, this is probably caused by limited data. The third shift is recognized in the late Pliocene, and the net magnitude of this shift is 0.8‰. The oxygen isotopic ratios in interval between the second and third shifts are constant with a variation of 1.8-3.3‰. However, two remarkable ^{18}O maxima are recognized around 6 and 8 Ma. In the interval between the third shift and the present, $\delta^{18}O$ values show a gradual increase.

During the Paleocene, the increase of $\delta^{18}O$ values in surface water is observed up to 61 Ma, and subsequently a ^{18}O minimum value (-2.0‰) is recognized in the earliest Eocene (58 Ma). The same pattern of isotopic change is found in oxygen isotopic records of bottom water. The oxygen isotopic records of surface water, however, exhibit a smaller magnitude of change (only 0.5 ‰) than those of bottom waters. The difference of $\delta^{18}O$ value between Sites 752 and 758 is relatively large (about 0.8‰) at that time. The ^{18}O minimum of surface water during the earliest Eocene (58 Ma) delayed by about 2 Ma than that of bottom waters. From 61 to 37 Ma, the distribution of $\delta^{18}O$ values are parallel between surface and bottom water around 1.8‰. During the Eocene, $\delta^{18}O$ values increase by 2.5‰ (from -2.1 to 0.4‰) in the entire water column, with the increase of surface $\delta^{18}O$ values being especially rapid from the early to early middle Eocene. As a result, the $\delta^{18}O$ difference between surface and bottom water is reduced to about 0.6‰ after the early middle Eocene. From the Oligocene to early Miocene, $\delta^{18}O$ values are constant around -0.2‰. No remarkable shift at the Oligocene / Eocene boundary is recognized. Then, $\delta^{18}O$ values of surface water are again separated from those of bottom water at this time, and the difference is about 1.5‰ during the Oligocene. During the Miocene, $\delta^{18}O$ values decrease from 20 Ma to 16 Ma, increase to a peak value (~0.2‰) at 12 Ma, and again decrease to about -1.0‰. However, $\delta^{18}O$ values at Site 253 tend to increase from 0.5 to 1.5 ‰ at that time. Hence, the scatter of $\delta^{18}O$ value increases, and the highest degree of scatter (reaching 3‰) is recorded at 6 Ma. Around the Miocene / Pliocene boundary, $\delta^{18}O$ values at Site 253 rapidly decrease, and as a

Table 3. Cenozoic calcareous nannofossil datum levels and corresponding zonal boundaries of Okada and Bukry (1980) and Martini (1971) with age estimates.

Event	Species	Zone (base) Okada and Bukry (1980)	Zone (base) Martini (1971)	Age (Ma)	Reference
Increase	*Emiliania huxleyi*			0.085	1
LO	*Helicosphaera inversa*			0.15	2
FO	*Emiliania huxleyi*	CN15	NN21	0.275	1, 3
LO	*Pseudoemiliania lacunosa*	CN14b	NN20	0.460	1, 3
FO	*Helicosphaera inversa*			0.48	2
Acme top	*Reticulofenestra* sp. A			0.83	2
FO	*Gephyrocapsa parallela*			0.89	2
Increase	*Gephyrocapsa oceanica*			0.90	4
Acme top	*Gephyrocapsa* (small)			0.93	5
LO	*Gephyrocapsa* (large)			1.10	2
LO	*Helicosphaera sellii*			1.19	2
FO	*Gephyrocapsa* (large)			1.36	2
LO	*Calcidiscus macintyrei*			1.45	3, 6
FO	*Gephyrocapsa oceanica*			1.57	2
FO	*Gephyrocapsa caribbeanica*			1.66	2
LO	*Discoaster triradiatus*			1.89	7
LO	*Discoaster brouweri*	CN13a	NN19	1.91	2
Increase	*Discoaster triradiatus*			2.07	7
LO	*Discoaster pentaradiatus*	CN12d	NN18	2.35	6, 8
LO	*Discoaster surculus*	CN12c	NN17	2.41	6
LO	*Discoaster tamalis*	CN12b		2.65	6, 7
LO	*Discoaster variabilis*			2.90	5
LO	*Sphenolithus* spp.			3.45	6
LO	*Sphenolithus neoabies*			3.51	8
LO	*Sphenolithus abies*			3.56	2
LO	*Reticulofenestra pseudoumbilica*	CN12a	NN16	3.56	6
FO	*Discoaster tamalis*	CN11b		3.8	3
LO	*Amaurolithus tricorniculatus*			3.7	3
FO	*Pseudoemiliania lacunosa*			4.05	8
FO	*Discoaster asymmetricus*			4.1	3
LO	*Amaurolithus delicatus*			4.11	9
LO	*Amaurolithus primus*	CN11a	NN15	4.37	9
LO	*Ceratolithus acutus*			4.43	9
FO	*Ceratolithus rugosus*	CN10c	NN13	4.66	9
FO	*Ceratolithus acutus*	CN10b		4.85	10
LO	*Triquetrorhabdulus rugosus*			4.90	10
LO	*Ceratolithus armatus*			5.06	5
LO	*Discoaster quinqueramus*	CN10a	NN12	5.26	5
LO	*Amaurolithus amplificus*			5.33	9
LO	*Discoaster berggrenii*			5.80	5
FO	*Amaurolithus amplificus*			6.02	9
FO	*Amaurolithus primus*	CN9b		6.70	10
FO	*Discoaster quinqueramus*			7.46	10
FO	*Discoaster berggrenii*	CN9a	NN11	8.00	9
LO	*Discoaster neohamatus*			8.10	8
FO	*Discoaster neorectus*	CN8b		8.5	3
FO	*Discoaster loeblichii*			8.5	3
LO	*Discoaster hamatus*	CN8a	NN10	8.67	10
LO	*Catinaster* spp.			8.77	10
FO	*Discoaster neohamatus*			8.96	10
LO	*Catinaster coalitus*			9.00	5
FO	*Catinaster calyculus*			10.00	3
LO	*Coccolithus miopelagicus*			10.23	2
FO	*Discoaster hamatus*	CN7	NN9	10.5	10
FO	*Catinaster coalitus*	CN6	NN8	11.1	10
FO	*Discoaster pentaradiatus*			12.0	3
FO	*Discoaster kugleri*		NN7	12.2	10
LO	*Coronocyclus nitescens*			12.7	9
LO	*Coccolithus floridanus*	CN5b		13.1	3, 10
LO	*Sphenolithus heteromorphus*	CN5a	NN6	13.6	10
FO	*Discoaster exilis*			15.4	3
LO	*Helicosphaera ampliaperta*	CN4	NN5	16.0	3, 10
Acme top	*Discoaster deflandrei*			16.1	9
FO	*Discoaster signus*			16.1	9
FO	*Sphenolithus heteromorphus*	CN3		18.4	10
LO	*Sphenolithus belemnos*		NN4	18.8	10
LO	*Triquetrorhabdulus carinatus*		NN3	19.5	10
FO	*Sphenolithus belemnos*	CN2		20.0	10
FO	*Discoaster druggii*	CN1c	NN2	23.6	10
LO	*Dictyococcites bisectus*	CN1a	NN1	23.7	3
LO	*Sphenolithus ciperoensis*			23.7	3
LO	*Crassidiscus backmanii*			24.8	11
FO	*Crassidiscus backmanii*			25.0	11
LO	*Sphenolithus distentus*	CP19b	NP25	26.0	11
LO	*Chiasmolithus altus*			28.2	3
FO	*Sphenolithus ciperoensis*	CP19a	NP24	30.2	3
FO	*Sphenolithus distentus*	CP18		31.2	11
LO	*Sphenolithus aff. distentus*			32.4	11
LO	*Reticulofenestra umbilica*	CP17	NP23	34.2	11
LO	*Bramletteius serraculoides*			34.2	11
LO	*Ericsonia obruta*			34.4	12
LO	*Ericsonia formosa*	CP16c	NP22	34.9	12
LO	*Isthmolithus recurvus*			34.9	3
LO	*Hayella situriformis*			35.1	11
FO	*Sphenolithus aff. distentus*			35.1	11
LO	*Chiasmolithus titus*			35.8	11
Acme top	*Ericsonia subdisticha*	CP16b		35.9	3
LO	*Reticulofenestra oamaruensis*			36.0	13
Increase	*Ericsonia obruta*			36.1	12
LO	*Discoaster saipanensis*	CP16a	NP21	36.7	3, 12
LO	*Discoaster barbadiensis*			36.8	11
LO	*Crirocentrum reticulatum*			37.0	11
FO	*Isthmolithus recurvus*	CP15b	NP19	37.8	3, 11
FO	*Chiasmolithus oamaruensis*			39.8	3
LO	*Chiasmolithus grandis*	CP15a	NP18	40.0	3
LO	*Campylosphaera dela*			40.6	11
LO	*Sphenolithus spiniger*			41.4	11
LO	*Sphenolithus furcatolithoides*			41.4	11
FO	*Dictyococcites bisectus*			41.4	11
FO	*Reticulofenestra reticulata*			42.1	13
LO	*Chiasmolithus solitus*	CP14b	NP17	43.4	11
LO	*Discoaster bifax*			43.4	11
LO	*Nannotetrina alata*			43.4	11
FO	*Reticulofenestra umbilica*			43.5	11
LO	*Cruciplacolithus staurion*			43.5	11
LO	*Nannotetrina fulgens*	CP14a		45.4	3
FO	*Discoaster bifax*			46.6	11
LO	*Chiasmolithus gigas*	CP13c		47.0	3
FO	*Sphenolithus furcatolithoides*			48.2	11
FO	*Chiasmolithus gigas*	CP13b		49.0	11
FO	*Nannotetrina fulgens*	CP13a	NP15	49.8	3
LO	*Discoaster lodoensis*			50.4	12
FO	*Reticulofenestra inflata*			52.0	3
FO	*Discoaster sublodoensis*	CP12	NP14	52.6	3
LO	*Tribrachiatus orthostylus*	CP11	NP13	53.7	3
FO	*Discoaster lodoensis*	CP10	NP12	55.3	3
LO	*Tribrachiatus contortus*	CP9b	NP11	56.3	3
FO	*Discoaster diastypus*			56.5	3
FO	*Tribrachiatus orthostylus*			56.6	3
LO	*Fasciculithus* spp.	CP9a	NP10	57.8	3
FO	*Tribrachiatus bramlettei*			57.8	3
FO	*Campylosphaera eodela*			58.2	3
FO	*Discoaster multiradiatus*	CP8	NP9	59.2	3
FO	*Discoaster mobilis*			59.8	3
FO	*Heliolithus reidelii*	CP7	NP8	60.0	3
FO	*Discoaster mohleri*	CP6	NP7	60.4	3
FO	*Heliolithus kleinpellii*	CP5	NP6	61.6	3
FO	*Ellipsolithus tympaniformis*			62.0	3
FO	*Fasciculithus* spp.	CP4	NP5	62.0	3
FO	*Ellipsolithus macellus*	CP3	NP4	63.7	3
FO	*Prinsius martinii*			63.8	3
FO	*Chiasmolithus danicus*	CP2	NP3	64.8	3
FO	*Cruciplacolithus tenuis*	CP1b	NP2	65.9	3
FO	*Biantholithus sparsus*	CP1a	NP1	66.4	3
FO	*Nephrolithus frequens*			69.0	
LO	*Reticulofenestra levis*			69.0	

Note: FO = first occurrence, LO = last occurrence. The references refer to the age column and represent (1) Thierstein et al. (1977); (2) Takayama and Sato (1987); (3) Berggren et al. (1985a, 1985b, 1985c); (4) Gartner (1977); (5) Gartner (1990); (6) Backman and Shackleton (1983); (7) Backman and Pestiaux (1986); (8) Rahman and Roth (1989); (9) Rio et al. (1990); (10) Backman et al. (1990); (11) Okada (1990); (12) Backman (1987); (13) Wei and Wise (1990).

Table 4. Nannofossil zonations for Indian and South Atlantic Ocean DSDP and ODP sites.

Event	Species	Zone (base) Okada and Bukry (1980)	Zone (base) Martini (1971)	Age (Ma)	Site 214*	Site 215	Site 216*	Site 237*	Site 238*	Site 253*	Site 525	Site 526	Site 527
FO	*Emiliania huxleyi*	CN15	NN21	0.275									
LO	*Pseudoemiliania lacunosa*	CN14b	NN20	0.460								3.23	
LO	*Helicosphaera sellii*			1.19									
FO	*Gephyrocapsa* (large)			1.36									
LO	*Calcidiscus macintyrei*			1.45									
FO	*Gephyrocapsa oceanica*			1.57									
LO	*Discoaster triradiatus*			1.89									
LO	*Discoaster brouweri*	CN13a	NN19	1.91							9.3	16.2	14
Increase	*Discoaster triradiatus*			2.07									
LO	*Discoaster pentaradiatus*	CN12d	NN18	2.35									
LO	*Discoaster surculus*	CN12c	NN17	2.41									18.97
LO	*Discoaster tamalis*	CN12b		2.65									
LO	*Discoaster variabilis*			2.90									
LO	*Sphenolithus* spp.			3.45									
LO	*Reticulofenestra pseudoumbilica*	CN12a	NN16	3.56							18.26		23.42
FO	*Discoaster tamalis*	CN11b		3.8									
LO	*Amaurolithus tricorniculatus*			3.7									
LO	*Amaurolithus primus*	CN11a	NN15	4.37							32.6	29.5	
FO	*Ceratolithus rugosus*	CN10c	NN13	4.66						19.3	47.82	35.45	
FO	*Ceratolithus acutus*	CN10b		4.85					138.3		57	47.2	59.1
LO	*Discoaster quinqueramus*	CN10a	NN12	5.26	92.9			82.5	144.4	24.50-25.08			
LO	*Discoaster berggrenii*			5.80									
FO	*Amaurolithus primus*	CN9b		6.70	119.4			100.0	186.3				
FO	*Discoaster quinqueramus*			7.46									
FO	*Discoaster berggrenii*	CN9a	NN11	8.00	133.3		111.0	111.1	214.6	39.98-41.18	103.78	67.87	104.12
FO	*Discoaster neorectus*	CN8b		8.5	133.3			120.6	218.3				
LO	*Discoaster hamatus*	CN8a	NN10	8.67	152.7		119.0	124.8	268.4	43.65-45.15	119.68	80.08	104.56
FO	*Discoaster neohamatus*			8.96									
FO	*Discoaster hamatus*	CN7	NN9	10.5	162.0			130.0	280.6	54.65-56.15	137.52	89.73	110.55
FO	*Catinaster coalitus*	CN6	NN8	11.1	170.8		124.5	130.0	290.5		139.58	94.21	113
FO	*Discoaster pentaradiatus*			12.0									
FO	*Discoaster kugleri*		NN7	12.2							156.6	106.75	
LO	*Coronocyclas nitescens*			12.7									
LO	*Coccolithus floridanus*	CN5b		13.1	181.1			135.5					
LO	*Sphenolithus heteromorphus*	CN5a	NN6	13.6	190.8		139.5	149.0		65.65-69.15	172.88	114.63	
FO	*Discoaster exilis*			15.4									
LO	*Helicosphaera ampliaperta*	CN4	NN5	16.0			149.0	158.5	362.1	74.00-76.58	193.15	116.65	
Acme top	*Discoaster deflandrei*			16.1									
FO	*Discoaster signus*			16.1									
FO	*Sphenolithus heteromorphus*	CN3		18.4	201.0		158.3		386.3				
LO	*Sphenolithus belemnos*		NN4	18.8							197	117.45	
LO	*Triquetrorhabdulus carinatus*		NN3	19.5						83.15-84.65	207.95	121.08	
FO	*Sphenolithus belemnos*	CN2		20.0	208.2		167.2	177.5	390.3				
FO	*Discoaster druggii*	CN1c	NN2	23.6				187.0	395.6	84.65-86.65	226.75	122	
LO	*Dictyococcites bisectus*	CN1a	NN1	23.7	221.2		195.4	193.0	453.9				
LO	*Sphenolithus ciperoensis*			23.7							256.65	160.09	
LO	*Sphenolithus distentus*	CP19b	NP25	26.0						89.65-91.15	278.6	170.2	
LO	*Chiasmolithus altus*			28.2									
FO	*Sphenolithus ciperoensis*	CP19a	NP24	30.2						96.15-98.95		184.1	
FO	*Sphenolithus distentus*	CP18		31.2									
LO	*Reticulofenestra umbilica*	CP17	NP23	34.2						111.53-114.80		209.6	113.84
LO	*Ericsonia formosa*	CP16c	NP22	34.9									
LO	*Isthmolithus recurvus*			34.9									
LO	*Reticulofenestra oamaruensis*			36.0									
LO	*Discoaster saipanensis*	CP16a	NP21	36.7								209.61	125.68
FO	*Isthmolithus recurvus*	CP15b	NP19	37.8						132.5		226.2	
FO	*Chiasmolithus oamaruensis*			39.8							278.61		
LO	*Chiasmolithus grandis*	CP15a	NP18	40.0									
FO	*Reticulofenestra reticulata*			42.1									
LO	*Chiasmolithus solitus*	CP14b	NP17	43.4									
FO	*Reticulofenestra umbilica*			43.5									
LO	*Nannotetrina fulgens*	CP14a		45.4									
LO	*Chiasmolithus gigas*	CP13c		47.0							279.1		138.85
FO	*Chiasmolithus gigas*	CP13b		49.0							283.89		140.77
FO	*Nannotetrina fulgens*	CP13a	NP15	49.8							291.65		
FO	*Discoaster sublodoensis*	CP12	NP14	52.6							310.55		
LO	*Tribrachiatus orthostylus*	CP11	NP13	53.7							329.55		
FO	*Discoaster lodoensis*	CP10	NP12	55.3		83.5					336.55		
LO	*Tribrachiatus contortus*	CP9b	NP11	56.3							349		
FO	*Discoaster diastypus*			56.5									
FO	*Tribrachiatus orthostylus*			56.6							372.61		
LO	*Fasciculithus* spp.	CP9a	NP10	57.8							391.55		
FO	*Tribrachiatus bramlettei*			57.8									
FO	*Discoaster multiradiatus*	CP8	NP9	59.2		114.5					401.88		
FO	*Heliolithus reidelii*	CP7	NP8	60.0							413.13		
FO	*Discoaster mohleri*	CP6	NP7	60.4		130.0					419.63		
FO	*Heliolithus kleinpellii*	CP5	NP6	61.6		150.0					428.35		
FO	*Ellipsolithus tympaniformis*			62.0							433.95		
FO	*Fasciculithus* spp.	CP4	NP5	62.0									
FO	*Ellipsolithus macellus*	CP3	NP4	63.7									
FO	*Prinsius martinii*			63.8									
FO	*Chiasmolithus danicus*	CP2	NP3	64.8									
FO	*Cruciplacolithus tenuis*	CP1b	NP2	65.9									
FO	*Biantholithus sparsus*	CP1a	NP1	66.4									
FO	*Nephrolithus frequens*			69.0									
LO	*Reticulofenestra levis*			69.0									

Table 4. (continued).

Event	Species	Zone (base) Okada and Bukry (1980)	Zone (base) Martini (1971)	Age (Ma)	Depth (mbsf) Site 528	Site 529	Site 658	Site 662	Site 663	Site 665	Site 667	Site 698
FO	*Emiliania huxleyi*	CN15	NN21	0.275			34.2-43.7	4.1-4.8	4.3-5.8			
LO	*Pseudoemiliania lacunosa*	CN14b	NN20	0.460		1.7	68.7-70.2	21.7-22.2	14.5-15.8	8.9-9.5	6.6-6.9	
LO	*Helicosphaera sellii*			1.19								
FO	*Gephyrocapsa*			1.36								
LO	*Calcidiscus macintyrei*			1.45	12.84		99.1-99.4	106.8-108.5	48.2-61.9	29.9-30.7	16.5-29.8	
FO	*Gephyrocapsa oceanica*			1.57								
LO	*Discoaster triradiatus*			1.89								
LO	*Discoaster brouweri*	CN13a	NN19	1.91	19.7	17.3	124.7-126.9	122.2-123.2	103.1-103.7	35.6-36.8		
Increase	*Discoaster triradiatus*			2.07			135.0-145.0	130.4-133.5	109.8-111.7	39.6-39.8		
LO	*Discoaster pentaradiatus*	CN12d	NN18	2.35			165.3-165.7	148.3-152.1	133.0-135.0	45.5-47.0	32.2-33.8	
LO	*Discoaster surculus*	CN12c	NN17	2.41			165.8-166.2	151.3-151.5	135.0-138.6	47.0-48.5	35.1-37.0	
LO	*Discoaster tamalis*	CN12b		2.65			197.7-201.3	159.5-160.5	141.6-143.2	50.7-51.2	40.5-41.7	
LO	*Discoaster variabilis*			2.90								
LO	*Sphenolithus*			3.45			281.4-290.9	189.7-193.9		63.8-64.4	48.8-49.6	
LO	*Reticulofenestra pseudoumbilica*	CN12a	NN16	3.56	27.85	19.05		193.9-196.7		65.0-65.4	49.6-54.2	
FO	*Discoaster tamalis*	CN11b		3.8								
LO	*Amaurolithus tricorniculatus*			3.7						67.1-69.9	58.3-67.8	
LO	*Amaurolithus primus*	CN11a	NN15	4.37	46.3	36.35						
FO	*Ceratolithus rugosus*	CN10c	NN13	4.66	55.6					72.7-73.8	75.8-78.3	
FO	*Ceratolithus acutus*	CN10b		4.85	55.61						79.7-85.1	
LO	*Discoaster quinqueramus*	CN10a	NN12	5.26							84.2-85.2	
LO	*Discoaster berggrenii*			5.80								
FO	*Amaurolithus primus*	CN9b		6.70							106.8-108.3	
FO	*Discoaster quinqueramus*			7.46							118.0-120.0	
FO	*Discoaster berggrenii*	CN9a	NN11	8.00	102.85							
FO	*Discoaster neorectus*	CN8b		8.5								
LO	*Discoaster hamatus*	CN8a	NN10	8.67	108.9							
FO	*Discoaster neohamatus*			8.96								
FO	*Discoaster hamatus*	CN7	NN9	10.5	115.34	37.46						
FO	*Catinaster coalitus*	CN6	NN8	11.1	117.69							
FO	*Discoaster pentaradiatus*			12.0								
FO	*Discoaster kugleri*		NN7	12.2	118.5							
LO	*Coronocyclas nitescens*			12.7								
LO	*Coccolithus floridanus*	CN5b		13.1							157.9-158.3	
LO	*Sphenolithus heteromorphus*	CN5a	NN6	13.6	118.51	55.25					160.3-160.9	
FO	*Discoaster exilis*			15.4								
LO	*Helicosphaera ampliaperta*	CN4	NN5	16.0	132.2	56.43					166.2-166.6	
Acme top	*Discoaster deflandrei*			16.1								
FO	*Discoaster signus*			16.1								
FO	*Sphenolithus heteromorphus*	CN3		18.4							207.7-208.0	
LO	*Sphenolithus belemnos*		NN4	18.8	132.74	69.73					211.3-211.7	
LO	*Triquetrorhabdulus carinatus*		NN3	19.5	145.21	74.05						
FO	*Sphenolithus belemnos*	CN2		20.0							244.7-229.8	
FO	*Discoaster druggii*	CN1c	NN2	23.6		82.05					250.4-257.8	
LO	*Dictyococcites bisectus*	CN1a	NN1	23.7								
LO	*Sphenolithus ciperoensis*			23.7		118.55					293.0-293.4	
LO	*Sphenolithus distentus*	CP19b	NP25	26.0		138.15					343.3-352.2	
LO	*Chiasmolithus altus*			28.2								
FO	*Sphenolithus ciperoensis*	CP19a	NP24	30.2							364.8-376.0	
FO	*Sphenolithus distentus*	CP18		31.2								
LO	*Reticulofenestra umbilica*	CP17	NP23	34.2		162.55						
LO	*Ericsonia formosa*	CP16c	NP22	34.9		186.07						
LO	*Isthmolithus recurvus*			34.9								
LO	*Reticulofenestra oamaruensis*			36.0								
LO	*Discoaster saipanensis*	CP16a	NP21	36.7	36.9	199.79						
FO	*Isthmolithus recurvus*	CP15b	NP19	37.8								
FO	*Chiasmolithus oamaruensis*			39.8	40.2							
LO	*Chiasmolithus grandis*	CP15a	NP18	40.0								
FO	*Reticulofenestra reticulata*			42.1								
LO	*Chiasmolithus solitus*	CP14b	NP17	43.4								
FO	*Reticulofenestra umbilica*			43.5								
LO	*Nannotetrina fulgens*	CP14a		45.4								
LO	*Chiasmolithus gigas*	CP13c		47.0								
FO	*Chiasmolithus gigas*	CP13b		49.0	253.5	223.15						
FO	*Nannotetrina fulgens*	CP13a	NP15	49.8		231						
FO	*Discoaster sublodoensis*	CP12	NP14	52.6								13.70-23.00
LO	*Tribrachiatus orthostylus*	CP11	NP13	53.7	269.5							23.00-32.50
FO	*Discoaster lodoensis*	CP10	NP12	55.3	284.8	247.15						
LO	*Tribrachiatus contortus*	CP9b	NP11	56.3								
FO	*Discoaster diastypus*			56.5	311.5							
FO	*Tribrachiatus orthostylus*			56.6	306.86							
LO	*Fasciculithus*	CP9a	NP10	57.8	313.2	264.5						62.80-71.02
FO	*Tribrachiatus bramlettei*			57.8								
FO	*Discoaster multiradiatus*	CP8	NP9	59.2		273.25						80.66-81.85
FO	*Heliolithus reidelii*	CP7	NP8	60.0		314.75						89.50-99.00
FO	*Discoaster mohleri*	CP6	NP7	60.4	346.7	319.8						
FO	*Heliolithus kleinpellii*	CP5	NP6	61.6		331.9						
FO	*Ellipsolithus tympaniformis*			62.0	379.7	348.7						
FO	*Fasciculithus*	CP4	NP5	62.0								
FO	*Ellipsolithus macellus*	CP3	NP4	63.7								
FO	*Prinsius martinii*			63.8								
FO	*Chiasmolithus danicus*	CP2	NP3	64.8	395.2	372.8						
FO	*Cruciplacolithus tenuis*	CP1b	NP2	65.9		383.63						
FO	*Biantholithus sparsus*	CP1a	NP1	66.4								
FO	*Nephrolithus frequens*			69.0								
LO	*Reticulofenestra levis*			69.0								

Table 4. (continued).

Event	Species	Zone (base)		Age	Site 699	Site 702	Site 709	Site 714	Site 716	Site 738	Site 748
		Okada and Bukry (1980)	Martini (1971)	(Ma)							
FO	*Emiliania huxleyi*	CN15	NN21	0.275							
LO	*Pseudoemiliania lacunosa*	CN14b	NN20	0.460							
LO	*Helicosphaera sellii*			1.19							
FO	*Gephyrocapsa*			1.36					34.8-36.3		
LO	*Calcidiscus macintyrei*			1.45			19.4-10.32		43.0-46.0		
FO	*Gephyrocapsa oceanica*			1.57			19.4-10.32		54.1-55.6		
LO	*Discoaster triradiatus*			1.89			20.92-19.4				
LO	*Discoaster brouweri*	CN13a	NN19	1.91			20.92-19.4		62.2-63.7		
Increase	*Discoaster triradiatus*			2.07							
LO	*Discoaster pentaradiatus*	CN12d	NN18	2.35			23.0-21.9		71.9-72.9		
LO	*Discoaster surculus*	CN12c	NN17	2.41			24.0-23.7				
LO	*Discoaster tamalis*	CN12b		2.65			28.5-27.3				
LO	*Discoaster variabilis*			2.90							
LO	*Sphenolithus*			3.45			34.0-33.4		103.8-105.3		
LO	*Reticulofenestra pseudoumbilica*	CN12a	NN16	3.56			36.3-35.5				
FO	*Discoaster tamalis*	CN11b		3.8							
LO	*Amaurolithus tricorniculatus*			3.7							
LO	*Amaurolithus primus*	CN11a	NN15	4.37							
FO	*Ceratolithus rugosus*	CN10c	NN13	4.66			54.8-53.3		123.2-129.2		
FO	*Ceratolithus acutus*	CN10b		4.85			57.8-56.3				
LO	*Discoaster quinqueramus*	CN10a	NN12	5.26			63.0-60.8		148.4-149.1		
LO	*Discoaster berggrenii*			5.80			107.6-104.6				
FO	*Amaurolithus primus*	CN9b		6.70							
FO	*Discoaster quinqueramus*			7.46							
FO	*Discoaster berggrenii*	CN9a	NN11	8.00							
FO	*Discoaster neorectus*	CN8b		8.5							
LO	*Discoaster hamatus*	CN8a	NN10	8.67			111.2-109.1	32.0-31.7			
FO	*Discoaster neohamatus*			8.96				53.9-52.8			
FO	*Discoaster hamatus*	CN7	NN9	10.5			114.2-112.7	55.8-55.6			
FO	*Catinaster coalitus*	CN6	NN8	11.1			115.7-114.2	62.0-61.35			
FO	*Discoaster pentaradiatus*			12.0							
FO	*Discoaster kugleri*		NN7	12.2				73.3-72.0			
LO	*Coronocyclas nitescens*			12.7				79.8-76.5			
LO	*Coccolithus floridanus*	CN5b		13.1				88.05-87.1			
LO	*Sphenolithus heteromorphus*	CN5a	NN6	13.6				88.05-87.1			
FO	*Discoaster exilis*			15.4							
LO	*Helicosphaera ampliaperta*	CN4	NN5	16.0				122.15-120.65			
Acme top	*Discoaster deflandrei*			16.1				127.55-126.75			
FO	*Discoaster signus*			16.1				127.55-126.75			
FO	*Sphenolithus heteromorphus*	CN3		18.4				163.3-163.0			
LO	*Sphenolithus belemnos*		NN4	18.8				166.6-165.3			
LO	*Triquetrorhabdulus carinatus*		NN3	19.5				166.6-165.3			
FO	*Sphenolithus belemnos*	CN2		20.0				171.1-169.6			
FO	*Discoaster druggii*	CN1c	NN2	23.6				179.3-177.8			
LO	*Dictyococcites bisectus*	CN1a	NN1	23.7				195.7-194.4			66.6-76.1
LO	*Sphenolithus ciperoensis*			23.7			201.1-198.1	197.2-195.7			
LO	*Sphenolithus distentus*	CP19b	NP25	26.0							
LO	*Chiasmolithus altus*			28.2							
FO	*Sphenolithus ciperoensis*	CP19a	NP24	30.2							
FO	*Sphenolithus distentus*	CP18		31.2							
LO	*Reticulofenestra umbilica*	CP17	NP23	34.2							
LO	*Ericsonia formosa*	CP16c	NP22	34.9							
LO	*Isthmolithus recurvus*			34.9							104.6-114.1
LO	*Reticulofenestra oamaruensis*			36.0						23.66-25.16	
LO	*Discoaster saipanensis*	CP16a	NP21	36.7							
FO	*Isthmolithus recurvus*	CP15b	NP19	37.8						39.26-40.66	123.6-133.1
FO	*Chiasmolithus oamaruensis*			39.8						69.7-71.16	142.6-152.1
LO	*Chiasmolithus grandis*	CP15a	NP18	40.0							
FO	*Reticulofenestra reticulata*			42.1						96.66-98.16	
LO	*Chiasmolithus solitus*	CP14b	NP17	43.4							152.1-161.6
FO	*Reticulofenestra umbilica*			43.5						118.46-119.96	
LO	*Nannotetrina fulgens*	CP14a		45.4							
LO	*Chiasmolithus gigas*	CP13c		47.0							
FO	*Chiasmolithus gigas*	CP13b		49.0							
FO	*Nannotetrina fulgens*	CP13a	NP15	49.8						196.8-205.26	
FO	*Discoaster sublodoensis*	CP12	NP14	52.6	452.62-449.10					226.26-227.79	
LO	*Tribrachiatus orthostylus*	CP11	NP13	53.7	464.08-468.10	200.23					268.0-277.5
FO	*Discoaster lodoensis*	CP10	NP12	55.3						255.79-264.76	277.5-287.0
LO	*Tribrachiatus contortus*	CP9b	NP11	56.3							
FO	*Discoaster diastypus*			56.5						278.9-284.30	
FO	*Tribrachiatus orthostylus*			56.6							315.5-320.5
LO	*Fasciculithus*	CP9a	NP10	57.8	487.10-499.45	239.63					320.5-330.0
FO	*Tribrachiatus bramlettei*			57.8							
FO	*Discoaster multiradiatus*	CP8	NP9	59.2		249.38				288.2-302.8	378.5-388.0
FO	*Heliolithus reidelii*	CP7	NP8	60.0		276.58					
FO	*Discoaster mohleri*	CP6	NP7	60.4						312.44-322.0	397.5-407.0
FO	*Heliolithus kleinpellii*	CP5	NP6	61.6						322.07-338.30	407
FO	*Ellipsolithus tympaniformis*			62.0							
FO	*Fasciculithus*	CP4	NP5	62.0							
FO	*Ellipsolithus macellus*	CP3	NP4	63.7							
FO	*Prinsius martinii*			63.8						359.5-360.85	
FO	*Chiasmolithus danicus*	CP2	NP3	64.8						364.35-364.85	
FO	*Cruciplacolithus tenuis*	CP1b	NP2	65.9						376.22-376.55	
FO	*Biantholithus sparsus*	CP1a	NP1	66.4							
FO	*Nephrolithus frequens*			69.0						409.14-411.04	416.5
LO	*Reticulofenestra levis*			69.0							

Table 4. (continued).

Event	Species	Zone (base) Okada and Bukry (1980)	Zone (base) Martini (1971)	Age (Ma)	Site 750	Site 752	Site 754	Site 756	Site 757	Site 758	Site 762*
FO	*Emiliania huxleyi*	CN15	NN21	0.275							
LO	*Pseudoemiliania lacunosa*	CN14b	NN20	0.460					2.3-3.8	6.0-7.5	4.4
LO	*Helicosphaera sellii*			1.19						15.6-17.1	
FO	*Gephyrocapsa*			1.36							
LO	*Calcidiscus macintyrei*			1.45					9.0-10.5		
FO	*Gephyrocapsa oceanica*			1.57							
LO	*Discoaster triradiatus*			1.89							
LO	*Discoaster brouweri*	CN13a	NN19	1.91		4.3	6.1-6.6	0.47-1.97	12.0-13.5	25.2-26.7	27.9
Increase	*Discoaster triradiatus*			2.07							
LO	*Discoaster pentaradiatus*	CN12d	NN18	2.35			6.6-8.1			33.3-34.8	
LO	*Discoaster surculus*	CN12c	NN17	2.41							35.9
LO	*Discoaster tamalis*	CN12b		2.65			9.6-11.1		15.5-17.0		
LO	*Discoaster variabilis*			2.90						37.8-39.3	
LO	*Sphenolithus*			3.45							
LO	*Reticulofenestra pseudoumbilica*	CN12a	NN16	3.56		10.3	15.7-16.2	4.50-6.00	23.0-23.6	44.4-45.9	64.4
FO	*Discoaster tamalis*	CN11b		3.8			17.7-19.2	8.00-8.50	26.6-28.1	57.0-58.5	
LO	*Amaurolithus tricorniculatus*			3.7							
LO	*Amaurolithus primus*	CN11a	NN15	4.37							
FO	*Ceratolithus rugosus*	CN10c	NN13	4.66							92.9
FO	*Ceratolithus acutus*	CN10b		4.85		19.1	22.7-25.3		38.2-39.7		
LO	*Discoaster quinqueramus*	CN10a	NN12	5.26					42.8-44.3	69.7-71.2	99.4
LO	*Discoaster berggrenii*			5.80							
FO	*Amaurolithus primus*	CN9b		6.70		25.1	31.8-34.9		52.5-54.0	83.1-84.6	
FO	*Discoaster quinqueramus*			7.46					62.2-63.6	102.4-103.9	
FO	*Discoaster berggrenii*	CN9a	NN11	8.00							111.9
FO	*Discoaster neorectus*	CN8b		8.5							
LO	*Discoaster hamatus*	CN8a	NN10	8.67				34.70-35.67	71.2-71.8	116.6-118.1	
FO	*Discoaster neohamatus*			8.96							
FO	*Discoaster hamatus*	CN7	NN9	10.5				37.30-38.80			118.4
FO	*Catinaster coalitus*	CN6	NN8	11.1							
FO	*Discoaster pentaradiatus*			12.0			46.5-48.5				
FO	*Discoaster kugleri*		NN7	12.2							
LO	*Coronocyclas nitescens*			12.7							
LO	*Coccolithus floridanus*	CN5b		13.1					80.9-81.5		
LO	*Sphenolithus heteromorphus*	CN5a	NN6	13.6		58.1	73.5-77.0	45.40-46.90	83.0-84.5		125.9
FO	*Discoaster exilis*			15.4			80.0-83.2		89.0-90.5		
LO	*Helicosphaera ampliaperta*	CN4	NN5	16.0							
Acme top	*Discoaster deflandrei*			16.1							
FO	*Discoaster signus*			16.1							
FO	*Sphenolithus heteromorphus*	CN3		18.4		73.1	86.7-89.7	54.70-56.20	95.7-97.2		
LO	*Sphenolithus belemnos*		NN4	18.8						144.0-145.5	133.5
LO	*Triquetrorhabdulus carinatus*		NN3	19.5							
FO	*Sphenolithus belemnos*	CN2		20.0			89.7-92.9		98.7-100.2		
FO	*Discoaster druggii*	CN1c	NN2	23.6					100.2-100.8		
LO	*Dictyococcites bisectus*	CN1a	NN1	23.7		91.7	107.1-108.6				144.9
LO	*Sphenolithus ciperoensis*			23.7				73.70-74.70	100.8-102.3	195.3-196.8	
LO	*Sphenolithus distentus*	CP19b	NP25	26.0							
LO	*Chiasmolithus altus*			28.2		93.4	116.8-113.8				
FO	*Sphenolithus ciperoensis*	CP19a	NP24	30.2				94.20-96.10	105.3-106.8	218.3-219.8	152.9
FO	*Sphenolithus distentus*	CP18		31.2					110.5-112.0	237.7-239.2	
LO	*Reticulofenestra umbilica*	CP17	NP23	34.2				117.70-119.20	115.0-116.5		162.4
LO	*Ericsonia formosa*	CP16c	NP22	34.9					119.5-120.1		173.4
LO	*Isthmolithus recurvus*			34.9							
LO	*Reticulofenestra oamaruensis*			36.0							
LO	*Discoaster saipanensis*	CP16a	NP21	36.7				134.90-136.40	123.1-124.6		200
FO	*Isthmolithus recurvus*	CP15b	NP19	37.8		104.3			129.1-129.8		222
FO	*Chiasmolithus oamaruensis*			39.8							
LO	*Chiasmolithus grandis*	CP15a	NP18	40.0					131.8-133.3		246
FO	*Reticulofenestra reticulata*			42.1							
LO	*Chiasmolithus solitus*	CP14b	NP17	43.4							272.5
FO	*Reticulofenestra umbilica*			43.5							
LO	*Nannotetrina fulgens*	CP14a		45.4					153.6-155.1		
LO	*Chiasmolithus gigas*	CP13c		47.0					158.4-159.9		
FO	*Chiasmolithus gigas*	CP13b		49.0					166.0-167.5		
FO	*Nannotetrina fulgens*	CP13a	NP15	49.8					174.7-175.3		307.5
FO	*Discoaster sublodoensis*	CP12	NP14	52.6					185.7-187.2		329.5
LO	*Tribrachiatus orthostylus*	CP11	NP13	53.7					202.0-203.5		334.5
FO	*Discoaster lodoensis*	CP10	NP12	55.3		114.3			211.7-213.2		369.5
LO	*Tribrachiatus contortus*	CP9b	NP11	56.3							393
FO	*Discoaster diastypus*			56.5							
FO	*Tribrachiatus orthostylus*			56.6							
LO	*Fasciculithus*	CP9a	NP10	57.8							407
FO	*Tribrachiatus bramlettei*			57.8		171.1					
FO	*Discoaster multiradiatus*	CP8	NP9	59.2		202.05				264.1-265.4	421.5
FO	*Heliolithus reidelii*	CP7	NP8	60.0		219.5					
FO	*Discoaster mohleri*	CP6	NP7	60.4						271.1-271.6	434
FO	*Heliolithus kleinpellii*	CP5	NP6	61.6		251.4					459.5
FO	*Ellipsolithus tympaniformis*			62.0	309.55-309.77	297.7				290.4-291.6	
FO	*Fasciculithus*	CP4	NP5	62.0							480
FO	*Ellipsolithus macellus*	CP3	NP4	63.7							489.5
FO	*Prinsius martinii*			63.8		318.7					
FO	*Chiasmolithus danicus*	CP2	NP3	64.8	346.42-346.44	345.1				292.1-295.6	529
FO	*Cruciplacolithus tenuis*	CP1b	NP2	65.9		353.46					552.5
FO	*Biantholithus sparsus*	CP1a	NP1	66.4	350.0	358.5					556
FO	*Nephrolithus frequens*			69.0		422.3				295.8-295.9	
LO	*Reticulofenestra levis*			69.0	394.6-394.4						

Table 5. Transition ages and depth (mbsf) for Indian and South Atlantic Ocean DSDP and ODP sites.

Normal polarity interval (Ma)	Transition	Depth (mbsf)																					
		Site 519	Site 521	Site 522	Site 523	Site 524	Site 525	Site 527	Site 528	Site 529	Site 659 Hole A	Site 665 Hole A	Site 689	Site 690	Site 699	Site 700	Site 702	Site 704	Site 709 Hole A	Site 744	Site 751	Site 752	Site 758 Hole A	Site 758 Hole B
0.00																								
0.73	Brunhes/Matyama?	8.94-9.02	3.40-3.43	4.32-4.51							22.8	14.8			10.59			34.51	9.00	3.80-6.30			10.90	10.70
0.91	Jaramillo(T)	13.89-14.11	3.70-4.33								28.6	19.3						38.41					14.20	14.25
0.98	Jaramillo(O)	31.63-32.01	5.16-5.30								31	21						44.27					15.30	15.25
1.66	Olduvai(T)	35.83-36.21	11.60-12.11	9.31-9.85								33.2			19.59			89.09		9.30-9.80				24.30
1.88	Olduvai(O)	42.00-42.63	13.31-13.69	10.53-10.98								36.4			21.19				21.35	9.80-10.3			26.00	26.40
2.47	Matuyama/Gauss	51.38-51.42	20.41-22.24	14.91-15.90								49.1		4.83	29.45			168.45	26.05	14.8-15.3			34.20	34.75
2.92	Kaena(T)	61.91-63.51												6.71				176.1					39.50	39.00
2.99	Kaena(O)													6.98				177.8					40.50	40.25
3.08	Mammoth(T)	65.31-65.53	30.41-30.65															179.1	30.55				41.90	41.40
3.18	Mammoth(O)																	181.5	31.65				42.90	42.60
3.40	Gauss/Gilbert	65.31-65.53	35.21-35.41	24.79-24.86											40.69			186.64	33.25	18.3-20.8				45.70
3.88	C3N-1 top	84.71-85.51											3.38	10.23				195.55		20.4				53.00
3.97	C3R-1 top												4.4	10.48				201.94		20.6				54.50
4.10	C3N-2 top	87.15-87.19											8.79	11.21				204.19					56.20	56.80
4.24	C3R-2 top												9.63	11.78				210.35					58.70	58.30
4.40	C3N-3 top	95.38-95.59											11.45	18.32				211.99					61.50	61.10
4.47	C3R-3 top												11.72					213.24					63.05	62.40
4.57	C3N-4 top	101.96-103.02											15.17					215.4			36.7		64.00	63.20
4.77	C3R-4 top												16.92					219.74			40.2		66.70	
5.35	C3AN-1 top	116.55-116.57													53.61			224.76			42.6		76.40	
5.53	C3AR-1 top																	231.04					80.50	80.40
5.68	C3AN-2 top	120.36-120.41																233.84					82.70	82.20
5.89	C3AR-2 top																	241.62		23.3-23.8	48.5		84.30	85.40
6.37	C3AN-3 top	121.84-121.92											18.09					251.25			50.6		90.20	89.40
6.50	C3AR-3 top												18.67					256.75					92.10	91.00
6.70	C4N-1 top												18.92					259.5						
7.41	C4R-3 top												20.17					275.85						
7.90	C4AN-1 top												22.15					290.06						
8.21	C4AR-1 top													20.07				318.55						
8.41	C4AN-2 top																	324.1						
8.50	C4AR-2 top												23.65					327.05						
8.71	C4AN-3 top												23.81					338.55						
8.80	C4AR-3 top												24.17											
8.92	C5N-1 top												24.67							24.3-24.8	54.4-57.2			
10.42	C5R-1 top												34.55	28.03				409.64		39.8-40.3				
10.54	C5N-2 top													29.53						40.3-41.92				
10.59	C5R-2 top													29.78						41.92-42.58				
11.03	C5N-3 top												37.55							50.42-51.39				
11.09	C5R-3 top												37.93							51.39-52.05				
11.55	C5AN-1 top												45.93	31.72				429.6						
11.73	C5AR-1 top												46.41	32.45										
11.86	C5AN-2 top												46.68	33.47										
12.12	C5AR-2 top												47.18	33.95							108			
12.83	C5AN-5 top												48.68	36.35										
13.01	C5AR-5 top												49.18	36.91										
13.20	C5AN-6 top												49.68	37.2										
13.46	C5AR-6 top												50.91	37.97										
13.69	C5AN-7 top												51.93	38.97						54.91-55.38				
14.08	C5AR-7 top												52.41	39.95										

Table 5. (continued).

Normal polarity interval (Ma)	Transition	Depth (mbsf)																						
		Site 519	Site 521	Site 522	Site 523	Site 524	Site 525	Site 527	Site 528	Site 529	Site 659 Hole A	Site 665 Hole A	Site 689	Site 690	Site 699	Site 700	Site 702	Site 704	Site 709 Hole A	Site 744	Site 751	Site 752	Site 758 Hole A	Site 758 Hole B
38.83	C16N-3 top													92.21						170.0-170.4				
39.24	C16R-3 top												144.77	95.70						172.3-173.4				
39.53	C17N-1 top				111.61-111.81								145.02	96.59										
40.43	C17R-1 top													99.04										
40.50	C17N-2 top													99.41										
40.70	C17R-2 top												151.73											
40.77	C17N-3 top												151.95											
41.11	C17R-3 top												152.73											
41.29	C18N top				123.41-124.99								153.70											
42.73	C18R top							136.31					161.17				71.84-71.96							
43.60	C19N top				140.05-140.25												84.25-85.26							
44.06	C19R top												163.16			48.45	86.45-86.55							
44.66	C20N top				147.75-147.95			137.61					165.55	106.27		55.76	98.65-98.75							
46.17	C20R top				162.11-162.31			138.71	248.59				171.11	118.23		68.60	113.34-113.45							
48.75	C21N top							143.45	257.05				183.23		405.65		157.25-157.35							
50.34	C21R top							148.09	258.24				197.89	123.63	434.68									
51.95	C22R top							153.59						130.48	455.21	152.01								
52.62	C22N top							154.73						132.23	464.65	164.16								
54.70	C23R-2 top							163.88						133.18		190.86								
55.14	C24N-1 top								277.81					137.33										
55.37	C24R-1 top													139.67										
55.66	C24N-2 top							172.93						144.42								135.00		
56.14	C24R-2 top													154.63								157.00		
58.64	C25N top					58.11-58.32								185.48								201.00		
59.24	C25R top													195.94								(212-218)		
60.21	C26N top													210.05		267.19						(222-229)		
60.75	C26R top							237.91		323.95				213.06								233.00		
63.03	C27N top					128.84-129.23		258.75	391.58							299.13						308.00		
63.54	C27R top							260.77														312.00		
64.29	C28N top					156.26-156.64	443.81	267.41					228.61									(336-349)		
65.12	C28R top						447.03	272.22																
65.50	C29N top					185.10-185.48	447.91	273.72	399.47							327.31								
66.17	C29R top						450.99	278.02	405.97	385.10				247.55		333.29						355.00		
66.74	C30N top					213.02-213.72	456.69	286.61	413.34	394.17				252.28								(360-364)		
68.42	C30R top						475.15						246.60									388.00		
68.52	C31N top					267.31-267.81	476.50	329.63					248.08									393.00		
69.40	C31R top					303.93-303.94	489.26		464.57				252.92	272.25		344.22						398.00		
71.37	C32N top						519.95						259.97	283.39		357.75								
71.65	C32R top												272.33	302.78										
71.91													277.32	308.02										
74.30																384.82								
80.17																407.45								
84.00																430.95								

Table 5. (continued).

Normal polarity interval (Ma)	Transition	Depth (mbsf)																						
		Site 519	Site 521	Site 522	Site 523	Site 524	Site 525	Site 527	Site 528	Site 529	Site 659 Hole A	Site 665 Hole A	Site 689	Site 690	Site 699	Site 700	Site 702	Site 704	Site 709 Hole A	Site 744	Site 751	Site 752	Site 758 Hole A	Site 758 Hole B
14.20	C5AN-8 top												52.85	40.2										
14.66	C5AR-8 top													41.68						58.14-59.22				
14.87	C5BN-1 top													42.16						59.75-60.38	109.55			
14.96	C5BR-1 top													42.41										
15.13	C5BN-2 top												56.53											
15.27	C5BR-2 top												57.4							60.91-61.81				
16.22	C5CN-1 top																			64.84-65.37	114			
16.98	C5CR-3 top																			66.85-66.95	123.2			
17.57	C5DN-1 top																	489.5		71.6-72.4	132.7			
17.90	C5DR-1 top													44.68				498.2		75.25-75.76				
18.12	C5DN-1 top												60.03	45.41						77.1				
18.14	C5DR-1 top												60.4	45.68						77.5				
18.56	C5EN top												61.76	46.68							152.1			
19.09	C5ER top																			81.0-82.4				
19.35	C6N top																			83.11-83.26				
20.45	C6R top								149.11											92.48-93.11				
20.88	C6AN-1 top																			94.40-94.86				
21.16	C6AR-1 top								153.21											96.46-96.90				
22.57	C6BN top			54.32-54.45																				
23.27	C6CN-1 top			55.51-55.71											87.57									
23.55	C6CN-2 top			57.01-57.21																				
24.04	C6CN-3 top			58.51-58.71																97.76				
24.21	C6CR-3 top														94.47									
25.50	C7N-1 top			63.70-64.21					170.96						115.35									
25.67	C7N-2 top												67.11											
25.97	C7R-2 top												67.88		127.69									
26.38	C7AN top			68.01-68.66									68.61		137.09					98.17-99.62				
26.56	C7AR top												68.88		140.38					99.98-100.49				
26.86	C8N-1 top			69.71-70.01									69.38	53.25	143.84					104.5-105.07				
26.93	C8R-1 top												70.11	54.75										
27.01	C8N-2 top												70.38	55.00										
27.74	C8R-2 top												75.98	60.11	156.14					111.56-112.07				
28.15	C9N-1 top			78.34-78.54					182.06				79.46	60.99	166.95					115.01-115.58				
28.74	C9R-1 top												85.05											
29.21	C9R-2 top													68.48	182.69									
29.73	C10N-1 top			86.49-86.68									89.82		189.34									
30.33	C10R-2 top												91.93		198.35									
31.23	C11N-1 top			95.37-96.24					190.36				100.23		208.34									
32.06	C11R-2 top												103.38	73.93	216.05					118.29-118.45				
32.46	C12N top			104.09-104.52									104.38	80.76						118.79-119.93				
32.90	C12R top				76.02-76.24				201.36				106.88	84.01						124.30-125.47				
35.29	C13N top			128.44-128.49	92.59-92.91				221.83				116.71							139.0-139.5				
35.87	C13R-2 top			134.15-134.35					226.03				119.70		284.55					146.5-146.77				
37.24	C15N-1 top			148.78-148.98									128.33							155.4-155.9				
37.68	C15R-2 top												134.02							157.9-158.3				
38.10	C16N-1 top			154.59-154.91									135.77							161.3-161.9				
38.34	C16R-1 top												139.45							162.4-163.4				
38.50	C16N-2 top												139.55							164.3-164.9				
38.79	C16R-2 top													91.95						166.68-168.9				

Table 6. Paleolatitude and paleolongitude for Indian and South Atlantic Ocean DSDP and ODP sites.

Age (Ma)	Latitude	Longitude
Site 214		
0	-11.3368	88.7180
10	-15.9456	84.8116
20	-20.5250	80.8046
35	-27.3647	75.6525
45	-30.3489	71.2536
55	-37.6345	66.5541
60	-43.5605	63.1810
66	-53.9952	55.9089
Site 216		
0	1.4622	90.2080
10	-3.2994	87.3183
20	-7.9936	83.9027
35	-15.1726	80.1364
45	-18.3758	76.4942
55	-25.8665	72.7479
60	-31.9171	70.1932
66	-42.8533	65.7410
Site 237		
0	-7.0832	58.1247
10	-8.1770	56.7058
20	-10.0566	55.1970
35	-13.5454	53.8467
45	-14.8039	52.7407
55	-15.9938	52.3575
60	-17.3310	51.9533
66	-22.4280	49.7591
Site 238		
0	-11.1535	70.5260
10	-14.1274	66.4282
20	-17.6872	62.1526
35	-22.4291	56.7264
45	-23.8565	52.5880
Site 709		
0	-3.9120	60.5517
10	-4.8220	58.9752
20	-6.4862	57.2805
35	-9.6658	55.6776
45	-10.7405	54.4558
55	-11.7185	53.9289
60	-12.9602	53.4716
66	-15.7036	52.4378
Site 738		
0	-62.7092	82.7875
10	-62.4770	80.2168
20	-62.8313	79.5958
35	-63.5433	78.9116
45	-62.6609	76.7674
55	-61.4366	74.9877
60	-61.6973	74.4524
66	-63.3389	73.4704
Site 744		
0	-61.5777	80.5910
10	-61.3221	78.0938
20	-61.6922	77.4088
35	-62.4115	76.6534
45	-61.4999	74.6470
55	-60.2574	72.9944
60	-60.5309	72.4101
66	-62.1785	71.2999
Site 748		
0	-58.4408	78.9815
10	-58.1638	76.6303
20	-58.5497	75.8385
35	-59.2735	75.0103
45	-58.3423	73.2131
55	-57.0886	71.7107
60	-57.3704	71.0416
66	-59.0207	69.8372
Site 750		
0	-57.5920	81.2395
10	-57.3442	78.9036
20	-57.7088	78.1143
35	-58.4260	77.3241
45	-57.5245	75.5062
55	-56.2898	73.9504
60	-56.5576	73.2808
66	-58.2030	72.1747
Site 751		
0	-57.7260	79.8148
10	-57.4782	77.4789
20	-57.8428	76.6896
35	-58.5600	75.8994
45	-57.6585	74.0815
55	-56.4238	72.5257
60	-56.6916	71.8561
66	-58.3370	70.7500
Site 752		
0	-30.8913	93.5775
10	-35.8046	88.0336
20	-40.4972	83.0759
35	-47.4277	75.2207
45	-49.7730	69.4555
55	-49.0639	67.5327
60	-49.4415	67.3313
66	-51.1781	67.0640
Site 754		
0	-30.9407	93.5658
10	-35.8529	88.0160
20	-40.5448	83.0540
35	-47.4727	75.1873
45	-49.8163	69.4157
55	-49.1061	67.4905
60	-49.4835	67.2886
66	-51.2198	67.0189
Site 756		
0	-27.3548	87.5973
10	-31.8147	82.1515
20	-36.2513	77.1224
35	-42.6070	69.4599
45	-45.2435	63.6150
55	-52.0742	56.5491
60	-57.6124	50.7719
66	-66.4441	34.9935
Site 757		
0	-17.0233	88.1802
10	-21.5704	83.7710
20	-26.0973	79.4448
35	-32.7713	73.5277
45	-35.6424	68.6980
55	-42.7977	63.3564
60	-48.6259	59.3740
66	-58.6726	49.9854
Site 758		
0	5.3842	90.3612
10	0.6002	87.7646
20	-4.1143	84.5032
35	-11.3592	81.0910
45	-14.6066	77.6362
55	-22.1319	74.0700
60	-28.1985	71.6449
66	-39.2081	67.6717
Site 762		
0	-19.8872	112.2540
10	-25.8986	108.4818
20	-31.0841	105.0744
35	-39.5450	100.8771
45	-42.8307	96.9645
55	-42.9795	95.3122
60	-43.3728	95.3188
66	-45.1141	96.0148
Site 689		
0.0	-64.5167	3.1000
5.9	-66.2000	4.9456
23.0	-69.0000	6.9186
37.7	-71.0000	11.9846
59.2	-67.1000	5.1890
66.2	-67.2000	3.4593
Site 690		
0.0	-65.1667	1.2000
5.9	-66.6000	3.3355
23.0	-69.2000	4.9584
37.7	-71.5000	10.3713
59.2	-67.5000	4.1512
66.2	-67.4000	1.6143
Site 698		
0.0	-51.4585	-33.0993
37.7	-58.0000	18.5531
59.2	-56.1000	9.2249
66.2	-57.1000	7.6105
Site 699		
0.0	-51.5423	-30.6770
37.7	-58.0000	16.1332
59.2	-56.1000	6.8033
66.2	-56.9000	4.8430
Site 700		
0.0	-51.5330	-30.2781
37.7	-58.0000	15.3265
59.2	-56.1000	6.2268
66.2	-56.9000	4.1512
Site 702		
0.0	-50.9464	-26.3686
37.7	-57.7000	12.0999
59.2	-55.5000	2.6521
66.2	-56.7000	1.6143
Site 704		
0.0	-46.8800	7.4217
5.9	-48.9000	7.8211
23.0	-53.6000	6.9186
Site 525		
0.0	-29.0712	2.9853
5.9	-31.9485	2.9528
23.0	-36.0485	2.1535
37.7	-39.2485	0.1930
59.2	-37.8485	-0.8445
66.2	-39.8485	-2.5742
Site 526		
0.0	-29.1227	3.1380
5.9	-32.0000	3.1054
23.0	-36.1000	2.3062
37.7	-39.3000	0.3457
59.2	-37.9000	-0.6919
66.2	-39.9000	-2.4215
Site 527		
0.0	-28.0415	1.7633
5.9	-30.9188	1.7308
23.0	-35.0188	0.9315
37.7	-38.2188	-1.0290
59.2	-36.8188	-2.0665
66.2	-38.8188	-3.7962
Site 528		
0.0	-28.5248	2.3240
5.9	-31.4022	2.2914
23.0	-35.5022	1.4922
37.7	-38.7022	-0.4683
59.2	-37.3022	-1.5059
66.2	-39.3022	-3.2355
Site 529		
0.0	-28.9305	2.7680
5.9	-31.8078	2.7354
23.0	-35.9078	1.9362
37.7	-39.1078	-0.0243
59.2	-37.7078	-1.0619
66.2	-39.7078	-2.7915
Site 516		
0.0	-30.2767	-35.6183
5.9	-31.8000	-34.0447
Site 517		
0.0	-30.9467	-38.0417
5.9	-32.7000	-36.6901
Site 518		
0.0	-29.9733	-38.1350
5.9	-31.7000	-36.4601
Site 519		
0.0	-26.1367	-11.6662
5.9	-28.2000	-12.3067
Site 521		
0.0	-26.0738	-10.2645
5.9	-28.1000	-10.3514
Site 522		
0.0	-26.1140	-5.1130
5.9	-28.1000	-5.6358
23.0	-33.3000	-6.6880
37.7	-35.0000	8.0666
Site 523		
0.0	-28.5522	-2.2513
5.9	-30.9000	-1.8403
23.0	-34.7000	-3.4593
37.7	-37.3000	-4.6095
59.2	-36.4000	-5.7655
Site 658		
0.0	20.7492	-18.5812
5.9	-19.0000	-18.7476
Site 366		
0.0	5.6783	-19.8517
5.9	3.9000	-22.0831
23.0	0.4000	-19.6028
37.7	-2.1000	-19.8207
Site 667		
0.0	4.5692	-21.9113
5.9	1.0000	-19.7827
23.0	-1.8000	-22.2550
37.7	-3.9000	-22.4712

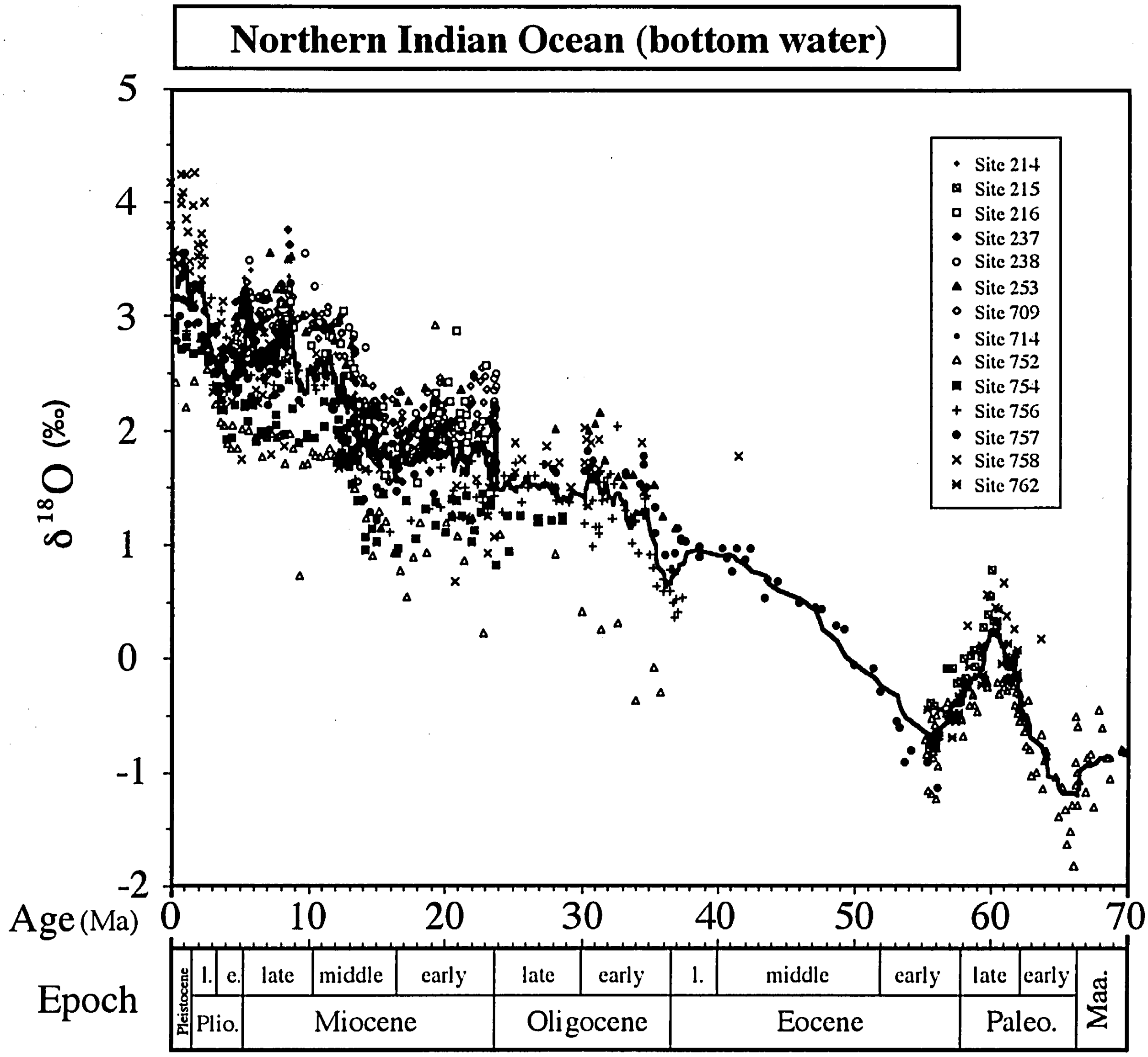

Fig. 36. Composite oxygen isotope record of bottom water in the Northern Indian Ocean region. All data corrected to dissolved inorganic carbon (DIC) of bottom water (See III-A-1 section). The smoothed curve is obtained by 15-point running average.

consequence there is less scatter in $\delta^{18}O$ values. Afterward, the general trends of surface $\delta^{18}O$ value are close to constant, although they exhibit a large fluctuation (~1.8‰). From the Miocene, the general trend of surface oxygen isotopic record shows the opposite pattern to that of bottom water, and consequently the $\delta^{18}O$ difference between surface and bottom water is expanded. Near the present-day, this difference reaches 4.5‰.

The carbon isotopic values of bottom water tend to increase about 2.5‰ from 70 to 65 Ma. Across the K/T boundary, no remarkable change in $\delta^{13}C$ values is found, however they fluctuate. Around the late / early Paleocene boundary (63 Ma), $\delta^{13}C$ shows a minimum value (~1.8‰). The carbon isotopic ratios rapidly increase from this minimum value to a maximum (~3.0‰) at 60 Ma within the late Paleocene, which shows the highest values among the Cenozoic data. Across the Paleocene / Eocene boundary, they exhibit a remarkable negative shift by 2.5‰ to the minimum value zone in the earliest Eocene (56-54 Ma). $\delta^{13}C$ values in the minimum zone are largely fluctuated, and are around 0.6‰. $\delta^{13}C$ values increase by 1.2‰ from 55 to 53 Ma and remain around 1.6‰ from the late early to late Eocene (53-37 Ma). Around the Oligocene / Eocene boundary, they increase slightly to 1.8‰. From the Oligocene, two remarkable carbon isotopic negative shifts are observed in the earliest Oligocene (33 Ma) and the latest Miocene (6 Ma, Chron-6

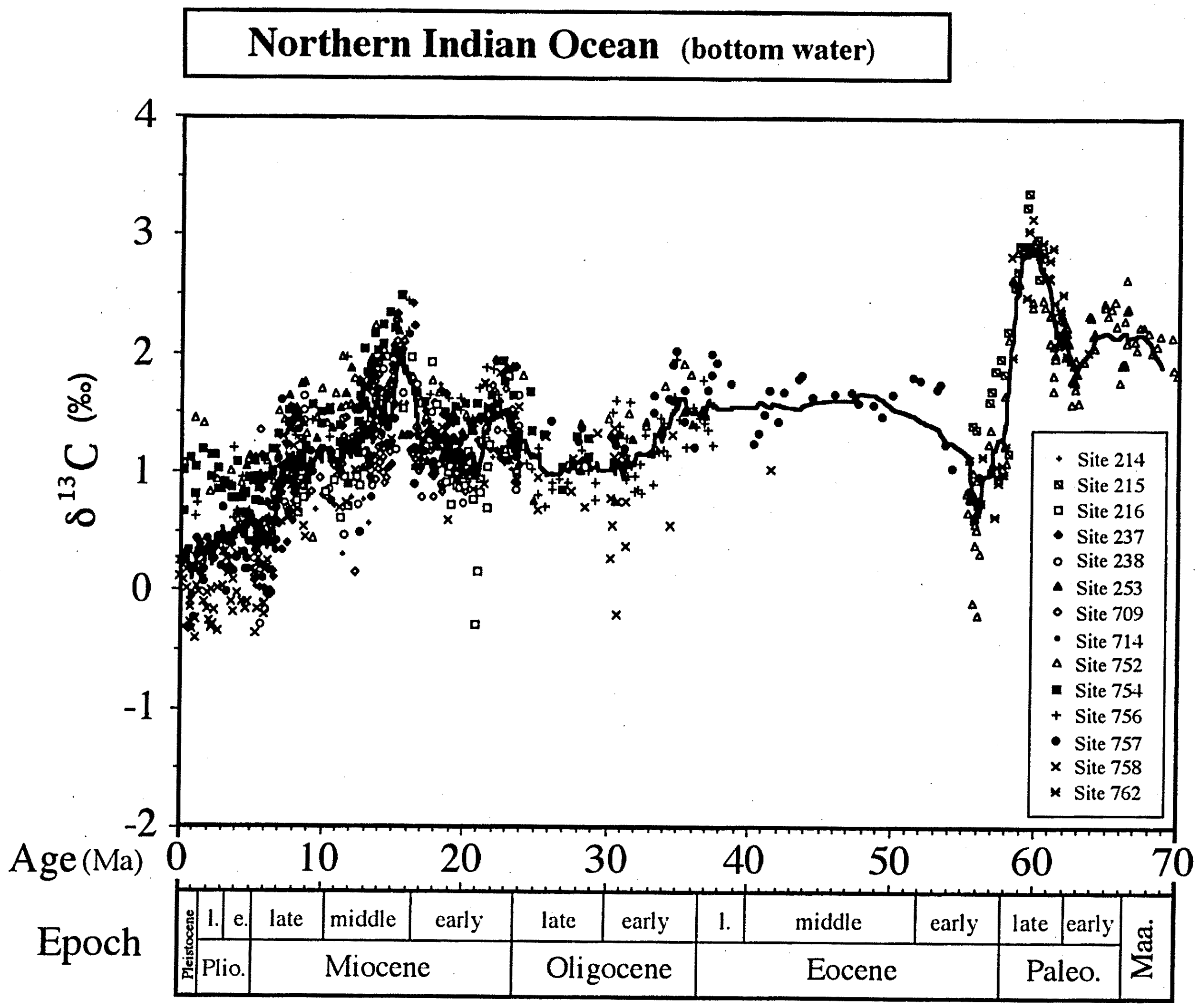

Fig. 37. Composite carbon isotope record of bottom water in the Northern Indian Ocean region. All data corrected to DIC of bottom water (See III-A-1 section). The smoothed curve is obtained by 15-point running average.

Shift: Vincent *et al.*, 1985). The magnitudes of these shifts are ~0.7‰ and ~0.8‰, respectively. During the interval between these two shifts, $\delta^{13}C$ values are constant at ~1.0‰ with a range of 1.0‰. In this interval, pronounced peaks are recognized in the earliest Miocene (23 Ma) and the middle Miocene (15 Ma, Monterey Excursion: Vincent and Berger, 1985). $\delta^{13}C$ ratios begin to increase from the Oligocene / Miocene boundary reaching a maximum value (~1.5‰) at 23 Ma, and subsequently decreasing at 20 Ma. It ratios increase again from 17 Ma, reaching a maximum value (~2.2‰) at 15 Ma, and decreasing to 1.0 ‰ at 12 Ma (the peak of the middle Miocene). The magnitude of the middle Miocene peak is higher than that of the earliest Miocene. After the shift in the latest Miocene, $\delta^{13}C$ values are generally constant around 0.5‰, but the degree of scatter is relatively high (~1.5‰).

The carbon isotopic ratios of surface water vary in a similar pattern to that of bottom waters during the Paleocene and Eocene. During the Paleocene, they are higher by ~0.5‰ than those of the bottom water. $\delta^{13}C$ differences between surface and bottom water increases to 0.8‰ at the earliest Eocene. From the middle Eocene to Oligocene, $\delta^{13}C$ values remain around 2.5‰ without any remarkable shifts. Consequently, the surface to bottom $\delta^{13}C$ difference expands to 1.1‰ in the late Oligocene. $\delta^{13}C$ values from the Oligocene / Miocene boundary to the early Miocene (20 Ma) decrease to a minimum value (~1.5‰). This minimum value is close to the present value, and at this time, the $\delta^{13}C$ difference between surface to bottom water is small (~0.4‰). During the Miocene, pronounced peaks are recognized at 15 and 8 Ma. For the peaks at 15 and 8 Ma, the values are ~2.7‰ and ~2.3‰, respectively. The peak at 15 Ma is remarkable in the carbon isotopic record of bottom water, whereas the peak at 8 Ma is weak, and consequently the surface to bottom difference increases more than 1.0‰ at this time. Although $\delta^{13}C$ values in surface water show a negative

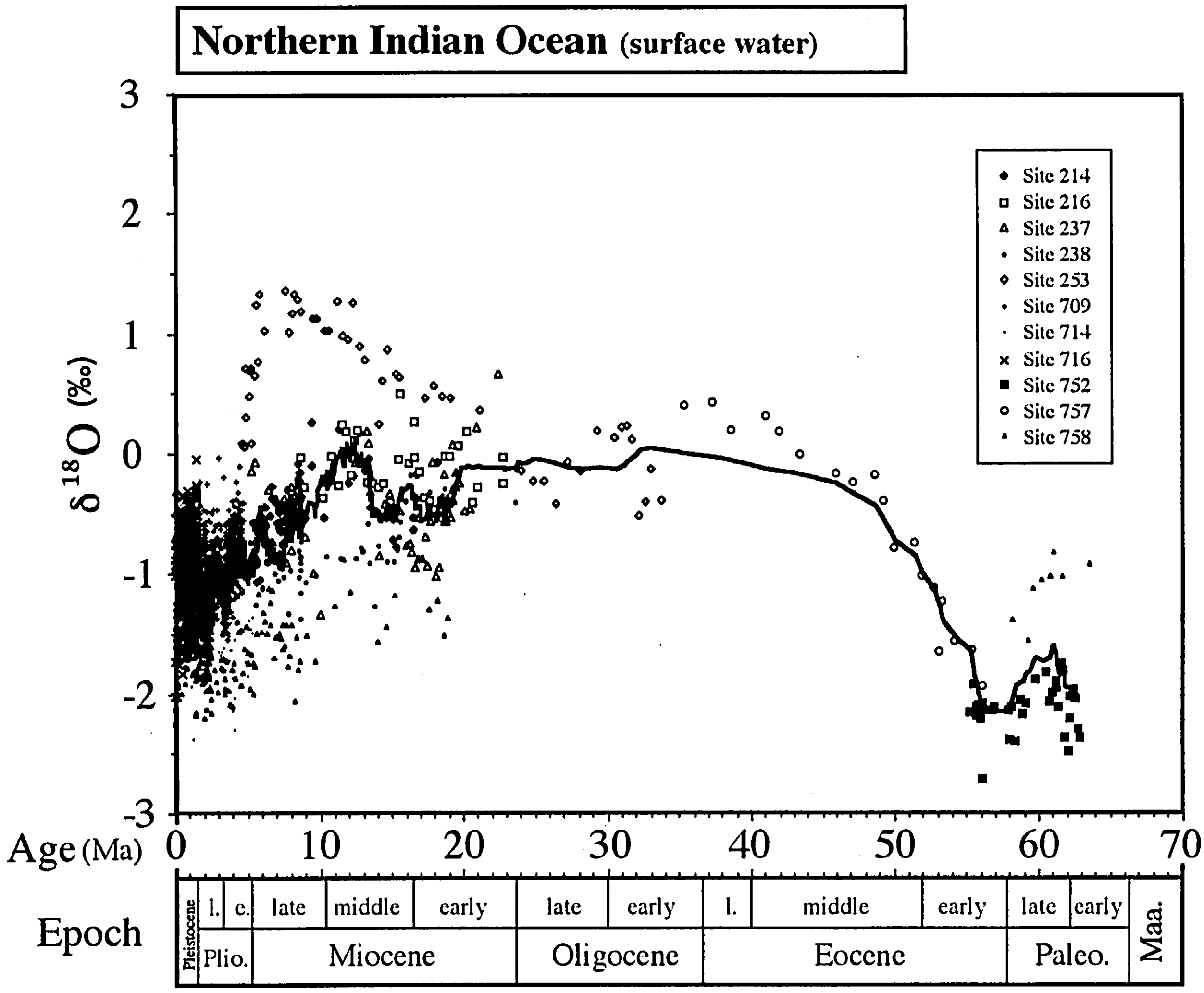

Fig. 38. Composite oxygen isotope record of surface water in the Northern Indian Ocean region. All data corrected to DIC of surface water (about 50 m below sea; See III-A-1 section). The smoothed curve is obtained by 15-point running average.

shift of 0.5‰ at ~6 Ma, the magnitude of this shift is smaller than that of the bottom waters. After the shift at 6 Ma, $\delta^{13}C$ values are constant around 1.4‰ with a low degree of scatter (~0.8‰). In this section, a weak peak (~0.3‰) is observed at 3 Ma. The carbon isotopic ratios of surface water are about 1.0‰ higher than those of bottom water.

C. Correlation of oxygen and carbon isotopes between the Indian Ocean and the South Atlantic Ocean

The isotopic records of the northern Indian Ocean are correlated with those of the Indian and South Atlantic Oceans. The general trends of carbon and oxygen isotopes in these ocean through the Cenozoic are illustrated in Figs. 40-53.

Oxygen isotopic record: During the late Maastrichtian, $\delta^{18}O$ values of bottom water in the Southern Ocean (Atlantic sector) are ~1.7‰ higher than those of the northern Indian Ocean. From 66 to 61 Ma within the Paleocene, although $\delta^{18}O$ values in the northern Indian Ocean rapidly increase, the increases in the South Atlantic and southern Indian Oceans are gradual. Consequently, the difference of $\delta^{18}O$ values between the northern Indian Ocean and the other oceans decreases to 0.4‰ in the ^{18}O maximum value at 61 Ma. Through the late Paleocene to Eocene, the same trends as those of the northern Indian Ocean are observed in all oceans. The $\delta^{18}O$ difference throughout the ocean is small. However, $\delta^{18}O$ values in the South Atlantic Ocean tend to be slightly higher than those of the other ocean. In the shift at the Oligocene / Eocene boundary, the net magnitude in the northern Indian Ocean is remarkably small (~0.6‰). The southern Indian Ocean exhibits a shift of ~0.8‰, the South Atlantic Ocean is ~ 0.6‰, the Southern Ocean (Atlantic sector) is ~1.0‰, and the Central Atlantic Ocean is ~1.0‰. This shift is generally large in the Antarctic Ocean, and tends to decrease northwards at this time. During the Oligocene, different trends in oxygen isotopes of bottom water are

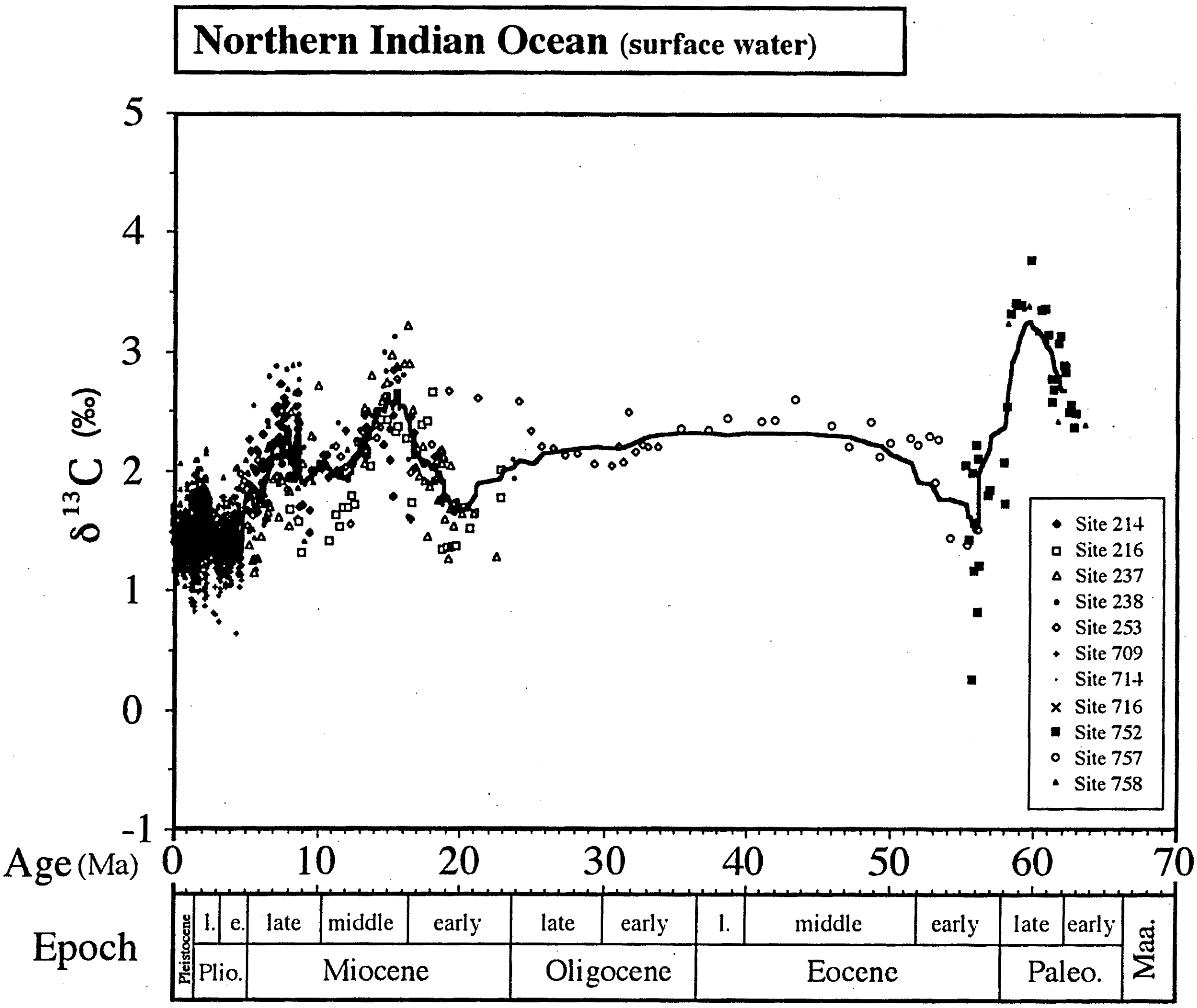

Fig. 39. Composite carbon isotope record of surface water in the Northern Indian Ocean region. All data corrected to DIC of surface water (about 50 m below sea; See III-A-1 section). The smoothed curve is obtained by 15-point running average.

recognized in each ocean. $\delta^{18}O$ values in the Southern Ocean (Atlantic sector) increase. In the northern Indian and Central Atlantic Oceans, they gradually increase, while they gradually decrease in the southern Indian and South Atlantic Oceans. Then, $\delta^{18}O$ values in the northern Indian, South and Central Atlantic Oceans become ~0.7‰, which is lower than those of the southern Indian and Southern Oceans. The shift in the middle Miocene is largest in the southern Indian Ocean (~0.9‰). The net magnitudes of this shift in the northern Indian and South Atlantic Oceans are ~0.8‰. In the Central Atlantic Ocean, the shift is remarkable small (~0.6‰). The decrease in $\delta^{18}O$ value before the shift is clearly observed in the southern Indian Ocean. The shift in the late Pliocene is most conspicuous in the Central Atlantic Ocean, and then the magnitude of shift reaches 1.3‰. The net magnitudes in other oceans are 1.1 to 0.6‰, and the northern Indian Ocean records the lowest magnitude. The magnitude of this shift tends to decrease southwards in the Atlantic Ocean side, and toward the Indian Ocean. Thus, $\delta^{18}O$ values appear to be highest in the Central Atlantic Ocean from the late Pliocene onwards.

From the Paleocene to Eocene, the oxygen isotopic records in surface water exhibit a similar pattern in all oceans. $\delta^{18}O$ values during the Paleocene, however, are different in each region. $\delta^{18}O$ values in the northern Indian Ocean are smallest at ~-2.0‰. The Southern Ocean and South Atlantic Oceans are ~1.5‰, which is larger than that of the northern Indian Ocean. In the South Atlantic Ocean, $\delta^{18}O$ values are larger at ~0.8‰ compared with the northern Indian Ocean. The magnitude of increase during the early Eocene is large in the northern Indian Ocean, and similar $\delta^{18}O$ values are recognized in the Indian and South Atlantic Oceans during the middle and late Eocene. In this interval, the surface to bottom $\delta^{18}O$ difference is also small (<1‰). A sharp increase at the Oligocene / Eocene boundary is recognized in the southern

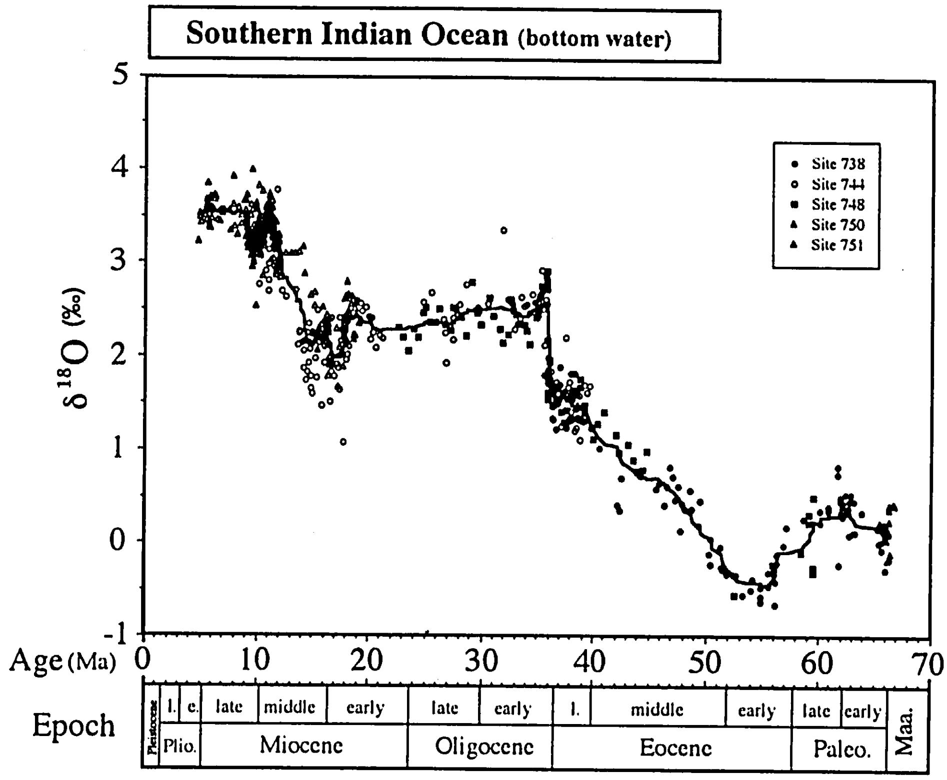

Fig. 40. Composite oxygen isotope record of bottom water in the Southern Indian Ocean region. All data corrected to DIC of bottom water (See III-A-1 section). The smoothed curve is obtained by 15-point running average.

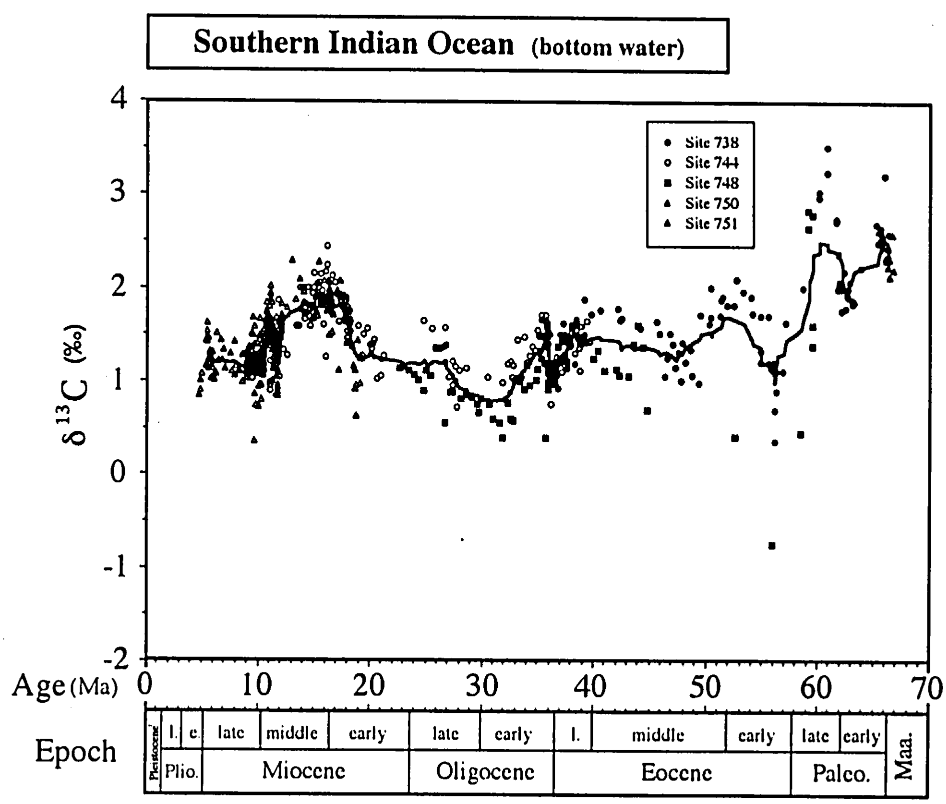

Fig. 41. Composite carbon isotope record of bottom water in the Southern Indian Ocean region. All data corrected to DIC of bottom water (See III-A-1 section). The smoothed curve is obtained by 15-point running average.

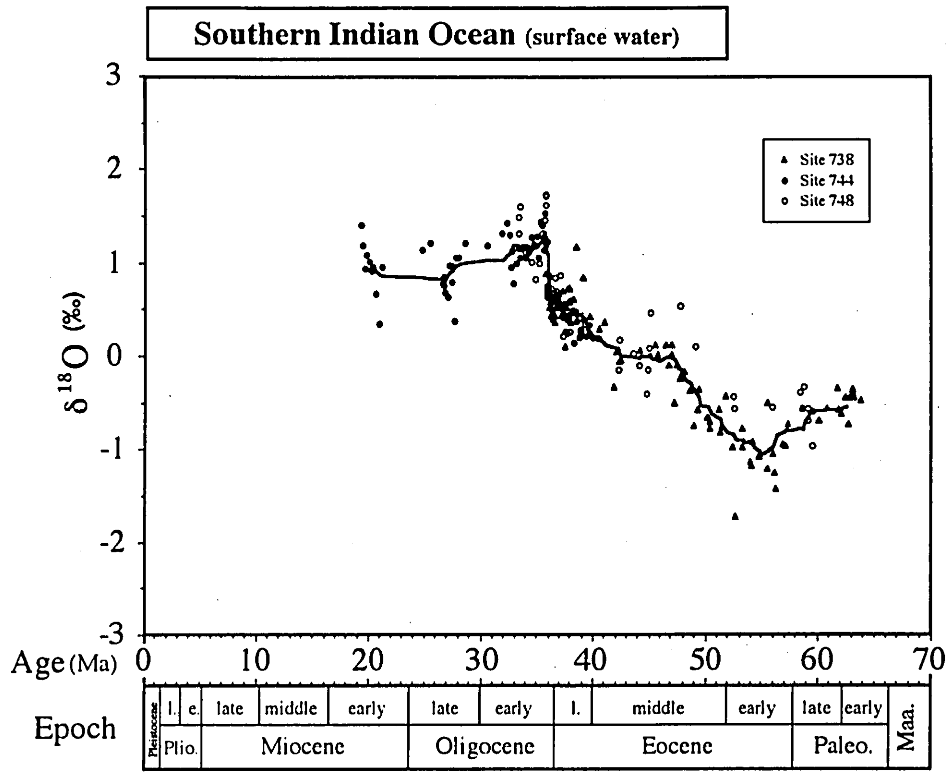

Fig. 42. Composite oxygen isotope record of surface water in the Southern Indian Ocean region. All data corrected to DIC of surface water (about 50 m below sea; See III-A-1 section). The smoothed curve is obtained by 15-point running average.

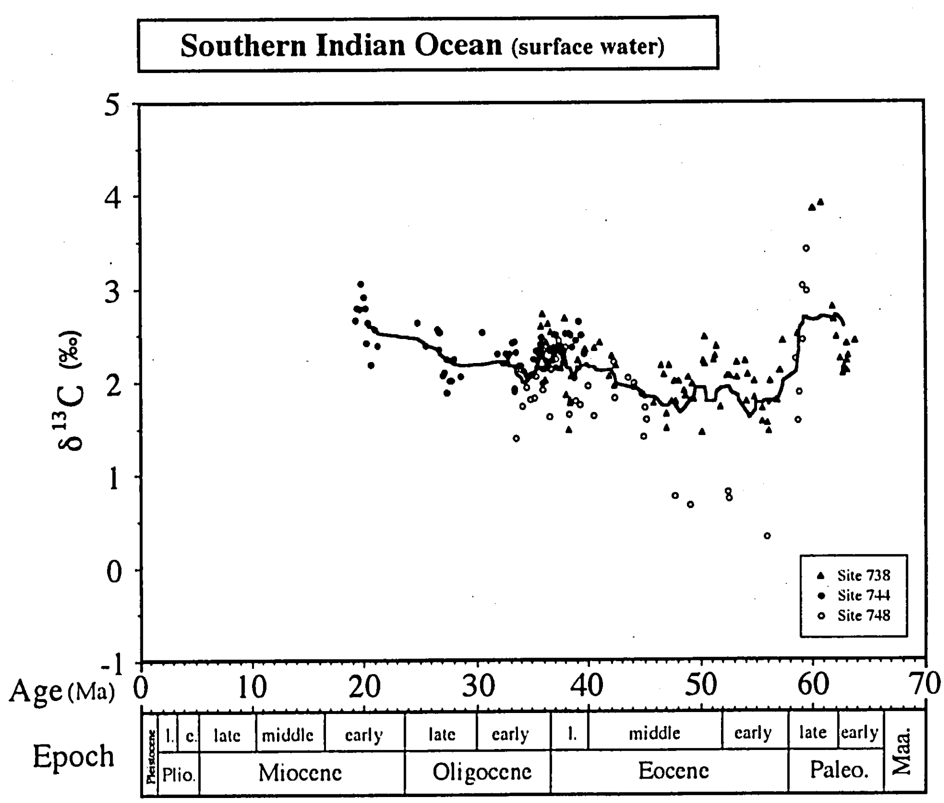

Fig. 43. Composite carbon isotope record of surface water in the Southern Indian Ocean region. All data corrected to DIC of surface water (about 50 m below sea; See III-A-1 section). The smoothed curve is obtained by 15-point running average.

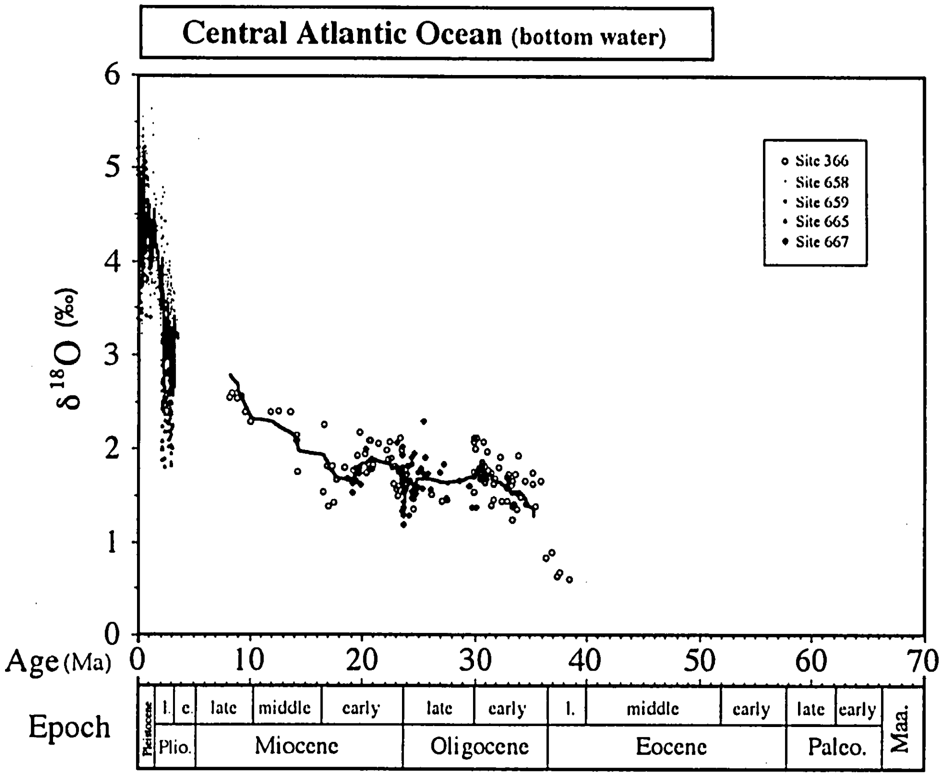

Fig. 44. Composite oxygen isotope record of bottom water in the Central Atlantic Ocean region. All data corrected to DIC of bottom water (See III-A-1 section). The smoothed curve is obtained by 15-point running average.

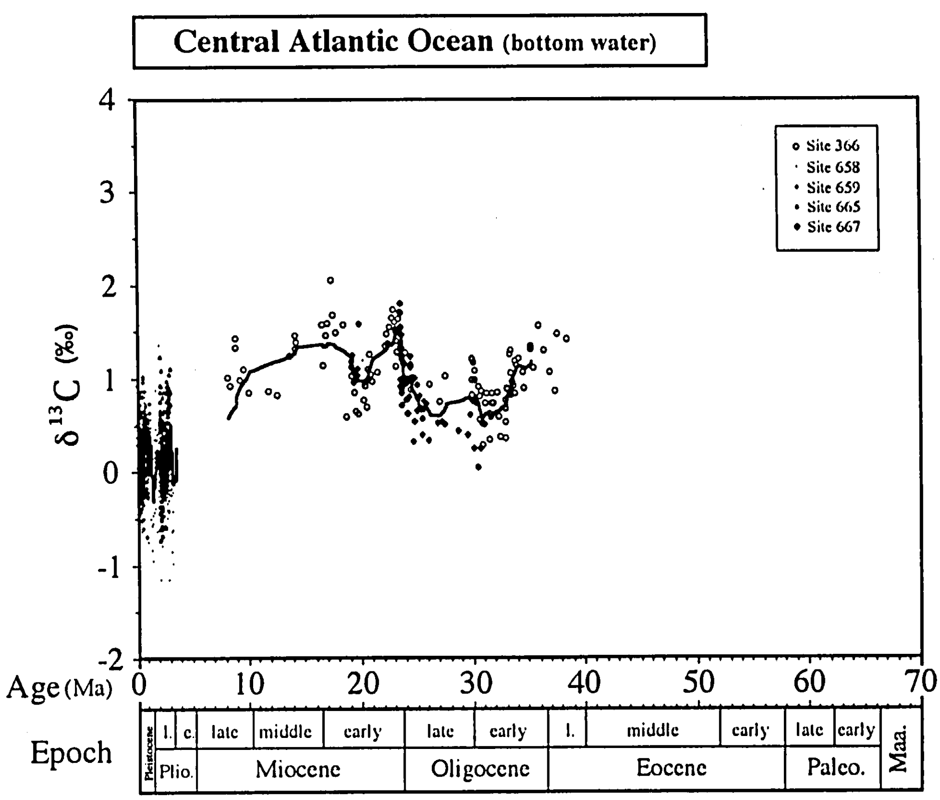

Fig. 45. Composite carbon isotope record of bottom water in the Central Atlantic Ocean region. All data corrected to DIC of bottom water (See III-A-1 section). The smoothed curve is obtained by 15-point running average.

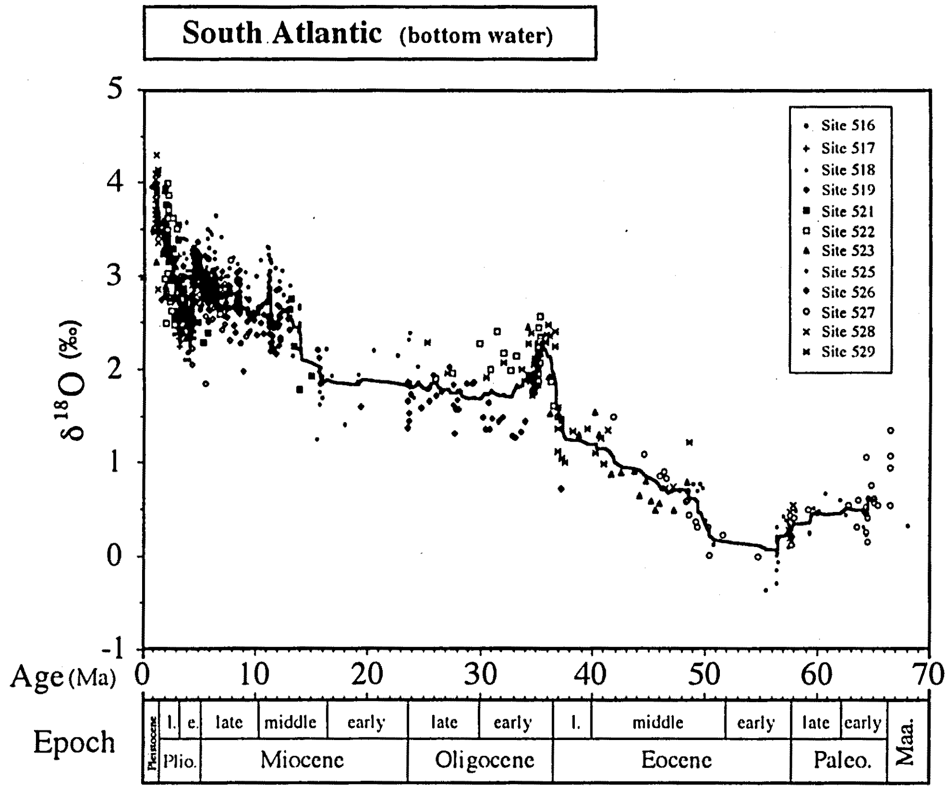

Fig. 46. Composite oxygen isotope record of bottom water in the South Atlantic Ocean region. All data corrected to DIC of bottom water (See III-A-1 section). The smoothed curve is obtained by 15-point running average.

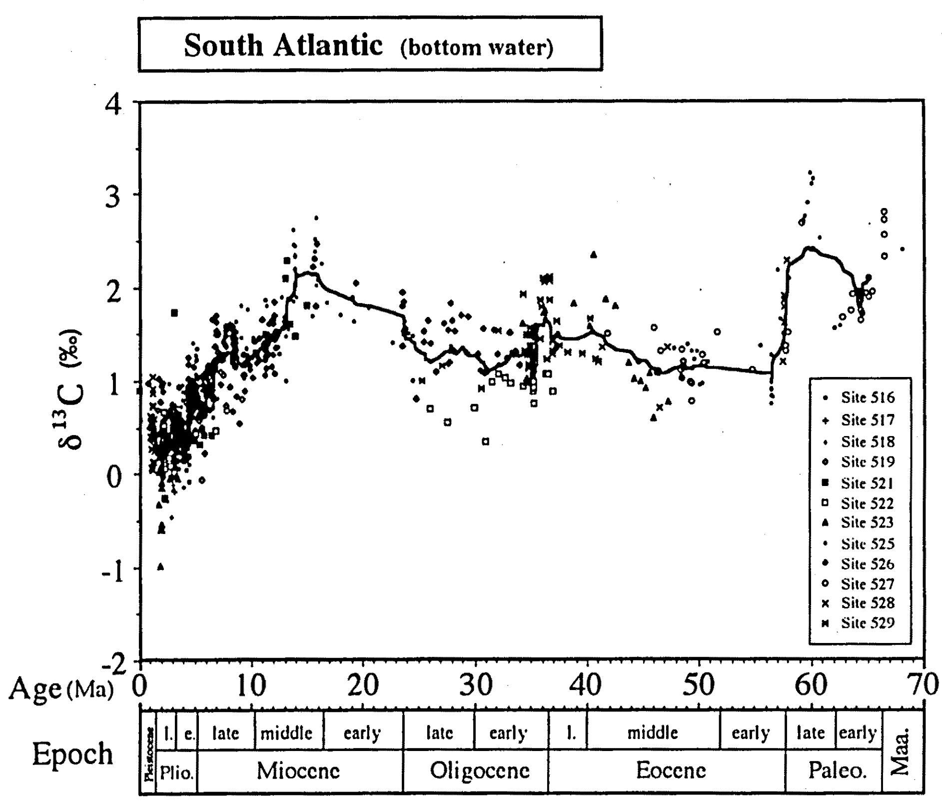

Fig. 47. Composite carbon isotope record of bottom water in the South Atlantic Ocean region. All data corrected to DIC of bottom water (See III-A-1 section). The smoothed curve is obtained by 15-point running average.

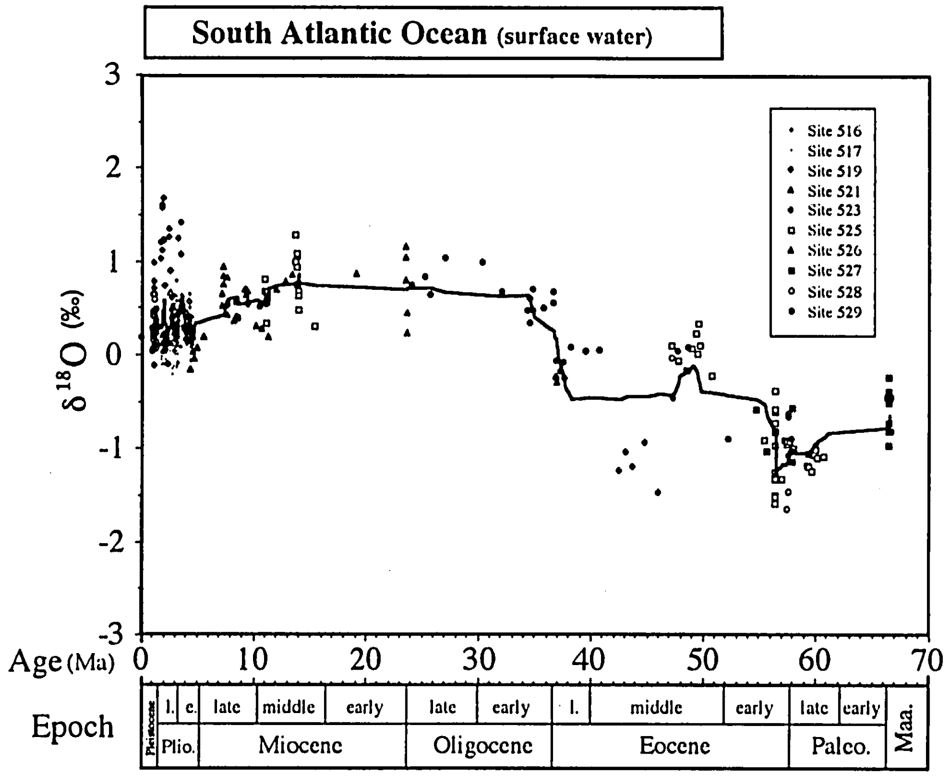

Fig. 48. Composite oxygen isotope record of surface water in the South Atlantic Ocean region. All data corrected to DIC of surface water (about 50 m below sea; See III-A-1 section). The smoothed curve is obtained by 15-point running average.

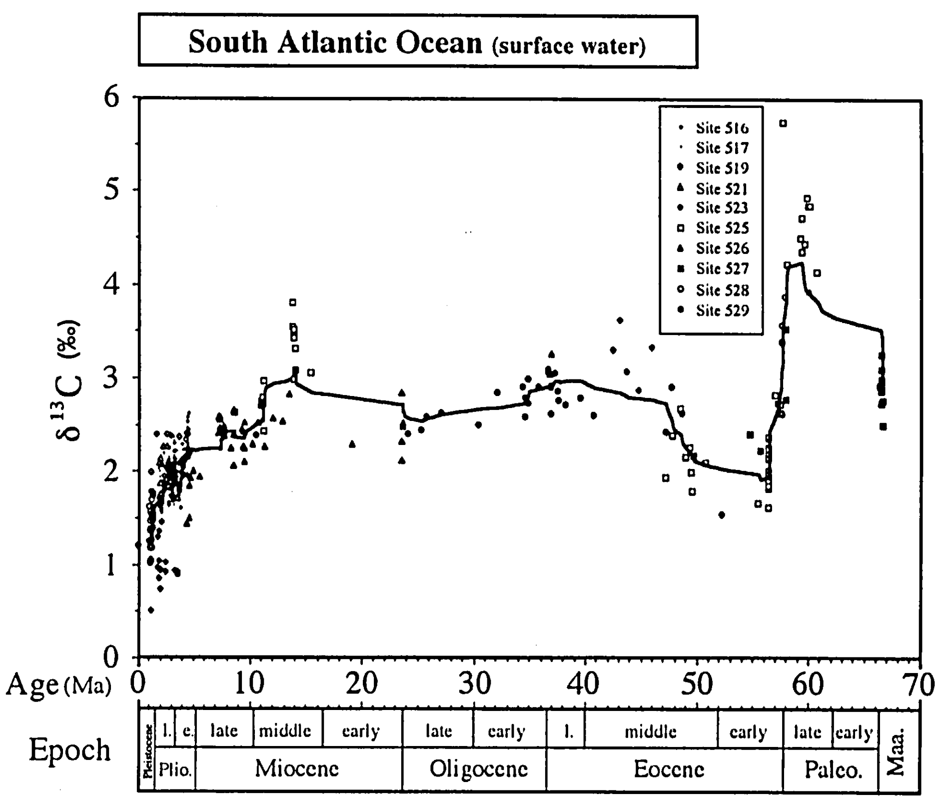

Fig. 49. Composite carbon isotope record of surface water in the South Atlantic Ocean region. All data corrected to DIC of surface water (about 50 m below sea; See III-A-1 section). The smoothed curve is obtained by 15-point running average.

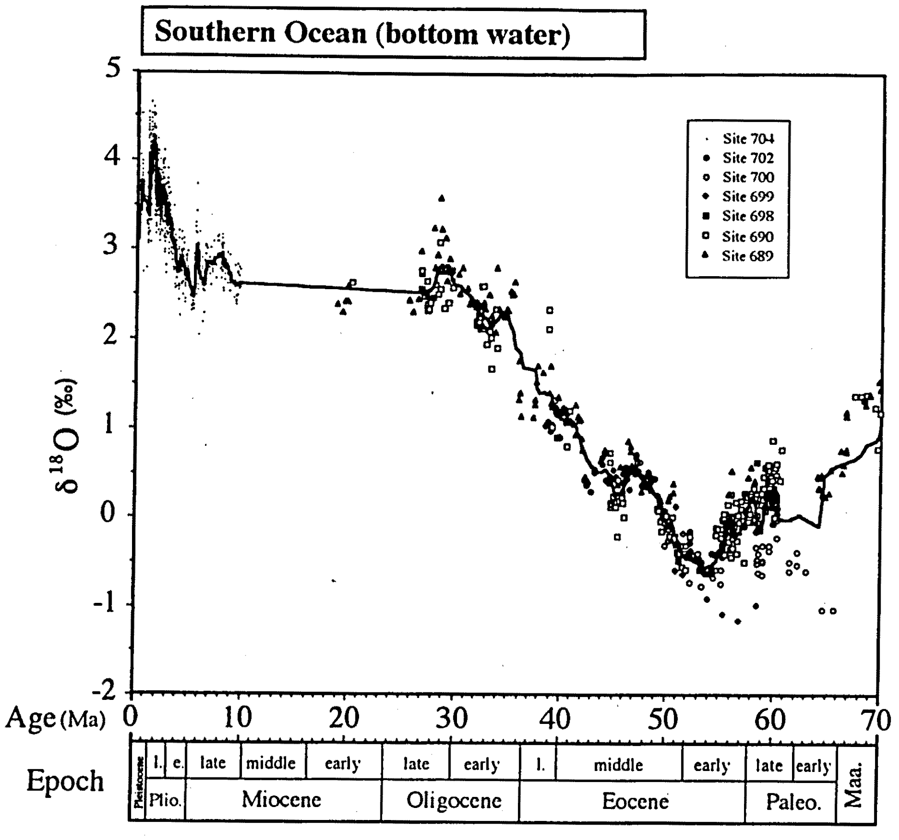

Fig. 50. Composite oxygen isotope record of bottom water in the Southern Ocean (Atlantic sector) region. All data corrected to DIC of bottom water (See III-A-1 section). The smoothed curve is obtained by 15-point running average.

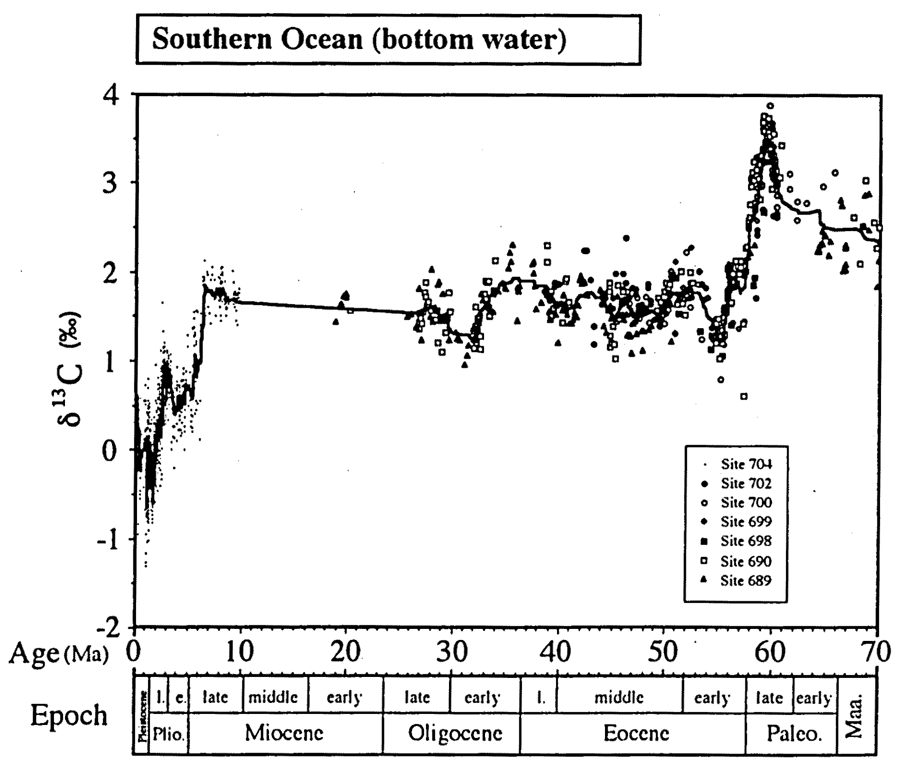

Fig. 51. Composite carbon isotope record of bottom water in the Southern Ocean (Atlantic sector) region. All data corrected to DIC of bottom water (See III-A-1 section). The smoothed curve is obtained by 15-point running average.

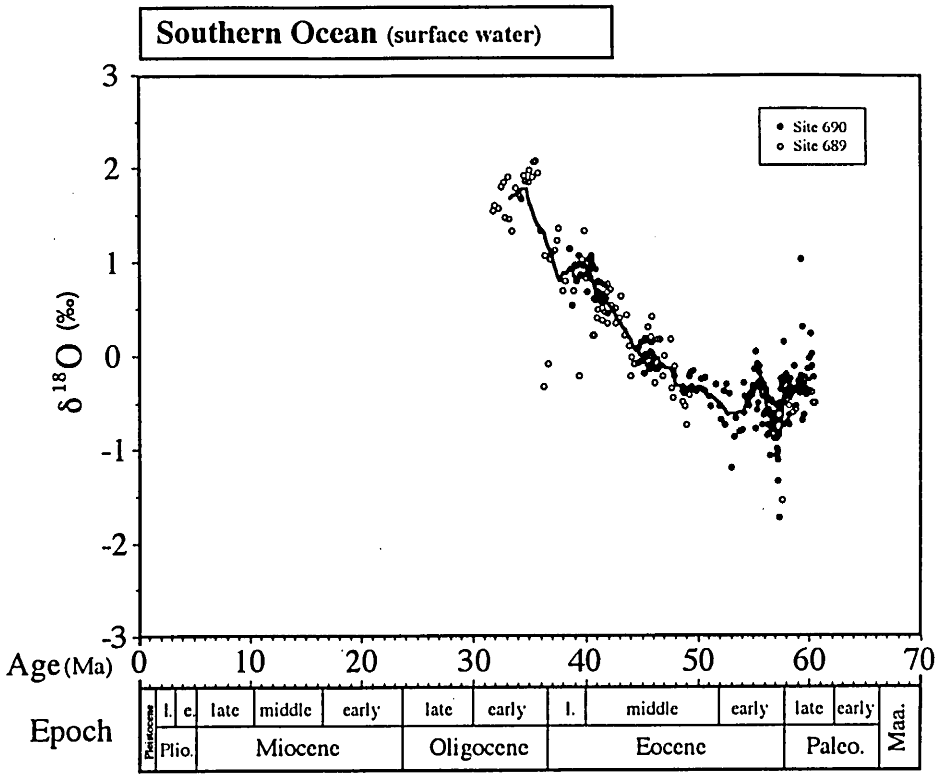

Fig. 52. Composite oxygen isotope record of surface water in the Southern Ocean (Atlantic sector) region. All data corrected to DIC of surface water (about 50 m below sea; See III-A-1 section). The smoothed curve is obtained by 15-point running average.

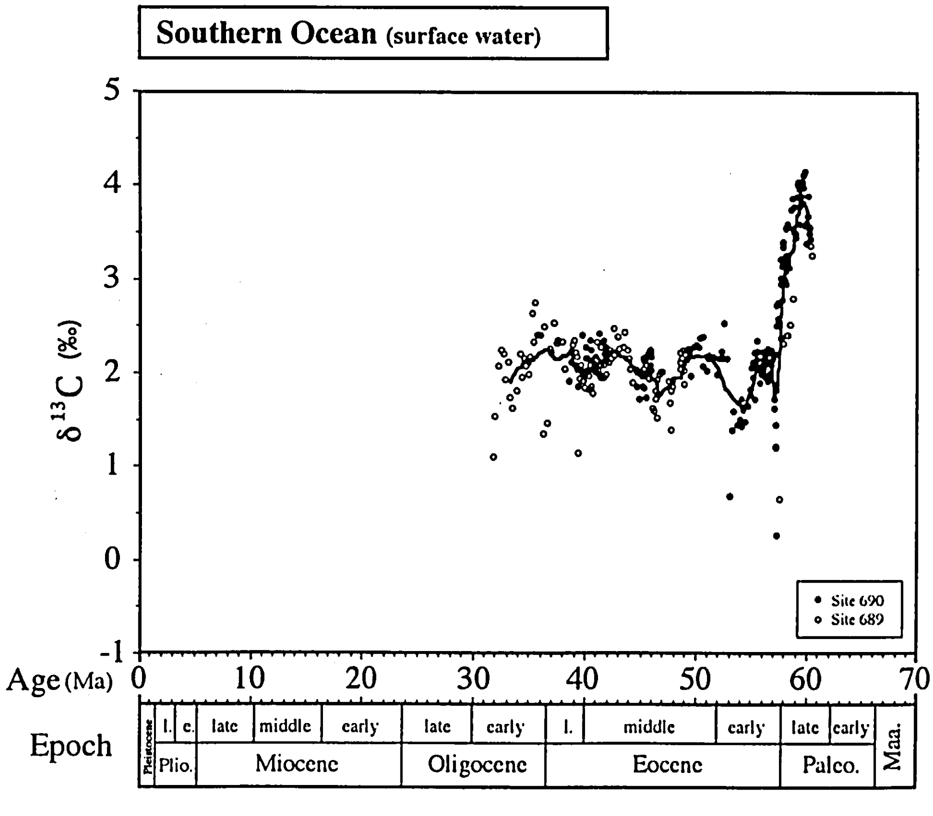

Fig. 53. Composite carbon isotope record of surface water in the Southern Ocean (Atlantic sector) region. All data corrected to DIC of surface water (about 50 m below sea; See III-A-1 section). The smoothed curve is obtained by 15-point running average.

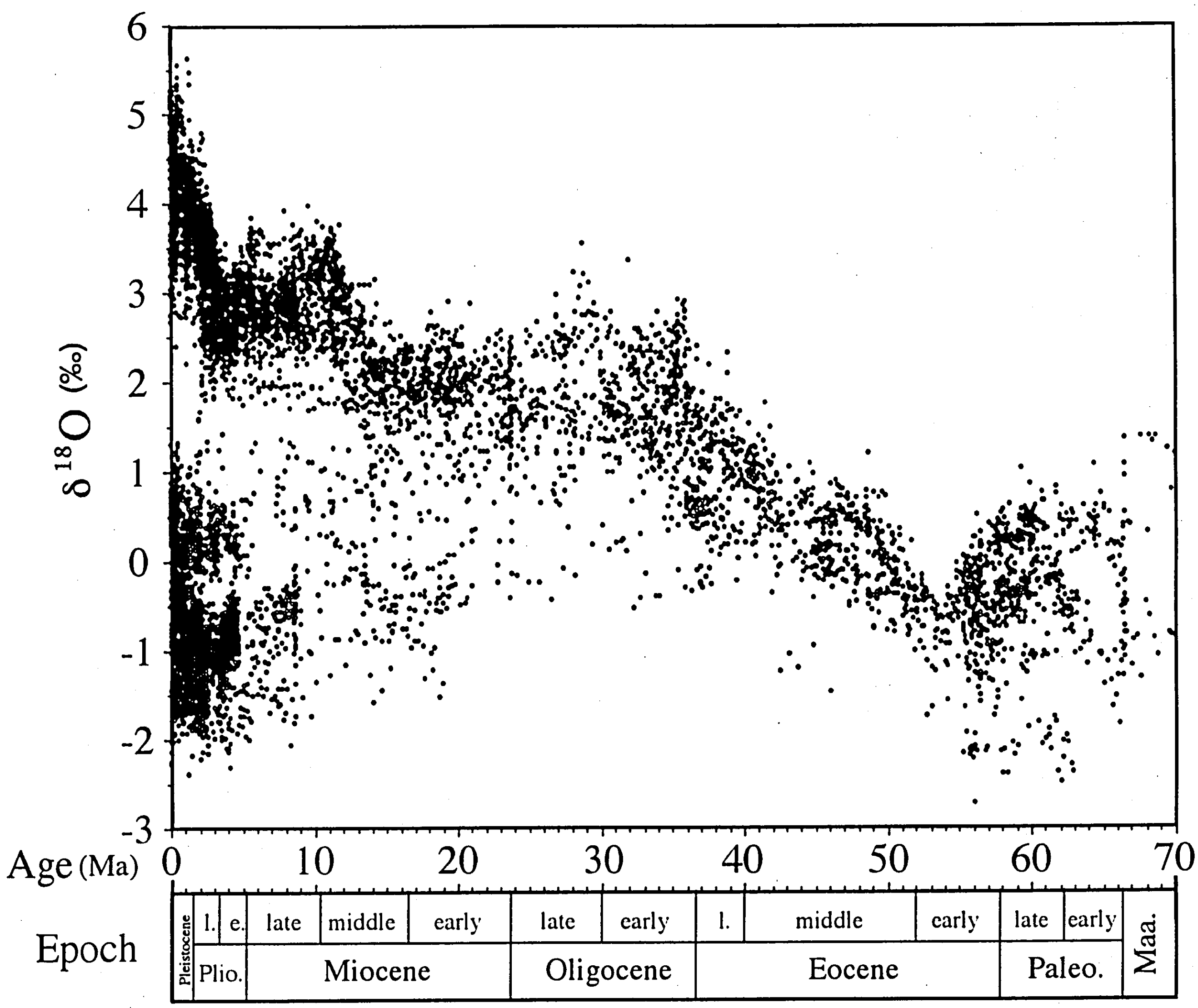

Fig. 54. All oxygen isotope data considered in this study. Open circle shows a DIC values of surface water (about 50 m below sea), and dot shows a DIC value of bottom water.

Indian, South Atlantic, and Southern Oceans. The net magnitudes are largest (~0.8‰) in the Southern Ocean, and tend to decrease southwards as found in the shift of the bottom water record. The following $\delta^{18}O$ values differ among the oceans during the Oligocene. $\delta^{18}O$ values in the northern Indian Ocean are lowest (~-0.2‰); the Southern Ocean, southern Indian, and South Atlantic Oceans, respectively, record the values of 2.0, 1.4, and 1.0‰, which are higher than those of the northern Indian Ocean. From the Miocene, although isotopes can only be recorded in the South Atlantic Ocean, the general trends are similar to those of the northern Indian Ocean. The degrees of decrease in those oceans are small from 12 Ma on consequently the $\delta^{18}O$ differences of those oceans expands to 1.4‰.

Carbon isotopic record: The carbon isotopic records of surface and bottom water through the Cenozoic exhibit the same pattern in the Indian and South Atlantic Oceans, except for a pronounced shift toward low values (by ~1.0‰) observed in the Southern Ocean (Atlantic sector) in the late Pliocene (2.5 Ma). The South Atlantic and northern Indian Oceans located in the same latitude record similar $\delta^{13}C$ values of bottom water. $\delta^{13}C$ values in the southern Indian Ocean are also similar with the exception of a lower value from the Eocene to late Oligocene. In the Central Atlantic Ocean, $\delta^{13}C$ values are slightly lower than those of the northern Indian Ocean. The difference of $\delta^{13}C$ values between the northern Indian and Southern Ocean varies according to age. $\delta^{13}C$ values in the Southern Ocean are close to those of the northern Indian Ocean in the late and middle Eocene, latest Pliocene, and Pleistocene, but they are higher through the Paleocene to early Eocene (0.5‰), and are higher through the Oligocene to early Pliocene (0.3‰).

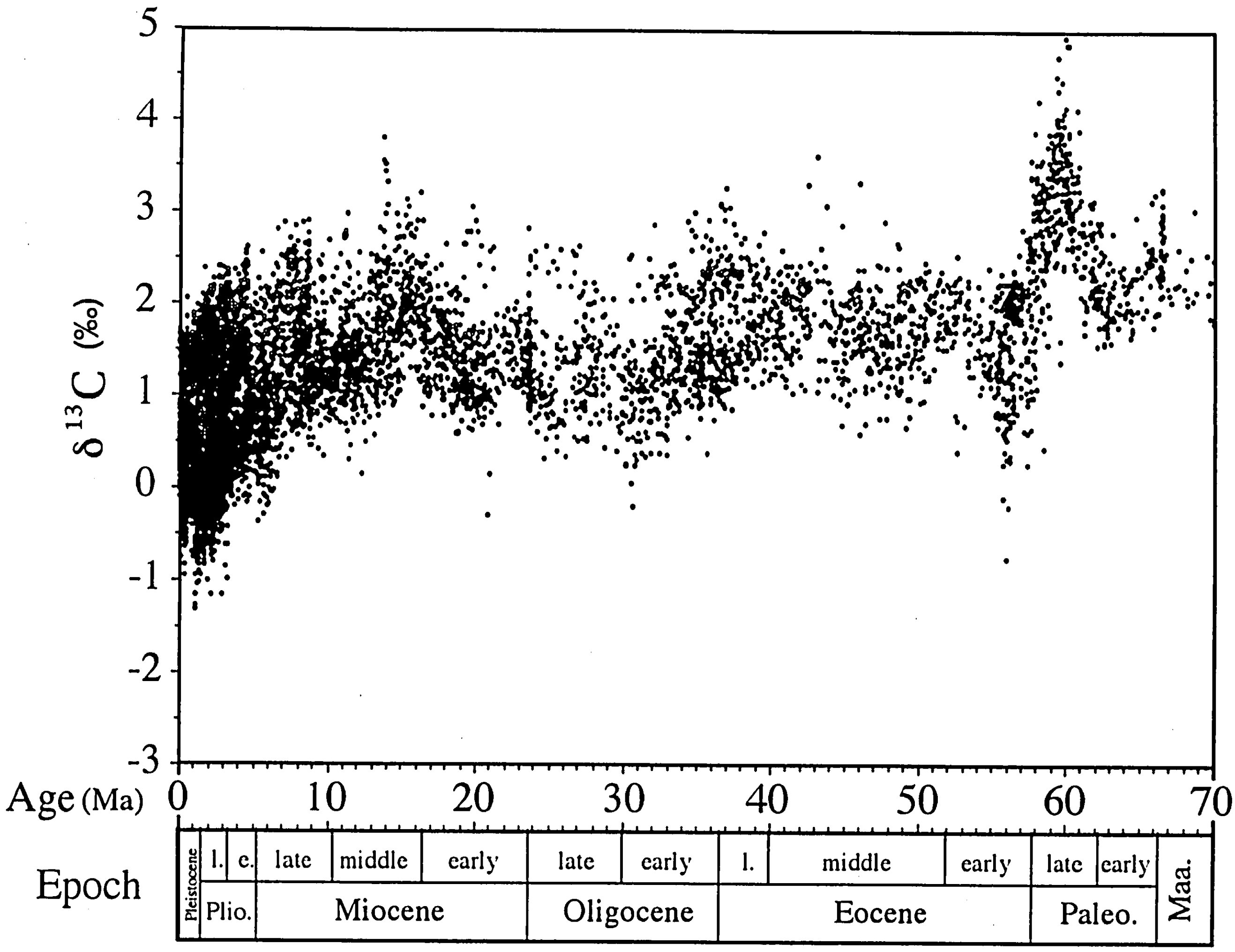

Fig. 55. All carbon isotope data considered in this study. Open circle shows a DIC values of surface water (about 50 m below sea), and dot shows a DIC value of bottom water.

For $\delta^{13}C$ values of surface water from the Paleocene to Oligocene, the southern Indian Ocean is generally similar to the northern Indian Ocean, however the former records 0.5‰, which is lower than that of the latter in the middle Eocene. During the Pleistocene, $\delta^{13}C$ values of the Central Atlantic Ocean are lower than those of the northern Indian Ocean (1.0‰). $\delta^{13}C$ values in the South Atlantic Ocean are higher throughout the Cenozoic 0.5 to 1.0‰. In the Southern Ocean (Atlantic sector), $\delta^{13}C$ values are 0.6‰ higher than those of the northern Indian Ocean during the Paleocene, which are similar to the early Eocene $\delta^{13}C$ values. They are slightly lower than those of the northern Indian Ocean in the middle and late Eocene.

The difference of $\delta^{13}C$ between surface and bottom water is smallest in the Southern Ocean (Atlantic sector), and largest in the South Atlantic Ocean. This difference tends to increase northwards. The Atlantic Ocean side exhibits larger difference than those of the Indian Ocean, although the two oceans are located at the same latitude.

D. General trends in the isotopic record

All oxygen and carbon isotope data used in this study are shown in Figs. 54 and 55. The general trends for oxygen and carbon isotopic records are similar in both the Indian and South Atlantic Oceans. In general, the oxygen and carbon isotopic values increase southwards.

The oxygen isotopic changes show a particular pattern from the Oligocene / Eocene boundary, that is, a gentle change followed by a sharp change in terms of a positive shift. Before and after the shift, a decrease in oxygen isotope values is recognized. The magnitudes of the shift of the Eocene / Oligocene boundary in surface and bottom water and the shift of the middle Miocene in bottom water tend to increase southwards. The shift of the late Pliocene tends to decrease southwards on the Atlantic ocean side, and decreases northwards on the Indian Ocean side. The difference in the magnitude of the shift may be caused by the difference in water mass structure.

As a general feature of carbon isotopes, the degree of variance of $\delta^{13}C$ tends to increase with a decrease in average

$\delta^{13}C$. This suggests that the carbon isotopic changes are related to ocean circulation velocity and marine productivity. The fluctuations in carbon isotopes from the latest Paleocene to early Eocene are remarkable in the Cenozoic record.

D. Distribution of oxygen and carbon isotopic values

The geographical distribution of oxygen and carbon isotopes are examined using reconstructed paleocoordinates and paleodepths. For the correlation among sites, the isotopic data are averaged in one million year intervals. The averaged values and standard deviations are shown in Table 7.

1. Oxygen isotopes

Maastrichtian: In the Maastrichtian, oxygen and carbon isotopic data are measured from Site 752 (around 50°S) in the northeastern Indian Ocean and Sites 689 and 690 (around 70°S) in the Atlantic sector of the Southern Ocean (Barrera and Huber, 1990). The oxygen isotopic values at Site 752 are constant at ~-0.9‰ with a slight fluctuation, whereas those at Sites 689 and 690 tend to increase slightly by ~1.0‰. The difference between sites results from geographic difference, rather than variation in water depth, because the estimated water depth at Site 752 is close to that of Site 689.

Paleocene: From the early Paleocene to the time of the ^{18}O maximum at 61 Ma, the latitudinal gradient of oxygen isotopes in bottom water in the South Atlantic Ocean (70°-30°S) shows a slightly increasing trend toward low-latitudes, and the latitudinal difference is less than 0.2‰ (Fig. 56). In the Indian Ocean, $\delta^{18}O$ values on the high-latitude side are only 0.1‰ , which are higher than those on the low-latitude side in this interval. However, the oxygen isotopic values at 50°S are lower than those on the high- and low-latitude sides (0.6-1.3‰). The oxygen isotopic values in the Indian Ocean side are lower than those of the Atlantic Ocean side at similar latitude and water depth (0.3-0.4‰). This difference tends to reduce in this interval. $\delta^{18}O$ values on the low-latitude side in surface water are lower than those on the high-latitude side, and the difference on both sides is about 0.5‰. In contrast, the $\delta^{18}O$ difference between surface and bottom water on the high-latitude side is lower than that on low-latitude sides. The oxygen isotopic values at about latitude 50°S in the Indian Ocean are lower than those of the high- and low-latitude sides, and similar to bottom water record (1.0-1.5‰). The surface to bottom difference of $\delta^{18}O$ values in this area is the largest among in the Indian and Atlantic Oceans reaching 1.6‰ at 62 Ma.

From 61 Ma in the Paleocene (Fig. 56), the oxygen isotopic values on the low-latitude side (around 40°S) in the Atlantic Ocean are close to those of the high-latitude side (~70°S). $\delta^{18}O$ values in mid-latitudes (~55°S) are 0.2-0.4‰, lower than those of both sides. In this area, $\delta^{18}O$ values in intermediate water depth (~1000m) are slightly higher than in deep water (~2000m). In surface water in the South Atlantic Ocean, the oxygen isotopic values on the low-latitude side are 0.6-0.8‰, lower than those on the high-latitude side, and the surface to bottom $\delta^{18}O$ difference on the low-latitude side is larger than that of the high-latitude sides. The latitudinal gradient of bottom water $\delta^{18}O$ in the Indian Ocean is similar to that of the Atlantic Ocean. The oxygen isotopic values on

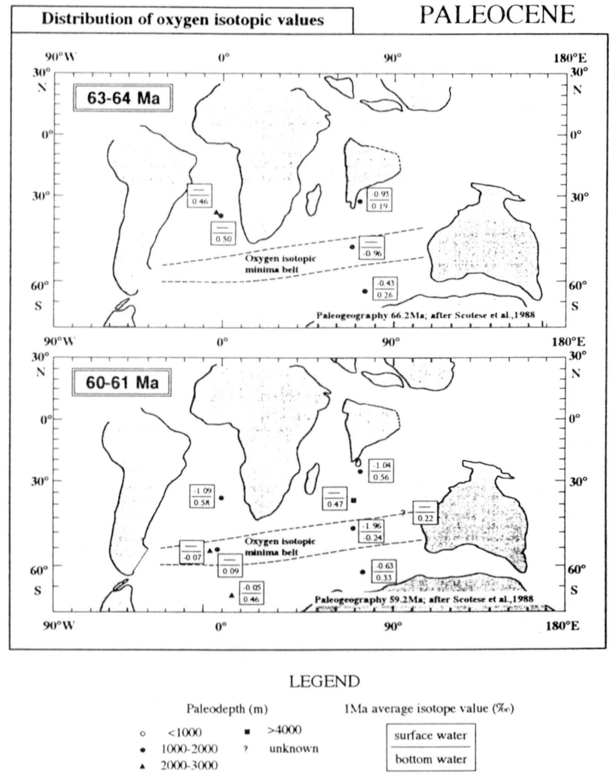

Fig. 56. Geographical distribution of oxygen isotopes during the Paleocene. The isotopic data are averaged in one million year intervals (Table 7).

the low-latitude side (~25°S) in bottom water are close to those on the high-latitude side (~65°S), and at mid-latitude (~50°S) records values lower by 0.6‰ than those of both sides. At high-latitudes, the oxygen isotopic values of bottom water in the Indian Ocean are close to those of the Atlantic Ocean. In surface water, the oxygen isotopic values on the low-latitude side in the Indian Ocean are 0.5-0.8‰, lower than those on the high-latitude side; furthermore those at mid-latitudes are 0.6-0.9‰, lower than those of the low-latitude side. The difference of $\delta^{18}O$ values between surface and bottom water is relatively large, being ~1.6‰ on the low-latitude side and ~0.8‰ on the high-latitude side. The difference at mid-latitudes is only 0.2‰, larger than the low-latitude side.

Remarkably low values of oxygen isotopes at mid-latitudes are observed in the Indian and South Atlantic Oceans (Fig. 56). Low values in the Indian Ocean are situated slightly northward, compared with those in the South Atlantic Ocean. Low values in both oceans may be geographically connected by a belt-form (here called the "oxygen isotopic minima belt"). The "oxygen isotopic minima belt" may also exist in the late Maastrichtian.

Eocene: The pattern of oxygen isotopes in the early Eocene is similar to that in the latest Paleocene (Fig. 57-1). The oxygen isotopic values at high-latitudes in the Atlantic Ocean are 0.3-0.5‰, higher than those at low-latitudes, with a smaller difference in the older part of the record. In this interval, $\delta^{18}O$ values in intermediate water (~1000 m) are

Table 7-1. Average oxygen and carbon isotopic data of the 1 Ma interval used in this study.

Interval (Ma)	$\delta^{18}O$ (‰)	$\delta^{13}C$ (‰)	No. of Data
Central Atlantic Ocean			
Site 98			
Benthic			
48−49	1.014	1.917	1
52−53	0.224±0.224	1.811±0.131	5
57−58	-0.162	1.392	1
58−59	-0.097	1.506	1
Site 366			
Benthic			
8·9	2.570±0.025	1.178±0.244	4
9·10	2.488±0.122	1.047±0.082	2
10−11	2.293	0.857	1
11−12	2.394	0.865	1
12−13	2.411	0.827	1
13−14	2.401	1.245	1
14−15	2.001±0.207	1.392±0.073	3
16−17	1.875±0.363	1.396±0.224	3
17−18	1.577±0.205	1.707±0.244	4
18−19	1.745±0.088	1.087±0.685	2
19−20	1.886±0.227	0.792±0.189	4
20−21	1.893±0.136	0.987±0.185	8
21−22	2.068	1.071	1
22−23	1.841±0.184	1.534±0.143	7
23−24	1.742±0.220	1.388±0.214	7
24−25	1.456±0.092	0.964±0.074	3
26−27	1.510	0.94	1
27−28	1.445±0.007	0.895±0.191	2
29−30	1.873±0.273	1.060±0.185	4
30−31	1.857±0.159	0.797±0.272	10
31−32	1.669±0.193	0.697±0.170	7
32−33	1.645±0.179	0.597±0.187	7
33−34	1.555±0.201	1.020±0.164	12
34−35	1.519±0.126	1.062±0.159	3
35−36	1.606±0.153	1.333±0.179	4
36−37	0.861±0.042	1.189±0.168	2
37−38	0.653±0.032	1.170±0.426	2
38−39	0.603	1.423	1
Site 658			
Benthic			
0·1	4.362±0.521	0.135±0.318	231
1·2	4.005±0.464	0.063±0.336	82
2·3	3.663±0.339	−0.010±0.350	133
3·4	3.309±0.251	−0.061±0.317	6
Planktonic			
0·1	0.241±0.474	0.327±0.340	237
1·2	0.229±0.336	0.572±0.304	90
2·3	0.680±0.115	0.546±0.144	4
Site 659			
Benthic			
0·1	4.419±0.495	0.252±0.376	163
Planktonic			
0·1	0.202±0.482	0.450±0.333	108
Site 662			
Planktonic			
0·1	−0.947±0.203		103
1·2	−1.020±0.293		81
Site 663			
Planktonic			
0·1	−0.628±0.441		108
Site 665			
Benthic			
2·3	2.699±0.353	0.288±0.458	134
3·4	2.140±0.214	0.610±0.306	12
Site 667			
Benthic			
19−20	1.678±0.091	1.158±0.191	8
20−21	1.890±0.143	0.976±0.021	2
23−24	1.613±0.219	1.247±0.414	23
Site 667			
Benthic			
24−25	1.668±0.208	0.862±0.281	11
25−26	1.794±0.228	0.690±0.158	8
26−27	1.554	0.342	1
27−28	1.678±0.185	0.529±0.013	3
28−29	1.661	0.438	1
29−30	1.484±0.160	0.506±0.151	2
30−31	1.572±0.172	0.186±0.114	3
31−32	1.666	0.511	1
South Atlantic Ocean			
Site 516			
Benthic			
2·3	2.932±0.249	0.420±0.177	12
3·4	2.552±0.159	0.340±0.164	38
4·5	2.544±0.318	0.353±0.158	33
Planktonic			
2·3	0.346±0.157	1.882±0.137	16
3·4	0.336±0.184	1.974±0.164	40
4·5	0.265±0.151	2.226±0.201	33
Site 517			
Benthic			
2·3	2.645±0.124	0.646±0.025	3
3·4	2.561±0.263	0.431±0.236	12
Planktonic			
1·2	−0.028±0.055	1.935±0.165	6
2·3	0.105±0.184	2.018±0.175	33
3·4	0.211±0.224	2.038±0.201	25
Site 518			
Benthic			
2·3	3.138±0.216	−0.070±0.205	6
3·4	2.537±0.216	0.384±0.223	23
4·5	2.540±0.167	0.231±0.210	5
Site 519			
Benthic			
1·2	3.108±0.523	0.589±0.133	2
2·3	3.064±0.489	0.442±0.418	3
3·4	2.876±0.082	0.529±0.152	4
4·5	2.438±0.224	0.442±0.221	8
5·6	2.691±0.306	0.604±0.260	11
6·7	2.699±0.135	0.926±0.143	5
7·8	2.585±0.241	1.116±0.213	6
8·9	2.333±0.277	0.741±0.173	4
9·10	2.423±0.106	0.933±0.184	2
Planktonic			
1·2	0.085±0.290	2.190±0.283	2
2·3	0.482±0.398	2.040±0.384	5
3·4	0.350±0.132	2.077±0.266	3
4·5	0.355±0.290	2.375±0.049	2
Site 521			
Benthic			
1·2	3.508±0.054	0.349±0.153	4
2·3	3.094±0.440	0.410±0.200	7
3·4	2.874±0.377	0.594±0.450	9
4·5	2.512±0.131	0.364±0.059	4
5·6	2.336±0.073	0.370±0.068	2
6·7	2.723	0.421	1
13−14	2.353±0.440	1.865±0.387	4
15−16	1.930	1.810	1
Planktonic			
1·2	0.147±0.047	1.9870.224	3
2·3	0.290±0.234	2.056±0.173	8
3·4	0.460±0.042	1.855±0.191	2
4·5	0.440	2.080	1
Site 522			
Benthic			
1·2	3.447±0.679	0.138±0.127	2
2·3	3.268±0.503	0.233±0.217	16
3·4	2.783±0.050	0.176±0.212	2

Table 7-2. (continued).

Interval (Ma)	$\delta^{18}O$ (‰)	$\delta^{13}C$ (‰)	No. of Data
Site 522			
Benthic			
4·5	2.508	0.294	1
5·6	2.708	0.436	1
6·7	2.588	0.464	1
26−27	1.893	0.693	1
27−28	1.956	0.556	1
29−30	2.273	0.713	1
30−31	1.996	0.356	1
31−32	2.410	0.980	1
32−33	2.076±0.127	1.056±0.028	2
33−34	2.146	0.966	1
34−35	1.936	0.946	1
35−36	2.193±0.169	1.199±0.217	32
36−37	1.659±0.196	1.006±0.104	3
Site 523			
Benthic			
1·2	3.391±0.376	−0.211±0.429	9
2·3	3.021±0.199	0.012±0.334	9
3·4	2.728±0.172	0.205±0.198	6
34−35	1.993±0.387	1.363±0.312	3
35−36	1.995±0.191	1.530±0.046	4
36−37	1.720±0.269	1.735±0.021	2
37−38	1.450	1.360	1
38−39	1.292	1.820	1
40−41	1.420±0.173	1.962±0.541	2
41−42	0.872	1.860	1
42−43	0.890	1.790	1
43−44	0.910	1.190	1
44−45	0.730±0.113	1.000±0.028	2
45−46	0.535±0.064	0.995±0.106	2
46−47	0.560	0.600	1
47−48	0.482	0.770	1
48−49	0.790	1.050	1
Planktonic			
1·2	1.182±0.358	1.005±0.248	9
2·3	1.259±0.059	0.907±0.127	4
3·4	1.241±0.175	0.916±0.025	3
42−43	−1.240	3.300	1
43−44	−1.115±0.106	3.345±0.389	2
44−45	−0.940	2.870	1
46−47	−1.470	3.330	1
47−48	−0.460	2.430	1
Site 524			
Benthic			
55−56	−0.583	0.339	1
56−57	−0.270±0.132	1.299±0.467	2
61−62	−0.246	2.283	1
64−65	−0.706±0.042	2.193±0.184	2
65−66	−0.172±0.327	2.319±0.372	5
66−67	−0.846±0.499	2.211±0.227	6
67−68	−0.921±0.799	1.733±0.014	2
Planktonic			
55−56	−1.350	1.960	1
56−57	−1.225±0.064	2.260±0.424	2
61−62	−1.060	2.770	1
62−63	−0.780	2.910	1
Site 525			
Benthic			
0·1	3.914	0.578	1
2·3	3.534±0.313	0.782±0.264	2
3·4	3.305±0.184	0.738±0.204	6
4·5	2.985±0.090	0.927±0.305	10
5·6	3.187±0.172	0.981±0.201	14
6·7	3.133±0.324	0.841±0.136	10
7·8	2.959±0.184	1.393±0.120	7
8·9	2.998±0.163	1.430±0.223	3
9·10	2.732±0.250	1.487±0.319	5
10−11	3.020±0.309	1.385±0.087	4
11−12	2.917±0.253	1.427±0.168	20
12−13	2.830±0.167	1.528±0.241	5
13−14	2.473±0.226	2.029±0.484	12
14−15	2.220	1.891	1
Site 525			
Benthic			
15−16	1.751±0.266	2.239±0.346	7
16−17	2.073±0.194	2.041±0.298	2
18−19	1.410	1.701	1
19−20	1.905±0.049	1.761±0.184	2
20−21	2.200	1.781	1
22−23	2.145	1.411	1
23−24	2.359±0.052	1.561±0.101	2
24−25	1.852±0.168	1.327±0.279	3
47−48	0.709	1.339	1
49−50	0.744±0.032	1.315±0.065	4
50−51	0.266±0.128	1.037±0.139	3
55−56	·0.362	1.378	1
56−57	0.065±0.189	0.928±0.143	10
57−58	0.282±0.145	1.672±0.299	5
58−59	0.488	2.098	1
59−60	0.397±0.121	2.900±0.221	6
60−61	0.578±0.127	2.843±0.445	2
61−62	0.608	1.558	1
62−63	0.448	1.588	1
63−64	0.499	1.919	1
64−65	0.407±0.174	1.882±0.108	4
68−69	0.328	2.402	1
Planktonic			
8·9	0.390	2.635	1
10−11	0.810	2.757	1
11−12	0.586±0.125	2.739±0.160	7
13−14	0.926±0.223	3.391±0.264	8
14−15	0.480	3.080	1
15−16	0.300	3.060	1
47−48	0.026±0.113	2.175±0.318	2
48−49	−0.154	2.680	1
49−50	0.147±0.127	2.082±0.184	5
50−51	−0.214	2.110	1
55−56	·0.914	1.670	1
56−57	−1.047±0.395	2.092±0.226	14
57−58	−1.006±0.178	3.332±1.347	5
58−59	−0.997	4.230	1
59−60	−1.126±0.092	4.631±0.231	6
60−61	−1.090±0.016	4.489±0.495	2
Site 526			
Benthic			
0·1	3.953	0.973	1
1·2	3.453±0.004	0.888±0.174	2
2·3	3.391±0.121	0.757±0.252	5
3·4	3.001±0.085	0.676±0.225	3
4·5	3.023±0.205	0.877±0.138	40
5·6	2.893±0.194	0.760±0.180	29
6·7	2.842±0.114	1.172±0.274	23
7·8	2.795±0.147	1.372±0.192	10
8·9	2.772±0.157	1.364±0.123	24
9·10	2.549±0.128	1.134±0.135	7
10−11	2.549±0.141	1.314±0.205	7
11−12	2.423±0.192	1.351±0.162	19
12−13	2.513±0.181	1.516±0.200	11
13−14	2.415	1.685	1
15−16	2.016±0.165	2.188±0.285	4
19−20	1.600	2.040	1
23−24	1.595±0.183	1.665±0.222	6
24−25	1.575	0.805	1
25−26	1.793±0.140	1.523±0.115	3
26−27	1.739±0.030	1.242±0.215	2
27−28	1.666±0.240	1.493±0.260	6
28−29	1.722±0.140	1.503±0.196	3
29−30	1.843±0.011	1.488±0.272	2
30−31	1.453±0.138	1.250±0.219	4
31−32	1.453±0.018	1.311±0.310	2
32−33	1.374±0.141	1.253±0.035	2
33−34	1.340±0.910	1.326±0.173	3
37−38	0.710	1.333	1
Planktonic			
4·5	0.019±0.128	1.743±0.256	5
5·6	0.189	1.949	1
7·8	0.689±0.178	2.486±0.078	8

Table 7-3. (continued).

Interval (Ma)	$\delta^{18}O$ (‰)	$\delta^{13}C$ (‰)	No. of Data	Interval (Ma)	$\delta^{18}O$ (‰)	$\delta^{13}C$ (‰)	No. of Data
Site 526				**Site 529**			
Planktonic				**Planktonic**			
8·9	0.481±0.115	2.338±0.248	4	35−36	0.501	2.919	1
9·10	0.642±0.061	2.339±0.155	6	36−37	0.234±0.456	2.935±0.216	4
10−11	0.294±0.021	2.409±0.170	2	37−38	−0.164±0.088	2.900±0.149	3
11−12	0.189	2.269	1	38−39	0.081	2.726	1
12−13	0.735±0.064	2.553±0.021	2	39−40	0.040	2.797	1
13−14	0.850	2.825	1	40−41	0.060	2.604	1
19−20	0.870	2.295	1	47−48	0.040	2.912	1
23−24	0.730±0.390	2.455±0.265	5	48−49	0.091	2.636	1
36−37	−0.225	3.045	1	52−53	−0.897	1.557	1
37−38	−0.283	3.264	1				
				Southern Ocean			
Site 527							
Benthic				**Site 689**			
4·5	2.975	0.765	1	**Benthic**			
7·8	3.165	0.685	1	18−19	2.382	1.439	1
41−42	1.498	1.508	1	19−20	2.428±0.117	1.702±0.049	2
44−45	1.088	1.208	1	25−26	2.427	1.494	1
46−47	0.861±0.035	1.331±0.230	3	26−27	2.571±0.361	1.563±0.218	3
48−49	0.586±0.111	1.171±0.128	4	27−28	2.498±0.040	1.465±0.159	4
49−50	0.332±0.033	0.915±0.110	3	28−29	3.081±0.314	1.706±0.251	6
50−51	0.158±0.212	1.228±0.057	2	29−30	2.838±0.183	1.476±0.185	5
51−52	0.228	1.518	1	30−31	2.664±0.151	1.263±0.047	3
54−55	−0.012	1.118	1	31−32	2.422±0.078	1.156±0.157	5
57−58	0.248±0.145	1.402±0.105	3	32−33	2.320±0.108	1.524±0.206	5
59−60	0.504	2.681	1	33−34	2.360±0.280	1.624±0.097	5
62−63	0.550	1.680	1	34−35	2.294±0.043	1.812±0.033	5
63−64	0.463±0.206	1.838±0.114	2	35−36	2.537±0.067	2.164±0.112	4
64−65	0.519±0.310	1.828±0.122	4	36−37	1.402±0.259	1.721±0.184	4
65−66	0.578±0.033	1.981±0.100	3	37−38	1.382±0.228	1.920±0.221	5
66−67	0.983±0.337	2.602±0.213	4	38−39	1.624	1.646	1
Planktonic				39−40	1.294±0.282	1.472±0.166	5
54−55	−0.574	2.410	1	40−41	1.149±0.064	1.564±0.103	6
55−56	−1.029	2.229	1	41−42	1.085±0.099	1.566±0.163	7
57−58	−0.850±0.412	3.164±0.531	2	42−43	0.624±0.232	1.859±0.088	4
66−67	−0.558±0.217	2.937±0.212	12	43−44	0.634	1.796	1
				44−45	0.593±0.167	1.448±0.131	4
Site 528				45−46	0.414±0.142	1.583±0.116	3
Benthic				46−47	0.630±0.166	1.334±0.144	7
1·2	3.763±0.312	0.477±0.249	27	47−48	0.427±0.104	1.296±0.136	4
2·3	2.740	0.641	1	48−49	0.357±0.046	1.353±0.031	3
4·5	2.835±0.078	0.840±0.085	2	49−50	0.102±0.130	1.449±0.033	2
41−42	1.349	1.359	1	50−51	0.121±0.246	1.698±0.266	6
46−47	0.728	0.718	1	55−56	0.262	2.079	1
47−48	0.421±0.186	1.718±0.365	7	56−57	0.520	2.032	1
Planktonic				57−58	0.450	2.162	1
1·2	0.294±0.171	1.422±0.232	29	58−59	0.490±0.113	2.252±0.057	2
47−48	−0.034	2.440	1	64−65	0.341±0.098	2.324±0.080	9
57−58	−1.057±0.421	3.252±0.511	6	65−66	0.409±0.177	2.256±0.113	2
				66−67	0.815±0.261	2.319±0.329	7
Site 529				68−69	1.334±0.060	2.615±0.213	3
Benthic				69−70	1.450±0.078	2.278±0.533	3
0·1	2.985	0.905	1	70−71	1.212	1.618	1
25−26	2.290	1.006	1	71−72	1.130±0.101	2.125±0.226	6
27−28	1.955	1.153	1	72−73	1.027±0.163	2.758±0.085	2
30−31	1.910	0.915	1	73−74	0.857±0.007	2.388±0.198	2
32−33	2.070	1.530	1	76−77	0.787±0.064	2.473±0.134	2
33−34	2.000	1.281	1	77−78	0.922	2.208	1
34−35	1.967±0.177	1.348±0.228	15	**Planktonic**			
35−36	2.320±0.044	1.698±0.222	3	31−32	1.578±0.039	1.325±0.304	2
36−37	1.985±0.512	1.715±0.393	9	32−33	1.672±0.184	2.111±0.140	4
37−38	1.024±0.035	1.504±0.184	2	33−34	1.618±0.271	1.823±0.207	4
38−39	1.334	1.299	1	34−35	1.799±0.107	2.074±0.107	5
39−40	1.360	1.290	1	35−36	1.994±0.069	2.458±0.233	5
40−41	1.119±0.139	1.364±0.261	3	36−37	0.602±0.755	1.992±0.543	5
48−49	1.214	1.174	1	37−38	1.203±0.120	2.355±0.134	4
Planktonic				38−39	0.773±0.109	2.230±0.128	4
0·1	0.185	1.205	1	39−40	0.833±0.425	1.954±0.346	9
10−11	0.519	2.389	1	40−41	0.731±0.269	2.012±0.128	16
24−25	0.751	2.409	1	41−42	0.592±0.149	2.112±0.111	12
25−26	0.740±0.129	2.525±0.093	2	42−43	0.516±0.125	2.236±0.138	5
27−28	1.041	2.639	1	43−44	0.260±0.299	2.293±0.099	6
30−31	0.991	2.509	1	44−45	−0.045±0.049	1.970±0.099	2
32−33	0.681	2.859	1	45−46	0.178±0.229	2.020±0.128	5
34−35	0.526±0.138	2.810±0.156	5	46−47	−0.077±0.155	1.799±0.183	10

Table 7-4. (continued).

Interval (Ma)	$\delta^{18}O$ (‰)	$\delta^{13}C$ (‰)	No. of Data
Site 689			
Planktonic			
47−48	−0.183±0.216	1.763±0.198	6
48−49	−0.464±0.140	2.100±0.127	7
49−50	−0.385±0.049	2.200±0.057	2
57−58	−0.750±0.694	1.787±0.976	3
58−59	−0.525±0.102	2.530±0.182	4
60−61	−0.463±0.064	3.387±0.158	3
Site 690			
Benthic			
20−21	2.624	1.556	1
26−27	2.678±0.106	1.452±0.069	4
27−28	2.437±0.107	1.643±0.142	8
28−29	2.687±0.269	1.416±0.149	4
29−30	2.565±0.190	1.441±0.251	5
31−32	2.154	1.326	1
32−33	2.239±0.184	1.371±0.184	13
33−34	2.035±0.213	1.815±0.205	7
38−39	2.214±0.156	2.201±0.134	2
39−40	1.103±0.169	1.655±0.127	5
40−41	1.075±0.192	1.727±0.228	5
44−45	0.372±0.268	1.522±0.343	6
45−46	0.167±0.167	1.480±0.261	9
46−47	0.087±0.117	1.679±0.004	2
49−50	−0.012±0.104	1.650±0.105	5
50−51	−0.079±0.106	1.884±0.062	4
51−52	−0.411±0.088	1.705±0.181	5
52−53	−0.411±0.186	1.875±0.125	3
54−55	−0.214±0.140	1.344±0.124	4
55−56	−0.089±0.156	1.583±0.291	19
56−57	−0.119±0.196	1.933±0.132	19
57−58	0.089±0.215	2.258±0.687	12
58−59	0.137±0.144	3.051±0.199	16
59−60	0.415±0.193	3.484±0.202	15
60−61	0.457±0.218	3.160±0.144	9
67−68	1.380	2.612	1
68−69	1.368±0.028	2.550±0.476	3
69−70	1.072±0.255	2.444±0.152	3
70−71	1.426±0.350	2.103±0.520	3
71−72	0.885±0.163	2.197±0.345	18
72−73	0.700±0.113	2.591±0.413	4
Planktonic			
38−39	0.835±0.431	2.015±0.134	2
39−40	0.958±0.090	2.100±0.224	4
40−41	0.913±0.145	2.222±0.097	5
41−42	0.630±0.125	2.197±0.191	6
44−45	0.025±0.106	1.900±0.140	4
45−46	−0.031±0.103	2.081±0.152	13
46−47	−0.130	2.030	1
49−50	−0.177±0.198	2.117±0.176	6
50−51	−0.332±0.077	2.240±0.154	6
51−52	−0.460±0.139	2.103±0.107	3
52−53	−0.500±0.192	2.250±0.165	5
53−54	−0.866±0.202	1.330±0.365	5
54−55	−0.439±0.115	1.633±0.134	7
55−56	−0.367±0.246	2.051±0.165	16
56−57	−0.661±0.180	2.122±0.110	21
57−58	−0.619±0.425	2.353±0.822	23
58−59	−0.394±0.169	3.384±0.272	17
59−60	−0.243±0.391	3.852±0.229	17
60−61	−0.045±0.159	3.604±0.164	6
Site 698			
Benthic			
51−52	−0.406±0.102	1.715±0.207	3
52−53	−0.448	1.709	1
53−54	−0.591	1.338	1
54−55	−0.614±0.021	1.205±0.114	2
55−56	−0.216±0.228	1.321±0.272	3
56−57	0.024	1.403	1
57−58	0.274	1.964	1
58−59	0.288±0.334	2.357±0.798	3
59−60	0.411±0.229	2.956±0.396	2
Site 699			
Benthic			
50−51	0.120	1.308	1
51−52	−0.475±0.259	1.895±0.190	3
52−53	−0.369	2.266	1
54−55	−0.916	1.707	1
55−56	−1.093	1.384	1
56−57	−1.160	1.361	1
58−59	−0.993	2.569	1
Site 700			
Benthic			
46−47	0.479±0.075	1.693±0.130	4
47−48	0.567±0.099	1.592±0.111	3
48−49	0.377±0.064	1.575±0.209	2
49−50	−0.314	1.415	1
50−51	−0.180±0.071	1.848±0.233	3
51−52	−0.308	2.221	1
52−53	−0.729	1.610	1
53−54	−0.588±0.264	1.552±0.442	2
54−55	−0.554±0.129	1.341±0.116	3
55−56	−0.592±0.147	1.087±0.247	3
58−59	−0.463±0.111	3.165±0.131	5
59−60	−0.351±0.261	3.417±0.409	7
60−61	−0.067±0.137	2.853±0.124	3
61−62	−0.554±0.066	3.020±0.126	2
62−63	−0.456±0.108	2.693±0.142	2
63−64	−0.595	2.780	1
64−65	−1.036	2.960	1
65−66	−1.028	3.127	1
Site 702			
Benthic			
38−39	1.047±0.026	1.753±0.024	3
39−40	1.069±0.157	1.811±0.095	4
40−41	1.132±0.064	1.660±0.005	2
42−43	0.358±0.061	2.129±0.191	3
43−44	0.582±0.075	1.499±0.258	4
44−45	0.451±0.064	1.695±0.080	4
45−46	0.483±0.016	1.984±0.005	2
46−47	0.478±0.112	1.951±0.295	4
47−48	0.532±0.123	1.648±0.091	7
48−49	0.427±0.069	1.692±0.125	6
49−50	0.173±0.146	1.538±0.115	6
50−51	−0.085	1.528	1
52−53	−0.278±0.121	1.802±0.083	3
53−54	−0.549±0.088	1.847±0.134	4
54−55	−0.406	1.370	1
55−56	−0.237±0.057	1.230±0.059	2
56−57	−0.157	1.431	1
57−58	0.120±0.195	1.899±0.394	3
58−59	0.095±0.228	2.196±0.420	3
59−60	0.277±0.121	3.400±0.199	9
60−61	0.090±0.110	2.738±0.206	4
Site 704			
Benthic			
0·1	3.475±0.435	0.114±0.509	48
1·2	3.834±0.343	−0.205±0.397	262
2·3	3.517±0.250	0.502±0.415	188
3·4	3.050±0.253	0.675±0.273	69
4·5	2.794±0.189	0.588±0.240	58
5·6	2.787±0.337	0.866±0.379	47
6·7	2.745±0.205	1.577±0.435	29
7·8	2.915±0.157	1.762±0.158	23
8·9	2.829±0.166	1.746±0.160	28
9·10	2.620±0.147	1.695±0.149	10
Northwestern Indian Ocean			
Site 237			
Benthic			
5·6	2.932±0.152	0.108±0.107	5
6·7	2.949±0.052	0.183±0.207	7
7·8	2.798±0.175	0.650±0.275	6
8·9	3.102±0.324	0.973±0.148	11

Table 7-5. (continued).

Interval (Ma)	$\delta^{18}O$ (‰)	$\delta^{13}C$ (‰)	No. of Data
Site 237			
Benthic			
9·10	2.950	1.180	1
12−13	3.010	1.290	1
13−14	2.550±0.208	1.263±0.365	6
14−15	2.070±0.157	1.570±0.336	3
15−16	2.255±0.035	2.170±0.212	2
16−17	1.835±0.218	1.797±0.538	6
17−18	1.968±0.080	1.413±0.100	6
18−19	1.948±0.146	1.328±0.237	12
19−20	1.869±0.088	1.165±0.111	12
20−21	1.990±0.173	1.083±0.153	3
21−22	2.095±0.163	1.205±0.021	2
22−23	2.000±0.057	1.150±0.042	2
23−24	1.835±0.223	1.285±0.420	4
Planktonic			
5·6	−0.446±0.297	1.338±0.201	6
6·7	−0.602±0.200	1.743±0.203	7
7·8	−0.616±0.215	2.001±0.258	6
8·9	−0.457±0.162	2.018±0.228	12
9·10	−0.843±0.219	2.175±0.163	2
10−11	−1.338	2.700	1
12−13	−0.078	2.090	1
13−14	−0.138±0.227	2.361±0.252	7
14−15	−0.531±0.278	2.600±0.121	3
15−16	−0.508±0.042	2.920±0.071	2
16−17	−0.784±0.145	2.616±0.467	6
17−18	−0.630±0.343	1.878±0.271	5
18−19	−0.536±0.249	1.936±0.191	11
19−20	−0.262±0.187	1.613±0.255	7
20−21	−0.238±0.398	1.657±0.029	3
22−23	0.662	1.280	1
Site 238			
Benthic			
5·6	3.137±0.233	0.097±0.276	6
6·7	3.152±0.061	0.448±0.438	5
7·8	2.948±0.159	0.810±0.176	6
8·9	3.076±0.138	1.182±0.295	9
9·10	3.550	−	1
10−11	3.260	0.850	1
11−12	2.825±0.304	0.955±0.686	2
12−13	2.885±0.035	0.945±0.318	2
13−14	2.438±0.304	1.150±0.233	4
14−15	2.300±0.411	1.733±0.125	3
15−16	1.935±0.325	1.735±0.409	4
16−17	2.020±0.453	1.560±0.255	2
17−18	2.035±0.082	1.333±0.128	4
18−19	2.135±0.290	0.985±0.120	2
19−20	2.110	0.740	1
23−24	2.262±0.147	1.206±0.215	11
Planktonic			
5·6	−0.886±0.297	2.047±0.270	7
6·7	−0.864±0.109	2.240±0.501	5
7·8	−1.067±0.156	2.536±0.316	5
8·9	−0.923±0.237	2.407±0.263	13
9·10	−1.014	2.270	1
10−11	−0.844	2.120	1
11−12	−0.860	2.400	1
12−13	−0.814±0.043	2.237±0.122	3
13−14	−0.882±0.294	2.379±0.158	4
14−15	−0.699±0.268	2.915±0.106	2
15−16	−0.618±0.213	2.860±0.143	6
16−17	−0.117±0.075	1.860±0.339	2
17−18	−0.318	1.910	1
18−19	−0.288	1.720	1
23−24	−0.264±0.190	2.020±0.113	2
Site 709			
Benthic			
4·5	3.120	0.270	1
5·6	3.125±0.100	0.716±0.382	11
7·8	3.138	1.060	1
8·9	3.170	0.780	1
9·10	2.995±0.021	0.885±0.078	2
10−11	2.914±0.072	0.989±0.184	5
Site 709			
Benthic			
11−12	2.916±0.075	1.167±0.158	11
12−13	2.775±0.159	1.024±0.587	4
13−14	1.972±0.203	1.476±0.352	14
14−15	2.105±0.175	1.324±0.329	24
15−16	1.970±0.223	1.945±0.330	6
16−17	2.024±0.128	1.108±0.096	9
17−18	1.936±0.136	0.936±0.157	5
18−19	1.971±0.134	1.023±0.130	4
19−20	2.224±0.149	1.107±0.114	12
20−21	2.053±0.142	0.955±0.116	4
21−22	2.328±0.089	1.720±0.005	2
22−23	2.322±0.177	1.708±0.206	8
23−24	2.127±0.187	1.301±0.323	8
Planktonic			
1·2	−0.856±0.220	1.320±0.195	173
2·3	−0.884±0.228	1.406±0.207	140
3·4	−0.957±0.239	1.372±0.175	248
4·5	−0.742±0.212	1.453±0.173	144
Site 714			
Benthic			
7·8	2.745±0.138	0.863±0.133	4
8·9	2.640±0.149	0.907±0.160	30
9·10	2.456±0.034	0.955±0.078	2
10−11	2.579±0.123	0.937±0.026	2
11−12	2.540±0.110	1.194±0.192	10
12−13	2.583±0.100	1.189±0.102	5
13−14	2.140	2.020	1
14−15	1.813	2.148	1
15−16	1.951±0.581	1.760±0.269	2
23−24	1.873±0.201	1.271±0.220	6
Planktonic			
0·1	−1.030±0.501		20
1·2	−1.242±0.514		19
2·3	−1.054±0.279		19
3·4	−1.433±0.351		19
4·5	−1.269±0.497		16
5·6	−1.428±0.051		5
7·8	−2.115±0.168	2.100±0.257	4
8·9	−1.985±0.258	1.951±0.203	27
9·10	−2.330±0.283	2.060±0.099	2
10−11	−1.610	1.540	1
11−12	−1.925±0.313	2.072±0.245	10
Site 716			
Planktonic			
0·1	−0.941±0.381		112
1·2	−0.861±0.318		65
Northeastern Indian Ocean			
Site 214			
Benthic			
5·6	3.133±0.222	0.267±0.259	6
6·7	2.771±0.250	0.756±0.394	7
7·8	2.967±0.097	1.300±0.138	12
8·9	3.069±0.220	1.173±0.103	11
9·10	2.220	0.680	1
10−11	2.557±0.074	0.963±0.225	3
11−12	2.570±0.156	0.550±0.339	2
12−13	2.705±0.134	0.825±0.078	2
13−14	2.305±0.228	0.970±0.261	5
14−15	1.780	1.410	1
15−16	1.745±0.148	1.565±0.007	2
18−19	1.945±0.064	1.395±0.488	2
19−20	1.900±0.170	1.145±0.290	2
20−21	1.900	0.980	1
21−22	1.970±0.057	1.130	2
22−23	2.030	1.350	1
23−24	1.970±0.028	1.050±0.028	2
Planktonic			
5·6	−0.821±0.197	1.984±0.210	8
6·7	−0.514±0.189	1.978±0.257	8
7·8	−0.542±0.120	2.407±0.188	18

Table 7-6. (continued).

Interval (Ma)	$\delta^{18}O$ (‰)	$\delta^{13}C$ (‰)	No. of Data
Site 214			
Planktonic			
8·9	−0.354±0.158	2.133±0.284	15
9·10	−0.127±0.400	1.622±0.124	3
10−11	−0.381±0.222	1.978±0.046	2
11−12	−0.016±0.314	2.165±0.233	2
12−13	−0.008±0.255	2.155±0.134	2
13−14	−0.228±0.152	2.303±0.135	5
14−15	−0.528	2.220	1
15−16	−0.631±0.141	2.168±0.301	4
16−17	−0.428±0.200	2.140±0.379	4
18−19	−0.069	2.110	1
Site 215			
Benthic			
55−56	−0.530±0.225	1.185±0.350	3
56−57	−0.080±0.000	1.647±0.064	2
57−58	−0.118±0.102	1.970±0.165	4
58−59	−0.035±0.108	2.343±0.791	4
59−60	0.270±0.221	3.074±0.218	5
60−61	0.470±0.269	2.829±0.169	3
Site 216			
Benthic			
8·9	3.041±0.119	0.850±0.121	7
10−11	2.850±0.141	0.875±0.078	2
11−12	2.773±0.090	0.757±0.175	3
12−13	2.810±0.245	1.065±0.181	4
13−14	2.453±0.194	1.477±0.110	3
14−15	2.030±0.087	1.760±0.201	3
15−16	1.910±0.424	1.735±0.290	2
16−17	1.807±0.084	1.727±0.212	3
17−18	1.835±0.021	1.565±0.502	2
18−19	1.895±0.235	1.130±0.292	4
19−20	2.062±0.151	0.940±0.133	9
20−21	2.195±0.325	0.735±0.521	8
21−22	2.077±0.121	1.034±0.229	7
22−23	2.193±0.335	1.367±0.387	3
Planktonic			
8·9	−0.333±0.158	1.787±0.270	7
10−11	−0.188±0.240	1.745±0.445	2
11−12	0.059±0.276	1.627±0.081	3
12−13	0.017±0.175	1.865±0.254	4
13−14	−0.238±0.014	2.105±0.092	2
14−15	−0.308±0.087	2.417±0.023	3
15−16	0.227±0.389	2.355±0.035	2
16−17	0.009±0.180	2.115±0.254	4
17−18	−0.373±0.021	2.405±0.021	2
18−19	−0.243±0.318	2.005±0.926	2
19−20	0.032±0.057	1.370±0.014	2
20−21	−0.165±0.316	1.627±0.087	3
22−23	−0.135±0.148	1.900±0.170	2
Site 253			
Benthic			
4·5	3.020±0.083	1.015±0.093	4
5·6	3.038±0.100	0.960±0.130	8
6·7	3.050±0.170	0.635±0.332	2
7·8	3.210±0.283	1.240±0.367	4
8·9	3.343±0.201	1.633±0.131	4
9·10	2.935±0.106	1.230±0.057	2
10−11	2.970±0.085	1.430±0.099	2
11−12	2.870±0.070	1.683±0.163	3
12−13	2.765±0.276	1.285±0.361	2
13−14	2.740	1.150	1
14−15	2.057±0.315	1.793±0.156	3
15−16	1.575±0.600	1.745±0.615	2
16−17	2.289±0.071	1.120±0.099	2
17−18	2.259	1.080	1
18−19	2.369	1.170	1
19−20	2.269	1.490	1
21−22	2.349	1.440	1
24−25	1.589	0.760	1
28−29	2.009	1.010	1
30−31	2.024±0.049	0.905±0.219	2
31−32	1.939±0.297	1.190±0.127	2
Site 253			
Benthic			
32−33	1.554±0.049	1.290±0.184	2
33−34	1.599	1.360	1
35−36	1.384±0.191	1.455±0.064	2
36−37	0.964±0.247	1.495±0.035	2
Planktonic			
4·5	0.288±0.297	1.920±0.041	4
5·6	0.743±0.399	1.746±0.175	8
6·7	1.020	2.010	1
7·8	1.185±0.247	1.985±0.205	2
8·9	1.240±0.076	2.173±0.156	4
9·10	1.120±0.000	2.000±0.007	2
10−11	1.025±0.007	2.130±0.007	2
11−12	1.067±0.177	2.115±0.080	3
12−13	1.075±0.247	1.840±0.403	2
13−14	0.780	2.315	1
14−15	0.573±0.311	2.415±0.178	3
15−16	0.645±0.021	2.800±0.049	2
16−17		2.000±0.021	2
17−18	0.515±0.071	2.142±0.106	2
18−19	0.475	2.157	1
19−20	0.455	2.657	1
21−22	0.110	2.607	1
24−25	−0.185±0.057	2.457±0.170	2
25−26	−0.235	2.197	1
26−27	−0.425	2.187	1
27−28	−0.075	2.137	1
28−29	−0.145	2.147	1
29−30	0.185	2.057	1
30−31	0.175±0.057	2.127±0.113	2
31−32	0.175±0.085	2.282±0.304	2
32−33	−0.355±0.200	2.194±0.032	3
33−34	−0.385	2.207	1
Site 752			
Benthic			
0·1	2.413	1.071	1
1·2	2.313±0.156	1.421±0.028	2
2·3	2.668±0.191	0.876±0.064	2
3·4	2.110±0.100	0.884±0.115	3
4·5	1.896±0.100	0.861±0.206	4
5·6	2.003±0.014	0.891±0.057	2
6·7	1.883±0.104	1.171±0.308	3
7·8	1.950±0.015	1.441±0.085	3
8·9	1.840±0.135	1.271±0.161	3
9·10	1.703±0.014	1.566±0.177	2
10−11	1.780±0.021	1.528±0.120	3
11−12	1.793±0.035	1.688±0.237	3
12−13	1.798±0.021	1.771±0.014	2
13−14	1.443±0.071	2.086±0.191	2
14−15	1.063±0.240	1.851±0.255	2
15−16	1.248±0.064	2.196±0.120	2
16−17	0.848±0.106	1.566±0.318	2
17−18	0.708±0.247	1.616±0.219	2
18−19	1.058±0.177	1.401±0.368	2
19−20	2.363±0.778	1.036±0.007	2
20−21	1.218±0.049	1.406±0.092	2
21−22	0.963±0.156	1.406±0.049	2
22−23	0.728±0.714	1.346±0.219	2
23−24	1.393	1.881	1
24−25	1.083	1.801	1
28−29	0.913	1.411	1
30−31	0.413	1.451	1
31−32	0.253	1.491	1
32−33	0.313	1.391	1
34−35	−0.377	1.721	1
35−36	−0.192±0.148	1.866±0.064	2
55−56	−0.789±0.199	0.655±0.282	13
56−57	−0.721±0.301	0.741±0.540	7
57−58	−0.588±0.086	1.325±0.293	3
58−59	−0.323±0.080	2.565±0.243	6
59−60	−0.308±0.140	2.578±0.274	3
60−61	−0.239±0.055	2.320±0.161	4
61−62	−0.222±0.090	2.083±0.193	12
62−63	−0.524±0.161	1.917±0.178	16

Table 7-7. (continued).

Interval (Ma)	$\delta^{18}O$ (‰)	$\delta^{13}C$ (‰)	No. of Data	Interval (Ma)	$\delta^{18}O$ (‰)	$\delta^{13}C$ (‰)	No. of Data
Site 752				**Site 756**			
Benthic				**Benthic**			
63−64	−0.955±0.179	2.066±0.307	5	23−24	1.355±0.081	1.167±0.047	3
64−65	−0.940±0.125	2.262±0.179	4	24−25	1.471±0.161	1.095±0.078	3
65−66	−1.386±0.179	2.175±0.274	6	25−26	1.567±0.174	0.911±0.255	3
66−67	−1.059±0.386	2.181±0.249	9	26−27	1.567±0.056	0.906±0.048	3
67−68	−0.875±0.345	2.168±0.087	4	27−28	1.592±0.097	1.010±0.085	3
68−69	−0.851±0.224	2.079±0.069	3	28−29	1.430±0.044	1.077±0.085	4
69−70	−0.821±0.019	1.941±0.172	3	29−30	1.397±0.032	0.841±0.099	2
70−71	−0.578±0.006	1.432±0.018	2	30−31	1.303±0.233	1.423±0.127	5
71−72	−1.105±0.371	1.433±0.150	2	31−32	1.400±0.217	1.108±0.228	9
Planktonic				32−33	1.608±0.335	1.020±0.224	4
55−56	−2.114±0.094	1.534±0.673	7	33−34	1.222±0.105	1.213±0.186	7
56−57	−2.232±0.270	1.567±0.527	5	34−35	1.200±0.260	1.561±0.298	5
57−58	−2.264±0.173	1.914±0.243	2	35−36	0.684±0.089	1.430±0.149	4
58−59	−2.177±0.149	3.175±0.416	4	36−37	0.571±0.146	1.516±0.146	6
59−60	−1.973±0.146	3.581±0.264	2	37−38	0.475±0.099	1.294±0.085	2
60−61	−1.957±0.128	3.291±0.119	3				
61−62	−1.976±0.228	2.843±0.218	6	**Site 757**			
62−63	−2.192±0.199	2.647±0.216	7	**Benthic**			
				0·1	3.088±0.201	0.108±0.277	5
Site 754				1·2	3.145±0.213	0.195±0.231	7
Benthic				2·3	2.800±0.196	0.342±0.106	5
0·1	2.847±0.113	0.936±0.230	3	3·4	2.632±0.186	0.309±0.210	9
1·2	2.741±0.073	1.015±0.190	3	4·5	2.505±0.127	0.429±0.166	8
2·3	2.696±0.088	0.997±0.133	6	5·6	2.506±0.118	0.363±0.132	6
3·4	2.240±0.196	0.885±0.110	6	6·7	2.625±0.290	0.648±0.272	7
4·5	2.249±0.227	0.808±0.125	4	7·8	2.356±0.227	1.158±0.282	5
5·6	2.189±0.071	0.922±0.150	4	8·9	2.825	1.355	1
6·7	1.957±0.038	1.120±0.168	4	9·10	2.415±0.213	1.089±0.124	2
7·8	2.092±0.059	1.469±0.067	2	10−11	2.464±0.014	0.957±0.291	2
8·9	2.078±0.163	1.331±0.170	2	11−12	2.309±0.155	1.141±0.118	3
9·10	1.933±0.036	1.492±0.076	3	12−13	2.484	0.491	1
10−11	1.933	1.531	1	13−14	2.118±0.150	1.255±0.266	3
11−12	2.169±0.112	1.182±0.254	3	14−15	1.354±0.127	1.464±0.076	4
12−13	1.873±0.132	1.523±0.234	16	16−17	1.528±0.069	1.050±0.220	2
13−14	1.681±0.226	1.798±0.284	11	17−18	1.719±0.084	1.187±0.114	3
14−15	1.058±0.096	2.222±0.131	3	18−19	1.784	1.117	1
15−16	1.232±0.210	2.233±0.250	3	19−20	1.443	1.293	1
16−17	0.953±0.028	1.670±0.012	2	23−24	1.687±0.053	1.218±0.001	2
17−18	1.223±0.226	1.301±0.410	2	25−26	1.584	1.429	1
18−19	1.313	1.511	1	27−28	1.666	1.256	1
19−20	1.273±0.141	1.493±0.088	2	28−29	1.634	1.379	1
20−21	1.285±0.136	1.482±0.113	4	30−31	1.723±0.077	1.284±0.038	4
21−22	1.238±0.164	1.530±0.083	4	31−32	1.619	1.206	1
22−23	1.287±0.160	1.764±0.179	3	33−34	1.620±0.021	1.575±0.102	2
23−24	1.228±0.271	1.580±0.235	4	34−35	1.631±0.132	1.790±0.210	4
24−25	1.100±0.222	1.513±0.243	2	35−36	1.219±0.163	1.568±0.182	2
25−26	1.263	1.311	1	36−37	0.922±0.011	1.350±0.182	2
26−27	1.221±0.017	0.952±0.128	2	37−38	1.069±0.051	1.856±0.131	4
27−28	1.213	1.301	1	38−39	0.941±0.066	1.748±0.001	2
28−29	1.227±0.020	1.212±0.114	5	40−41	0.878±0.099	1.353±0.121	3
				41−42	0.916±0.068	1.562±0.177	2
Site 756				42−43	0.974	1.677	1
Benthic				43−44	0.618±0.122	1.812±0.021	2
1·2	3.003±0.187	0.683±0.086	2	44−45	0.684	1.635	1
2·3	3.026±0.573	0.398±0.052	3	45−46	0.488	1.664	1
3·4	2.623±0.333	0.681±0.312	5	47−48	0.451±0.010	1.638±0.057	2
4·5	2.699±0.084	0.757±0.148	4	48−49	0.294	1.575	1
5·6	2.652±0.136	0.574±0.247	6	49−50	0.110±0.222	1.575±0.133	2
6·7	2.498±0.167	0.676±0.093	5	51−52	−0.187±0.141	1.793±0.019	2
7·8	2.446±0.133	1.168±0.160	4	53−54	−0.681±0.192	1.563±0.282	3
8·9	2.523±0.084	1.221±0.140	3	54−55	−0.799	1.044	1
9·10	2.535	1.434	1	55−56	−0.903	0.849	1
10−11	2.376±0.030	1.184±0.141	2	56−57	−1.141	0.972	1
11−12	2.498±0.131	1.581±0.547	2	**Planktonic**			
12−13	2.143±0.167	1.312±0.042	3	35−36	0.402	2.367	1
13−14	1.572	1.359	1	37−38	0.430	2.343	1
14−15	1.645	1.603	1	38−39	0.197	2.445	1
15−16	1.394±0.245	2.174±0.270	3	40−41	0.317	2.421	1
17−18	1.214±0.000	1.534±0.159	2	41−42	0.182	2.431	1
18−19	1.479±0.233	1.444±0.245	2	43−44	0.006	2.609	1
19−20	1.509±0.245	1.567±0.067	2	45−46	−0.159	2.390	1
20−21	1.616±0.193	1.493±0.143	4	47−48	−0.231	2.212	1
21−22	1.629±0.115	1.824±0.089	3	48−49	−0.170	2.413	1
22−23	1.446±0.083	1.442±0.306	3	49−50	−0.583±0.275	2.182±0.083	2

Table 7-8. (continued).

Interval (Ma)	$\delta^{18}O$ (‰)	$\delta^{13}C$ (‰)	No. of Data
Site 757			
Planktonic			
51−52	−0.872±0.194	2.259±0.033	2
52−53	−1.115	2.302	1
53−54	−1.433±0.292	2.094±0.255	2
54−55	−1.552	1.458	1
55−56	−1.636	1.395	1
56−57	−1.933	1.523	1
Site 758			
Benthic			
0·1	3.751±0.314	0.022±0.227	13
1·2	3.640±0.407	−0.021±0.225	12
2·3	3.242±0.533	−0.079±0.216	9
3·4	2.699±0.209	0.188±0.220	9
4·5	2.703±0.209	0.061±0.205	7
5·6	2.645±0.369	0.030±0.292	8
6·7	2.528±0.226	0.666±0.301	7
7·8	2.536±0.336	0.904±0.256	8
8·9	2.535±0.361	0.825±0.312	6
10−11	2.676	1.151	1
11−12	2.269±0.325	0.722±0.033	2
12−13	1.679	1.008	1
14−15	1.796±0.120	1.468±0.214	3
15−16	1.669	1.569	1
17−18	1.848	1.014	1
18−19	1.793±0.062	0.985±0.556	2
19−20	2.045±0.015	1.097±0.189	3
20−21	1.549±0.616	1.060±0.252	4
21−22	1.510±0.235	1.400±0.442	3
22−23	1.805±0.208	1.627±0.182	3
23−24	1.347±0.264	1.287±0.169	7
25−26	1.758±0.134	0.983±0.317	3
27−28	1.786±0.121	0.975±0.192	2
28−29	1.715	0.712	1
29−30	1.500	1.330	1
30−31	1.684±0.259	0.728±0.514	8
31−32	1.790±0.183	0.574±0.264	2
34−35	1.675±0.303	0.938±0.541	2
41−42	1.775	1.033	1
58−59	0.291	2.836	1
59−60	0.340±0.320	3.031±0.163	2
60−61	0.563±0.158	2.731±0.118	2
61−62	0.321±0.075	2.221±0.150	2
63−64	0.185	2.023	1
Planktonic			
0·1	−1.250±0.409	1.411±0.185	142
1·2	−1.478±0.232	1.621±0.222	121
2·3	−1.599±0.251	1.654±0.173	81
3·4	−1.903±0.135	1.542±0.180	12
4·5	−1.605±0.231	1.741±0.245	10
5·6	−1.701±0.259	1.740±0.320	10
6·7	−1.358±0.193	2.074±0.223	8
7·8	−1.568±0.116	2.181±0.226	9
8·9	−1.710±0.248	2.382±0.395	5
9·10	−1.624±0.148	1.655±0.346	2
11−12	−1.069±0.276	2.108±0.134	2
12−13	−1.154	2.178	1
14−15	−1.507±0.095	2.610±0.145	2
15−16	−1.184	2.562	1
17−18	−1.299	2.062	1
18−19	−1.369±0.148	1.969±0.102	3
58−59	−1.383	3.239	1
59−60	−1.340±0.301	3.372±0.010	2
60−61	−1.037±0.025	3.132±0.044	2
61−62	−0.922±0.140	2.609±0.271	2
63−64	−0.927	2.388	1
Site 762			
Benthic			
55−56	−0.559±0.168	0.869±0.359	2
56−57	−0.547±0.116	0.973±0.197	3
57−58	−0.460±0.128	0.987±0.168	8
58−59	−0.074	1.977	1
59−60	−0.183±0.040	2.817±0.297	3
60−61	0.216±0.187	2.821±0.107	5
Site 762			
Benthic			
61−62	−0.042±0.172	2.337±0.273	9
Southern Indian Ocean			
Site 738			
Benthic			
35−36	2.034±0.394	1.440±0.223	5
36−37	1.475±0.167	1.106±0.099	9
37−38	1.543±0.220	1.447±0.141	9
38−39	1.547±0.188	1.505±0.190	5
39−40	1.272±0.049	1.800±0.109	2
40−41	1.012	1.763	1
42−43	0.484±0.187	1.706±0.062	3
44−45	0.727	1.583	1
45−46	0.612±0.035	1.582±0.085	2
46−47	0.610±0.205	1.279±0.236	3
47−48	0.469±0.220	1.264±0.174	5
48−49	0.430±0.114	1.212±0.135	3
49−50	0.187	0.982	1
50−51	0.023±0.257	1.753±0.151	5
51−52	−0.290±0.040	1.869±0.042	3
52−53	−0.343±0.000	1.962±0.198	2
53−54	−0.553	1.972	1
54−55	−0.511±0.095	1.581±0.294	5
55−56	−0.383±0.099	1.452±0.353	2
56−57	−0.292±0.204	0.939±0.314	7
57−58	0.182	1.628	1
58−59	0.262	2.013	1
60−61	0.332±0.073	3.192±0.241	4
61−62	0.462±0.414	2.314±0.383	5
62−63	0.376±0.130	1.964±0.134	9
63−64	0.257±0.162	1.950±0.182	3
65−66	−0.033±0.164	2.710±0.293	5
66−67	−0.163	2.582	1
Planktonic			
35−36	0.757±0.107	2.597±0.120	3
36−37	0.497±0.087	2.353±0.182	7
37−38	0.503±0.192	2.358±0.160	9
38−39	0.615±0.323	1.793±0.209	5
39−40	0.627±0.292	2.287±0.075	2
40−41	0.293	2.365	1
41−42	0.009±0.491	2.241±0.257	2
42−43	−0.018±0.053	2.139±0.164	3
44−45	0.062	1.939	1
45−46	0.062±0.071	1.765	2
46−47	0.009±0.160	2.127±0.074	3
47−48	−0.157±0.218	1.814±0.246	6
48−49	−0.305±0.111	1.911±0.081	3
49−50	−0.564±0.191	1.940±0.118	3
50−51	−0.680±0.072	2.110±0.386	5
51−52	−0.676±0.208	2.120±0.351	3
52−53	−1.355±0.531	2.060±0.000	2
53−54	−0.879±0.134	2.127±0.110	2
54−55	−1.078±0.099	1.980±0.179	5
55−56	−0.855±0.502	1.640±0.099	2
56−57	−1.173±0.215	1.708±0.240	4
57−58	−0.850±0.156	2.270±0.226	2
58−59	−0.560	2.500	1
60−61	−0.625±0.092	3.870±0.042	2
61−62	−0.465±0.163	2.730±0.099	2
62−63	−0.563±0.144	2.243±0.165	4
63−64	−0.426±0.047	2.288±0.134	5
Site 744			
Benthic			
9·10	3.131±0.021	1.090±0.085	2
10−11	3.023±0.212	1.338±0.235	5
11−12	3.051±0.381	1.217±0.356	6
12−13	2.657±0.041	1.305±0.035	2
13−14	2.287±0.236	1.788±0.203	5
14−15	1.937±0.237	1.810±0.141	12
15−16	2.033±0.334	1.994±0.187	7
16−17	1.989±0.292	1.977±0.372	8
17−18	2.068±0.316	1.774±0.142	19
18−19	2.292±0.238	1.592±0.138	5

Table 7-9. (continued).

Interval (Ma)	$\delta^{18}O$ (‰)	$\delta^{13}C$ (‰)	No. of Data
Site 744			
Benthic			
19−20	2.491±0.060	1.433±0.130	4
20−21	2.220±0.121	1.260±0.200	5
21−22	2.176	1.280	1
24−25	2.576	1.650	1
25−26	2.666	1.560	1
26−27	2.226±0.208	1.385±0.151	4
27−28	2.360±0.128	1.020±0.197	5
28−29	2.651±0.148	1.130±0.014	2
30−31	2.556	1.050	1
31−32	3.356	0.990	1
32−33	2.502±0.125	1.128±0.090	5
33−34	2.476±0.125	1.253±0.240	4
34−35	2.559±0.083	1.298±0.077	4
35−36	2.412±0.348	1.532±0.154	9
36−37	1.696±0.196	1.158±0.286	5
37−38	1.690±0.339	1.274±0.161	5
38−39	1.312±0.141	1.440±0.168	8
39−40	1.656±0.044	1.527±0.112	3
Planktonic			
19−20	1.122±0.181	2.839±0.151	5
20−21	0.760±0.259	2.519±0.227	5
21−22	0.956	2.389	1
24−25	1.146	2.629	1
25−26	1.206	2.389	1
26−27	0.766±0.075	2.494±0.098	4
27−28	0.799±0.256	2.054±0.117	6
28−29	1.131±0.106	2.149±0.127	2
30−31	1.186	2.539	1
31−32	1.316	2.299	1
32−33	1.114±0.261	2.257±0.045	15
33−34	1.091±0.083	2.337±0.123	4
34−35	1.159±0.092	2.107±0.049	4
35−36	1.217±0.259	2.242±0.142	8
36−37	0.560±0.111	2.257±0.107	5
37−38	0.528±0.172	2.285±0.096	5
38−39	0.344±0.168	2.402±0.181	6
39−40	0.313±0.087	2.489±0.171	3
Site 748			
Benthic			
22−23	2.292	1.149	1
23−24	2.174±0.114	1.118±0.048	3
24−25	2.321±0.182	0.957±0.081	2
25−26	2.407±0.095	1.180±0.159	3
26−27	2.409±0.125	0.955±0.573	2
27−28	2.394±0.179	0.885±0.007	2
28−29	2.310±0.141	0.830±0.028	2
29−30	2.515±0.195	0.765±0.069	4
30−31	2.521±0.126	0.677±0.117	2
31−32	2.211±0.098	0.477±0.117	2
32−33	2.437±0.196	0.650±0.104	3
33−34	2.310±0.036	1.027±0.132	3
34−35	2.270±0.198	0.985±0.049	2
35−36	2.393±0.530	1.178±0.323	12
36−37	1.620±0.110	1.184±0.187	5
37−38	1.350±0.057	1.425±0.168	5
38−39	1.662±0.071	1.484±0.097	4
39−40	1.431±0.055	1.420±0.000	2
40−41	1.260±0.145	1.233±0.106	3
41−42	1.164	1.129	1
42−43	0.970	1.070	1
43−44	0.903±0.143	1.355±0.280	3
44−45	0.880±0.141	1.040±0.491	2
52−53	−0.560	0.410	1
55−56	−0.220	−0.750	1
58−59	−0.090	0.450	1
59−60	0.092±0.359	2.251±0.695	5
Planktonic			
33−34	1.377±0.212	1.839±0.310	4
34−35	0.997±0.170	1.831±0.101	3
35−36	1.287±0.387	2.190±0.211	10
36−37	0.745±0.104	2.097±0.213	7
37−38	0.455±0.259	2.379±0.098	5
38−39	0.334±0.121	1.941±0.378	3
39−40	0.344	1.761	1
40−41	0.201±0.009	1.801±0.226	2
42−43	0.012±0.229	2.021±0.268	2
43−44	0.034	2.041	1
44−45	−0.217±0.159	1.757±0.306	3
45−46	0.274±0.269	1.661±0.099	2
47−48	0.534	0.771	1
49−50	0.104	0.671	1
52−53	−0.496±0.085	0.776±0.049	2
55−56	−0.546	0.331	1
58−59	−0.426±0.115	1.904±0.330	3
59−60	−0.699±0.187	2.964±0.395	4
Site 750			
Benthic			
65−66	0.195±0.021	2.555±0.073	4
66−67	0.173±0.217	2.341±0.131	12
Site 751			
Benthic			
4·5	3.410±0.133	0.955±0.105	4
5·6	3.570±0.137	1.297±0.160	18
6·7	3.578±0.101	1.24±0.168	9
7·8	3.593±0.209	1.196±0.148	5
8·9	3.489±0.145	1.135±0.093	12
9·10	3.313±0.252	1.202±0.215	41
10−11	3.354±0.172	1.372±0.262	54
11−12	3.319±0.226	1.407±0.273	55
12−13	3.005±0.128	1.658±0.109	8
13−14	3.099±0.003	2.073±0.211	3
14−15	2.727±0.393	1.779±0.124	4
15−16	2.325±0.179	1.878±0.172	11
16−17	2.164±0.219	1.835±0.162	17
17−18	2.224±0.334	1.672±0.326	8
18−19	2.481±0.194	1.316±0.361	12
19−20	2.360±0.024	1.106±0.192	2

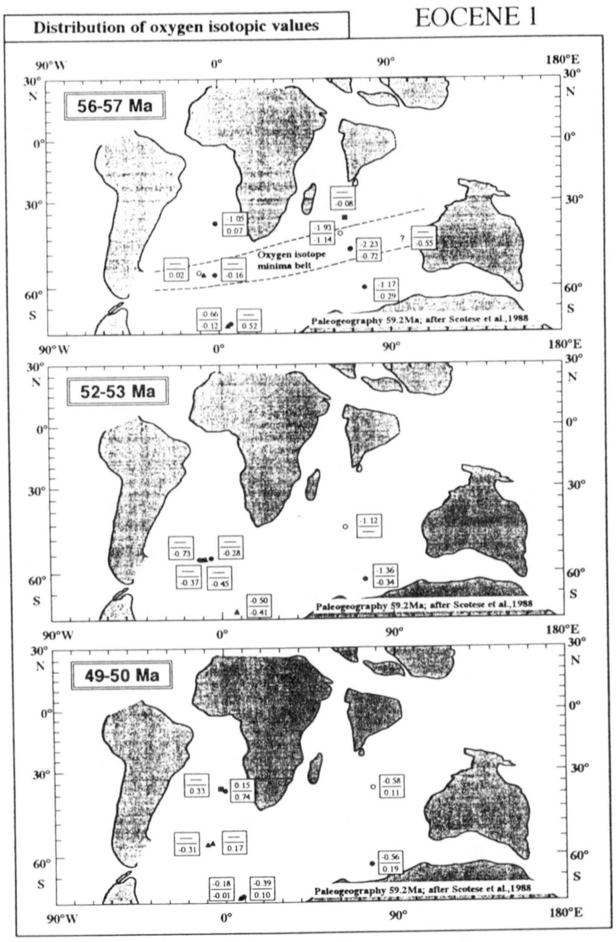

Fig. 57-1. Geographical distribution of oxygen isotopes during the Eocene. The isotopic data are averaged in one million year intervals (Table 7). See legend of Fig. 56.

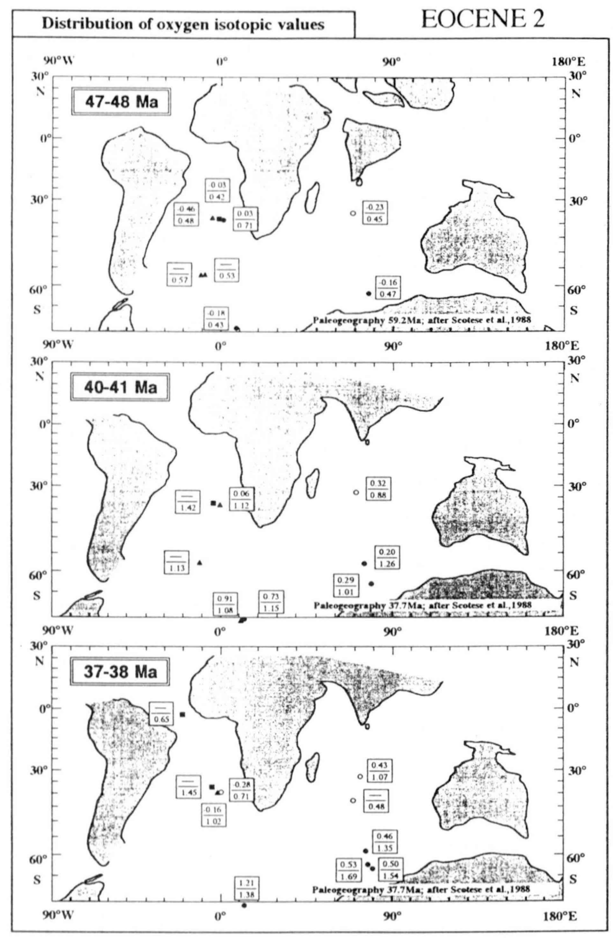

Fig. 57-2. (continued).

distinctly high. Latitudinal difference of surface water $\delta^{18}O$ at this time is smaller than that in the latest Paleocene; for example the difference between 40°S and 70°S ranges from 0.2-0.4‰. Distinctly lower values of $\delta^{18}O$ of surface and bottom water in the Indian and South Atlantic Oceans became close to $\delta^{18}O$ values at high-latitudes in this interval, and those values became close to values recognized at the middle/early Eocene boundary. As a result, "oxygen isotopic minima belt" in the Indian and South Atlantic Oceans disappear at this time. $\delta^{18}O$ values in the Indian Ocean are slightly lower than those in the Atlantic Ocean.

During the middle Eocene, the oxygen isotopic values of bottom water in the Atlantic Ocean tend to increase northward from high-latitudes, and the oxygen isotopic difference between the high- and low-latitude sides (around 70°-40°S) is 0.2-0.6‰ at the same depth. From 49 to 51 Ma, $\delta^{18}O$ values of intermediate water (~2000m) at high-latitudes are 0.2-0.3‰ lower than those of deep water. In contrast, $\delta^{18}O$ values of intermediate water (1000-2000m) at high-latitudes are 0.3-0.5‰ higher than those from 47 to 43 Ma. The benthic $\delta^{18}O$ values at 40 Ma are close to values at depths shallower than 2500 m. In surface water of the Atlantic Ocean, $\delta^{18}O$ values at low-latitude are about 0.3‰ higher than those at high-latitudes during the period 51-48 Ma (Fig. 57). In the Indian Ocean, the oxygen isotopic values of bottom water tend to increase southward from low-latitudes in the middle Eocene, and the latitudinal difference of $\delta^{18}O$ value between 35°S and 65°S is 0.1-0.4‰ at a different water depth (Fig. 57-2). This difference tends to be expanded. The oxygen isotopes of intermediate water (1000-1500m) at high-latitudes in the Indian Ocean show relatively high values in comparison with deep water, which is a similar oxygen isotopic record to the Atlantic Ocean. No latitudinal gradient of oxygen isotopes is observed in surface water of the Indian Ocean.

In the late Eocene, the oxygen isotopic values of bottom water in the Atlantic Ocean tend to decrease toward low-latitudes the opposite pattern to the middle Eocene, and then the latitudinal difference between 70°S and 0° is about 0.6‰ (Fig. 57-2). The pattern of oxygen isotopes in surface water is similarly to that in bottom water. The latitudinal difference between 70° and 40°S in surface water is about 0.6-1.4‰. Although the latitudinal gradient of oxygen isotopes in the Indian Ocean in the late Eocene is close to that of the middle Eocene, the latitudinal difference of $\delta^{18}O$ values between 65°S and 35°S is expanded by 0.3-0.6‰.

Oligocene: In the Atlantic Ocean, the oxygen isotopic values of bottom water in the Oligocene exhibit a decreasing trend toward low-latitudes, and the gradient at the late Oligocene is steeper than that of the early Oligocene (Fig. 58). The latitudinal difference from 70°S to 0° at ~2000m water depth ranges from 0.8-1.0‰ in the earliest Oligocene (36-34 Ma). This difference is rapidly reduced in the 34-33 Ma interval, and becomes to 0.4-0.6‰ in the late early Oligocene (34-30 Ma). This difference is again expanded by 0.6-1.2‰ in the late Oligocene. The oxygen isotopic values in intermediate water (~2000 m paleodepth) at high-latitudes are relatively higher than those in deep water. The water column gradient in other regions around the Atlantic Ocean shows a decreasing trend toward shallower depth. $\delta^{18}O$ values in surface water around the Atlantic Ocean also tend to decrease northward from the high-latitude side during the Oligocene. The latitudinal difference of $\delta^{18}O$ value in surface water between 70°S and 40°S is 1.0-1.4‰, and show a reducing trend.

The oxygen isotopic values of bottom water in the Indian Ocean tend to decrease northward from high-latitudes similar to the oxygen isotopic record in the Atlantic Ocean. No latitudinal difference is recognized to the north of 40°S. At 2000 m paleodepth, the latitudinal difference between 65°S and 10°S is constant throughout the Oligocene (approximately 0.9‰). The latitudinal difference (65°S-35°S) in surface water is 1.4‰ from 35 to 32 Ma, reducing to ~1.0‰ at 32-31 Ma, and tends expand gently from 32 to 24 Ma. At 1000m paleodepth, the latitudinal difference between 60°S and 30°S is ~0.7‰ with a small fluctuation throughout the Oligocene. This fluctuation may reflect an isotopic change in surface water. The water column gradient in the Indian Ocean exhibits a decreasing trend toward shallower depths.

Miocene: During the Miocene, the oxygen isotopic values of bottom water in the Atlantic Ocean show a decrease north-ward from the high-latitude side, which is similar to the Oligocene isotopic record (Fig. 59-1). At 2500m water depth, the $\delta^{18}O$ difference between the high- and low-latitude sides (around 35°S-5°N) is relatively large from 25-20 Ma and 13-7 Ma, respectively (0.3-0.8‰). In these intervals, the largest differences are recognized at 24-23 Ma and 11-10 Ma, respectively. The water column gradient tends to decrease

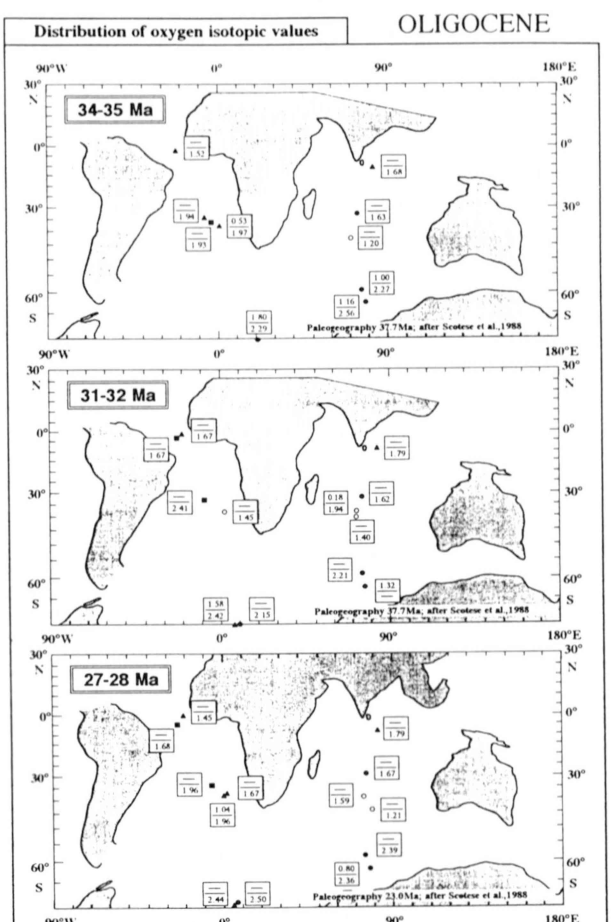

Fig. 58. Geographical distribution of oxygen isotopes during the Oligocene. The isotopic data are averaged in one million year intervals (Table 7). See legend of Fig. 56.

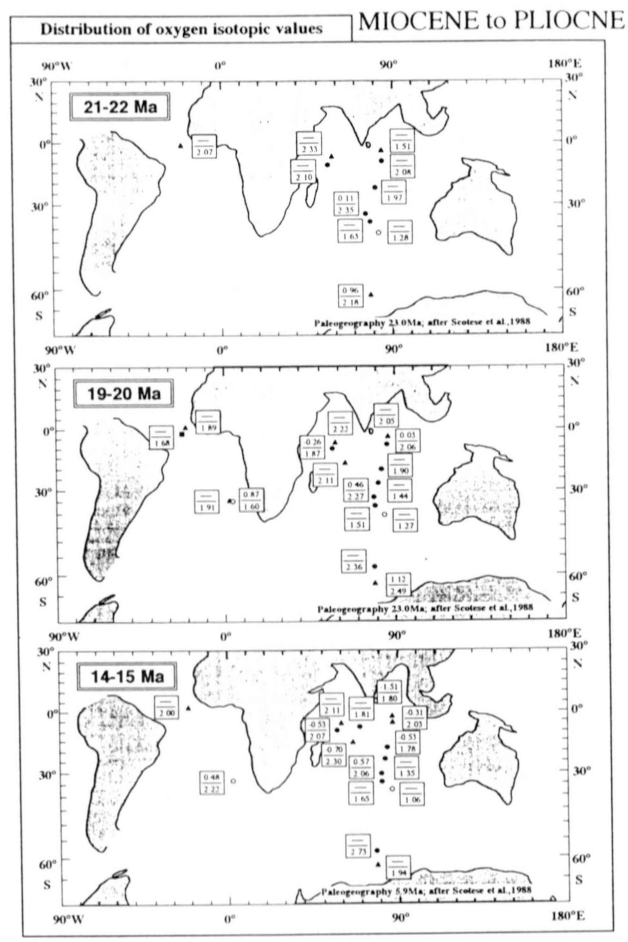

Fig. 59. Geographical distribution of oxygen isotopes from Miocene to Pliocene. The isotopic data are averaged in one million year intervals (Table 7). See legend of Fig. 56.

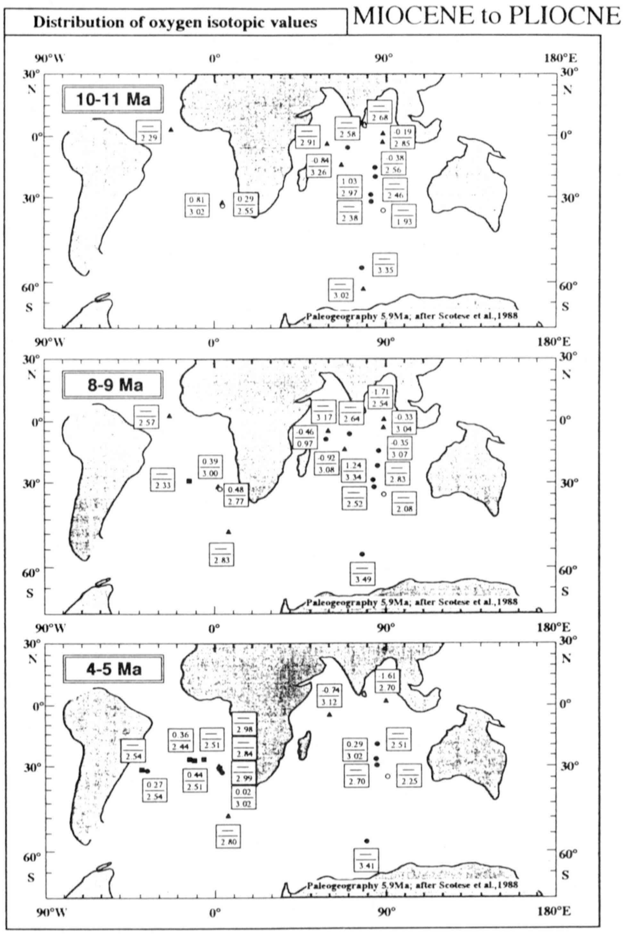

Fig. 59-2. (continued).

with depth in these intervals. In contrast, the latitudinal difference of $\delta^{18}O$ (around 35°S-5°N) is small at 20-13 Ma (<0.25‰) and in terms of the $\delta^{18}O$ water column is constant between 1000-2500m depths.

The oxygen isotopic values of bottom water in the Indian Ocean exhibit a general decrease northward from the high-latitude side and westward from the east side during the Miocene. The latitudinal difference of $\delta^{18}O$ values between 60°S and 35°S is from 0.5 to 1.5‰ at a water depth of 1500 m, and this difference is small at 26-23 Ma, 18-15 Ma, 13-12 Ma, and 9-8 Ma intervals, whereas it is large from 15-13 Ma (Fig. 59). The 18-15 Ma interval corresponds to the oxygen isotopic minima zone in the Miocene, and the 15-13 Ma interval corresponds to a shift in the middle Miocene. $\delta^{18}O$ values at 1500 m paleodepth between 55°E to 85°E show a range of 0.2-0.8 ‰ at the 15-9 Ma interval. This difference is not observed at other intervals in the Miocene. At a water depth of 2000m, the latitudinal difference between 60°S and 10°S in terms of $\delta^{18}O$ value is less than 0.5‰, and is relatively small at 22-20 Ma and 18-15 Ma. The latitudinal difference between 60°S and 10°S shows an increase north-ward from high-latitudes from 15 to 13 Ma. Relations are reverse to the general gradients. Therefore, the latitudinal gradient of deep water is in contrast to that of shallow water (1500m). The longitudinal difference of $\delta^{18}O$ at 2000m paleodepth between 55°E and 85°E is consistently 0.1-0.2‰ throughout the Miocene. The latitudinal difference of $\delta^{18}O$ in surface water is large in the Indian Ocean during the Miocene: for example this difference at 35°-5°S is 1.9-3.0 ‰. This difference is largest at 9-8 Ma, which corresponds to the ^{18}O maximum at 8 Ma. The longitudinal difference of $\delta^{18}O$ values in surface water during the Miocene gradually expands to the ^{18}O maximum at 8 Ma, and reduces afterward.

Pliocene-Pleistocene: The oxygen isotopic latitudinal gradient from the Pliocene to Pleistocene in the Atlantic Ocean decreases south-ward at depths shallower than 4000 m, opposite to the pattern in the Miocene (Fig. 59-2). The latitudinal differences of $\delta^{18}O$ between 50°S-30°S and 50°S-20°N at a water depth of 2500 m are less than 0.2 ‰ in the shift of the late Pliocene (5-3 Ma), whereas they expand to 0.5 and 1.2‰ respectively after the shift of the late Pliocene (3-0 Ma). The latitudinal gradient of $\delta^{18}O$ below the 4000m paleodepth in the Atlantic Ocean decreases to the north. The latitudinal difference in oxygen isotopes between 30°S and 0° is ~0.6 ‰ at 4500m depth. The oxygen isotopic ratios in surface water tend to increase toward high-latitude, and the latitudinal difference between 0° and 30°S is ~1.0‰. In the Indian Ocean, $\delta^{18}O$ values of bottom water at depths <3000m tend to decrease north-ward from the Pliocene on, which is the opposite relation to the gradient in the Atlantic Ocean. The oxygen isotopic values in the Indian Ocean are lower than those of the Atlantic Ocean.

2. Carbon isotopes

Maastrichtian: In the Maastrichtian, the carbon isotopic values at Site 752 in the Indian Ocean are ~0.4‰, lower than those of Site 689 in the Atlantic sector of the Southern Ocean. Although Sites 689 and 690 are situated at different water depths, $\delta^{13}C$ values at Site 689 are close to those of Site 690. Therefore, the carbon isotopic column in the Atlantic sector of Southern Ocean may be uniform.

Paleocene: In general, carbon isotopic values at the low-latitudes in the Atlantic Ocean are higher than those at the high-latitudes (Fig. 60). The ^{13}C latitudinal gradient is relatively large from 66-61 Ma: for example the latitudinal difference between 55°S and 40°S is ~1.0‰ at a water depth of 2000m. In this interval, a water column gradient is not observed at low-latitudes. In contrast, the latitudinal difference in carbon isotopes between 70°S and 40°S is small at 61-58 Ma, <0.3‰ at 1000-2500m water depth. At the 61-60 Ma section, $\delta^{13}C$ values at mid-latitudes (60°S-40°S) are uniform at 1000-2500 m paleodepth, however the $\delta^{13}C$ values at high-latitudes are relatively low. The ^{13}C difference between those regions and Site 690 at 70°S are relatively large. At the 60-59 Ma interval, which show the highest values of $\delta^{13}C$, they are uniform in the water mass between 70° and 55°S in the 1500-2500 m paleodepth, and between 55°S and ~40°S at 1000 m. The ^{13}C difference of these water masses, however, is relatively large. The surface carbon isotopic values at 61-58 Ma interval are relatively high at low-latitudes.

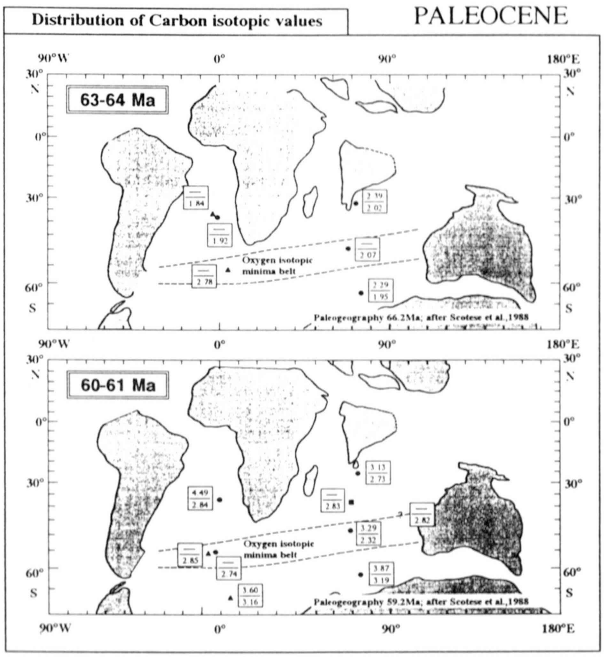

Fig. 60. Geographical distribution of carbon isotopes during the Paleocene. The isotopic data are averaged in one million year intervals (Table 7). See legend of Fig. 56.

In the Indian Ocean, the carbon isotopic latitudinal difference at ~1000 m between 65°S 50°S is ~0.5‰ from 67 to 64 Ma, with higher values at high-latitudes. At 64-61 Ma, $\delta^{13}C$ values of bottom water between 65°S and 30°S are uniform. In this area, $\delta^{13}C$ values are the lowest at 50°S. In this interval, $\delta^{13}C$ values of surface water at mid-latitudes (~50°S) are 0.1-0.4‰, higher than those on the low- and high-latitude sides (around 30°-60°S). Consequently, the surface to bottom difference is the largest at mid-latitudes. In the 61-58 Ma interval for highest values of $\delta^{13}C$, the latitudinal difference of $\delta^{13}C$ at ~1000m is relatively large: $\delta^{13}C$ values on the high-latitude side (~60°S) are ~0.5‰ higher than those on the low-latitude side (~30°S), and ~0.9‰ higher than those of mid-latitudes (~50°S), which are the lowest values in this area. The carbon isotopic values in surface water decrease toward low-latitudes, and the ^{13}C latitudinal difference between 60° and 50°S is relatively large (approximately 0.75‰). In contrast, $\delta^{13}C$ values between 50°-30°S exhibit a relatively small difference (<0.2‰). In general, the carbon isotopic values on the Atlantic Ocean side are slightly higher than those of the Indian Ocean side at high-latitudes.

Eocene: The carbon isotopic values of bottom water on the Atlantic Ocean side decrease toward low-latitudes through the Eocene (Fig. 61). In the early Eocene, the latitudinal difference of $\delta^{13}C$ in bottom water tends to expand from 58 to 56 Ma, then reduce to 52 Ma (Fig. 61-1). The largest latitudinal difference of $\delta^{13}C$ at 57-56 Ma corresponds to a ^{13}C minimum value, and the latitudinal difference between 70 and 40°S at 1000m paleodepth reaches 1.1 ‰. The carbon isotopic column gradient of bottom water in the 58-56 Ma interval shows a decrease with depth, whereas the gradient increases during the 56-52 Ma interval. This gradient is remarkable at mid-latitudes (~55°S). No surface latitudinal difference in $\delta^{13}C$ value is observed in the 57 to 55 Ma interval. As for other intervals in the early Eocene, $\delta^{13}C$ values in surface water show slight latitudinal differences, and are randomly distributed. The benthic latitudinal gradient of $\delta^{13}C$ on the Indian Ocean side shows a decrease toward low-latitudes similar to that on the Atlantic Ocean side. The latitudinal difference in $\delta^{13}C$ tends to expand from 58 to 56 Ma. Carbon isotopic values decrease from the Atlantic to Indian Ocean sides at high-latitudes. A regional difference in $\delta^{13}C$ is recognized in the Indian and South Atlantic Oceans during the ^{13}C minima zone (57-55 Ma). The $\delta^{13}C$ variance increases between the southern and northern parts of the South Atlantic Ocean. The same feature can be observed in $\delta^{13}C$ between the South Atlantic and Indian Oceans.

In the 52-49 Ma interval of the middle Eocene, the carbon isotopic values of intermediate water (~2000 m) in the South Atlantic Ocean (70-55°S latitude) are relatively high. A ^{13}C latitudinal difference is not observed in this area. In the 49-44 Ma interval on the Atlantic Ocean side, the carbon

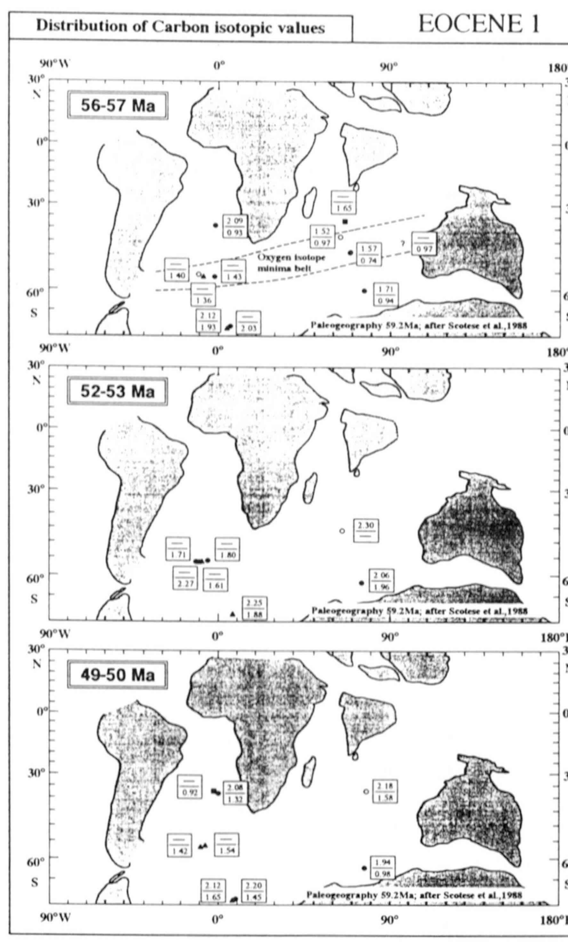

Fig. 61-1. Geographical distribution of carbon isotopes during the Eocene. The isotopic data are averaged in one million year intervals (Table 7). See legend of Fig. 56.

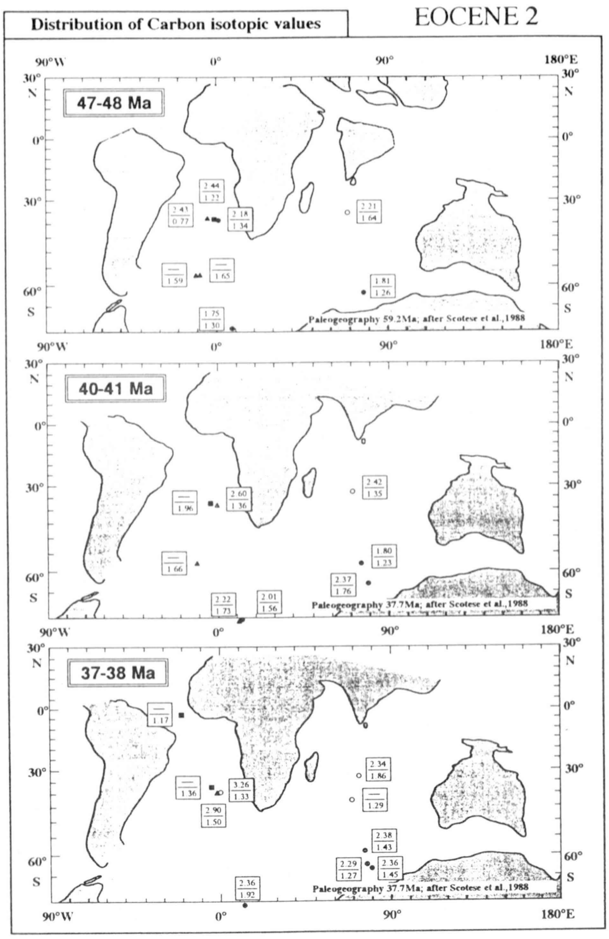

Fig. 61-2. (continued).

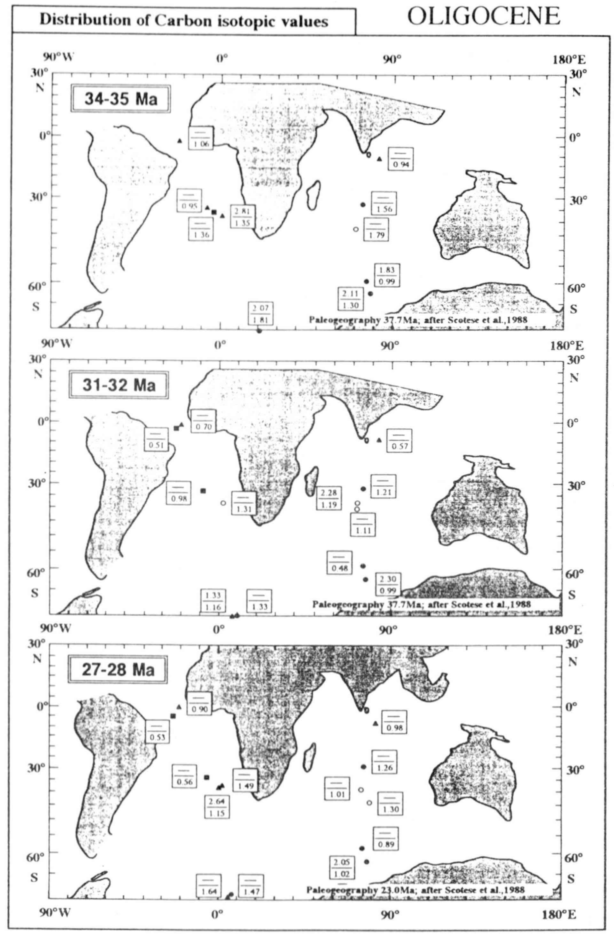

Fig. 62. Geographical distribution of carbon isotopes during the Oligocene. The isotopic data are averaged in one million year intervals (Table 7). See legend of Fig. 56.

isotopic values are lowest at low-latitudes (~40°S) in deep water (2500-3000 m paleodepth). This trend is noted in the 48-46 Ma interval (Fig. 61-2). The ^{13}C latitudinal difference is relatively small except for the area showing the lowest value, and is less than 0.6 ‰ in this interval. In the 44-40 Ma interval, $\delta^{13}C$ values differ by <0.6 ‰ according to latitude. In surface water, a latitudinal difference in $\delta^{13}C$ between 70°S and 40°S in the middle Eocene is not recognized in the 52-49 Ma interval, whereas isotopic differences are 0.55-0.75 ‰ in the 49-40 Ma interval, with higher values at low-latitudes. In the Indian Ocean, carbon isotopic values in low-latitudes tend to be higher than those at high-latitudes at different water depths through the middle Eocene. The ^{13}C latitudinal difference in the 43-40 Ma interval is 0.4-0.6 ‰ in intermediate water (~1000 m paleodepth). In this interval, the carbon isotopic values of deep water at high-latitude (>1500 m) are the highest among the Indian Ocean sites, while the lowest values are found at intermediate water (~1000 m). At high-latitudes, the carbon isotopic values of deep water (>1500 m paleodepth) in the Indian Ocean are close to those of the Atlantic Ocean during the middle Eocene. Between 60° and 40°S, $\delta^{13}C$ values of surface water at low-latitudes tend to be slightly higher than those at high-latitudes.

In the late Eocene, the ^{13}C latitudinal difference (70-0°S) in the Atlantic Ocean is <0.8 ‰ in bottom water. $\delta^{13}C$ values in intermediate water (~1500 m) are lower than those of deep water (~2000 m) at high-latitudes (~70°S). The carbon isotopes in the water column are close to constant at mid-latitudes (~40°S). $\delta^{13}C$ values in surface water at mid-latitudes (~40°S) are 0.7-1.0 ‰, higher than those at high-latitudes (~70°S). In the Indian Ocean, the carbon isotopic at low-latitude are higher than those at high-latitudes at shallower than 2000m paleodepth throughout the late Eocene. The latitudinal difference of $\delta^{13}C$ at that time is 0.1-0.4 ‰ between 60°S and 35°S, which is smaller than that in the late middle Eocene. Carbon isotopic values in the Indian Ocean are lower than those in the Atlantic Ocean, and the difference of $\delta^{13}C$ in those oceans tends to expand throughout the middle Eocene.

Oligocene: Carbon isotopes on the Atlantic Ocean side shows decrease gradually toward low-latitudes (Fig. 62).

The ^{13}C latitudinal difference between 70°S and 0° at a water depth of ~2000m is 0.6-1.0‰ up to ~32 Ma, and 0.4-0.6‰ from 32 Ma to 26 Ma. This difference tends to expand from 30 Ma. The latitudinal difference of $\delta^{13}C$ at 2500-3500 m between 70°S and 0° is 0.8-1.1 ‰ in the 32-26 Ma interval with an increase in upper stratigraphic levels. Surface carbon isotopes exhibit a high values at low-latitudes. Carbon isotopic values of intermediate water (<1500 m paleodepth) on the Indian Ocean side increase toward low-latitudes. The ^{13}C latitudinal difference reduces upward, and is <0.2‰ in the 27-24 Ma interval. Conversely, carbon isotopic values in deep water (>1500 m paleodepth) decrease toward low-latitudes. At high-latitudes (~60°S), $\delta^{13}C$ values in intermediate water (~1000 m) are lower than those in deep water during the Oligocene. Although this trend cannot be found in low-latitudes by 31 Ma, $\delta^{13}C$ values are low at ~1000m after 31 Ma, with high values at ~2000m paleodepth.

Miocene: During the Miocene, carbon isotopes in bottom water on the Atlantic Ocean side decrease toward low-latitudes (Fig. 63). The latitudinal difference of $\delta^{13}C$ at 2500m between 35°S and 5°N is less than 0.4‰ in the 24-22 Ma interval, corresponding to a ^{13}C maximum in the earliest Miocene (23 Ma). A value of 0.5-0.7‰ at 19-14 Ma corresponds to a ^{13}C maximum in the middle Miocene (15 Ma), whereas there are large variation between 0.8 to 1.0‰ from 21-19 Ma. From 8 to 14 Ma, the ^{13}C latitudinal difference between 35°S and 5°N at 2500m paleodepth tends to reduce from 0.8 to 0.2 ‰. The water column gradient in the 1000-3000 m depth interval is small (<0.3 ‰). $\delta^{13}C$ values at >3000m differ by ~0.5‰ from this depth section, particularly during the late Miocene.

The latitudinal gradient of carbon isotopic values in the Indian Ocean decrease toward low-latitudes at the same water depth. Carbon isotopic values in the Indian Ocean transect show a longitudinal decrease eastward from 24 Ma to 9 Ma, whereas they increase eastward from 9 Ma to 5 Ma. In the water column of the northern Indian Ocean, lower $\delta^{13}C$ values are observed at 1500-2000m, and $\delta^{13}C$ values are relatively high immediately above and below this interval. The ^{13}C latitudinal gradient in surface water tends to decrease northward from high-latitudes. The ^{13}C latitudinal difference is large up to 19 Ma, and then is greater than 1.0‰ between 60° and 5°S. After 19 Ma, the ^{13}C latitudinal difference is relatively small during the Miocene.

Pliocene-Pleistocene: During the Pliocene, carbon

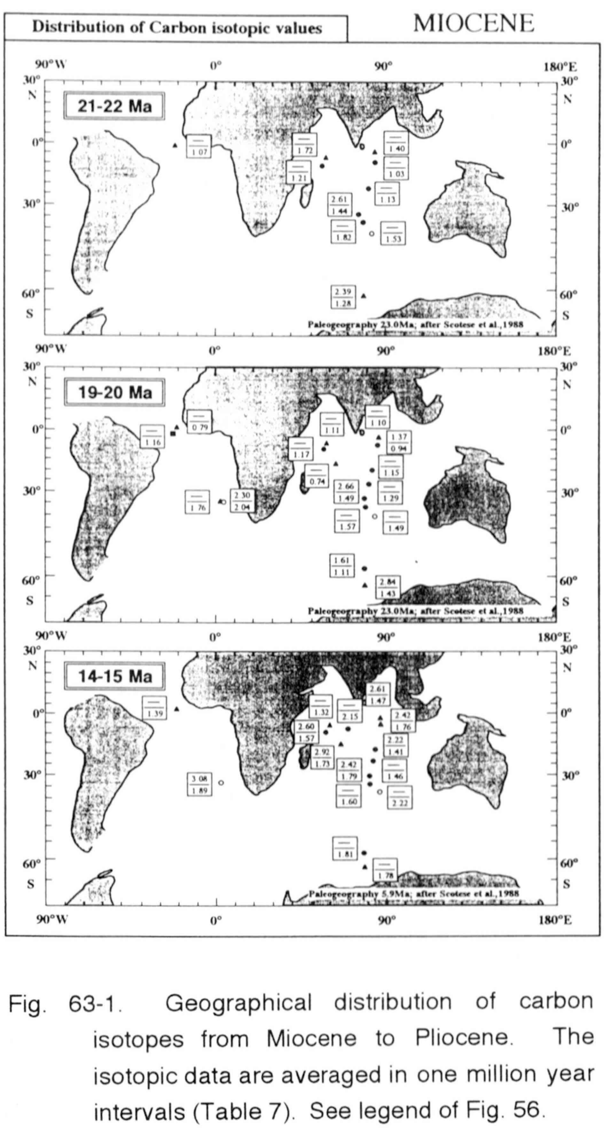

Fig. 63-1. Geographical distribution of carbon isotopes from Miocene to Pliocene. The isotopic data are averaged in one million year intervals (Table 7). See legend of Fig. 56.

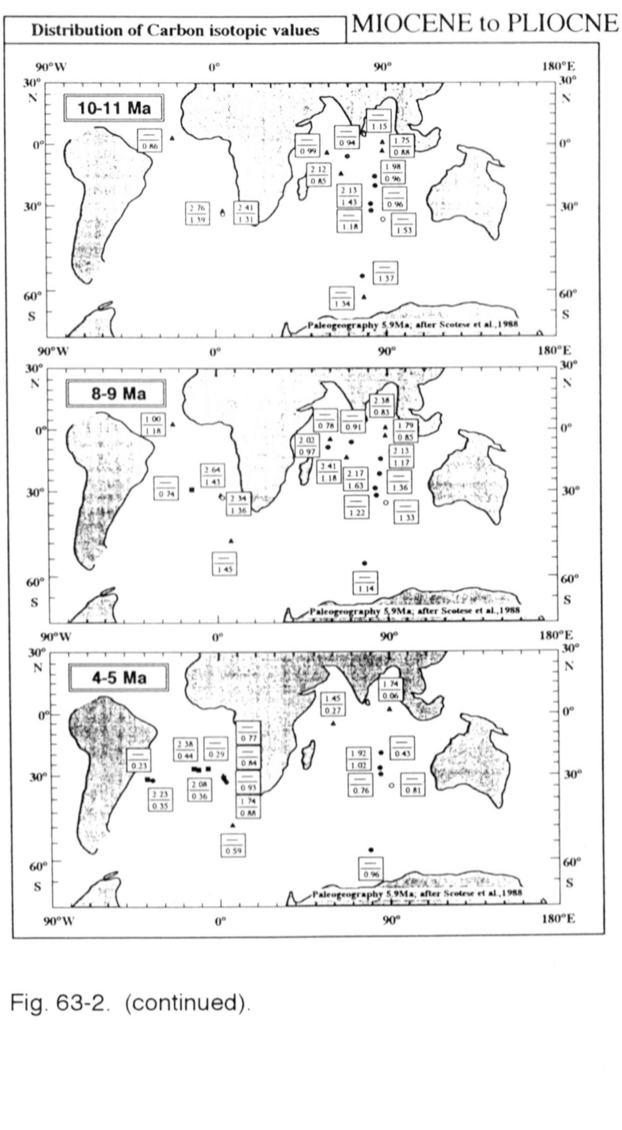

Fig. 63-2. (continued).

isotopic values on the Atlantic Ocean side tend to decrease northward. At 2500m water depth, $\delta^{13}C$ values around 30°S are 0.1-0.2‰, higher than those at 50°S. The latitudinal difference at 2000m between 30°S and 20°N is ~0.8‰. This difference decreases throughout the Pleistocene. The water column gradient of $\delta^{13}C$ is relatively large, and $\delta^{13}C$ values at >4500m paleodepth are particularly low. From 30°S-20°N, the surface carbon isotopic values on the south side are 0.8-1.5 ‰, higher than the north side, with low values in the young part. During the Pleistocene and Pliocene, the gradient of carbon isotopic values in the Indian Ocean decreased a northward at high-latitudes. In the 5 to 4 Ma interval, $\delta^{13}C$ values between 60°S and 25°S are uniform (<0.25‰). In general, the carbon isotopic values at depth >2500m are low during the Pleistocene and Pliocene.

IV. Paleoceanographic reconstruction of the Indian and South Atlantic Oceans

A. Paleo-ocean circulation viewed from carbon and oxygen isotopic ratios

Carbon isotopic ratios in sea water are mainly influenced by the biological production of organic carbon and the decomposition of organic matter. $\delta^{13}C$ values in surface water are generally 1‰ higher than those of bottom water (Kroopnick, 1974; 1980; Berger and Vincent, 1986). This is caused by selective absorption of ^{12}C-enriched CO_2 by phytoplankton in surface water. On the other hand, Kroopnick (1974, 1980) investigated the $\delta^{13}C$ values of DIC (dissolved inorganic carbon) of the modern ocean, and noted that the $\delta^{13}C$ values depend on the circulation velocity of deep water. Modern $\delta^{13}C$ distribution of DIC in the Atlantic Ocean show a southward decrease from the Northern hemisphere (Kroopnick, 1974; 1980; Leonard et al., 1983; Duplessy et al., 1984; Woodruff and Savin, 1989). This gradient is explained by a supply of ^{12}C by oxidative resolution of ^{12}C-enriched organic carbon through flow of deep water. $\delta^{13}C$ values in aged deep water are low because of high ^{12}C. Therefore, a ^{13}C gradient indicates the deep water flow (Woodruff and Savin, 1989).

$\delta^{13}C$ values of DIC have been recorded in the carbonate of foraminiferal tests (e.g., Shackleton et al., 1984; Woodruff and Savin, 1989). Woodruff and Savin (1989) showed that the distribution pattern of foraminiferal $\delta^{13}C$ are similar to the modern distribution of water DIC $\delta^{13}C$, and they concluded that the benthic $\delta^{13}C$ gradient can be used to tracer ancient ocean circulation. Based on this evidence, they proposed the existence of Tethyan Indian Saline Water (TISW), flowing from the Tethys into the northern Indian Ocean.

In this study, the paleo-directions of deep flow are deduced from the foraminiferal $\delta^{13}C$ gradient. In the case of a single direction of deep-water flow, the relationship between $\delta^{13}C$ values and migration distance are characterized by a linear function (Fig. 64-A). If this relationship is not recognized, the geographical distribution of $\delta^{13}C$ may represent the some water mass flow (Fig. 64-B).

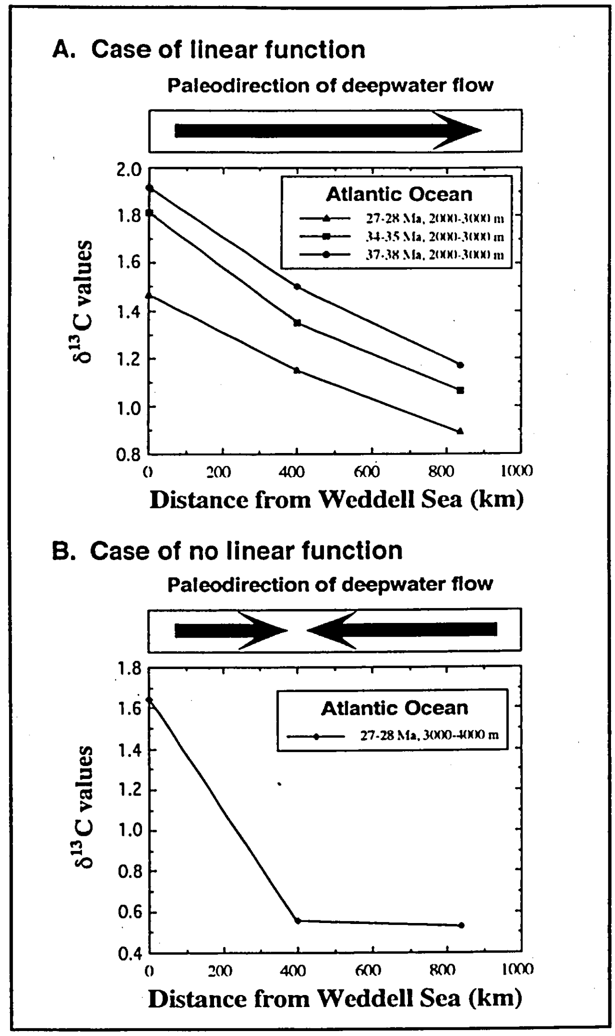

Fig. 64. Paleodirection of deep water flow and the ^{13}C gradient. A. In the case of a linear function, the paleodirection indicates a single direction flow. B. For no linear function, the paleodirection indicates some water-mass flow.

B. Isotopic water of column structure

The water column structure of oxygen and carbon isotopes from the late Maastrichtian to Pleistocene has been reconstructed, shown in Figs. 65 and 66. The relationship between the estimated water depth and isotopic data at representative ages are shown in Figs. 67 and 68. Each reconstruction covers a relatively large area (i.e., for the northeastern Indian Ocean region; the latitudinal range is about 35°), therefore even small regional differences can be recognized. The reconstruction of the Neogene in the southern Indian and Southern Oceans cannot be illustrated because of few data.

1. Oxygen isotopes

During the Paleocene, oxygen isotopic ratios of the northeastern Indian Ocean increased in a linear fashion with depth down to 1500m, and become constant below this level. The differences between the $\delta^{18}O$ values of surface and

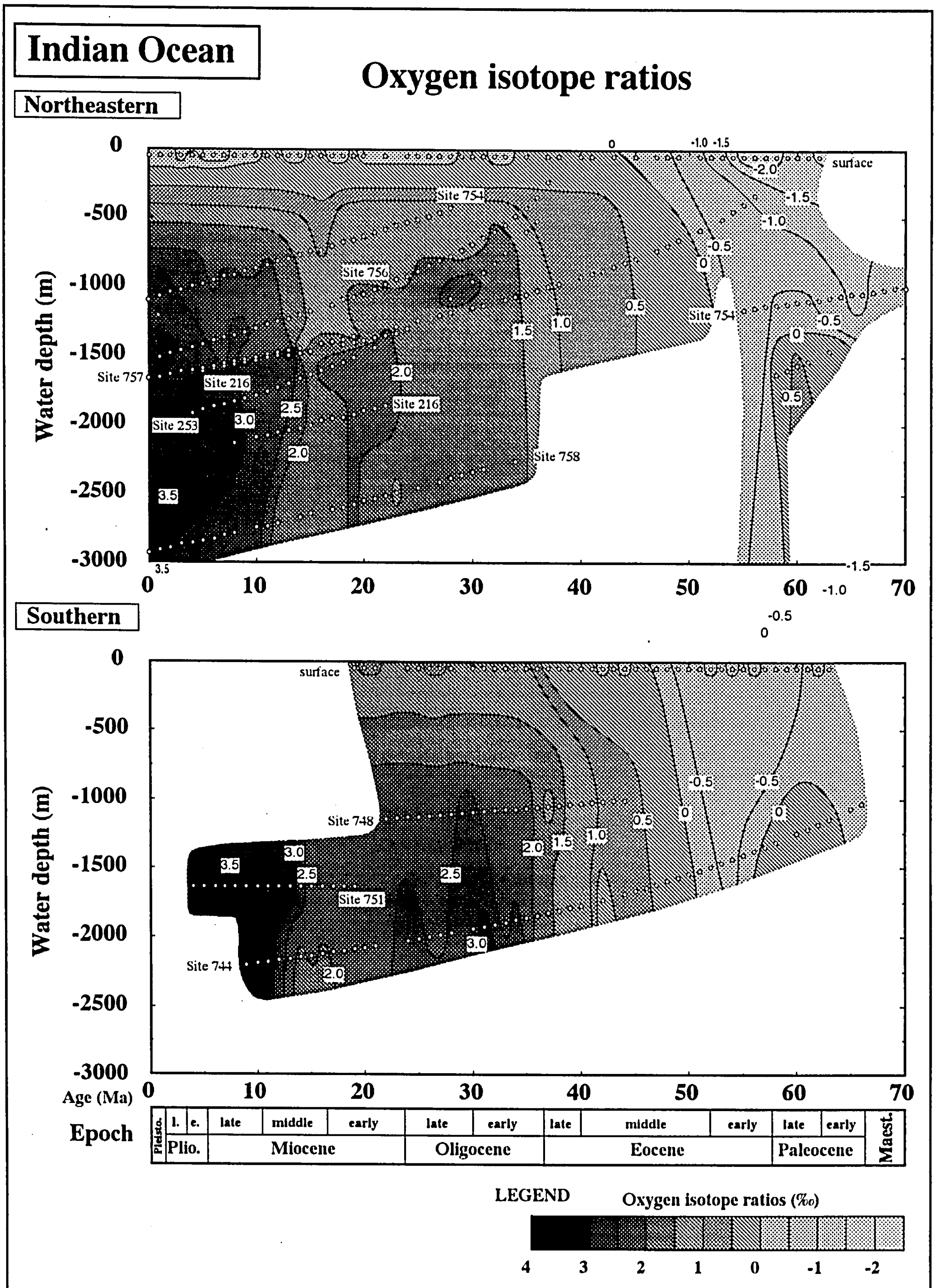

Fig. 65-1 DIC $\delta^{18}O$ value of water column at the Cenozoic in the four ocean region. The isotopic data are averaged in one million year intervals (Table 7). Paleodepth is mainly reconstructed using published data calculated from a subsidence curve of the "backtrack method" (See III-A-3 section).

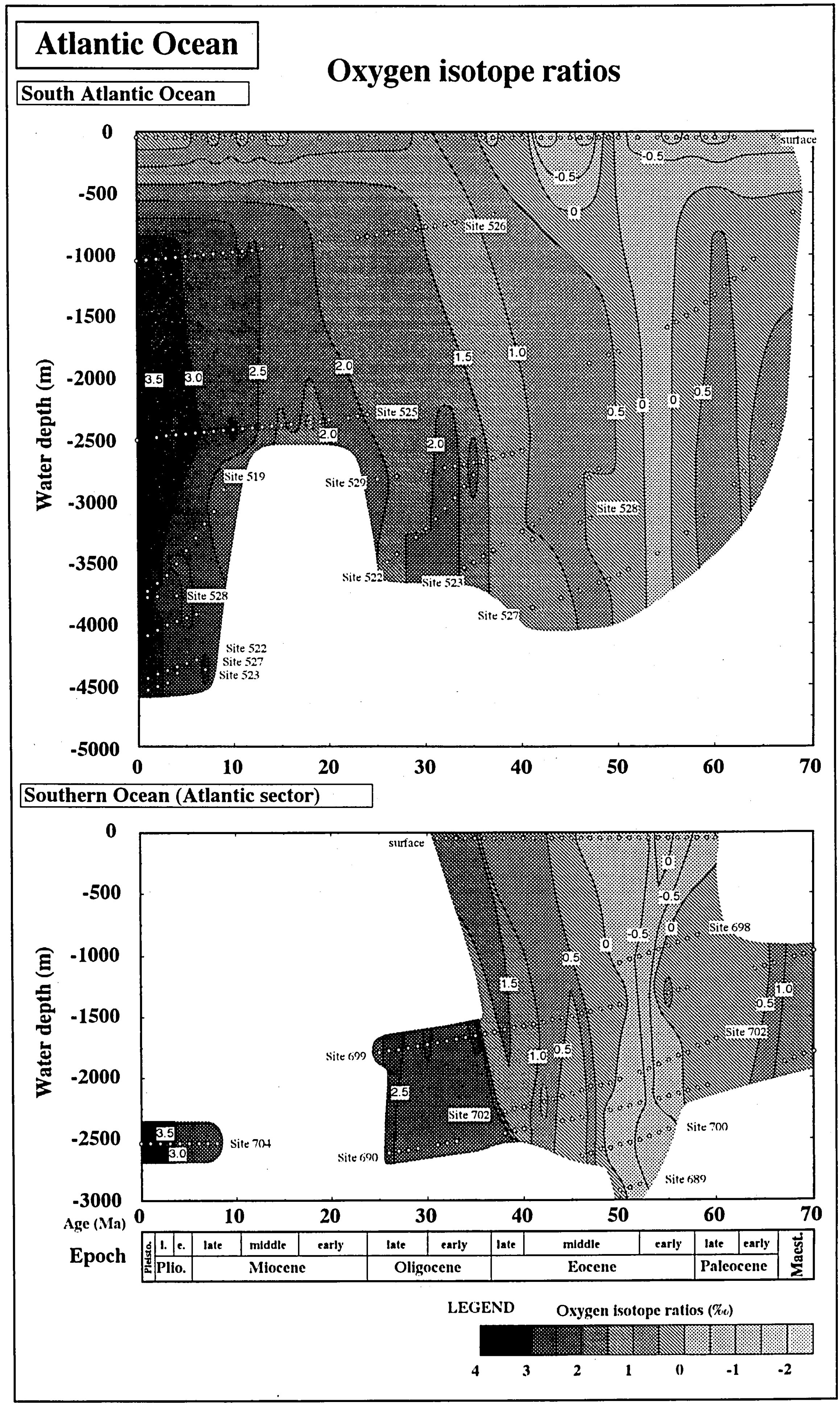

Fig. 65-2. (continued).

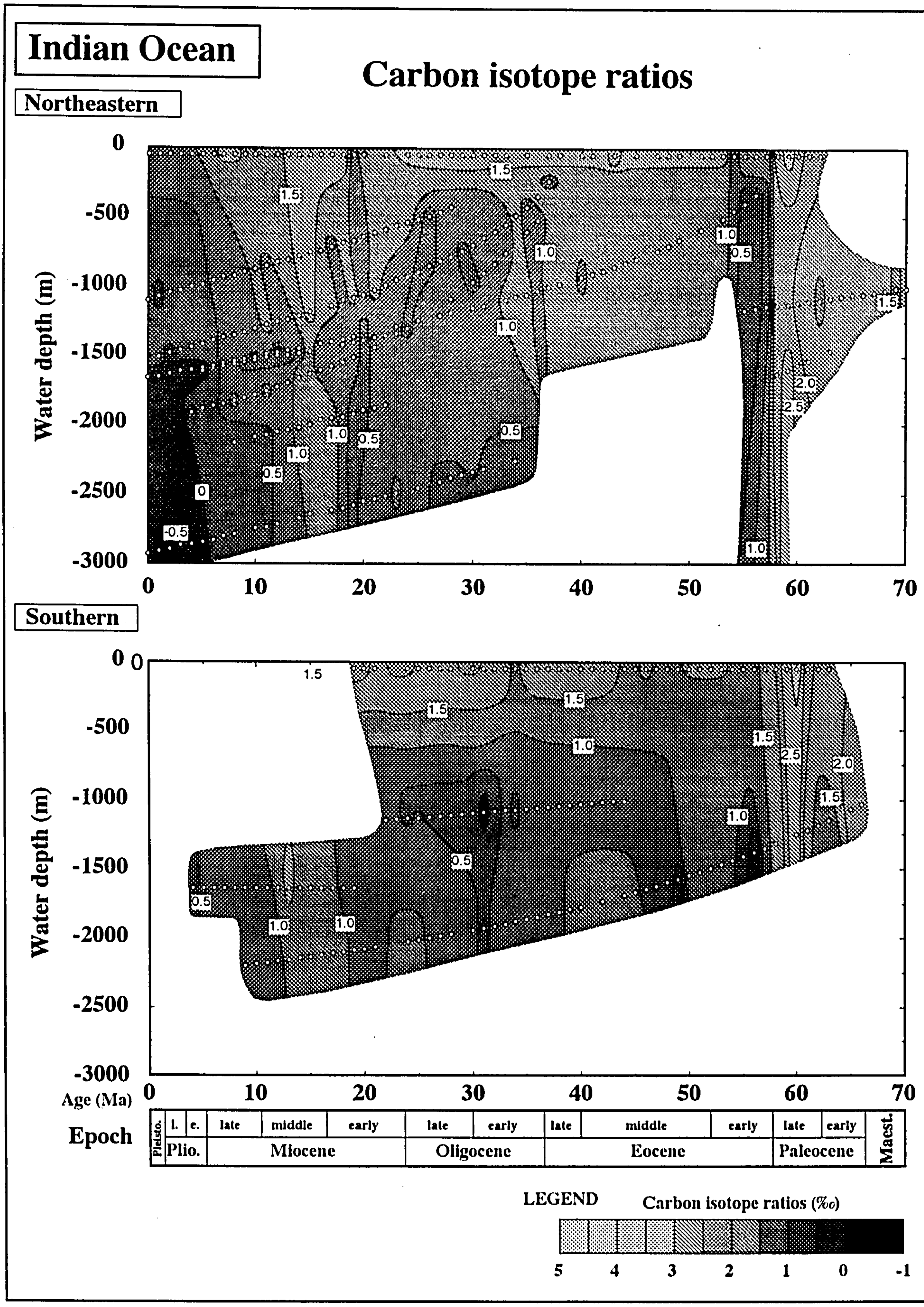

Fig. 66-1 DIC $\delta^{13}C$ value of water column in the Cenozoic in the four ocean region. The isotopic data are averaged in one million year intervals (Table 7). Paleodepth is mainly reconstructed using published data calculated from a subsidence curve of the "backtrack method" (See III-A-3 section).

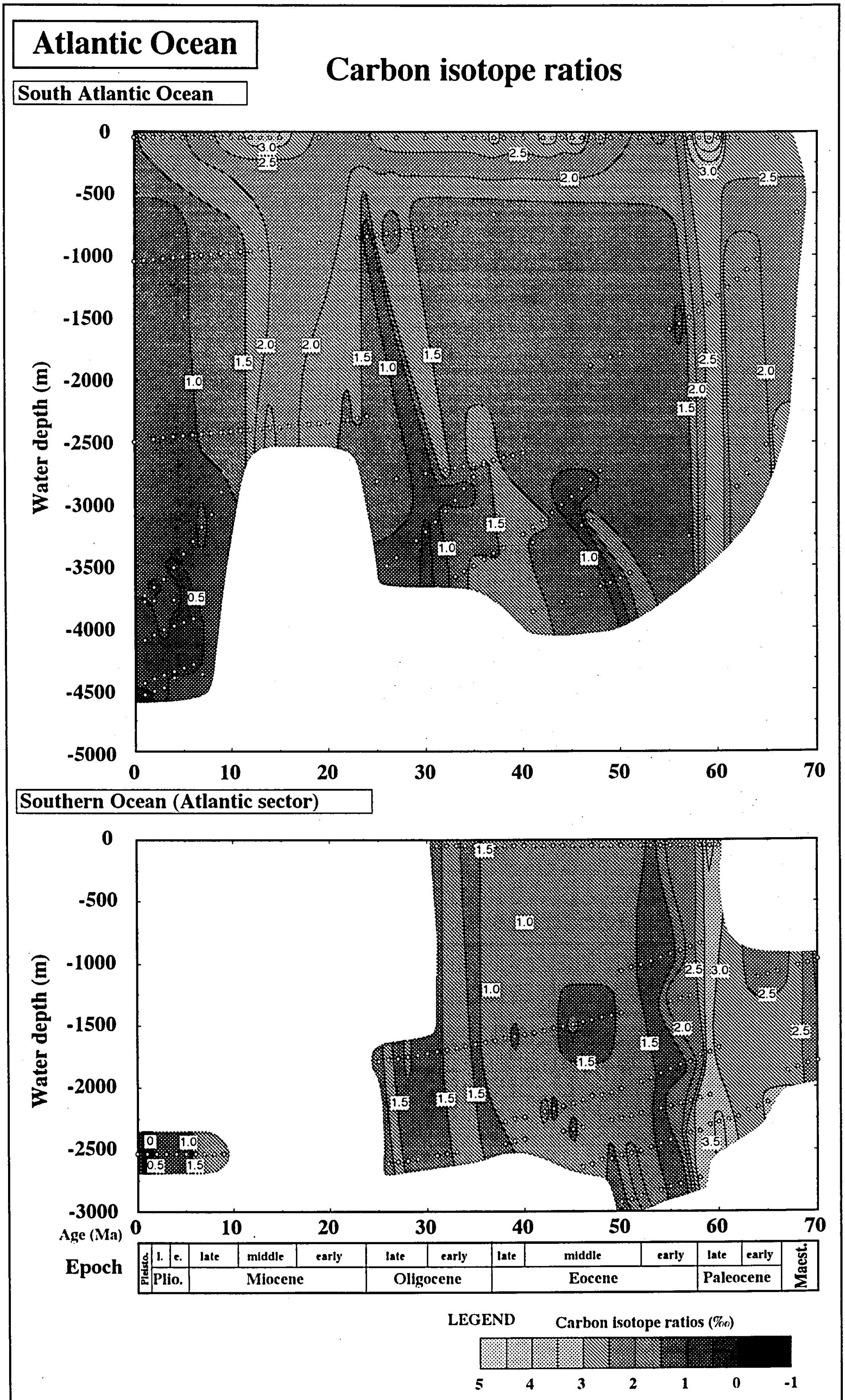

Fig. 66-2. (continued).

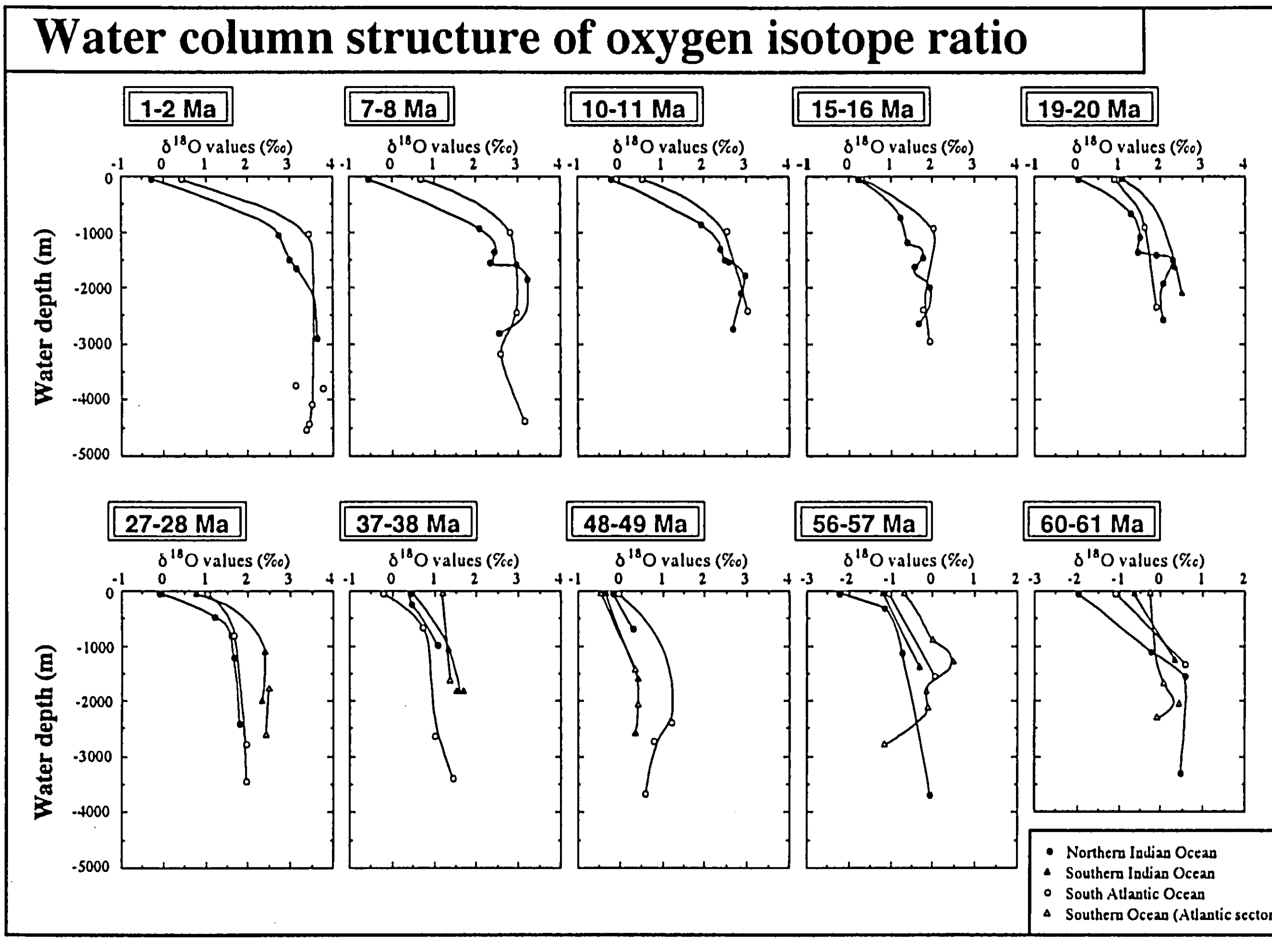

Fig. 67 Vertical change of DIC $\delta^{18}O$ value at representative age in the four ocean region. The isotopic data are averaged in one million year intervals (Table 7). Paleodepth is mainly reconstructed by published data calculated from a subsidence curve of the "backtrack method" (See IV-A-3 section).

bottom water are relatively large (up to ~2.5‰). The water columns in other oceans exhibit the same gradient to that of the northeastern Indian Ocean except for the Southern Ocean (Atlantic sector), which shows homogeneous values through the water column. A ^{18}O maximum at 61 Ma is observed in all the oceans except for the Southern Ocean (Atlantic sector), and is particularly high at the northeastern Indian Ocean region. The surface to bottom difference in oxygen isotopes of the northeastern Indian Ocean region during this time is the largest in the Paleocene section.

In the ^{18}O minimum zone within the early Eocene, $\delta^{18}O$ values are low through the entire water column, and the surface to bottom difference is relatively small. In the northeastern Indian Ocean, bottom water oxygen isotopes increase with increasing depth. During the increase of the middle and late Eocene, the surface to bottom difference in oxygen isotopes is relatively small, and the isotopic difference according to depth in bottom water is also small, especially in the Southern Ocean where the entire water column records relatively homogeneous values.

The shift at the Oligocene / Eocene boundary is remarkable in the Southern Ocean. During the Oligocene, $\delta^{18}O$ values rapidly increased from the surface to depths of about 1000m, and gradually increased from 1000m.

In the early Miocene, the water column in the northeastern Indian Ocean was divided into intermediate and deep water by a conspicuous discontinuity at about 1500m. $\delta^{18}O$ values of intermediate water are ~0.6‰, higher than those of deep water. The difference between $\delta^{18}O$ values of surface and intermediate water during this time is similar to that of Oligocene sections. In the ^{18}O minima zone of the Miocene, the intermediate/deep water boundary is indistinct, and the surface to bottom difference reduces. After the shift of the middle Miocene, this conspicuous discontinuity is again observed around 1500m, and the surface to bottom difference increases. All sections of bottom water show high values at the 8 Ma ^{18}O maximum. From the latest Miocene to early Pliocene, $\delta^{18}O$ values are distinctively high in the water column from 1600-2500m paleodepth. These discontinuities are only recognized in the northern Indian Ocean. During the Miocene, the water column gradient in the South Atlantic

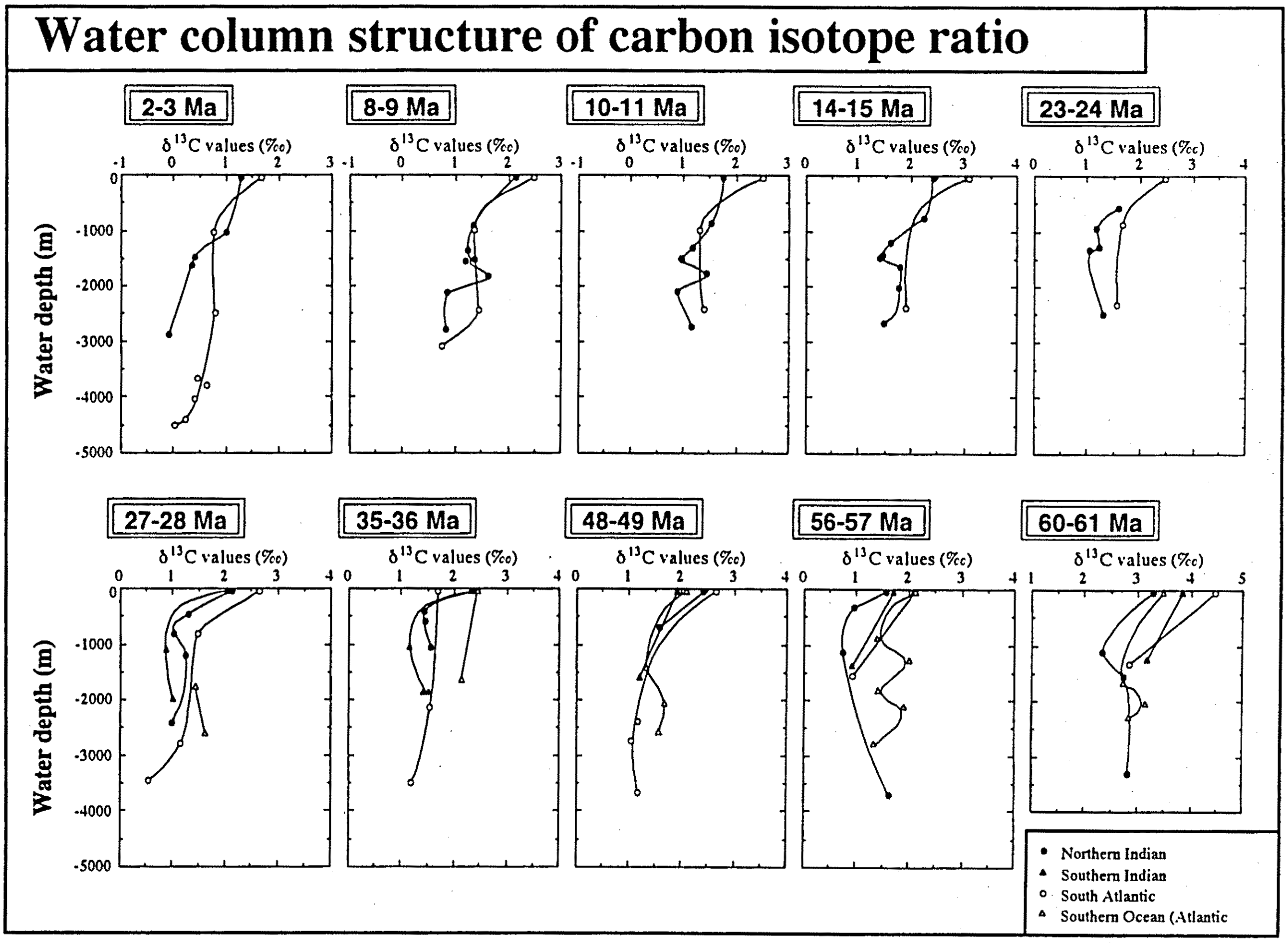

Fig. 68 Vertical change of DIC $\delta^{13}C$ value at representative age in the four ocean region. The isotopic data are averaged in one million year intervals (Table 7). Paleodepth is mainly reconstructed by published data calculated from a subsidence curve of the "backtrack method" (See IV-A-3 section).

Ocean displays a trend of gradual increase with depth. From the late middle Miocene to early Pliocene, $\delta^{18}O$ values are relatively high in intermediate water (1000-2800 m).

After the shift of the late Pliocene, the surface to bottom differences in oxygen isotope values expanded in the Indian and South Atlantic Oceans. In bottom water, $\delta^{18}O$ values tended to increase with depth in the northern Indian Ocean, and were uniform in the South Atlantic Ocean.

2. Carbon isotopes

During the Paleocene, carbon isotopes in the water column of the northeastern Indian Ocean region showed an increase by 0.5‰ from 400 to 1200m, and were uniform below 1200m. In the Southern Ocean (Atlantic sector), the surface to bottom water difference of carbon isotope was relatively small. The surface to bottom water differences, however, were large except for the Southern Ocean (Atlantic sector). The shift at the Paleocene / Eocene boundary is remarkable as observed in other deep sea sections.

The minimum value zone within the early Eocene exhibits a similar pattern in all oceans, as in the Paleocene. The surface to bottom difference at this time is slightly smaller than those in the Paleocene. Although the intermediate water (500-1500 m) in the southern Indian Ocean shows relatively low values, the carbon isotopic ratios of bottom water are uniform from the minimum value zone in the early Eocene to the shift in the earliest Oligocene in all oceans. The surface to bottom difference is the largest (1.5-2.0‰) in the South Atlantic Ocean. In contrast to this, $\delta^{13}C$ values of bottom water are close to that of surface water of the Southern Ocean. The surface to bottom difference in the Indian Ocean is 0.5-1.0‰. Although the water column exhibits a general decreasing trend with increasing paleodepth during the late Oligocene, $\delta^{13}C$ values from 400-1000m in the northeastern Indian Ocean and of 400-1500m in the southern Indian Ocean are relatively low. The surface to bottom difference in this interval is larger than that of the early Oligocene in the northeastern Indian Ocean. At the ^{13}C maximum at 23 Ma (near the Miocene / Oligocene boundary), the entire water column records are roughly homogeneous.

From the Miocene onward, the carbon isotopic values through the water column in the northeastern Indian Ocean show a gradual decrease with depth. At approximately

1500m, carbon isotopic values are remarkably low (0.2-0.5‰) during the Miocene. From 11 to 7 Ma, a discontinuity is observed at a depth of 2000m, and $\delta^{13}C$ values below 2000m deep reduce by ~0.5‰. $\delta^{13}C$ values of surface water increase from 6 to 10 Ma, consequently the surface-bottom difference increases. From the Pliocene to Pleistocene, a discontinuity with a value of 0.6‰ is recognized at 1300m paleodepth. No discontinuity is recognized in other oceans after the Miocene.

C. Source of deep water

Ocean regions with high $\delta^{13}C$ values is close to the source of bottom water (Miller et al., 1987) because the ^{13}C-enriched surface water produced from the source region flows into the bottom water. Therefore, the oxygen and carbon isotopic ratio of bottom water in these regions is also close to that of surface water. The oxygen isotopic ratio of bottom water in the source region exhibits the highest value, because this water is characterized by either colder or highly saline waters. Based on water density, the source water may have flowed to a warmer and less saline deep area.

In the South Atlantic and Indian Oceans, the averaged value of $\delta^{13}C$ in one million year intervals are plotted as a function of paleo-latitude (Fig. 69). Throughout the Cenozoic, carbon isotopic values are high on the high latitude side of the Southern Ocean, and tend to decrease toward middle to low latitudes. In the former region, oxygen isotopic ratios are higher, and the carbon isotopic values of bottom water are also close to those of surface water. This suggests that the source water formed at a high latitude in the Southern Ocean throughout the Cenozoic. Bottom water influenced by this source water may correspond to AABW (Antarctic Bottom Water) or its prototype.

During the Paleocene, $\delta^{18}O$ and $\delta^{13}C$ values in the northern part of the South Atlantic and Indian Oceans are also distinctly high. The ^{13}C difference between surface and bottom water is small in the northern part of Indian Ocean (Site 758), which is similar to that of the Southern Ocean (Site 690). This shows that the source water exists in the northern part of the South Atlantic and the Indian Oceans. This water may be warm and highly saline, because this source water probably formed at low latitude. Brass et al. (1982) called such deep water "Warm Saline Deep Water (WSDW)", and considered that this water was formed by the concentration of saline water through evaporation in the Tethyan Sea or lower latitudes. The gradient of carbon isotopic ratios in the Indian Ocean supports the supposition that WSDW may have formed in the Tethyan Sea.

High $\delta^{13}C$ values are recognized at mid latitudes (~30°S) from the Miocene. This is probably caused by the influence of AAIW (Antarctic Intermediate Water).

During Miocene, the carbon isotopic values are high at 10°S in the northwestern Indian Ocean. This may be influenced by TISW (Tethyan Indian Saline Water) as proposed by Woodruff and Savin (1989).

D. Reconstruction of paleo-ocean circulation

During the Paleocene, two water masses (proto-AABW and WSDW) probably existed in the South Atlantic and Indian Oceans. The gradient of oxygen and carbon isotope ratios shows that Proto-AABW flowed northward

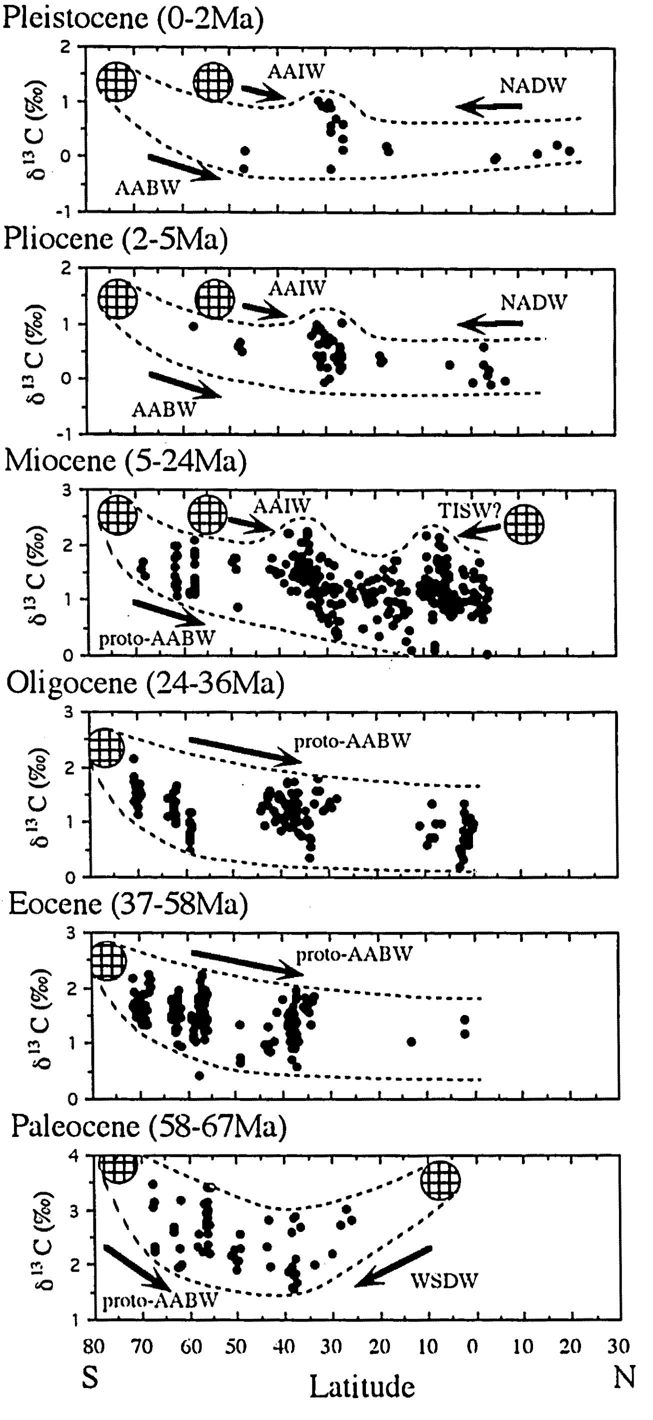

Fig. 69 ^{13}C latitudinal change of one million average values during the each period. Carbon isotopic ratios of source water show a high value. In general, carbon isotopic values decrease from high to low latitudes.

from the Southern Ocean, and that WSDW flowed probably southward from the Tethyan Sea. In the South Atlantic and Indian Oceans during the Paleocene, an "oxygen isotopic minima belt" existed at mid-latitudes (50-60°S). $\delta^{18}O$ values in this belt are 0.6-1.6‰, lower than that of high- and low latitudes. $\delta^{18}O$ values at Site 752 are lowest among the "oxygen isotopic minima belt". The "oxygen isotopic minima belt" may have been caused by the confluence of Proto-AABW and WSDW, as pointed out by Nomura et al.(1992), because the carbon isotopic ratio is lowest among the ^{13}C gradient. Across the Paleocene / Eocene boundary, a sudden decrease in carbon isotopic ratios has been recognized from 59 to 56 Ma (Kennett and Stott, 1990; Barrera and Huber, 1991; Zachos et al., 1992a). However, the distribution of oxygen and carbon isotopes is similar to that of the Paleocene. Therefore, the ocean circulation system seems to be similar to that of the Paleocene.

After 56 Ma, the ^{13}C latitudinal gradient shows that Proto-AABW flowed into the South Atlantic and Indian Oceans from high latitudes. Until about 50 Ma, $\delta^{18}O$ values at Site 757 in the northern Indian Ocean are higher than that at Site 689 in the Southern Ocean. This suggests that WSDW remained an influence in the Indian Ocean until about 50 Ma, and that WSDW flowing from the north part of Indian Ocean disappeared after that. This water mass may have been reduced with the closing of the Tethyan Sea. WSDW on the Atlantic Ocean side, however, may have flowed until about 40 Ma judging from the ^{13}C geographical gradient of the South Atlantic Ocean. The carbon and oxygen isotopic ratios at Site 738, where the paleodepth is slightly deeper than at Site 748, show similar values to those at Sites 689 and 690. This indicates that the water mass flowed into deep water in the southern Indian Ocean from the Southern Ocean. This water mass can be referred to as the proto-type of CPDW (Circumpolar Deep Water).

The sharp change in oxygen isotopic ratios and low carbon isotopic ratios are recognized at ~1000 m depth in the northern Indian Ocean at about 30 Ma. The water mass in the deep part may be equivalent to the proto-type of AABW (Proto-AABW), and the water mass in the shallow part is equivalent to the present AAIW. AAIW may be formed by melting of sea ice, as in the present ocean, based on the lower $\delta^{18}O$ values.

Carbon isotopic ratios in the northwestern Indian Ocean are higher during the Miocene. This supports the scenario of Woodruff and Savin (1989), where a warm saline plume (Tethyan / Indian Saline Water: TISW) flowed into the northern Indian Ocean from the Tethyan Sea. However, a northward decrease of the carbon isotope gradient is recognized in the intermediate water of the northeastern Indian Ocean. This suggests that TISW is not the main flow in the Indian Ocean. This intermediate water is probably the Antarctic Intermediate Water (AAIW), which formed by melting of sea ice, because the $\delta^{18}O$ values of intermediate water are low in comparison with that of deep water. The sharp change of oxygen isotopic ratios in the water column of the northern Indian Ocean, assuming that the AAIW / Proto-AABW boundary, are recognized at ~2000 m paleodepth. The boundary is deeper than that recognized in the late Oligocene. During the late Miocene, the AAIW / Proto-AABW boundary deepens to the north, as indicated by the distribution of low $\delta^{13}C$ values. This may be caused by the northward movement of Proto-AABW. As a result, AAIW flows into the deeper part of the northern Indian Ocean.

After the late Pliocene, ocean circulation of the deep sea is the same as the present circulation. The oxygen isotopic ratios of Central Atlantic Ocean are higher than those of the South Atlantic Ocean. The carbon isotopic gradient shows a southward decrease in the South Atlantic Ocean. These features indicate a water mass corresponding to NADW in the modern ocean. Before the early Pliocene, positive evidence of NADW is not recognized in the South Atlantic Ocean. This indicates that NADW developed rapidly near the early/late Pliocene boundary (about 3 Ma), and affected to AABW and CPDW.

VI. Concluding Remarks

(1) Oxygen and carbon isotopic ratios were studied in Cenozoic sediments at six sites (Sites 752, 754, 756, 757, 758, and 762) of ODP Legs 121 and 122 in the northeastern Indian Ocean. They recorded such global events as the sharp increase of $\delta^{18}O$ values near the middle Miocene and Eocene / Oligocene boundary, the increase of $\delta^{18}O$ values in the Eocene (Miller et al., 1987), the chron-6 shift and the chron-16 shift of $\delta^{13}C$ ratios (Vincent et al., 1980; 1985), and the drastic change of $\delta^{13}C$ and $\delta^{18}O$ values across the Paleocene / Eocene boundary.

(2) Benthic and planktonic foraminiferal isotopic were data converted into δ values of dissolved inorganic carbon of marine water on the basis of the adjustment values calculated from foraminiferal interspecific differences in isotopic ratios. Those data are compiled from the Indian Ocean and the South Atlantic Oceans. The general trends of oxygen and carbon isotopic records are similar in all studied oceans. However, the oxygen and carbon isotopic values show an increase southwards.

(3) Averaged isotopic values in one million year intervals are calculated at each ODP and DSDP site, and the time and spatial distributions of the oxygen and carbon isotopic values are examined based on the estimated paleodepth and paleocoordinates. In the Paleocene water column, vertical change in isotopic ratios is not observed. In the Miocene, a notable oxygen isotopic discontinuity and low carbon isotopic values are recognized at ~1500m paleodepth in the northeastern Indian Ocean. This suggests that two water masses may have existed in the Miocene water column of the Indian Ocean. The modern ocean shows a complicated water circulation in the Indian Ocean (Warren, 1984). Based on those results, it is concluded that the water column structure became more complicated from Paleocene to the Recent.

(4) The source of deep water is discussed using the ^{13}C geographical gradient. In the South Atlantic and Indian Oceans, the source water may be formed on the high latitude side of the Southern Ocean through the Cenozoic because the carbon isotopic values are consistently high on the high latitude side of the Southern Ocean. The bottom water formed in the source region should correspond to AABW (Antarctic Bottom Water) or its prototype. In the Paleocene, the $\delta^{18}O$ and $\delta^{13}C$ values in the northern part of the South Atlantic and Indian Oceans also are remarkably high. This water may be

"Warm Saline Deep Water (WSDW)". High $\delta^{13}C$ values are recognized at mid latitudes (~30°S) from the Miocene onwards. This is probably caused by the influence of AAIW (Antarctic Intermediate Water). During the Miocene, carbon isotopes showed high values at 10°S in the northwestern Indian Ocean. This may be due to the influence of TISW (Tethyan Indian Saline Water; Woodruff and Savin, 1989).

(5) The circulation patterns of deep water within the Cenozoic have been reconstructed from isotopic evidence. The gradient of oxygen and carbon isotopic values reveals that Proto-AABW flowed northward from the Southern Ocean, and that WSDW flowed southward probably from the Tethyan Sea. WSDW is characterized by high temperature and high salinity. WSDW may have formed in the shallow Tethyan Sea associated with high evaporation. This water mass rapidly reduced with the closing of the Tethyan Sea across the Paleocene/Eocene boundary, and disappeared at about 50 Ma in the Indian Ocean, but it may have developed until 40 Ma in the South Atlantic Ocean. After 56 Ma, the ^{13}C latitudinal gradient shows that Proto-AABW flowed into the South Atlantic and Indian Oceans from high latitude, including the present Weddell Sea region. During the Paleocene and early Eocene, an "Oxygen isotopic minima belt" is recognized at mid-latitudes in the South Atlantic and Indian Oceans. A sharp change in oxygen isotopic ratios and a low value zone of carbon isotopic ratios formed at 1000-2000 m depths in the water column of the northern Indian Ocean after 30 Ma. This sharp change may indicate the formation of the AAIW/Proto-AABW boundary. AAIW may have flowed northward from high latitude judging from the northward decrease of the carbon isotope gradient. NADW (North Atlantic Deep Water) rapidly developed during the early/late Pliocene boundary time (~3 Ma), and affected AABW and CPDW.

Acknowledgment

I express sincere gratitude to Prof. Y. Okimura of Hiroshima University for his invaluable discussion and suggestions, and for his critical reading of the manuscript. Special thanks are due to Associate Prof. R. Nomura of Shimane University for his continuous guidance and encouragement during the course of this study. Thanks are also due to Prof. N. Niitsuma and Associate Prof. H. Wada of Shizuoka University for helpful discussion and technical advice concerning isotope analysis. I would like to thank Drs. M. Miyamoto, T. Yano, and A. Kano of Hiroshima University for valuable discussions and critical reading of the manuscript. I also wish to thank Dr P. Morris, Shimane University for reading the manuscript, and Dr. H. Nishi of Tohoku University for identification of planktonic foraminifera. Thanks are also due to Prof. I. Hara , Prof. S. Takeno, Prof. S. Honda, and Prof. Y. Sano of Hiroshima University for their important advice and encouragement. I would like to thank Dr. T. Matsumoto, Dr. T. Naka, and Mr. H. Yamasaki, and friends of Hiroshima University and Shizuoka University for helpful advice.

Reference

Backman, J., 1987. Quantitative calcareous nannofossil biochronology of middle Eocene through early Oligocene sediment from DSDP Site 522 and 523. *Abh. Geol. Bundesanst. (Austria)*, 39:21-31.

Backman, J., Duncan, R. A., et al., 1988. *Proc. ODP, Init. Repts.* 115: College Station, TX (Ocean Drilling Program).

Backman, J., and Pestiaux, P., 1986. Pliocene *Discoaster* abundance variations, Deep Sea Drilling Project Site 606: biochronology and Paleoenvironmental implication. *In* Ruddiman, W. F., Kidd, R. B., Thomas, E., et al., *Init. Repts. DSDP*, 94, Pt. 2: Washington (U.S.Govt. Printing Office), 903-910.

Backman, J., Schneider, D. A., Rio, D., and Okada, H., 1990. Neogene low-latitude magnetostratigraphy from Site 710 and revised age estimates of Miocene nannofossil datum events. *In* Backman, J., Duncan, R. A., Peterson, L. C., et al., *Proc. ODP, Sci. Results*, 115: College Station, TX (Ocean Drilling Program), 271-276.

Backman, J., and Shackleton, N. J., 1983. Quantitative biochronology of Pliocene and early Pleistocene calcareous nannofossils from the Atlantic, Pacific and Indian oceans. *Mar. Micropaleontol.*, 8:141-170.

Baldauf, J. G., Thomas, E., Clement, B., Takayama, T., Weaver, P. P. E., Backman, J., Jenkins, G., Mudie, P. J., and Westberg-Smith, M. J., 1987. Magnetostratigraphic and biostratigraphic synthesis, Deep Sea Drilling Project Leg 94. *In* Ruddiman, W. F., Kidd, R. B., Thomas, E., et al., *Init. Repts. DSDP*, 94, Pt. 2: Washington (U.S.Govt. Printing Office), 1159-1205.

Barrera, E. and Huber, T., 1990. Evolution of Antarctic waters during the Maestrichian: Foraminifer oxygen and carbon isotope ratios, Leg 113. *In* Barker, P. F., Kennett, J. P., et al., *Proc. ODP, Sci. Results*, 113: College Station, TX (Ocean Drilling Program), 813-827.

Barrera, E. and Huber, T., 1991. Paleocene and early Neogene oceanography of the southern Indian Ocean : Leg 119 foraminifer stable isotope results. *In* Barron, J., Larsen, B., et al., *Proc. ODP, Sci. Results*, 115: College Station, TX (Ocean Drilling Program), 693-717.

Barton, C. E., and Bloemendal, J., 1986. Paleomagnetism of sediments collected during Leg 90, southwest Pacific. In Kennett, J. P., von der Borch, C. C., et al., Init. Repts. DSDP, 90: Washington (U.S.Govt. Printing Office), 1273-1316.

Be, A. W. H., 1977. An ecologic, zoogeographic and taxonomic review of recent planktonic foraminifera. *In* Ramsay, A. T. S. (Ed.), *Oceanic Micropaleontology*, Vol.1: 1-88

Belanger, P. E., Curry, W. B., and Matthews, R. K., 1981. Core-top evaluation of benthic foraminiferal isotopic ratios for paleoceanographic interpretations. *Palaeogeogr., Palaeoclimatol., Palaeoecol.*, 33: 205-220.

Berger, W. H., and Vincent, E., 1986. Deep-sea carbonates: reading the carbon-isotope signal. *Geol. Rundsch.*, 75: 249-269.

Berggren, W. A., Kent, D. V., and Flynn, J. J., 1985a. Jurassic to Paleogene: Part 2. Paleogene geochronology and chronostratigraphy. *In* Snelling, N. J. (Ed.), *The Chronology of the Geological Record*, Geol. Soc. London Mem. 10:141-195.

Berggren, W. A., Kent, D. V., and Van Caouverring, J. A., 1985b. The Neogene: Part 2. Neogene geochronology and chronostratigraphy. *In* Snelling, N. J. (Ed), *The Chronology of the Geological Record*, Mem. Geol. Soc. (London), 10: 211-260.

Berggren, W. A., Kent, D. V., Flynn, J. J. and Van Caouverring, J. A., 1985c. Cenozoic geochronology. *Geol. Soc. Am. Bull.*, 96: 1407-1418.

Blattner, P. and Hulston, J. R., 1978. Proportional variations of geochemical $\delta^{18}O$ scales -- an interlaboratory comparison. *Geochim. Cosmochim. Acta*, 42: 59-62.

Boersma, A., and Mikkelsen, N., 1990. Miocene-age primary productivity episodes and oxygen minima in the central equatorial Indian Ocean. *In* Duncan, R. A., Backman, J., Peterson, L. C., et al., *Proc. ODP, Sci. Results*, 115: College Station, TX (Ocean Drilling Program), 589-609.

Brass, G. W., Southam, J. R., and Pererson, W. H., 1982. Warm saline bottom water in the ancient ocean. *Nature*, 296: 620-623.

Clement, B. M., and Robinson, F., 1987. The magnetostratigraphy of Leg 94 sediments. *In* Ruddiman, W. F., Kidd, R. B., Thomas, E., et al., *Init. Repts. DSDP*, 94, Pt. 2: Washington (U.S.Govt. Printing Office), 635-650.

Craig H., 1965. The measurement of oxygen isotope paleotempertures. *In* Tongiorgi, E.(Ed.), *Proc. Stable Isotope in Oceanographic Studies and Paleotempertures, Spoleto*, 2: 1-87.

Duplessy, J. C., Shackleton, N. J., Matthews, R. K., Prell, W. L., Ruddiman, W. F., Caralp, M., and Hendy, C. H., 1984. ^{13}C record of benthic foraminifera in the last interglacial ocean: implications for the carbon cycle and global deepwater circulation. *Quat. Res.*, 21: 225-243.

Epstein, S., Buchsbaum, R., Lowenstam, H., and Urey, H. C., 1951. Carbonate-water isotopic temperature scale. *Geol. Soc. Am. Bull.*, 62: 417-426.

Finger, W., 1984. Carbonate dissolution facies of late Miocene to Pleistocene sediments from Leg 73, Sites 519 and 520 (South Atlantic). *In* Hsü, K. J., LaBrecque, J. L., et al., *Init. Repts. DSDP*, 73: Washington (U.S. Govt. Printing Office), 765-769

Ganssen, G., and Sarnthein, M., 1983. Stable-isotope composition of foraminifers: The surface and bottom water record of coastal upwelling. *In* Seuss, E., and Thiede, J. (Ed.) , *Coastal Upwelling: Its Sediment Record, Part A*, 99-121.

Gartner, S., Jr., 1977. Calcareous nannofossil biostratigraphy and reyised zonation of the Pleistocene. *Mar. Micropaleontol.*, 2: 1-25.

Gartner, S., 1990. Neogene calcareous nannofossil biostratigraphy, Leg 116 (Central Indian Ocean). *In* Cochran, J. R., Stow, D. A. V., et al., *Proc. ODP, Sci. Results*, 116: College Station, TX (Ocean Drilling Program), 165-187.

Haq, B. U., Hardenbol, J., and Vail, P R., 1987. Chronology of fluctuating sea levels since the Triassic. *Science*, 235: 1156-1167.

Hodell, D. A., Muller, D. W., Ciesielski, P. F., and Mead G. A., 1991. Synthesis of oxygen and carbon isotopic results from Site 704 : Implications for major climatic-geochemical transitions duting the late Neogene. *In* Ciesielski, P. F., Kristoffersen, Y., et al., *Proc. ODP, Sci. Results*, 115: College Station, TX (Ocean Drilling Program), 475-480.

Horibe, Y. and Oba, T., 1969. Paleotemperatures of deep-sea cores from the Indian Ocean by oxygen isotope method. *Kaseki (Fossils), Special Issue*, 21-29. (in Japanese).

Hsü, K. J., McKenzie, J. A., Oberhänsli, H., Weissert, H., and Wright, R. C., 1984. South Atlantic Cenozoic paleoceanography. *In* Hsü, K. J., LaBrecque, J. L., et al., *Init. Repts. DSDP, 73*: Washington (U.S. Govt. Printing Office), 771-785.

Katz, M. E., and Miller, K. G., 1991. Early Paleogene benthic foraminiferal assemblage and stable isotope composition in the Southern Ocean, Ocean Drilling Program, Leg 114. *In* Ciesielski, P. F., Kristoffersen, Y., et al., *Proc. ODP, Sci. Results*, 114: College Station, TX (Ocean Drilling Program), 481-516.

Kennett, J. P., and Stott, L. D., 1990. Proteus and Proto-oceanus: ancestral Paleogene ocean as revealed from Antarctic stable isotopic results: ODP Leg 113. *In* Barker, P. F., Kennett, J. P., et al., *Proc. ODP, Sci. Results*, 113: College Station, TX (Ocean Drilling Program), 865-880.

Kidd, R. B. and Davies, T. A., 1978. Indian Ocean sediment distribution since the Late Jurassic. *Mar. Geol.* 26: 49-70.

Kroopnick, P. M., 1974. The dissolved O_2-CO_2-^{13}C system in the eastern equatorial Pacific. *Deep-sea Res.*, 21: 211-227.

Kroopnick, P. M., 1980. The distribution of ^{13}C of ΣCO_2 in the Atlantic Ocean. *Eart. Planet. Sci. Lett.*, 49:469-484.

Kroopnick, P. M., 1985. The distribution of ^{13}C of ΣCO_2 in the world oceans. *Deep-sea Res.*, 32: 57-84.

Larson, R. L., Pitman III, W. C., Golovchenko, X., Cande, S. C., Dewey, J. F., Haxby, W. F., and Labrecque, J. L., 1985. The Bedrock Geology of the World. Freeman, New York.

Leonard, K. A., Williams, D. F., and Thunell, R. C., 1983. Pliocene paleoclimatic and paleoceanographic history of the South Atlantic Ocean: stable isotopic records from Leg 72 DSDP Sites 516A and 517. *In* Kennett, J. P., von der Borch, C. C., et al., *Init. Repts. DSDP*, 72: Washington (U.S.Govt. Printing Office), 895-906.

Lohman, W. H., 1986. Calcareous nannoplankton biostratigraphy of the southern Coral Sea, Tasman Sea, and southwestern Pacific Ocean. Deep Sea Drilling Project Leg 90: Neogene and Quaternary. *In* Kennett, J. P., von der Borch, C. C., et al., *Init. Repts. DSDP*, 90: Washington (U.S.Govt. Printing Office), 763-795.

Mackensen, A. and Berggren, W. A., 1992. Paleogene benthic foraminifers from the Southern Indian Ocean (Kerguelen Plateau): biostratigraphy and paleoecology. *In* Wise, S. W., Jr., Schlich, R., et al., *Proc. ODP, Sci. Results*, 120: College Station, TX (Ocean Drilling Program), 603-630.

Martini, E., 1971. Standard Tertiary and Quaternary calcareous nannoplankton zonation. *In* Farinacci, A. (Ed.), *Proceedings of the Second International Conference on Planktonic Microfossils, Roma:* Rome (Tecnoscienza), 739-785.

McKenzie, J. A., Weissert, H., Poore, R. Z., Wright, R. C., Percival, S. F. Jr., Oberhänsli, H., and Casey, M., 1984. Paleoceanogrphic implications of stable-isotope data from upper Miocene-Lower Pliocene sediments from the Southeast Atlantic (Deep Sea Drilling Project Site 519). *In* Hsü, K. J., LaBrecque, J. L., et al., *Init. Repts. DSDP, 73*: Washington (U.S. Govt. Printing Office), 717-724.

Miller, K. G., Fairbanks, R. G., and Mountain, G. S., 1987. Tertiary oxygen isotope synthesis, sea level history, and continental margin erosion. *Paleoceanography*, 2:1-19.

Miller, K. G., Wright, J. D., and Brower, A., 1989. Oligocene to Miocene stable isotope stratigraphy and planktonic foraminifer biostratigraphy of the Sierrab Leone Rise (DSDP Site 366 and ODP Site 667). *In* Ruddiman, W., Sarnthein, M., et al., *Proc. ODP, Sci. Results*, 108: College Station, TX (Ocean Drilling Program), 279-294.

Moore, T. C. Jr., Rabinowitz, P. D., Borella, P. E., Shackleton, N. J., and Boersma, A., 1984. History of the Walvis Ridge. *In* Moore, T. C. Jr., Rabinowitz, P. D., et al., *Init. Repts. DSDP, 74*: Washington (U.S. Govt. Printing Office), 737-747

Nomura, R., 1991a, Paleoceanography of upper Maastrichtian to Eocene benthic foraminiferal assemblages at Site 752, 753 and 754, eastern Indian Ocean. *In* Weissel, J., Peirce, J., Taylor, E., Alt, J., et al., *Proc. ODP, Sci. Results*, 121: College Station, TX (Ocean Drilling Program), 3-29.

Nomura, R., 1991b, Oligocene to Pleistocene benthic foraminifera assemblages at Site 754 and 756, eastern Indian Ocean. *In* Weissel, J., Peirce, J., Taylor, E., Alt, J., et al., *Proc. ODP, Sci. Results*, 121: College Station, TX (Ocean Drilling Program), 31-75.

Nomura, R., Seto, K., and Niitsuma, N., 1992. Late Cenozoic deep-sea benthic foraminiferal changes and isotopic records in the Eastern Indian Ocean. *In* Saito, (Ed.), *Studies in Benthic Foraminifera*, BENTHOS'90, Sendai, 1990, 227-233.

Nomura, R., Seto, K., and Niitsuma, N., 1992. Warm Saline Deep Water (WSDW) Chikyu Monthly, 6, 161-166. (in Japanese).

Oberhänsli, H., 1986. Latest Cretaceous-Early Neogene oxygen and carbon isotopic record at DSDP sites in the Indian Ocean. *Mar. Micropaleontol.*, 10:91-117.

Oberhänsli, H., McKenzie, J. A., Toumarkine, M., and Weissert, H., 1984. A paleoclimatic and paleoceanographic record of the Paleogene in the central South Atlantic (Leg 73, Sites 522, 523, and 524). *In* Hsü, K. J., LaBrecque, J. L., et al., *Init. Repts. DSDP, 73*: Washington (U.S. Govt. Printing Office), 737-747

Okada, H., 1990. Quaternary and Paleogene calcareous nannofossils, Leg 115. In Duncan, R. A., Backman, J., Peterson, L. C., et al., Proc. ODP, Sci. Results, 115: College Station, TX (Ocean Drilling Program), 129-174.

Okada, H., and Bukry, D.; 1980. Supplementary modification and introduction of code number to the low-latitude coccolith biostratigraphic zonation (Bukry, 1973; 1975). *Mar. Micropaleontol.*, 5:321-325.

Peirce, J., Weissel, J., et al., 1989. *Proc. ODP, Init. Repts.*, 121: College Station, TX (Ocean Drilling Program).

Poore, R. Z., and Matthews, R. K., 1984. Late Eocene-Oligocene oxygen- and carbon-isotopic record from South Atlantic Ocean, deep sea drilling Project Site 522. *In* Hsü, K. J., LaBrecque, J. L., et al., *Init. Repts. DSDP, 73*: Washington (U.S. Govt. Printing Office), 725-735

Poore, R. A., Tauxe, L., Percival, S F., Jr., LaBrecque, J. L., Wright, R., Peterson, N. P., Smith, C. C., Tucker, P., and Hsü, K. J., 1983. Late Cretaceous-Cenozoic magnetostratigraphic and biostratigraphic correlations for the South Atlantic Ocean, DSDP Leg 73. *Palaeogeogr. Palaeoclimatol. Palaeoecol.*, 42:127-148.

Rahman, A., and Roth, P. H., 1989. Late Neogene calcareous nannofossil biostratigraphy of the Gulf of Aden region based on calcareous nannofossils. Mar. Micropaleontol., 15:1-27.

Rea, D. K., Lohmann, K. C., MacLeod, N. D., House, M. A., Hovan, S. A., and Martin, G. D., 1991. Oxygen and carbon isotopic records the oozes of ODP Sites 752, 754, 756, and 757, eastern Indian Ocean. *In* Peirce, J., Weissel, J., et al., *Proc. ODP, Sci. Results*, 121: College Station, TX (Ocean Drilling Program), 229-240.

Rio, D., Fornaciari, F., and Raffi, I., 1990. Late Oligocene through early Pleistocene calcareous nannofossils from western equatorial Indian Ocean (Leg 115). *In* Duncan, R. A., Backman, J., Peterson, L. C., et al., *Proc. ODP, Sci. Results*, 115: College Station, TX (Ocean Drilling Program), 167-185.

Sarnthein, M. and Tiedemann, R., 1989. Toward a high-resolution stable isotope stratigraphy of the last 3.4 million years: Sites 658 and 659 off Northwest Africa. *In* Ruddiman, W., Sarnthein, M., et al., *Proc. ODP, Sci. Results*, 108: College Station, TX (Ocean Drilling Program), 529-538.

Scotese C. R., Gahagan L. M., and Larson R. L., 1988. Plate tectonic reconstructions of the Cretaceous and Cenozoic ocean basins. *Tectonophysics*, 155: 27-48.

Savin, S. M. and Woodruff, F., 1990. Isotopic Evidence for temperature and productivity in the Tertiary oceans. *In* Burnett, W. C. and Riggs, S. P. (Ed.), ***Phosphate Deposits of the World, vol.3, Genesis of Neogene to recent Phosphorites***, 241-259.

Seto, K., Nomura, R., and Niitsuma, N., 1991. *DATA REPORT:* Oxygen and carbon isotope records of the upper Maastrichtian to lower Eocene benthic foraminifers at Site 752 in the eastern Indian Ocean. *In* Peirce, J., Weissel, J. , Taylor, E., Alt, J., et al., *Proc. ODP, Sci. Results*, 121: College Station, TX (Ocean Drilling Program), 885-889.

Shackleton, N. J., Backman, J., Zimmerman, H. B., Kent, D. V., Hall, M. A., Roberts, D. G., Schnitker, D., Baldauf, J. G., Desprairies, A., Homrighausen, R., Guddlestun, P., Keene, J. B., Kalttenback, A. J., Krumsiek, K. A. O., Morton, A C., Murray, J. W., and Westberg-Smith, J., 1984. Oxygen isotope calibration of the onset of icerafting in DSDP Site 522A: history of glaciation in the North Atlantic region. *Nature*, 307: 620-623.

Shackleton, N. J., Corfield, R. M., and Hall, M. A., 1985. Stable isotope data and the ontogeny of Paleocene planktonic foraminifera. *J. Foraminiferal. Res.*, 15: 321-336.

Shackleton, N. J., and Hall, M. A., 1990. Pliocene oxygen isotope stratigraphy of Hole 709C. *In* Duncan, R. A., Backman, J., Peterson, L. C., et al., *Proc. ODP, Sci. Results,* 115: College Station, TX (Ocean Drilling Program), 529-538.

Stott, L. D. and Kennett, J. P., 1990. Antarctic Paleogene planktonic foraminifer biostratigraphy: ODP Leg 113, Sites 689 and 690. *In* Barker, P. F., Kennett, J. P., et al., *Proc. ODP, Sci. Results*, 113: College Station, TX (Ocean Drilling Program), 549-569.

Stott, L. D., Kennett, J. P., Shackleton, N. J., and Corfield, R. M., 1990. The evolution of Antarctic surface waters during the Paleogene: inferences from stable isotopic composition of planktonic foraminifers, ODP Leg 113. *In* Barker, P. F., Kennett, J. P., et al., *Proc. ODP, Sci. Results*, 113: College Station, TX (Ocean Drilling Program), 849-863.

Takayama, T., and Sato, T., 1987. Coccolith biostratigraphy of the North Atlantic Ocean, Deep Sea Drilling Project Leg 94. *In* Ruddiman, W. F., Kidd, R. B., Thomas, E., et al., *Init. Repts. DSDP*, 94, Pt. 2: Washington (U.S.Govt. Printing Office), 651-702.

Thierstein, H. R., Geitzenauer, K. R., Molfino, B., and Shackleton, N. J., 1977. Global synchroneity of late Quaternary coccolith datum levels: validation by oxygen isotope. *Geology*, 5:400-404.

Urey, H. C., 1947, The thermodynamic properties of isotopic substances. *J. chem. Soc.*, 562-581.

Urey, H. C., Lowenstam, H. A., Epstein, S., and McKinney, C. R., 1951, Measurement of paleotemperatures and temperatures of the Upper Cretaceous of England, Denmark, and the south-eastern United States. *Geol. Soc. Am. Bull.*, 62: 399-416.

Vincent, E., Killingley, J. S., and Berger, W. H., 1980. The Magnetic Epoch-6 carbon shift: a change in the ocean's $^{13}C/^{12}C$ ratio 6.2 million years ago. *Mar. Micropaleontol.*, 5: 185-203.

Vincent, E., Killingley, J. S., and Berger, W. H., 1985. Miocene oxygen and carbon isotope stratigraphy of the tropical Indian Ocean. *In* Kennet, J. P. (Ed.), *The Miocene Ocean: Paleoceanography and Biogeography. Mem. Geol. Soc. Am.*, 163: 103-130.

Vincent, E., Shackleton, N. J., and Hall, M. A., 1991. Miocene oxygen and carbon isotope stratigraphy of planktonic foraminifers at Sites 709 and 758, tropical Indian Ocean. *In* Peirce, J., Weissel, J., et al., *Proc. ODP, Sci. Results*, 121: College Station, TX (Ocean Drilling Program), 241-252.

Wada, H., Fujii, N., and Niitsuma, N., T., 1984. Analytical method of stable isotope for ultra-small amounts of carbon dioxide with MAT 250 Mass-spectrometer. *Geosci. Rep. Shizuoka Univ.*, 10: 103-112.

Wada, H., Nagai, Y., Ando, T., and Niitsuma, N., 1991. New trap system for Purification of Carbon Dioxide equipped to the inlet system of MAT 250 Mass-Spectrometer. *Geosci. Rep. Shizuoka Univ.*, 17: 161-167.

Wada, H., Niitsuma, N., and Saito, T., 1982. Carbon and oxygen isotopic measurement of ultra-small samples. *Geosci. Rep. Shizuoka Univ.*, 7: 35-50.

Weissert, H. J., Mckenzie, J. A., Wright, R. C., Clark, M., Oberhänsli, H., and Casey, M., 1984. Paleoclimatic record of the Pliocene at deep sea drilling project Sites 519, 521, 522, and 523 (Central South Atlantic). *In* Hsü, K. J., LaBrecque, J. L., et al., *Init. Repts. DSDP, 73*: Washington (U.S. Govt. Printing Office), 701-715.

Woodruff, F., and Chamber, R., 1991. Middle Miocene benthic foraminiferal oxygen and carbon isotopes and stratigraphy: Southern Ocean Site 744. *In* Barron, J., Larsen, B., et al., *Proc. ODP, Sci. Results*, 119: College Station, TX (Ocean Drilling Program), 935-939.

Woodruff, F., and Savin, S., 1989. Miocene deepwater oceanography. *Paleoceanography*, 4: 87-140.

Woodruff, F., Savin, S. M., and Abel, L.,1990. Miocene benthic foraminifera oxygen and carbon isotopes, Site 709, Indian Ocean. *In* Backman, J., Duncan, R. A., Peterson, L. C., et al., *Proc. ODP, Sci. Results*, 115: College Station, TX (Ocean Drilling Program), 519-528.

Zachos, J. C., Berggren, W. A., Aubry, M. P., and Mackensen, A., 1992a. Isotope and trace element geochemistry of Eocene and Oligocene foraminifers from Site 748, Kerguelen Plateau. *In* Wise, S. W., Jr., Schlich, R., et al., *Proc. ODP, Sci. Results*, 120: College Station, TX (Ocean Drilling Program), 839-854.

Zachos, J. C., Breza, J., and Wise, S. W., Jr., 1992b. Early Oligocene ice-sheet expansion on Antarctica: sedimentological and isotope evidence from Kerguelen Plateau. *Geology*. 20: 569-573.

Savin, S. M. and Woodruff, F., 1990. Isotopic Evidence for temperature and productivity in the Tertiary oceans. *In* Burnett, W. C. and Riggs, S. P. (Ed.), *Phosphate Deposits of the World, vol.3, Genesis of Neogene to recent Phosphorites*, 241-259.

Seto, K., Nomura, R., and Niitsuma, N., 1991. *DATA REPORT:* Oxygen and carbon isotope records of the upper Maastrichtian to lower Eocene benthic foraminifers at Site 752 in the eastern Indian Ocean. *In* Peirce, J., Weissel, J. , Taylor, E., Alt, J., et al., *Proc. ODP, Sci. Results*, 121: College Station, TX (Ocean Drilling Program), 885-889.

Shackleton, N. J., Backman, J., Zimmerman, H. B., Kent, D. V., Hall, M. A., Roberts, D. G., Schnitker, D., Baldauf, J. G., Desprairies, A., Homrighausen, R., Guddlestun, P., Keene, J. B., Kalttenback, A. J., Krumsiek, K. A. O., Morton, A C., Murray, J. W., and Westberg-Smith, J., 1984. Oxygen isotope calibration of the onset of icerafting in DSDP Site 522A: history of glaciation in the North Atlantic region. *Nature*, 307: 620-623.

Shackleton, N. J., Corfield, R. M., and Hall, M. A., 1985. Stable isotope data and the ontogeny of Paleocene planktonic foraminifera. *J. Foraminiferal. Res.*, 15: 321-336.

Shackleton, N. J., and Hall, M. A., 1990. Pliocene oxygen isotope stratigraphy of Hole 709C. *In* Duncan, R. A., Backman, J., Peterson, L. C., et al., *Proc. ODP, Sci. Results,* 115: College Station, TX (Ocean Drilling Program), 529-538.

Stott, L. D. and Kennett, J. P., 1990. Antarctic Paleogene planktonic foraminifer biostratigraphy: ODP Leg 113, Sites 689 and 690. *In* Barker, P. F., Kennett, J. P., et al., *Proc. ODP, Sci. Results*, 113: College Station, TX (Ocean Drilling Program), 549-569.

Stott, L. D., Kennett, J. P., Shackleton, N. J., and Corfield, R. M., 1990. The evolution of Antarctic surface waters during the Paleogene: inferences from stable isotopic composition of planktonic foraminifers, ODP Leg 113. *In* Barker, P. F., Kennett, J. P., et al., *Proc. ODP, Sci. Results*, 113: College Station, TX (Ocean Drilling Program), 849-863.

Takayama, T., and Sato, T., 1987. Coccolith biostratigraphy of the North Atlantic Ocean, Deep Sea Drilling Project Leg 94. *In* Ruddiman, W. F., Kidd, R. B., Thomas, E., et al., *Init. Repts. DSDP*, 94, Pt. 2: Washington (U.S.Govt. Printing Office), 651-702.

Thierstein, H. R., Geitzenauer, K. R., Molfino, B., and Shackleton, N. J., 1977. Global synchroneity of late Quaternary coccolith datum levels: validation by oxygen isotope. *Geology*, 5:400-404.

Urey, H. C., 1947, The thermodynamic properties of isotopic substances. *J. chem. Soc.*, 562-581.

Urey, H. C., Lowenstam, H. A., Epstein, S., and McKinney, C. R., 1951, Measurement of paleotemperatures and temperatures of the Upper Cretaceous of England, Denmark, and the south-eastern United States. *Geol. Soc. Am. Bull.*, 62: 399-416.

Vincent, E., Killingley, J. S., and Berger, W. H., 1980. The Magnetic Epoch-6 carbon shift: a change in the ocean's $^{13}C/^{12}C$ ratio 6.2 million years ago. *Mar. Micropaleontol.*, 5: 185-203.

Vincent, E., Killingley, J. S., and Berger, W. H., 1985. Miocene oxygen and carbon isotope stratigraphy of the tropical Indian Ocean. *In* Kennet, J. P. (Ed.), *The Miocene Ocean: Paleoceanography and Biogeography. Mem. Geol. Soc. Am.*, 163: 103-130.

Vincent, E., Shackleton, N. J., and Hall, M. A., 1991. Miocene oxygen and carbon isotope stratigraphy of planktonic foraminifers at Sites 709 and 758, tropical Indian Ocean. *In* Peirce, J., Weissel, J., et al., *Proc. ODP, Sci. Results*, 121: College Station, TX (Ocean Drilling Program), 241-252.

Wada, H., Fujii, N., and Niitsuma, N., T., 1984. Analytical method of stable isotope for ultra-small amounts of carbon dioxide with MAT 250 Mass-spectrometer. *Geosci. Rep. Shizuoka Univ.*, 10: 103-112.

Wada, H., Nagai, Y., Ando, T., and Niitsuma, N., 1991. New trap system for Purification of Carbon Dioxide equipped to the inlet system of MAT 250 Mass-Spectrometer. *Geosci. Rep. Shizuoka Univ.*, 17: 161-167.

Wada, H., Niitsuma, N., and Saito, T., 1982. Carbon and oxygen isotopic measurement of ultra-small samples. *Geosci. Rep. Shizuoka Univ.*, 7: 35-50.

Weissert, H. J., Mckenzie, J. A., Wright, R. C., Clark, M., Oberhänsli, H., and Casey, M., 1984. Paleoclimatic record of the Pliocene at deep sea drilling project Sites 519, 521, 522, and 523 (Central South Atlantic). *In* Hsü, K. J., LaBrecque, J. L., et al., *Init. Repts. DSDP, 73*: Washington (U.S. Govt. Printing Office), 701-715.

Woodruff, F., and Chamber, R., 1991. Middle Miocene benthic foraminiferal oxygen and carbon isotopes and stratigraphy: Southern Ocean Site 744. *In* Barron, J., Larsen, B., et al., *Proc. ODP, Sci. Results*, 119: College Station, TX (Ocean Drilling Program), 935-939.

Woodruff, F., and Savin, S., 1989. Miocene deepwater oceanography. *Paleoceanography*, 4: 87-140.

Woodruff, F., Savin, S. M., and Abel, L.,1990. Miocene benthic foraminifera oxygen and carbon isotopes, Site 709, Indian Ocean. *In* Backman, J., Duncan, R. A., Peterson, L. C., et al., *Proc. ODP, Sci. Results*, 115: College Station, TX (Ocean Drilling Program), 519-528.

Zachos, J. C., Berggren, W. A., Aubry, M. P., and Mackensen, A., 1992a. Isotope and trace element geochemistry of Eocene and Oligocene foraminifers from Site 748, Kerguelen Plateau. *In* Wise, S. W., Jr., Schlich, R., et al., *Proc. ODP, Sci. Results*, 120: College Station, TX (Ocean Drilling Program), 839-854.

Zachos, J. C., Breza, J., and Wise, S. W., Jr., 1992b. Early Oligocene ice-sheet expansion on Antarctica: sedimentological and isotope evidence from Kerguelen Plateau. *Geology*. 20: 569-573.

Zachos, J. C., Rea, D. K., Seto, K., Niitsuma, N., and Nomura, R., 1992c. Paleogene and early Neogene deep water paleoceanography of the Indian Ocean as determined from benthic foraminifera stable carbon and oxygen isotope records. *Am. Geophys. Union Monograph*, 70: 351-385.

Zahn, R., Winn, K., and Sarnthein, M., 1986. Benthic foraminiferal d[13]C and accumulation rates of organic carbon: *Uvigerina pergrina* group and *Cibicidoides wuellerstorfi*. *Paleoceanography*, 1: 27-42.

Zijderveld, J. D., Zachariasse, J. W., Verhallen, P. J. J., and Hilgen, F. J., 1986. The age of the Miocene/Pliocene boundary. *Newsl. Stratigr.*, 16:169-181.

Koji SETO
Department of Geology, Faculty of Science, Shimane University, Matsue, 690, Japan.

From 1, Oct., 1995
Department of Geoscience, Interdisciplinary Faculty of Science and Engineering, Shimane University, Matsue, 690, Japan.

Appendix A-1. Oxygen and carbon isotopic data from Legs 121 and 122.

Benthic Foraminifera

Leg 121 Site 752 Hole A

Anomalinoides danicus

Core & Section	Interval	Depth (mbsf)	Age (Ma)	Specimen size D (μm)	Specimen size T (μm)	$\delta^{18}O$	$\delta^{13}C$	$\delta^{18}O$ ave.	$\delta^{13}C$ ave.
13X-1	0.70-0.75	113.60	55.27	658	380	-0.770	0.314	-0.840	0.170
13X-1	0.70-0.75	113.60	55.27	607	354	-0.935	0.050		
13X-1	0.70-0.75	113.60	55.27	405	253	-0.816	0.146		
13X-2	0.70-0.75	115.10	55.34	658	405	-1.039	-0.056	-1.026	0.122
13X-2	0.70-0.75	115.10	55.34	392	253	-1.068	0.003		
13X-2	0.70-0.75	115.10	55.34	405	304	-0.971	0.419		
13X-4	0.62-0.67	118.02	55.46	557	278	-1.021	-0.072	-0.856	0.079
13X-4	0.62-0.67	118.02	55.46	481	278	-0.875	0.081		
13X-4	0.62-0.67	118.02	55.46	405	228	-0.673	0.229		
14X-1	0.70-0.75	123.30	55.70	506	278	-1.456	-0.890	-1.371	-0.648
14X-1	0.70-0.75	123.30	55.70	506	304	-1.233	-0.684		
14X-1	0.70-0.75	123.30	55.70	455	278	-1.538	-0.995		
14X-1	0.70-0.75	123.30	55.70	405	228	-1.255	-0.022		
14X-2	0.72-0.75	124.82	55.76	620	329	-1.041	-0.175	-0.886	0.079
14X-2	0.72-0.75	124.82	55.76	455	304	-0.728	0.321		
14X-2	0.72-0.75	124.82	55.76	481	278	-0.887	0.091		
14X-3	0.70-0.75	126.30	55.83	607	329	-0.851	0.228	-0.998	0.021
14X-3	0.70-0.75	126.30	55.83	481	253	-1.214	-0.239		
14X-3	0.70-0.75	126.30	55.83	405	228	-0.930	0.074		
14X-4	0.62-0.68	127.72	55.89	506	304	-0.920	-0.077	-0.825	-0.016
14X-4	0.62-0.68	127.72	55.89	417	253	-0.762	0.028		
14X-4	0.62-0.68	127.72	55.89	455	253	-0.793	0.001		
15X-1	0.70-0.75	133.00	56.12	481	278	-1.218	-0.287	-1.126	-0.230
15X-1	0.70-0.75	133.00	56.12	455	278	-1.012	-0.137		
15X-1	0.70-0.75	133.00	56.12	519	278	-1.148	-0.267		
15X-2	0.69-0.72	134.49	56.19	481	278	-0.536	0.441	-0.872	0.209
15X-2	0.69-0.72	134.49	56.19	455	278	-0.917	0.150		
15X-2	0.69-0.72	134.49	56.19	417	253	-1.162	0.036		
15X-4	0.70-0.73	137.50	55.71	481	304	-0.828	0.279	-0.799	0.356
15X-4	0.70-0.73	137.50	55.71	417	228	-0.744	0.357		
15X-4	0.70-0.73	137.50	55.71	455	278	-0.824	0.433		
15X-5	0.70-0.75	139.00	55.75	531	304	-0.622	0.412	-0.700	0.277
15X-5	0.70-0.75	139.00	55.75	430	253	-0.748	0.164		
15X-5	0.70-0.75	139.00	55.75	405	228	-0.730	0.254		
16X-1	0.70-0.75	142.70	55.83	430	253	-0.963	0.216	-0.861	0.234
16X-1	0.70-0.75	142.70	55.83	405	228	-0.728	0.343		
16X-1	0.70-0.75	142.70	55.83	506	278	-0.893	0.143		
16X-2	0.70-0.75	144.20	55.86	380	215	-1.014	-0.234	-1.047	-0.150
16X-2	0.70-0.75	144.20	55.86	380	202	-1.124	-0.219		
16X-2	0.70-0.75	144.20	55.86	405	278	-1.002	0.003		
16X-4	0.59-0.65	147.09	55.92	380	240	-0.809	0.349	-0.973	0.120
16X-4	0.59-0.65	147.09	55.92	455	228	-1.136	-0.109		
16X-5	0.25-0.30	148.25	55.95	455	278	-0.778	0.283	-0.768	0.395
16X-5	0.25-0.30	148.25	55.95	481	278	-0.663	0.421		
16X-5	0.25-0.30	148.25	55.95	430	253	-0.864	0.480		
17X-1	0.70-0.75	152.40	56.04	531	354	-1.459	-0.815	-1.420	-0.746
17X-1	0.70-0.75	152.40	56.04	405	228	-1.568	-0.833		
17X-1	0.70-0.75	152.40	56.04	405	228	-1.343	-0.634		
17X-1	0.70-0.75	152.40	56.04	430	253	-1.311	-0.702		
17X-2	0.64-0.66	153.84	56.07	392	215	-0.968	0.194	-0.968	0.194
17X-3	0.70-0.75	155.40	56.11	607	354	-0.532	0.507	-0.679	0.418
17X-3	0.70-0.75	155.40	56.11	455	228	-0.821	0.370		
17X-3	0.70-0.75	155.40	56.11	430	228	-0.683	0.376		
18X-1	0.71-0.75	162.11	56.74	506	304	-1.226	0.281	-0.747	0.642
18X-1	0.71-0.75	162.11	56.74	430	253	-0.379	0.824		
18X-1	0.71-0.75	162.11	56.74	380	202	-0.637	0.820		
18X-2	0.67-0.70	163.57	56.91	405	278	-0.621	0.794	-0.561	0.810
18X-2	0.67-0.70	163.57	56.91	405	228	-0.501	0.825		
19X-1	0.70-0.75	171.80	57.82	582	380	-0.718	1.009	-0.672	1.041
19X-1	0.70-0.75	171.80	57.82	582	202	-0.748	1.024		
19X-1	0.70-0.75	171.80	57.82	481	278	-0.733	0.979		
19X-1	0.70-0.75	171.80	57.82	405	278	-0.589	1.031		
19X-1	0.70-0.75	171.80	57.82	430	228	-0.570	1.163		
19X-2	0.71-0.74	173.31	57.86	607	380	-0.811	0.607	-0.727	0.683
19X-2	0.71-0.74	173.31	57.86	607	329	-0.705	0.729		

Benthic Foraminifera

Leg 121 Site 752 Hole A

Anomalinoides danicus

Core & Section	Interval	Depth (mbsf)	Age (Ma)	Specimen size D (μm)	Specimen size T (μm)	$\delta^{18}O$	$\delta^{13}C$	$\delta^{18}O$ ave.	$\delta^{13}C$ ave.
19X-2	0.71-0.74	173.31	57.86	557	329	-0.664	0.712		
19X-3	0.75-0.79	174.85	57.91	455	278	-0.672	0.647	-0.769	0.698
19X-3	0.75-0.79	174.85	57.91	506	304	-0.848	0.769		
19X-3	0.75-0.79	174.85	57.91	481	329	-0.786	0.679		
20X-1	0.70-0.75	181.40	58.09	430	278	-0.008	2.129	-0.189	1.889
20X-1	0.70-0.75	181.40	58.09	455	304	-0.112	2.025		
20X-1	0.70-0.75	181.40	58.09	430	278	-0.447	1.513		
21X-1	0.70-0.75	191.10	58.36	455	329	-0.420	2.127	-0.389	2.105
21X-1	0.70-0.75	191.10	58.36	506	304	-0.403	2.109		
21X-1	0.70-0.75	191.10	58.36	607	329	-0.343	2.079		
21X-2	0.70-0.73	192.60	58.40	632	405	-0.492	2.041	-0.633	1.966
21X-2	0.70-0.73	192.60	58.40	506	380	-0.581	2.022		
21X-2	0.70-0.73	192.60	58.40	380	253	-0.824	1.834		
22X-1	0.70-0.75	200.80	58.63	430	304	-0.590	2.375	-0.577	2.315
22X-1	0.70-0.75	200.80	58.63	405	253	-0.643	2.410		
22X-1	0.70-0.75	200.80	58.63	531	354	-0.499	2.160		
22X-3	0.70-0.75	203.80	58.76	430	304	-1.412	1.912	-0.837	2.071
22X-3	0.70-0.75	203.80	58.76	455	278	-0.701	1.994		
22X-3	0.70-0.75	203.80	58.76	430	253	-0.397	2.306		
23X-1	0.54-0.56	210.34	59.04	430	304	-0.845	2.284	-0.845	2.284
25X-2	0.75-0.79	231.35	60.63	506	329	-0.609	1.986	-0.609	1.986
26X-1	0.97-1.00	239.77	60.96	455	304	-0.662	1.955	-0.610	2.035
26X-1	0.97-1.00	239.77	60.96	481	329	-0.657	2.449		
26X-1	0.97-1.00	239.77	60.96	683	455	-0.511	1.702		
27X-3	0.70-0.75	252.10	61.33	810	506	-0.397	1.432	-0.359	1.473
27X-3	0.70-0.75	252.10	61.33	430	278	-0.321	1.513		
28X-1	0.70-0.75	258.80	61.53	430	278	-0.714	1.586	-0.472	1.635
28X-1	0.70-0.75	258.80	61.53	708	430	-0.289	1.704		
28X-1	0.70-0.75	258.80	61.53	632	380	-0.414	1.614		
28X-4	0.72-0.76	263.32	61.67	683	278	-0.184	1.631	-0.184	1.631
28X-5	0.70-0.75	264.80	61.72	683	430	-0.554	1.903	-0.487	1.958
28X-5	0.70-0.75	264.80	61.72	607	354	-0.527	1.970		
28X-5	0.70-0.75	264.80	61.72	607	380	-0.364	2.155		
28X-5	0.70-0.75	264.80	61.72	582	405	-0.504	1.804		
29X-1	0.70-0.75	268.40	61.83	784	455	-0.562	1.817	-0.609	1.856
29X-1	0.70-0.75	268.40	61.83	607	304	-0.772	1.862		
29X-1	0.70-0.75	268.40	61.83	683	380	-0.492	1.890		
29X-2	0.68-0.71	269.88	61.87	506	329	-0.367	1.731	-0.594	1.706
29X-2	0.68-0.71	269.88	61.87	531	342	-0.707	1.616		
29X-2	0.68-0.71	269.88	61.87	405	278	-0.708	1.770		
29X-5	0.70-0.73	274.40	62.01	683	405	-0.816	1.568	-0.636	1.603
29X-5	0.70-0.73	274.40	62.01	481	278	-0.596	1.627		
29X-5	0.70-0.73	274.40	62.01	430	304	-0.495	1.613		
29X-6	0.78-0.81	275.98	62.06	620	380	-0.609	1.651	-0.465	1.636
29X-6	0.78-0.81	275.98	62.06	860	430	-0.422	1.665		
29X-6	0.78-0.81	275.98	62.06	708	405	-0.363	1.593		
30X-1	0.73-0.76	278.13	62.12	582	380	-0.355	1.640	-0.465	1.708
30X-1	0.73-0.76	278.13	62.12	430	278	-0.567	1.715		
30X-1	0.73-0.76	278.13	62.12	430	278	-0.473	1.769		
31X-1	0.70-0.75	280.10	62.18	455	278	-0.798	1.725	-0.684	1.733
31X-1	0.70-0.75	280.10	62.18	455	278	-0.537	1.908		
31X-1	0.70-0.75	280.10	62.18	506	304	-0.718	1.566		
31X-2	0.77-0.80	281.67	62.23	506	354	-0.701	1.706	-0.595	1.609
31X-2	0.77-0.80	281.67	62.23	759	455	-0.686	1.617		
31X-2	0.77-0.80	281.67	62.23	708	430	-0.397	1.505		
31X-4	0.75-0.79	284.65	62.32	822	481	-0.660	1.432	-0.640	1.464
31X-4	0.75-0.79	284.65	62.32	658	392	-0.619	1.497		
31X-5	0.70-0.75	286.10	62.36	481	304	-0.644	1.443	-0.644	1.443
32X-1	0.70-0.75	289.40	62.46	784	455	-1.069	1.294	-0.964	1.119
32X-1	0.70-0.75	289.40	62.46	658	380	-1.101	1.244		
32X-1	0.70-0.75	289.40	62.46	582	430	-0.801	0.841		
32X-1	0.70-0.75	289.40	62.46	506	329	-0.883	1.096		
32X-5	0.70-0.75	295.40	62.65	430	329	-0.821	1.432	-1.011	1.433
32X-5	0.70-0.75	295.40	62.65	380	228	-1.200	1.434		

Appendix A-2. (continued).

Core & Section	Interval	Depth (mbsf)	Age (Ma)	Specimen size D (μm)	Specimen size T (μm)	$\delta^{18}O$	$\delta^{13}C$	$\delta^{18}O$ ave.	$\delta^{13}C$ ave.
Leg 121 Site 752 Hole A									
Cibicidoides velascoensis									
20X-1	0.70-0.75	181.40	58.09	582	380	-0.512	1.284	-0.505	1.470
20X-1	0.70-0.75	181.40	58.09	557	380	-0.555	1.413		
20X-1	0.70-0.75	181.40	58.09	430	278	-0.447	1.714		
21X-1	0.70-0.75	191.10	58.36	607	380	-0.371	2.110	-0.305	2.156
21X-1	0.70-0.75	191.10	58.36	658	380	-0.232	2.115		
21X-1	0.70-0.75	191.10	58.36	557	380	-0.313	2.244		
21X-2	0.70-0.73	192.60	58.40	595	329	-0.386	2.080	-0.379	2.091
21X-2	0.70-0.73	192.60	58.40	506	354	-0.457	2.141		
21X-2	0.70-0.73	192.60	58.40	430	304	-0.292	2.053		
22X-1	0.70-0.75	200.80	58.63	531	354	-0.394	2.227	-0.387	2.360
22X-1	0.70-0.75	200.80	58.63	506	354	-0.429	2.457		
22X-1	0.70-0.75	200.80	58.63	455	329	-0.337	2.396		
22X-2	0.75-0.79	202.35	58.70	455	304	-0.423	2.149	-0.369	2.200
22X-2	0.75-0.79	202.35	58.70	455	329	-0.390	2.158		
22X-2	0.75-0.79	202.35	58.70	417	304	-0.292	2.292		
22X-3	0.70-0.75	203.80	58.76	506	329	-0.435	2.318	-0.384	2.292
22X-3	0.70-0.75	203.80	58.76	506	354	-0.373	2.297		
22X-3	0.70-0.75	203.80	58.76	405	304	-0.343	2.260		
23X-1	0.54-0.56	210.34	59.04	354	253	-0.536	2.369	-0.626	2.375
23X-1	0.54-0.56	210.34	59.04	354	253	-0.716	2.380		
24X-2	0.70-0.75	221.22	59.81	569	405	-0.253	1.938	-0.253	1.938
25X-1	0.79-0.84	229.89	60.53	468	329	-0.395	2.018	-0.326	2.122
25X-1	0.79-0.84	229.89	60.53	493	380	-0.257	2.225		
25X-3	0.79-0.84	232.89	60.74	380	278	-0.581	2.162	-0.581	2.162
26X-5	0.97-1.00	245.77	61.14	405	253	-0.370	1.412	-0.370	1.412
30X-1	0.73-0.76	278.13	62.12	455	329	-0.447	1.593	-0.478	1.642
30X-1	0.73-0.76	278.13	62.12	481	380	-0.428	1.764		
30X-1	0.73-0.76	278.13	62.12	481	405	-0.559	1.569		
31X-1	0.70-0.75	280.10	62.18	658	380	-0.611	1.430	-0.598	1.467
31X-1	0.70-0.75	280.10	62.18	557	354	-0.665	1.396		
31X-1	0.70-0.75	280.10	62.18	405	278	-0.518	1.576		
31X-4	0.75-0.79	284.65	62.32	746	392	-0.450	1.469	-0.345	1.374
31X-4	0.75-0.79	284.65	62.32	392	291	-0.211	1.191		
31X-4	0.75-0.79	284.65	62.32	430	304	-0.372	1.463		
32X-1	0.70-0.75	289.40	62.46	708	380	-0.685	1.103	-0.774	1.168
32X-1	0.70-0.75	289.40	62.46	658	354	-0.787	1.107		
32X-1	0.70-0.75	289.40	62.46	455	278	-0.850	1.295		
33X-1	0.68-0.71	299.08	62.76	607	380	-0.987	0.952	-0.987	0.952
33X-3	0.57-0.60	301.97	62.85	380	228	-0.781	0.948	-0.719	1.012
33X-3	0.57-0.60	301.97	62.85	380	278	-0.656	1.076		
Nuttallides truempyi									
22X-1	0.70-0.75	200.80	58.63	405	253	-0.566	1.752	-0.538	1.890
22X-1	0.70-0.75	200.80	58.63	430	278	-0.515	1.983		
22X-1	0.70-0.75	200.80	58.63	455	278	-0.533	1.934		
22X-3	0.70-0.75	203.80	58.76	481	278	-0.508	1.442	-0.508	1.442
Nuttallides truempyi (5 specimens)									
13X-1	0.70-0.75	113.60	55.27	253-380	177-202	-1.094	-0.149		
13X-4	0.62-0.67	118.02	55.46	153-329	152-177	-1.971	-0.146		
15X-4	0.70-0.73	137.50	55.71	253-304	177-202	-1.116	0.014		
18X-1	0.71-0.75	162.11	56.74	304-405	202-253	-0.739	0.226		
19X-1	0.70-0.75	171.80	57.82	278-304	177	-0.894	0.638		
19X-3	0.75-0.79	174.85	57.91	278-354	152-202	-1.112	-0.143		
20X-1	0.70-0.75	181.40	58.09	304-380	177-228	-0.506	0.933		
22X-1	0.70-0.75	200.80	58.63	278-329	177-202	-0.550	1.818		
23X-1	0.54-0.56	210.34	59.04	253-304	202	-0.581	1.873		
26X-1	0.97-1.00	239.77	60.96	304-354	177-253	-0.302	1.215		
Oridorsalis umbonatus									
21X-1	0.70-0.75	191.10	58.36	481	253	-0.164	1.518	-0.221	1.613
21X-1	0.70-0.75	191.10	58.36	455	304	-0.278	1.708		
Stensioina beccariiformis									
16X-4	0.59-0.65	147.09	55.92	481	253	-0.612	0.903	-0.524	0.887
16X-4	0.59-0.65	147.09	55.92	493	278	-0.577	0.787		
16X-4	0.59-0.65	147.09	55.92	430	253	-0.381	0.971		
20X-1	0.70-0.75	181.40	58.09	481	253	-0.853	0.345	-0.699	0.703
20X-1	0.70-0.75	181.40	58.09	430	228	-0.675	1.014		
20X-1	0.70-0.75	181.40	58.09	405	253	-0.568	0.749		
Leg 121 Site 752 Hole A									
Stensioina beccariiformis (Cont.)									
21X-1	0.70-0.75	191.10	58.36	506	278	-0.468	1.386	-0.533	1.422
21X-1	0.70-0.75	191.10	58.36	430	253	-0.387	1.431		
21X-1	0.70-0.75	191.10	58.36	481	278	-0.745	1.448		
21X-2	0.70-0.73	192.60	58.40	468	253	-0.570	1.495	-0.599	1.501
21X-2	0.70-0.73	192.60	58.40	455	228	-0.627	1.508		
22X-1	0.70-0.75	200.80	58.63	506	253	-0.586	1.652	-0.566	1.581
22X-1	0.70-0.75	200.80	58.63	506	278	-0.562	1.594		
22X-1	0.70-0.75	200.80	58.63	531	304	-0.549	1.498		
22X-2	0.75-0.79	202.35	58.70	430	228	-0.517	1.436	-0.527	1.361
22X-2	0.75-0.79	202.35	58.70	519	304	-0.604	1.392		
22X-2	0.75-0.79	202.35	58.70	455	253	-0.460	1.254		
22X-3	0.70-0.75	203.80	58.76	557	278	-0.436	1.294	-0.600	1.466
22X-3	0.70-0.75	203.80	58.76	506	253	-0.649	1.557		
22X-3	0.70-0.75	203.80	58.76	455	253	-0.715	1.546		
23X-1	0.54-0.56	210.34	59.04	430	329	-0.710	1.755	-0.699	1.689
23X-1	0.54-0.56	210.34	59.04	506	278	-0.567	1.654		
23X-1	0.54-0.56	210.34	59.04	481	253	-0.820	1.659		
24X-1	0.70-0.73	220.20	59.72	582	278	-0.468	1.293	-0.419	1.242
24X-1	0.70-0.73	220.20	59.72	582	329	-0.390	1.276		
24X-1	0.70-0.73	220.20	59.72	582	304	-0.399	1.156		
24X-2	0.70-0.75	221.22	59.81	531	278	-0.493	1.181	-0.465	1.193
24X-2	0.70-0.75	221.22	59.81	569	278	-0.529	1.274		
24X-2	0.70-0.75	221.22	59.81	417	228	-0.372	1.125		
25X-1	0.79-0.84	229.89	60.53	557	304	-0.492	1.191	-0.419	1.251
25X-1	0.79-0.84	229.89	60.53	380	202	-0.347	1.428		
25X-1	0.79-0.84	229.89	60.53	380	202	-0.417	1.135		
25X-2	0.75-0.79	231.35	60.63	557	304	-0.627	0.891	-0.408	1.068
25X-2	0.75-0.79	231.35	60.63	481	266	-0.343	1.136		
25X-2	0.75-0.79	231.35	60.63	455	253	-0.253	1.178		
26X-1	0.97-1.00	239.77	60.96	557	329	-0.623	0.866	-0.553	0.919
26X-1	0.97-1.00	239.77	60.96	582	304	-0.717	0.914		
26X-1	0.97-1.00	239.77	60.96	506	253	-0.319	0.978		
26X-2	0.82-0.85	241.12	61.00	468	253	-0.398	0.815	-0.403	0.886
26X-2	0.82-0.85	241.12	61.00	493	304	-0.404	0.873		
26X-2	0.82-0.85	241.12	61.00	455	253	-0.407	0.970		
26X-5	0.97-1.00	245.77	61.14	455	329	-0.402	0.814	-0.389	0.864
26X-5	0.97-1.00	245.77	61.14	557	304	-0.413	0.591		
26X-5	0.97-1.00	245.77	61.14	430	228	-0.351	1.187		
26X-6	0.82-0.86	247.12	61.18	506	278	-0.352	0.686	-0.492	0.623
26X-6	0.82-0.86	247.12	61.18	380	202	-0.632	0.560		
27X-1	0.70-0.75	249.10	61.24	531	278	-0.492	0.255	-0.418	0.484
27X-1	0.70-0.75	249.10	61.24	455	253	-0.323	0.813		
27X-1	0.70-0.75	249.10	61.24	405	228	-0.440	0.384		
27X-2	0.78-0.82	250.68	61.29	607	291	-0.257	0.718	-0.276	0.758
27X-2	0.78-0.82	250.68	61.29	468	253	-0.476	0.717		
27X-2	0.78-0.82	250.68	61.29	468	253	-0.094	0.838		
27X-3	0.70-0.75	252.10	61.33	481	253	-0.268	0.739	-0.364	0.765
27X-3	0.70-0.75	252.10	61.33	430	278	-0.277	0.660		
27X-3	0.70-0.75	252.10	61.33	405	202	-0.546	0.897		
28X-1	0.70-0.75	258.80	61.53	531	304	-0.182	0.952	-0.244	0.829
28X-1	0.70-0.75	258.80	61.53	506	329	-0.323	0.715		
28X-1	0.70-0.75	258.80	61.53	481	278	-0.226	0.821		
28X-2	0.55-0.58	260.15	61.58	582	329	-0.367	0.708	-0.422	0.885
28X-2	0.55-0.58	260.15	61.58	481	278	-0.451	0.826		
28X-2	0.55-0.58	260.15	61.58	468	253	-0.447	1.122		
28X-4	0.72-0.76	263.32	61.67	531	266	-0.678	0.879	-0.543	0.923
28X-4	0.72-0.76	263.32	61.67	506	228	-0.445	0.889		
28X-4	0.72-0.76	263.32	61.67	481	253	-0.506	1.002		
28X-5	0.70-0.75	264.80	61.72	582	329	-0.416	0.606	-0.377	0.887
28X-5	0.70-0.75	264.80	61.72	481	278	-0.409	0.943		
28X-5	0.70-0.75	264.80	61.72	455	278	-0.305	1.111		
29X-1	0.70-0.73	268.40	61.83	531	278	-0.576	0.941	-0.615	1.034
29X-1	0.70-0.73	268.40	61.83	506	278	-0.845	1.090		
29X-1	0.70-0.73	268.40	61.83	506	278	-0.423	1.071		
29X-2	0.68-0.71	269.88	61.87	430	253	-0.392	0.963	-0.392	0.963
29X-4	0.72-0.76	272.92	61.96	367	228	-0.507	1.080	-0.507	1.080

Appendix A-3. (continued).

Core & Section	Interval	Depth (mbsf)	Age (Ma)	Specimen size D (μm)	Specimen size T (μm)	$\delta^{18}O$	$\delta^{13}C$	$\delta^{18}O$ ave.	$\delta^{13}C$ ave.
Leg 121 Site 752 Hole A									
Stensioina beccariiformis			(Cont.)						
29X-5	0.70-0.73	274.40	62.01	506	329	-0.408	0.800	-0.722	0.596
29X-5	0.70-0.73	274.40	62.01	506	304	-0.913	0.623		
29X-5	0.70-0.73	274.40	62.01	481	253	-0.844	0.366		
29X-6	0.78-0.81	275.98	62.06	443	240	-0.282	0.928	-0.263	0.813
29X-6	0.78-0.81	275.98	62.06	506	291	-0.306	0.692		
29X-6	0.78-0.81	275.98	62.06	468	266	-0.200	0.820		
30X-1	0.73-0.76	278.13	62.12	455	304	-0.574	0.986	-0.559	0.992
30X-1	0.73-0.76	278.13	62.12	455	253	-0.361	0.932		
30X-1	0.73-0.76	278.13	62.12	455	253	-0.743	1.058		
31X-1	0.70-0.75	280.10	62.18	481	278	-0.773	0.943	-0.813	0.877
31X-1	0.70-0.75	280.10	62.18	455	278	-0.785	0.779		
31X-1	0.70-0.75	280.10	62.18	455	253	-0.881	0.908		
31X-2	0.77-0.80	281.67	62.23	493	228	-0.597	0.733	-0.577	0.846
31X-2	0.77-0.80	281.67	62.23	430	215	-0.565	0.671		
31X-2	0.77-0.80	281.67	62.23	430	228	-0.569	1.135		
31X-4	0.75-0.79	284.65	62.32	506	228	-0.661	0.900	-0.779	0.782
31X-4	0.75-0.79	284.65	62.32	531	304	-0.714	0.612		
31X-4	0.75-0.79	284.65	62.32	481	228	-0.960	0.833		
31X-5	0.70-0.75	286.10	62.36	405	278	-1.021	0.839	-0.784	0.706
31X-5	0.70-0.75	286.10	62.36	430	253	-0.689	0.721		
31X-5	0.70-0.75	286.10	62.36	455	253	-0.641	0.558		
32X-1	0.70-0.75	289.40	62.46	455	304	-0.800	0.583	-0.712	0.686
32X-1	0.70-0.75	289.40	62.46	405	253	-0.476	0.847		
32X-1	0.70-0.75	289.40	62.46	380	202	-0.861	0.627		
32X-2	0.71-0.75	290.91	62.51	531	278	-0.936	0.114	-0.773	0.381
32X-2	0.71-0.75	290.91	62.51	468	266	-0.763	0.460		
32X-2	0.71-0.75	290.91	62.51	430	215	-0.618	0.569		
32X-4	0.71-0.74	293.91	62.60	481	240	-0.626	0.539	-0.732	0.564
32X-4	0.71-0.74	293.91	62.60	405	202	-0.912	0.624		
32X-4	0.71-0.74	293.91	62.60	405	228	-0.656	0.528		
32X-5	0.70-0.75	295.40	62.65	430	228	-0.857	0.780	-0.925	0.636
32X-5	0.70-0.75	295.40	62.65	430	228	-0.906	0.407		
32X-5	0.70-0.75	295.40	62.65	443	278	-1.012	0.722		
32X-6	0.81-0.84	297.01	62.70	430	253	-0.648	0.844	-0.779	0.754
32X-6	0.81-0.84	297.01	62.70	481	266	-0.740	0.776		
32X-6	0.81-0.84	297.01	62.70	430	228	-0.949	0.643		
33X-1	0.68-0.71	299.08	62.76	405	253	-0.976	0.568	-0.827	0.505
33X-1	0.68-0.71	299.08	62.76	519	253	-0.809	0.453		
33X-1	0.68-0.71	299.08	62.76	531	278	-0.697	0.495		
33X-2	0.71-0.73	300.61	62.81	506	266	-0.578	0.627	-0.578	0.627
33X-3	0.57-0.60	301.97	62.85	405	228	-1.334	0.843	-1.018	0.638
33X-3	0.57-0.60	301.97	62.85	455	202	-0.922	0.822		
33X-3	0.57-0.60	301.97	62.85	430	278	-0.797	0.250		
Leg 121 Site 752 Hole B									
Cibicidoides velascoensis									
5R-3	0.50-0.53	300.50	62.80	708	430	-0.761	1.025	-0.948	1.103
5R-3	0.50-0.53	300.50	62.80	481	304	-1.175	1.275		
5R-3	0.50-0.53	300.50	62.80	582	354	-0.907	1.010		
6R-1	0.44-0.47	307.04	63.00	708	380	-1.310	0.861	-1.321	0.859
6R-1	0.44-0.47	307.04	63.00	658	329	-1.234	0.874		
6R-1	0.44-0.47	307.04	63.00	455	228	-1.419	0.841		
6R-3	0.99-1.02	310.59	63.36	481	405	-1.010	1.059	-1.044	1.017
6R-3	0.99-1.02	310.59	63.36	405	228	-1.210	1.159		
6R-3	0.99-1.02	310.59	63.36	607	405	-0.913	0.833		
7R-1	0.82-0.85	316.92	63.66	607	354	-0.968	1.527	-0.956	1.481
7R-1	0.82-0.85	316.92	63.66	658	405	-0.955	1.515		
7R-1	0.82-0.85	316.92	63.66	734	405	-0.946	1.401		
7R-5	0.76-0.78	322.86	63.81	430	329	-1.076	1.491	-1.207	1.518
7R-5	0.76-0.78	322.86	63.81	430	304	-1.606	1.661		
7R-5	0.76-0.78	322.86	63.81	455	278	-0.939	1.402		
8R-2	0.91-0.94	326.85	63.91	455	278	-1.399	1.185	-1.455	1.218
8R-2	0.91-0.94	326.85	63.91	430	253	-1.697	1.370		
8R-2	0.91-0.94	326.85	63.91	430	304	-1.269	1.099		
8R-6	1.01-1.04	332.91	64.05	658	354	-0.950	1.214	-1.037	1.267
8R-6	1.01-1.04	332.91	64.05	886	506	-1.193	1.243		
8R-6	1.01-1.04	332.91	64.05	430	278	-0.969	1.345		

Core & Section	Interval	Depth (mbsf)	Age (Ma)	Specimen size D (μm)	Specimen size T (μm)	$\delta^{18}O$	$\delta^{13}C$	$\delta^{18}O$ ave.	$\delta^{13}C$ ave.
Leg 121 Site 752 Hole B									
Cibicidoides velascoensis			(Cont.)						
9R-1	0.42-0.45	335.82	64.13	860	481	-0.873	1.327	-0.846	1.279
9R-1	0.42-0.45	335.82	64.13	632	354	-0.851	1.222		
9R-1	0.42-0.45	335.82	64.13	683	354	-0.814	1.288		
10R-1	1.05-1.08	346.15	64.84	632	430	-0.898	1.355	-1.024	1.310
10R-1	1.05-1.08	346.15	64.84	531	304	-1.189	1.250		
10R-1	1.05-1.08	346.15	64.84	481	304	-0.986	1.326		
10R-2	1.00-1.02	347.60	65.06	481	278	-1.664	1.215	-1.492	1.224
10R-2	1.00-1.02	347.60	65.06	455	329	-1.496	1.289		
10R-2	1.00-1.02	347.60	65.06	430	278	-1.317	1.168		
10R-3	1.12-1.15	349.22	65.30	430	253	-0.858	1.533	-1.394	1.462
10R-3	1.12-1.15	349.22	65.30	481	304	-1.747	1.497		
10R-3	1.12-1.15	349.22	65.30	430	253	-1.577	1.355		
10R-4	0.79-0.81	350.39	65.48	481	329	-1.530	1.624	-1.572	1.539
10R-4	0.79-0.81	350.39	65.48	455	253	-1.889	1.524		
10R-4	0.79-0.81	350.39	65.48	405	253	-1.298	1.468		
10R-6	1.00-1.02	353.60	65.96	430	253	-1.696	0.988	-1.493	0.912
10R-6	1.00-1.02	353.60	65.96	430	253	-1.376	1.015		
10R-6	1.00-1.02	353.60	65.96	430	253	-1.407	0.732		
10R-7	0.41-0.43	354.51	66.10	405	253	-1.269	0.825	-1.217	0.880
10R-7	0.41-0.43	354.51	66.10	405	228	-1.164	0.934		
11R-1	0.44-0.47	355.24	66.18	632	329	-1.576	1.422	-1.064	1.177
11R-1	0.44-0.47	355.24	66.18	531	304	-0.810	1.093		
11R-1	0.44-0.47	355.24	66.18	405	202	-0.805	1.015		
11R-2	0.44-0.47	356.74	66.28	632	380	-1.084	1.467	-1.158	1.443
11R-2	0.44-0.47	356.74	66.28	658	380	-0.976	1.354		
11R-2	0.44-0.47	356.74	66.28	405	304	-1.413	1.509		
11R-3	0.38-0.41	358.18	66.37	734	405	-0.524	0.984	-0.593	1.352
11R-3	0.38-0.41	358.18	66.37	582	506	-0.593	1.153		
11R-3	0.38-0.41	358.18	66.37	455	253	-0.661	1.919		
11R-3	0.64-0.66	358.44	66.38	506	278	-0.815	1.797	-1.075	1.719
11R-3	0.64-0.66	358.44	66.38	455	329	-1.354	1.648		
11R-3	0.64-0.66	358.44	66.38	455	304	-1.055	1.711		
11R-3	1.12-1.14	358.92	66.42	430	278	-0.792	1.661	-0.990	1.609
11R-3	1.12-1.14	358.92	66.42	430	253	-1.233	1.516		
11R-3	1.12-1.14	358.92	66.42	430	278	-0.946	1.650		
12R-1	1.04-1.07	365.44	66.96	810	405	-0.833	0.937	-0.728	1.018
12R-1	1.04-1.07	365.44	66.96	506	304	-0.524	1.163		
12R-1	1.04-1.07	365.44	66.96	430	278	-0.827	0.955		
12R-3	0.10-0.13	367.50	67.10	531	329	-0.662	1.314	-0.888	1.242
12R-3	0.10-0.13	367.50	67.10	557	405	-0.870	1.157		
12R-3	0.10-0.13	367.50	67.10	607	405	-1.132	1.256		
12R-5	0.54-0.57	370.94	67.32	405	278	-1.757	1.142	-1.193	1.214
12R-5	0.54-0.57	370.94	67.32	380	253	-1.090	1.203		
12R-5	0.54-0.57	370.94	67.32	734	455	-0.733	1.297		
13R-1	0.40-0.43	374.40	67.54	683	455	-1.239	1.195	-0.900	1.187
13R-1	0.40-0.43	374.40	67.54	658	380	-0.855	1.129		
13R-1	0.40-0.43	374.40	67.54	455	253	-0.606	1.238		
13R-5	0.65-0.68	380.65	67.95	810	455	-0.648	1.271	-0.523	1.275
13R-5	0.65-0.68	380.65	67.95	708	405	-0.429	1.225		
13R-5	0.65-0.68	380.65	67.95	455	253	-0.491	1.330		
14R-1	0.69-0.72	384.29	68.18	557	405	-0.547	1.133	-0.744	1.338
14R-1	0.69-0.72	384.29	68.18	544	329	-0.628	1.261		
14R-1	0.69-0.72	384.29	68.18	784	405	-1.057	1.621		
14R-5	0.62-0.65	390.22	68.46	658	405	-1.256	1.413	-0.929	1.268
14R-5	0.62-0.65	390.22	68.46	632	380	-0.838	1.233		
14R-5	0.62-0.65	390.22	68.46	708	405	-0.692	1.159		
15R-1	1.19-1.22	394.49	68.78	506	380	-0.954	1.328	-1.147	1.291
15R-1	1.19-1.22	394.49	68.78	531	354	-1.414	1.293		
15R-1	1.19-1.22	394.49	68.78	380	228	-1.072	1.251		
15R-5	1.12-1.15	400.42	69.53	632	380	-0.768	1.159	-0.734	1.287
15R-5	1.12-1.15	400.42	69.53	886	531	-0.678	1.287		
15R-5	1.12-1.15	400.42	69.53	380	228	-0.757	1.414		
16R-1	0.15-0.18	403.15	69.67	506	329	-0.711	1.074	-0.863	0.957
16R-1	0.15-0.18	403.15	69.67	506	329	-0.936	0.861		
16R-1	0.15-0.18	403.15	69.67	481	304	-0.943	0.936		
16R-3	1.36-1.39	407.36	69.89	759	455	-1.294	0.968	-1.308	0.962

Appendix A-4. (continued).

Core & Section	Interval	Depth (mbsf)	Age (Ma)	Specimen size D (μm)	Specimen size T (μm)	$\delta^{18}O$	$\delta^{13}C$	$\delta^{18}O$ ave.	$\delta^{13}C$ ave.
Leg 121 Site 752 Hole B									
Cibicidoides velascoensis				(Cont.)					
16R-3	1.36-1.39	407.36	69.89	632	380	-1.898	1.112		
16R-3	1.36-1.39	407.36	69.89	430	278	-0.732	0.806		
17R-1	1.03-1.06	413.63	70.22	531	405	-0.476	0.322	-1.067	0.531
17R-1	1.03-1.06	413.63	70.22	557	329	-1.331	0.817		
17R-1	1.03-1.06	413.63	70.22	380	202	-1.395	0.454		
17R-5	0.66-0.69	419.26	70.52	835	455	-0.683	0.748	-0.679	0.595
17R-5	0.66-0.69	419.26	70.52	734	455	-0.288	0.364		
17R-5	0.66-0.69	419.26	70.52	531	329	-1.065	0.673		
19R-1	0.42-0.45	432.02	71.19	582	329	-0.727	0.605	-0.680	0.678
19R-1	0.42-0.45	432.02	71.19	658	380	-0.553	0.644		
19R-1	0.42-0.45	432.02	71.19	582	329	-0.760	0.784		
19R-3	0.49-0.52	435.09	71.35	810	455	-1.644	0.638	-1.336	0.626
19R-3	0.49-0.52	435.09	71.35	683	380	-0.926	0.579		
19R-3	0.49-0.52	435.09	71.35	759	430	-1.437	0.661		
Stensioina beccariiformis									
5R-3	0.50-0.53	300.50	62.80	582	278	-0.892	0.596	-0.826	0.563
5R-3	0.50-0.53	300.50	62.80	531	304	-0.707	0.601		
5R-3	0.50-0.53	300.50	62.80	506	278	-0.932	0.616		
5R-3	0.50-0.53	300.50	62.80	430	228	-0.701	0.546		
5R-3	0.50-0.53	300.50	62.80	430	202	-0.896	0.458		
6R-1	0.44-0.47	307.04	63.00	405	202	-1.306	0.562	-1.250	0.392
6R-1	0.44-0.47	307.04	63.00	430	228	-1.242	0.255		
6R-1	0.44-0.47	307.04	63.00	430	253	-1.201	0.358		
6R-3	0.99-1.02	310.59	63.36	430	228	-1.428	0.695	-1.216	0.733
6R-3	0.99-1.02	310.59	63.36	405	202	-1.380	0.709		
6R-3	0.99-1.02	310.59	63.36	405	228	-0.839	0.796		
7R-1	0.82-0.85	316.92	63.66	405	228	-0.811	1.098	-0.891	1.125
7R-1	0.82-0.85	316.92	63.66	405	253	-0.789	1.123		
7R-1	0.82-0.85	316.92	63.66	405	253	-1.073	1.155		
7R-5	0.76-0.78	322.86	63.81	455	278	-1.672	1.141	-1.369	1.109
7R-5	0.76-0.78	322.86	63.81	430	202	-1.177	1.091		
7R-5	0.76-0.78	322.86	63.81	405	202	-1.259	1.094		
8R-2	0.91-0.94	326.85	63.91	455	253	-1.152	0.869	-1.120	0.956
8R-2	0.91-0.94	326.85	63.91	506	253	-1.122	0.922		
8R-2	0.91-0.94	326.85	63.91	455	228	-1.087	1.077		
8R-6	1.01-1.04	332.91	64.05	455	253	-1.018	0.918	-1.069	0.977
8R-6	1.01-1.04	332.91	64.05	430	253	-0.858	1.029		
8R-6	1.01-1.04	332.91	64.05	430	228	-1.330	0.985		
9R-1	0.42-0.45	335.82	64.13	455	253	-1.020	0.792	-1.009	0.863
9R-1	0.42-0.45	335.82	64.13	455	253	-1.134	0.929		
9R-1	0.42-0.45	335.82	64.13	506	278	-0.872	0.868		
10R-1	0.50-0.52	345.60	64.76	430	253	-1.428	1.223	-1.111	1.145
10R-1	0.50-0.52	345.60	64.76	430	228	-0.834	1.163		
10R-1	0.50-0.52	345.60	64.76	405	253	-1.070	1.050		
10R-1	1.05-1.08	346.15	64.84	405	253	-1.187	1.186	-1.252	1.244
10R-1	1.05-1.08	346.15	64.84	380	228	-1.399	1.125		
10R-1	1.05-1.08	346.15	64.84	380	202	-1.170	1.420		
10R-2	1.00-1.02	347.60	65.06	380	228	-1.355	1.073	-1.432	1.098
10R-2	1.00-1.02	347.60	65.06	405	228	-1.264	1.098		
10R-2	1.00-1.02	347.60	65.06	380	202	-1.676	1.122		
10R-3	1.12-1.15	349.22	65.30	455	202	-1.328	1.300	-1.211	1.215
10R-3	1.12-1.15	349.22	65.30	405	228	-0.986	1.199		
10R-3	1.12-1.15	349.22	65.30	380	253	-1.320	1.147		
10R-4	0.79-0.81	350.39	65.48	380	202	-1.872	1.262	-1.656	1.267
10R-4	0.79-0.81	350.39	65.48	380	228	-1.508	1.201		
10R-4	0.79-0.81	350.39	65.48	405	228	-1.588	1.337		
10R-5	0.50-0.52	351.60	65.66	455	228	-1.744	1.027	-1.744	1.027
10R-6	0.50-0.52	353.10	65.88	380	202	-1.662	0.489	-1.780	0.657
10R-6	0.50-0.52	353.10	65.88	380	202	-1.897	0.825		
10R-6	1.00-1.02	353.60	65.96	380	202	-1.391	0.739	-1.391	0.739
11R-2	1.00-1.02	357.30	66.31	405	202	-1.230	0.977	-1.391	0.904
11R-2	1.00-1.02	357.30	66.31	405	202	-0.973	1.159		
11R-2	1.00-1.02	357.30	66.31	380	177	-1.970	0.577		
11R-3	0.38-0.41	358.18	66.37	405	228	-0.726	1.375	-0.873	1.374
11R-3	0.38-0.41	358.18	66.37	405	202	-1.019	1.373		
11R-3	0.64-0.66	358.44	66.38	380	202	-1.238	1.211	-1.375	1.010
Leg 121 Site 752 Hole B									
Stensioina beccariiformis				(Cont.)					
11R-3	0.64-0.66	358.44	66.38	380	202	-1.511	0.808		
11R-3	1.12-1.14	358.92	66.42	380	228	-1.695	1.239	-1.252	1.253
11R-3	1.12-1.14	358.92	66.42	405	228	-0.962	1.487		
11R-3	1.12-1.14	358.92	66.42	405	228	-1.099	1.032		
12R-1	1.04-1.07	365.44	66.96	405	202	-1.284	0.958	-1.473	1.019
12R-1	1.04-1.07	365.44	66.96	380	202	-1.532	1.133		
12R-1	1.04-1.07	365.44	66.96	380	202	-1.603	0.966		
12R-3	0.10-0.13	367.50	67.10	380	202	-0.807	0.903	-0.982	0.812
12R-3	0.10-0.13	367.50	67.10	405	202	-1.182	0.879		
12R-3	0.10-0.13	367.50	67.10	405	228	-0.956	0.653		
12R-5	0.54-0.57	370.94	67.32	405	304	-1.310	1.104	-1.123	1.084
12R-5	0.54-0.57	370.94	67.32	455	329	-0.949	0.929		
12R-5	0.54-0.57	370.94	67.32	430	228	-1.110	1.218		
13R-1	0.40-0.43	374.40	67.54	405	228	-1.823	1.012	-1.621	0.888
13R-1	0.40-0.43	374.40	67.54	380	253	-1.223	0.618		
13R-1	0.40-0.43	374.40	67.54	455	253	-1.817	1.033		
13R-5	0.65-0.68	380.65	67.95	455	253	-0.506	1.113	-0.543	1.049
13R-5	0.65-0.68	380.65	67.95	405	202	-0.643	0.924		
13R-5	0.65-0.68	380.65	67.95	380	202	-0.479	1.110		
14R-1	0.69-0.72	384.29	68.18	430	253	-0.743	0.722	-0.721	0.823
14R-1	0.69-0.72	384.29	68.18	405	228	-0.403	0.707		
14R-1	0.69-0.72	384.29	68.18	405	228	-1.016	1.039		
14R-5	0.62-0.65	390.22	68.46	405	228	-1.104	0.956	-1.169	0.888
14R-5	0.62-0.65	390.22	68.46	405	253	-1.097	0.836		
14R-5	0.62-0.65	390.22	68.46	417	253	-1.305	0.872		
15R-1	1.19-1.22	394.49	68.78	481	304	-1.181	0.988	-1.294	1.011
15R-1	1.19-1.22	394.49	68.78	430	228	-1.546	1.022		
15R-1	1.19-1.22	394.49	68.78	380	202	-1.155	1.024		
15R-5	1.12-1.15	400.42	69.53	380	202	-1.153	0.836	-0.982	1.000
15R-5	1.12-1.15	400.42	69.53	506	278	-0.834	1.064		
15R-5	1.12-1.15	400.42	69.53	405	253	-0.958	1.100		
16R-1	0.15-0.18	403.15	69.67	430	253	-0.885	0.660	-1.027	0.674
16R-1	0.15-0.18	403.15	69.67	380	202	-1.223	0.616		
16R-1	0.15-0.18	403.15	69.67	380	202	-0.972	0.745		
16R-3	1.36-1.39	407.36	69.89	380	228	-0.870	0.479	-1.126	0.648
16R-3	1.36-1.39	407.36	69.89	380	228	-1.246	0.850		
16R-3	1.36-1.39	407.36	69.89	430	278	-1.262	0.615		
17R-1	1.03-1.06	413.63	70.22	405	278	-0.499	0.280	-0.733	0.152
17R-1	1.03-1.06	413.63	70.22	380	202	-0.924	0.251		
17R-1	1.03-1.06	413.63	70.22	380	202	-0.775	-0.075		
17R-5	0.66-0.69	419.26	70.52	380	202	-0.797	0.221	-0.772	0.291
17R-5	0.66-0.69	419.26	70.52	380	228	-0.647	0.357		
17R-5	0.66-0.69	419.26	70.52	405	228	-0.873	0.294		
19R-1	0.42-0.45	432.02	71.19	405	228	-0.779	0.102	-1.055	0.058
19R-1	0.42-0.45	432.02	71.19	380	177	-1.541	0.221		
19R-1	0.42-0.45	432.02	71.19	380	202	-0.845	-0.150		
Stensioina beccariiformis (11 specimens)									
9R-1	0.42-0.45	335.82	64.13	253-354	127-177	-1.040	0.826		
10R-1	0.50-0.52	345.60	64.76	202-304	127-202	-1.423	1.293		
10R-1	1.05-1.08	346.15	64.84	253-354	152-202	-1.258	1.145		
10R-2	1.00-1.02	347.60	65.06	202-354	127-202	-1.779	1.139		
10R-3	1.12-1.15	349.22	65.30	253-354	152-177	-1.479	1.145		
10R-4	0.79-0.81	350.39	65.48	253-354	152-202	-1.445	1.203		
10R-5	0.50-0.52	351.60	65.66	177-278	101-278	-1.969	1.039		
10R-6	0.50-0.52	353.10	65.88	202-354	127-202	-1.685	0.475		
10R-6	1.00-1.02	353.60	65.96	253-354	127-177	-1.626	0.661		
10R-7	0.41-0.43	354.51	66.10	253-304	127-202	-2.040	0.725		
11R-1	0.44-0.47	355.24	66.18	278-304	152-177	-0.727	0.715		
11R-1	1.02-1.04	355.82	66.22	202-354	101-202	-1.341	0.712		
11R-2	0.44-0.47	356.74	66.28	253-380	152-202	-1.136	1.082		
11R-2	1.00-1.02	357.30	66.31	253-354	152-202	-1.614	0.879		
11R-3	0.38-0.41	358.18	66.37	278-354	152-202	-0.746	1.468		
11R-3	0.64-0.66	358.44	66.38	253-354	127-202	-1.056	1.325		
11R-3	1.12-1.14	358.92	66.42	278-354	152-202	-1.344	1.097		
12R-1	1.04-1.07	365.44	66.96	253-354	152-202	-1.303	0.809		
12R-3	0.10-0.13	367.50	67.10	278-354	152-202	-1.206	0.861		

Appendix A-5. (continued).

Core & Section	Interval	Depth (mbsf)	Age (Ma)	Specimen size D (μm)	Specimen size T (μm)	$\delta^{18}O$	$\delta^{13}C$	$\delta^{18}O$ ave.	$\delta^{13}C$ ave.
Leg 121 Site 752 Hole B									
Stensioina beccariiformis (11 specimens) (Cont.)									
12R-5	0.54-0.57	370.94	67.32	253-354	127-202	-1.010	0.949		
13R-1	0.40-0.43	374.40	67.54	304-354	177-202	-1.416	1.159		
13R-5	0.65-0.68	380.65	67.95	253-354	152-202	-0.805	0.916		
14R-1	0.69-0.72	384.29	68.18	278-354	127-202	-0.938	0.803		
14R-5	0.62-0.65	390.22	68.46	253-354	152-202	-1.005	0.840		
15R-1	1.19-1.22	394.49	68.78	253-329	152-177	-1.259	0.889		
15R-5	1.12-1.15	400.42	69.53	253-354	152-202	-1.049	0.867		
16R-1	0.15-0.18	403.15	69.67	253-354	152-202	-1.047	0.660		
16R-3	1.36-1.39	407.36	69.89	228-329	127-177	-0.979	0.576		
17R-1	1.03-1.06	413.63	70.22	253-354	127-202	-0.841	0.279		
17R-5	0.66-0.69	419.26	70.52	253-354	152-202	-0.819	0.192		
19R-1	0.42-0.45	432.02	71.19	278-354	152-202	-1.056	0.189		
19R-3	0.49-0.52	435.09	71.35	253-354	152-202	-1.581	0.336		
Leg 121 Site 754 Hole A									
Oridorsalis umbonatus									
1H-1	0.70-0.75	0.70	0.21	405	228	2.801	-0.319	2.945	-0.325
1H-1	0.70-0.75	0.70	0.21	582	354	3.032	-0.204		
1H-1	0.70-0.75	0.70	0.21	506	304	3.003	-0.451		
1H-3	0.70-0.75	3.70	1.11	405	228	2.593	-0.013	2.818	-0.186
1H-3	0.70-0.75	3.70	1.11	405	304	2.995	-0.273		
1H-3	0.70-0.75	3.70	1.11	455	253	2.867	-0.272		
2H-1	0.70-0.75	6.80	2.11	506	253	2.565	0.063	2.700	-0.050
2H-1	0.70-0.75	6.80	2.11	455	253	2.750	-0.026		
2H-1	0.70-0.75	6.80	2.11	405	228	2.785	-0.187		
2H-3	0.70-0.75	9.80	2.60	531	329	2.695	0.025	2.604	-0.140
2H-3	0.70-0.75	9.80	2.60	506	278	2.580	-0.263		
2H-3	0.70-0.75	9.80	2.60	481	228	2.537	-0.181		
3H-1	0.70-0.75	16.40	3.60	506	304	2.329	-0.045	2.182	-0.125
3H-1	0.70-0.75	16.40	3.60	481	253	2.180	-0.310		
3H-1	0.70-0.75	16.40	3.60	455	253	2.036	-0.019		
3H-5	0.70-0.75	22.40	4.55	557	329	2.483	-0.320	2.467	-0.341
3H-5	0.70-0.75	22.40	4.55	481	278	2.554	-0.331		
3H-5	0.70-0.75	22.40	4.55	481	253	2.363	-0.373		
4H-1	0.70-0.75	26.00	5.25	493	278	2.309	-0.301	2.235	-0.246
4H-1	0.70-0.75	26.00	5.25	481	278	2.192	-0.188		
4H-1	0.70-0.75	26.00	5.25	455	253	1.944	-0.089		
4H-1	0.70-0.75	26.00	5.25	430	253	2.496	-0.405		
4H-5	0.70-0.75	32.00	6.43	481	304	1.917	0.078	1.967	0.016
4H-5	0.70-0.75	32.00	6.43	405	228	2.105	0.165		
4H-5	0.70-0.75	32.00	6.43	405	228	1.878	-0.194		
5H-1	0.70-0.75	35.60	7.54	683	405	2.224	0.713	2.050	0.516
5H-1	0.70-0.75	35.60	7.54	506	278	2.034	0.245		
5H-1	0.70-0.75	35.60	7.54	405	202	1.892	0.589		
5H-5	0.70-0.75	41.60	9.79	531	329	2.236	0.561	1.962	0.504
5H-5	0.70-0.75	41.60	9.79	531	278	1.817	0.510		
5H-5	0.70-0.75	41.60	9.79	405	253	1.832	0.442		
6H-1	0.70-0.75	45.20	11.14	506	304	2.096	0.341	2.042	0.394
6H-1	0.70-0.75	45.20	11.14	519	278	2.004	0.367		
6H-1	0.70-0.75	45.20	11.14	506	278	2.025	0.475		
6H-5	0.70-0.75	51.20	12.21	430	253	2.241	0.698	2.096	0.532
6H-5	0.70-0.75	51.20	12.21	481	253	2.074	0.455		
6H-5	0.70-0.75	51.20	12.21	531	304	1.974	0.444		
7H-1	0.70-0.75	54.80	12.42	506	253	1.914	0.346	1.938	0.535
7H-1	0.70-0.75	54.80	12.42	481	278	1.975	0.646		
7H-1	0.70-0.75	54.80	12.42	455	228	1.925	0.614		
7H-3	0.70-0.75	57.80	12.59	582	354	1.928	0.628	1.716	0.749
7H-3	0.70-0.75	57.80	12.59	506	329	1.683	0.847		
7H-3	0.70-0.75	57.80	12.59	506	278	1.626	0.716		
7H-3	0.70-0.75	57.80	12.59	430	228	1.628	0.805		
7H-5	0.70-0.75	60.80	12.77	455	253	2.035	0.857	1.924	0.708
7H-5	0.70-0.75	60.80	12.77	430	228	1.709	0.456		
7H-5	0.70-0.75	60.80	12.77	430	240	2.028	0.811		
8H-1	0.70-0.75	64.50	12.98	506	291	1.751	0.526	1.755	0.544
8H-1	0.70-0.75	64.50	12.98	455	278	1.792	0.493		
8H-1	0.70-0.75	64.50	12.98	455	253	1.722	0.612		
8H-3	0.70-0.75	67.50	13.15	430	304	1.667	0.228	1.528	0.103
Leg 121 Site 754 Hole A									
Oridorsalis umbonatus (Cont.)									
8H-3	0.70-0.75	67.50	13.15	392	228	1.388	-0.022		
8H-5	0.70-0.75	70.50	13.33	430	228	1.875	0.487	1.734	0.504
8H-5	0.70-0.75	70.50	13.33	405	228	1.636	0.435		
8H-5	0.70-0.75	70.50	13.33	405	228	1.691	0.590		
9H-1	0.70-0.75	74.20	13.54	506	278	1.556	1.315	1.395	1.175
9H-1	0.70-0.75	74.20	13.54	531	304	1.376	1.427		
9H-1	0.70-0.75	74.20	13.54	430	253	1.252	0.782		
9H-3	0.70-0.75	77.20	14.15	506	354	0.971	1.200	1.077	1.244
9H-3	0.70-0.75	77.20	14.15	481	304	1.102	1.055		
9H-3	0.70-0.75	77.20	14.15	455	278	1.158	1.476		
9H-5	0.70-0.75	80.20	15.00	506	278	1.283	1.578	1.231	1.216
9H-5	0.70-0.75	80.20	15.00	506	304	1.139	1.001		
9H-5	0.70-0.75	80.20	15.00	506	354	1.272	1.068		
10H-1	0.70-0.75	83.90	16.45	481	253	1.061	0.827	0.933	0.678
10H-1	0.70-0.75	83.90	16.45	430	253	0.766	0.446		
10H-1	0.70-0.75	83.90	16.45	405	202	0.973	0.760		
10H-5	0.70-0.75	89.90	19.28	506	304	1.292	0.665	1.372	0.555
10H-5	0.70-0.75	89.90	19.28	405	253	1.476	0.361		
10H-5	0.70-0.75	89.90	19.28	405	253	1.349	0.639		
11H-1	0.70-0.75	93.60	20.51	531	278	1.345	0.407	1.240	0.424
11H-1	0.70-0.75	93.60	20.51	455	329	1.273	0.569		
11H-1	0.70-0.75	93.60	20.51	582	304	1.103	0.296		
11H-5	0.70-0.75	99.60	21.86	531	354	1.136	0.700	1.222	0.647
11H-5	0.70-0.75	99.60	21.86	557	354	1.186	0.585		
11H-5	0.70-0.75	99.60	21.86	632	430	1.345	0.655		
12H-1	0.70-0.75	103.30	22.68	455	304	1.444	1.021	1.295	0.939
12H-1	0.70-0.75	103.30	22.68	455	304	1.271	0.822		
12H-1	0.70-0.75	103.30	22.68	493	329	1.171	0.974		
12H-3	0.70-0.75	106.30	23.35	405	253	1.046	0.513	1.343	0.648
12H-3	0.70-0.75	106.30	23.35	405	228	1.468	0.448		
12H-3	0.70-0.75	106.30	23.35	430	253	1.516	0.982		
12H-5	0.70-0.75	109.30	24.58	531	304	1.287	0.853	1.257	0.684
12H-5	0.70-0.75	109.30	24.58	481	278	1.287	0.773		
12H-5	0.70-0.75	109.30	24.58	405	253	1.196	0.426		
13X-1	0.70-0.75	113.00	26.81	430	278	1.261	-0.217	1.209	0.042
13X-1	0.70-0.75	113.00	26.81	405	202	1.330	0.332		
13X-1	0.70-0.75	113.00	26.81	392	228	1.037	0.011		
13X-3	0.70-0.75	116.00	28.62	405	253	1.006	-0.164	1.241	0.292
13X-3	0.70-0.75	116.00	28.62	405	202	1.429	0.361		
13X-3	0.70-0.75	116.00	28.62	430	228	1.288	0.680		
Leg 121 Site 756 Hole B									
Oridorsalis umbonatus									
1H-1	0.70-0.75	0.70	1.10	531	304	2.887	-0.435	2.870	-0.378
1H-1	0.70-0.75	0.70	1.10	506	278	2.635	-0.299		
1H-1	0.70-0.75	0.70	1.10	481	278	3.100	-0.516		
1H-1	0.70-0.75	0.70	1.10	582	329	2.857	-0.263		
1H-3	0.70-0.75	3.70	2.93	506	304	3.031	-0.800	3.169	-0.553
1H-3	0.70-0.75	3.70	2.93	455	278	3.175	-0.567		
1H-3	0.70-0.75	3.70	2.93	430	253	3.302	-0.293		
1H-5	0.70-0.75	6.70	3.68	607	304	2.587	-0.337	2.653	-0.383
1H-5	0.70-0.75	6.70	3.68	531	304	2.847	-0.382		
1H-5	0.70-0.75	6.70	3.68	481	253	2.526	-0.430		
2H-5	0.70-0.75	15.20	5.06	481	278	2.670	-0.407	2.494	-0.593
2H-5	0.70-0.75	15.20	5.06	481	278	2.424	-0.943		
2H-5	0.70-0.75	15.20	5.06	481	278	2.389	-0.428		
3H-1	0.70-0.75	18.80	5.71	531	304	2.985	-0.508	2.663	-0.790
3H-1	0.70-0.75	18.80	5.71	506	304	2.707	-0.988		
3H-1	0.70-0.75	18.80	5.71	455	253	2.297	-0.873		
3H-3	0.70-0.75	21.80	6.25	658	354	2.506	-0.629	2.634	-0.391
3H-3	0.70-0.75	21.80	6.25	607	304	2.635	-0.157		
3H-3	0.70-0.75	21.80	6.25	430	278	2.715	-0.621		
3H-3	0.70-0.75	21.80	6.25	582	329	2.680	-0.158		
3H-5	0.70-0.75	24.80	6.79	557	329	2.275	-0.308	2.411	-0.223
3H-5	0.70-0.75	24.80	6.79	506	304	2.455	-0.346		
3H-5	0.70-0.75	24.80	6.79	455	278	2.503	-0.016		
4H-1	0.70-0.75	28.40	7.44	455	253	2.447	0.175	2.394	0.219

Appendix A-6. (continued).

Core & Section	Interval	Depth (mbsf)	Age (Ma)	Specimen size D (μm)	Specimen size T (μm)	$\delta^{18}O$	$\delta^{13}C$	$\delta^{18}O$ ave.	$\delta^{13}C$ ave.
Leg 121 Site 756 Hole B									
Oridorsalis umbonatus (Cont.)									
4H-1	0.70-0.75	28.40	7.44	455	253	2.321	0.274		
4H-1	0.70-0.75	28.40	7.44	430	304	2.413	0.207		
4H-3	0.70-0.75	31.40	7.99	430	253	2.645	0.302	2.573	0.305
4H-3	0.70-0.75	31.40	7.99	506	278	2.563	0.255		
4H-3	0.70-0.75	31.40	7.99	557	278	2.511	0.359		
4H-5	0.70-0.75	34.40	8.53	455	228	2.367	0.218	2.449	0.265
4H-5	0.70-0.75	34.40	8.53	455	228	2.551	0.301		
4H-5	0.70-0.75	34.40	8.53	506	304	2.428	0.277		
5H-1	0.70-0.75	38.00	10.47	455	228	2.390	0.281	2.397	0.284
5H-1	0.70-0.75	38.00	10.47	481	278	2.362	0.270		
5H-1	0.70-0.75	38.00	10.47	506	329	2.440	0.300		
5H-3	0.70-0.75	41.00	11.63	481	304	2.463	0.976	2.590	0.967
5H-3	0.70-0.75	41.00	11.63	531	304	2.561	0.991		
5H-3	0.70-0.75	41.00	11.63	506	304	2.745	0.934		
5H-5	0.70-0.75	44.00	12.78	481	278	1.893	0.224	1.950	0.271
5H-5	0.70-0.75	44.00	12.78	506	278	2.117	0.253		
5H-5	0.70-0.75	44.00	12.78	430	253	1.839	0.337		
6H-1	0.70-0.75	47.60	14.35	481	253	1.291	0.650	1.645	0.603
6H-1	0.70-0.75	47.60	14.35	405	228	1.965	0.773		
6H-1	0.70-0.75	47.60	14.35	430	228	1.679	0.387		
6H-3	0.70-0.75	50.60	15.90	632	253	1.693	1.541	1.574	1.439
6H-3	0.70-0.75	50.60	15.90	557	354	1.517	1.439		
6H-3	0.70-0.75	50.60	15.90	481	304	1.513	1.336		
6H-5	0.70-0.75	53.60	17.45	506	354	1.545	0.997	1.214	0.646
6H-5	0.70-0.75	53.60	17.45	430	253	1.168	0.570		
6H-5	0.70-0.75	53.60	17.45	405	253	0.930	0.372		
7H-1	0.70-0.75	56.90	18.81	582	405	1.717	0.827	1.643	0.617
7H-1	0.70-0.75	56.90	18.81	481	329	1.636	0.526		
7H-1	0.70-0.75	56.90	18.81	430	253	1.577	0.497		
7H-3	0.70-0.75	59.90	19.66	481	354	1.258	0.419	1.335	0.614
7H-3	0.70-0.75	59.90	19.66	481	380	1.498	0.776		
7H-3	0.70-0.75	59.90	19.66	506	329	1.248	0.647		
7H-5	0.70-0.75	62.90	20.51	481	354	1.712	0.691	1.425	0.449
7H-5	0.70-0.75	62.90	20.51	455	304	1.395	0.556		
7H-5	0.70-0.75	62.90	20.51	430	228	1.167	0.099		
8H-1	0.70-0.75	66.30	21.47	531	354	1.455	1.061	1.512	0.881
8H-1	0.70-0.75	66.30	21.47	455	304	1.350	0.715		
8H-1	0.70-0.75	66.30	21.47	455	278	1.732	0.868		
8H-3	0.70-0.75	69.30	22.31	506	354	1.348	0.613	1.421	0.649
8H-3	0.70-0.75	69.30	22.31	481	329	1.505	0.722		
8H-3	0.70-0.75	69.30	22.31	506	329	1.410	0.611		
8H-5	0.70-0.75	72.30	23.16	531	380	1.386	0.464	1.270	0.113
8H-5	0.70-0.75	72.30	23.16	481	304	1.359	-0.300		
8H-5	0.70-0.75	72.30	23.16	455	278	1.065	0.176		
9H-1	0.70-0.75	75.90	24.23	455	278	1.324	0.234	1.290	0.183
9H-1	0.70-0.75	75.90	24.23	405	228	1.222	0.273		
9H-1	0.70-0.75	75.90	24.23	405	278	1.325	0.041		
9H-3	0.70-0.75	78.90	25.16	557	354	1.775	0.035	1.715	0.199
9H-3	0.70-0.75	78.90	25.16	481	329	1.583	0.280		
9H-3	0.70-0.75	78.90	25.16	455	304	1.787	0.281		
9H-5	0.70-0.75	81.90	26.09	531	354	1.736	0.050	1.599	-0.148
9H-5	0.70-0.75	81.90	26.09	430	278	1.391	-0.120		
9H-5	0.70-0.75	81.90	26.09	430	278	1.670	-0.374		
10H-1	0.70-0.75	85.60	27.24	557	329	1.781	-0.255	1.703	-0.081
10H-1	0.70-0.75	85.60	27.24	506	329	1.632	0.009		
10H-1	0.70-0.75	85.60	27.24	405	228	1.696	0.002		
10H-3	0.70-0.75	88.60	28.17	506	304	1.480	0.233	1.487	0.194
10H-3	0.70-0.75	88.60	28.17	455	278	1.626	0.066		
10H-3	0.70-0.75	88.60	28.17	481	278	1.355	0.283		
10H-5	0.70-0.75	91.60	29.10	531	405	1.569	0.092	1.419	-0.089
10H-5	0.70-0.75	91.60	29.10	455	304	1.508	-0.079		
10H-5	0.70-0.75	91.60	29.10	455	278	1.179	-0.280		
11H-1	0.70-0.75	95.30	30.23	455	278	1.325	0.185	1.182	0.300
11H-1	0.70-0.75	95.30	30.23	481	253	1.292	0.465		
11H-1	0.70-0.75	95.30	30.23	455	304	0.930	0.250		
11H-3	0.70-0.75	98.30	30.74	506	304	1.314	0.407	1.385	0.383

Core & Section	Interval	Depth (mbsf)	Age (Ma)	Specimen size D (μm)	Specimen size T (μm)	$\delta^{18}O$	$\delta^{13}C$	$\delta^{18}O$ ave.	$\delta^{13}C$ ave.
Leg 121 Site 756 Hole B									
Oridorsalis umbonatus (Cont.)									
11H-3	0.70-0.75	98.30	30.74	430	253	1.306	0.440		
11H-3	0.70-0.75	98.30	30.74	405	253	1.536	0.301		
11H-5	0.70-0.75	101.30	31.26	405	253	1.031	0.097	1.100	0.289
11H-5	0.70-0.75	101.30	31.26	405	253	1.030	0.472		
11H-5	0.70-0.75	101.30	31.26	405	228	1.239	0.298		
Leg 121 Site 756 Hole C									
Oridorsalis umbonatus									
4X-1	0.70-0.75	101.60	31.31	531	329	1.336	0.032	1.622	-0.057
4X-1	0.70-0.75	101.60	31.31	506	304	1.770	-0.066		
4X-1	0.70-0.75	101.60	31.31	531	380	1.760	-0.138		
4X-3	0.70-0.75	104.60	31.82	455	278	1.606	-0.112	1.588	-0.031
4X-3	0.70-0.75	104.60	31.82	455	253	1.375	-0.188		
4X-3	0.70-0.75	104.60	31.82	455	329	1.783	0.207		
4X-5	0.70-0.75	107.60	32.34	455	278	1.492	-0.166	1.540	-0.173
4X-5	0.70-0.75	107.60	32.34	455	278	1.576	-0.176		
4X-5	0.70-0.75	107.60	32.34	455	253	1.552	-0.178		
5X-2	0.65-0.70	111.47	33.00	455	329	1.426	0.169	1.348	0.165
5X-2	0.65-0.70	111.47	33.00	430	304	1.209	0.099		
5X-2	0.65-0.70	111.47	33.00	405	253	1.408	0.227		
5X-5	0.70-0.75	114.16	33.46	506	278	1.106	0.383	1.220	0.193
5X-5	0.70-0.75	114.16	33.46	455	304	1.380	0.160		
5X-5	0.70-0.75	114.16	33.46	430	278	1.173	0.036		
5X-7	0.70-0.75	116.31	33.83	481	278	1.180	0.083	1.212	0.183
5X-7	0.70-0.75	116.31	33.83	405	253	1.114	0.083		
5X-7	0.70-0.75	116.31	33.83	632	405	1.343	0.383		
6X-1	0.70-0.75	120.90	34.56	506	329	1.384	1.003	1.312	0.636
6X-1	0.70-0.75	120.90	34.56	506	304	1.244	0.626		
6X-1	0.70-0.75	120.90	34.56	455	253	1.308	0.278		
6X-3	0.70-0.75	123.90	34.99	455	329	0.893	0.524	0.918	0.443
6X-3	0.70-0.75	123.90	34.99	430	253	1.004	0.628		
6X-3	0.70-0.75	123.90	34.99	430	278	0.856	0.176		
7X-1	0.70-0.75	130.50	35.95	506	278	0.595	0.525	0.595	0.525
7X-3	0.70-0.75	133.50	36.39	430	253	0.852	0.614	0.785	0.461
7X-3	0.70-0.75	133.50	36.39	405	253	0.696	0.315		
7X-3	0.70-0.75	133.50	36.39	405	202	0.807	0.455		
7X-5	0.70-0.75	136.50	36.82	430	228	0.265	0.329	0.361	0.412
7X-5	0.70-0.75	136.50	36.82	430	304	0.231	0.128		
7X-5	0.70-0.75	136.50	36.82	430	253	0.586	0.778		
Leg 121 Site 757 Hole B									
Anomalinoides danicus									
15H-5	0.70-0.75	136.50	40.98	405	278	0.449	0.885	0.449	0.885
16H-5	0.70-0.75	146.20	43.38	632	380	0.208	1.229	0.278	1.237
16H-5	0.70-0.75	146.20	43.38	683	430	0.262	1.184		
16H-5	0.70-0.75	146.20	43.38	759	455	0.363	1.297		
17H-5	0.70-0.75	155.80	45.88	734	430	0.272	0.995	0.310	1.117
17H-5	0.70-0.75	155.80	45.88	658	380	0.303	1.158		
17H-5	0.70-0.75	155.80	45.88	708	405	0.355	1.199		
18H-1	0.70-0.75	159.50	47.09	708	380	0.425	1.157	0.420	1.176
18H-1	0.70-0.75	159.50	47.09	430	278	0.415	1.194		
18H-5	0.70-0.75	165.50	48.67	557	405	0.148	0.988	0.178	1.034
18H-5	0.70-0.75	165.50	48.67	582	329	0.289	1.105		
18H-5	0.70-0.75	165.50	48.67	455	253	0.096	1.010		
19H-1	0.70-0.75	169.20	49.24	582	380	0.057	0.878	0.089	0.934
19H-1	0.70-0.75	169.20	49.24	430	253	0.208	1.023		
19H-1	0.70-0.75	169.20	49.24	430	329	0.001	0.901		
20X-1	0.70-0.75	175.40	49.90	607	354	-0.212	1.172	-0.225	1.122
20X-1	0.70-0.75	175.40	49.90	557	405	-0.386	0.936		
20X-1	0.70-0.75	175.40	49.90	455	278	-0.077	1.257		
20X-5	0.70-0.75	181.40	51.37	506	304	-0.240	1.259	-0.256	1.273
20X-5	0.70-0.75	181.40	51.37	481	278	-0.182	1.358		
20X-5	0.70-0.75	181.40	51.37	430	304	-0.345	1.201		
21X-1	0.70-0.75	183.40	51.85	557	304	-0.407	1.317	-0.433	1.340
21X-1	0.70-0.75	183.40	51.85	443	228	-0.470	1.360		
21X-1	0.70-0.75	183.40	51.85	405	202	-0.421	1.344		
22X-1	0.70-0.75	193.10	53.05	557	278	-0.771	1.081	-0.736	1.099
22X-1	0.70-0.75	193.10	53.05	531	278	-0.613	1.132		

Appendix A-7. (continued).

Core & Section	Interval	Depth (mbsf)	Age (Ma)	Specimen size D (μm)	Specimen size T (μm)	$\delta^{18}O$	$\delta^{13}C$	$\delta^{18}O$ ave.	$\delta^{13}C$ ave.
Leg 121 Site 757 Hole B									
Anomalinoides danicus				(Cont.)					
22X-1	0.70-0.75	193.10	53.05	455	253	-0.824	1.084		
22X-3	0.70-0.75	196.10	53.25	531	304	-0.705	1.227	-0.786	1.132
22X-3	0.70-0.75	196.10	53.25	531	304	-0.802	1.147		
22X-3	0.70-0.75	196.10	53.25	455	253	-0.851	1.023		
23X-1	0.70-0.75	202.70	53.70	683	430	-0.933	0.806	-1.079	0.692
23X-1	0.70-0.75	202.70	53.70	582	380	-1.050	0.677		
23X-1	0.70-0.75	202.70	53.70	455	228	-1.253	0.592		
23X-3	0.70-0.75	205.70	54.19	632	367	-0.965	0.500	-0.977	0.497
23X-3	0.70-0.75	205.70	54.19	632	354	-0.874	0.552		
23X-3	0.70-0.75	205.70	54.19	582	329	-1.091	0.438		
24X-1	0.58-0.61	212.28	55.27	911	506	-1.112	0.222	-1.081	0.302
24X-1	0.58-0.61	212.28	55.27	582	329	-1.106	0.300		
24X-1	0.58-0.61	212.28	55.27	531	278	-1.024	0.384		
24X-4	0.58-0.61	216.78	56.01	683	304	-1.403	0.351	-1.319	0.425
24X-4	0.58-0.61	216.78	56.01	658	380	-1.287	0.375		
24X-4	0.58-0.61	216.78	56.01	582	405	-1.268	0.550		
Oridorsalis umbonatus									
1H-2	0.70-0.75	2.03	0.31	557	304	2.904	-0.752	3.158	-0.691
1H-2	0.70-0.75	2.03	0.31	481	278	3.333	-0.762		
1H-2	0.70-0.75	2.03	0.31	506	354	3.238	-0.558		
2H-1	0.70-0.75	5.20	0.78	506	329	3.502	-1.131	3.330	-1.310
2H-1	0.70-0.75	5.20	0.78	455	278	3.389	-1.386		
2H-1	0.70-0.75	5.20	0.78	455	329	3.100	-1.412		
2H-3	0.70-0.75	8.20	1.22	632	455	3.539	-0.550	3.117	-0.559
2H-3	0.70-0.75	8.20	1.22	455	278	2.711	-0.601		
2H-3	0.70-0.75	8.20	1.22	430	278	3.102	-0.525		
2H-5	0.70-0.75	11.20	1.67	607	405	3.089	-0.631	3.281	-0.819
2H-5	0.70-0.75	11.20	1.67	506	354	3.241	-0.764		
2H-5	0.70-0.75	11.20	1.67	506	278	3.514	-1.063		
3H-1	0.70-0.75	14.70	2.32	632	405	2.761	-0.472	2.830	-0.640
3H-1	0.70-0.75	14.70	2.32	557	304	2.674	-0.835		
3H-1	0.70-0.75	14.70	2.32	455	304	3.054	-0.612		
3H-3	0.70-0.75	17.70	2.84	582	354	2.937	-0.334	2.909	-0.572
3H-3	0.70-0.75	17.70	2.84	607	354	3.155	-0.785		
3H-3	0.70-0.75	17.70	2.84	557	329	2.636	-0.598		
3H-5	0.70-0.75	20.70	3.22	557	304	3.072	-0.797	2.923	-1.005
3H-5	0.70-0.75	20.70	3.22	531	304	2.864	-1.145		
3H-5	0.70-0.75	20.70	3.22	481	304	2.832	-1.073		
4H-1	0.70-0.75	24.30	3.62	582	354	2.555	-0.704	2.605	-0.602
4H-1	0.70-0.75	24.30	3.62	506	304	2.641	-0.505		
4H-1	0.70-0.75	24.30	3.62	506	329	2.620	-0.598		
4H-3	0.70-0.75	27.30	3.80	531	304	2.661	-0.556	2.630	-0.504
4H-3	0.70-0.75	27.30	3.80	531	304	2.420	-0.502		
4H-3	0.70-0.75	27.30	3.80	506	329	2.810	-0.454		
5H-1	0.70-0.75	33.90	4.39	557	278	2.752	-0.675	2.696	-0.676
5H-1	0.70-0.75	33.90	4.39	531	329	2.647	-0.732		
5H-1	0.70-0.75	33.90	4.39	506	304	2.690	-0.621		
5H-3	0.70-0.75	36.90	4.66	632	329	2.313	-0.785	2.358	-0.737
5H-3	0.70-0.75	36.90	4.66	481	278	2.501	-0.565		
5H-3	0.70-0.75	36.90	4.66	455	329	2.261	-0.862		
6H-1	0.70-0.75	43.50	5.26	607	354	2.461	-0.509	2.515	-0.658
6H-1	0.70-0.75	43.50	5.26	481	278	2.615	-0.572		
6H-1	0.70-0.75	43.50	5.26	455	278	2.470	-0.893		
6H-3	0.70-0.75	46.50	5.70	557	304	2.327	-0.683	2.295	-0.892
6H-3	0.70-0.75	46.50	5.70	455	228	2.076	-1.026		
6H-3	0.70-0.75	46.50	5.70	430	278	2.483	-0.968		
6H-5	0.70-0.75	49.50	6.14	632	380	2.813	-0.387	2.793	-0.409
6H-5	0.70-0.75	49.50	6.14	506	304	2.657	-0.493		
6H-5	0.70-0.75	49.50	6.14	430	278	2.910	-0.346		
7H-1	0.70-0.75	53.20	6.69	506	253	2.727	-0.635	2.463	-0.584
7H-1	0.70-0.75	53.20	6.69	405	202	2.221	-0.582		
7H-1	0.70-0.75	53.20	6.69	405	228	2.440	-0.535		
7H-3	0.70-0.75	56.20	6.93	607	354	2.305	-0.134	2.221	-0.120
7H-3	0.70-0.75	56.20	6.93	557	278	2.086	-0.057		
7H-3	0.70-0.75	56.20	6.93	531	278	2.272	-0.170		
8H-1	0.70-0.75	62.90	7.46	481	253	2.555	0.174	2.602	0.233
Leg 121 Site 757 Hole B									
Oridorsalis umbonatus				(Cont.)					
8H-1	0.70-0.75	62.90	7.46	506	278	2.684	0.292		
8H-1	0.70-0.75	62.90	7.46	557	278	2.568	0.234		
8H-3	0.70-0.75	65.90	7.88	481	329	2.340	-0.174	2.368	-0.094
8H-3	0.70-0.75	65.90	7.88	455	278	2.223	-0.236		
8H-3	0.70-0.75	65.90	7.88	481	278	2.540	0.129		
8H-5	0.70-0.75	68.90	8.30	481	253	2.916	0.272	2.825	0.355
8H-5	0.70-0.75	68.90	8.30	506	329	2.823	0.444		
8H-5	0.70-0.75	68.90	8.30	557	304	2.737	0.350		
9H-1	0.70-0.75	72.50	9.13	481	228	2.534	0.092	2.565	0.176
9H-1	0.70-0.75	72.50	9.13	531	278	2.549	0.095		
9H-1	0.70-0.75	72.50	9.13	531	304	2.611	0.340		
9H-3	0.70-0.75	75.50	10.50	481	304	2.433	0.173	2.474	0.162
9H-3	0.70-0.75	75.50	10.50	481	253	2.332	0.167		
9H-3	0.70-0.75	75.50	10.50	557	278	2.658	0.145		
9H-5	0.70-0.75	78.50	11.87	557	354	2.361	0.318	2.188	0.226
9H-5	0.70-0.75	78.50	11.87	481	329	2.296	0.177		
9H-5	0.70-0.75	78.50	11.87	455	278	1.908	0.183		
10H-1	0.70-0.75	82.20	13.30	632	329	2.185	0.302	2.106	0.328
10H-1	0.70-0.75	82.20	13.30	455	253	2.148	0.253		
10H-1	0.70-0.75	82.20	13.30	455	228	1.984	0.430		
10H-3	0.70-0.75	85.20	14.04	632	329	1.562	0.608	1.397	0.468
10H-3	0.70-0.75	85.20	14.04	455	278	1.511	0.476		
10H-3	0.70-0.75	85.20	14.04	455	253	1.117	0.321		
10H-5	0.70-0.75	88.20	14.94	683	405	1.148	0.565	1.217	0.561
10H-5	0.70-0.75	88.20	14.94	607	380	1.330	0.477		
10H-5	0.70-0.75	88.20	14.94	455	253	1.172	0.642		
11H-1	0.70-0.75	91.90	16.36	708	329	1.680	0.294	1.576	0.205
11H-1	0.70-0.75	91.90	16.36	531	304	1.811	0.382		
11H-1	0.70-0.75	91.90	16.36	506	304	1.238	-0.060		
11H-3	0.70-0.75	94.90	17.71	658	405	1.756	0.591	1.625	0.310
11H-3	0.70-0.75	94.90	17.71	531	329	1.478	0.091		
11H-3	0.70-0.75	94.90	17.71	506	329	1.641	0.248		
11H-5	0.70-0.75	97.90	19.17	607	380	1.185	-0.208	1.443	0.293
11H-5	0.70-0.75	97.90	19.17	531	329	1.622	0.643		
11H-5	0.70-0.75	97.90	19.17	481	253	1.522	0.444		
12H-1	0.70-0.75	101.50	23.70	531	278	1.656	0.376	1.649	0.219
12H-1	0.70-0.75	101.50	23.70	455	278	1.814	0.258		
12H-1	0.70-0.75	101.50	23.70	405	228	1.477	0.023		
12H-3	0.70-0.75	104.50	27.96	582	329	1.707	0.534	1.666	0.256
12H-3	0.70-0.75	104.50	27.96	481	278	1.706	0.259		
12H-3	0.70-0.75	104.50	27.96	455	253	1.586	-0.024		
12H-5	0.70-0.75	107.50	30.48	607	380	1.950	0.318	1.826	0.274
12H-5	0.70-0.75	107.50	30.48	582	354	1.737	0.117		
12H-5	0.70-0.75	107.50	30.48	506	329	1.791	0.387		
13H-1	0.70-0.75	111.20	31.19	455	278	1.682	0.386	1.619	0.206
13H-1	0.70-0.75	111.20	31.19	531	304	1.621	0.087		
13H-1	0.70-0.75	111.20	31.19	405	278	1.554	0.146		
13H-3	0.70-0.75	114.20	33.17	455	253	1.549	0.420	1.605	0.503
13H-3	0.70-0.75	114.20	33.17	430	278	1.695	0.626		
13H-3	0.70-0.75	114.20	33.17	481	253	1.570	0.464		
13H-5	0.70-0.75	117.20	34.45	531	354	1.772	0.537	1.710	0.599
13H-5	0.70-0.75	117.20	34.45	455	304	1.583	0.745		
13H-5	0.70-0.75	117.20	34.45	506	304	1.775	0.514		
14H-1	0.70-0.75	120.80	35.34	455	253	0.932	0.180	1.104	0.439
14H-1	0.70-0.75	120.80	35.34	506	304	1.192	0.630		
14H-1	0.70-0.75	120.80	35.34	506	304	1.187	0.508		
14H-5	0.70-0.75	126.80	37.28	683	531	0.920	1.192	1.053	0.991
14H-5	0.70-0.75	126.80	37.28	481	304	1.085	0.806		
14H-5	0.70-0.75	126.80	37.28	481	329	1.155	0.974		
15H-1	0.70-0.75	130.50	38.55	455	253	1.077	0.896	0.987	0.749
15H-1	0.70-0.75	130.50	38.55	455	253	1.186	0.905		
15H-1	0.70-0.75	130.50	38.55	430	253	0.699	0.446		
15H-5	0.70-0.75	136.50	40.98	481	329	0.961	0.522	0.925	0.537
15H-5	0.70-0.75	136.50	40.98	468	278	0.867	0.522		
15H-5	0.70-0.75	136.50	40.98	380	228	0.947	0.567		
16H-1	0.70-0.75	140.20	41.89	430	253	1.059	0.599	0.868	0.436

Appendix A-8. (continued).

Core & Section	Interval	Depth (mbsf)	Age (Ma)	Specimen size D (μm)	Specimen size T (μm)	$\delta^{18}O$	$\delta^{13}C$	$\delta^{18}O$ ave.	$\delta^{13}C$ ave.
Leg 121 Site 757 Hole B									
Oridorsalis umbonatus (Cont.)									
16H-1	0.70-0.75	140.20	41.89	430	278	0.825	0.322		
16H-1	0.70-0.75	140.20	41.89	430	266	0.721	0.387		
16H-5	0.70-0.75	146.20	43.38	455	253	0.526	0.741	0.609	0.810
16H-5	0.70-0.75	146.20	43.38	481	304	0.585	0.643		
16H-5	0.70-0.75	146.20	43.38	582	354	0.716	1.047		
17H-1	0.70-0.75	149.80	44.27	607	380	0.684	0.635	0.684	0.635
18H-1	0.70-0.75	159.50	47.09	506	304	0.398	0.672	0.319	0.634
18H-1	0.70-0.75	159.50	47.09	405	253	0.240	0.559		
18H-1	0.70-0.75	159.50	47.09	405	240	0.318	0.670		
18H-5	0.70-0.75	165.50	48.67	506	329	0.288	0.662	0.233	0.569
18H-5	0.70-0.75	165.50	48.67	405	240	0.146	0.374		
18H-5	0.70-0.75	165.50	48.67	405	228	0.266	0.672		
20X-5	0.70-0.75	181.40	51.37	455	278	-0.097	0.792	-0.097	0.792
21X-1	0.70-0.75	183.40	51.85	380	228	-0.319	0.670	-0.319	0.670
22X-1	0.70-0.75	193.10	53.05	455	278	-0.560	0.729	-0.535	0.757
22X-1	0.70-0.75	193.10	53.05	417	253	-0.509	0.784		
22X-3	0.70-0.75	196.10	53.25	430	240	-0.587	0.770	-0.584	0.818
22X-3	0.70-0.75	196.10	53.25	405	228	-0.622	0.917		
22X-3	0.70-0.75	196.10	53.25	417	215	-0.542	0.768		
Leg 121 Site 758 Hole A									
Anomalinoides danicus									
28X-2	0.75-0.80	259.15	58.18	481	278	0.203	2.132	0.203	2.132
28X-6	0.75-0.80	265.15	59.27	455	278	0.310	2.483	0.085	2.220
28X-6	0.75-0.80	265.15	59.27	443	253	-0.046	2.054		
28X-6	0.75-0.80	265.15	59.27	430	253	-0.009	2.122		
30X-1	0.75-0.80	277.05	60.86	405	240	0.508	1.908	0.508	1.908
Cibicidoides wuellerstorfi									
12X-1	0.75-0.80	103.15	7.46	557	202	2.581	0.884	2.547	0.964
12X-1	0.75-0.80	103.15	7.46	493	177	2.531	1.005		
12X-1	0.75-0.80	103.15	7.46	569	253	2.530	1.003		
12X-4	0.75-0.80	107.65	7.84	557	215	2.659	0.988	2.581	1.060
12X-4	0.75-0.80	107.65	7.84	506	202	2.625	1.106		
12X-4	0.75-0.80	107.65	7.84	835	253	2.460	1.086		
14X-3	0.75-0.80	125.45	11.66	531	190	2.220	0.738	2.155	0.837
14X-3	0.75-0.80	125.45	11.66	506	177	2.106	0.785		
14X-3	0.75-0.80	125.45	11.66	696	278	2.140	0.987		
Cibicidoides mundulus									
10H-1	0.75-0.80	83.85	5.83	443	278	2.528	-0.061	2.528	-0.061
12X-1	0.75-0.80	103.15	7.46	443	228	2.702	0.883	2.702	0.883
18X-1	0.75-0.80	161.15	20.37	506	253	1.869	0.849	1.869	0.849
23X-1	0.70-0.75	209.40	27.47	380	190	1.940	0.608	1.896	0.759
23X-1	0.70-0.75	209.40	27.47	392	177	1.852	0.909		
23X-3	0.75-0.80	212.45	28.33	443	228	1.640	0.830	1.640	0.830
24X-1	0.58-0.63	218.88	30.15	417	228	2.235	0.717	2.215	0.747
24X-1	0.58-0.63	218.88	30.15	455	228	2.165	0.853		
24X-1	0.58-0.63	218.88	30.15	506	253	2.244	0.671		
27X-1	0.75-0.80	248.05	41.42	430	202	1.777	1.118	1.865	1.149
27X-1	0.75-0.80	248.05	41.42	468	253	2.044	1.176		
27X-1	0.75-0.80	248.05	41.42	392	215	1.775	1.152		
Gyroidina soldanii									
9H-4	0.75-0.80	78.65	5.45	367	278	2.834	-0.800	2.834	-0.800
10H-1	0.75-0.80	83.85	5.83	481	291	3.307	-0.944	3.307	-0.944
10H-4	0.75-0.80	88.35	6.22	367	278	2.677	-0.704	2.778	-0.691
10H-4	0.75-0.80	88.35	6.22	392	253	2.878	-0.677		
12X-1	0.75-0.80	103.15	7.46	392	304	2.785	-0.375	2.785	-0.375
14X-1	0.75-0.80	122.45	10.56	430	291	2.758	0.428	2.758	0.428
15X-1	0.75-0.80	132.15	14.14	658	493	2.109	0.455	2.109	0.455
17X-3	0.75-0.80	154.45	19.73	443	316	2.033	0.267	2.033	0.267
18X-1	0.75-0.80	161.15	20.37	531	380	1.831	-0.033	1.831	-0.033
18X-3	0.75-0.80	164.15	20.65	430	304	2.161	0.047	2.387	0.321
18X-3	0.75-0.80	164.15	20.65	468	342	2.613	0.594		
23X-1	0.70-0.75	209.40	27.47	380	291	2.172	0.212	2.088	0.227
23X-1	0.70-0.75	209.40	27.47	392	304	2.003	0.241		
23X-3	0.75-0.80	212.45	28.33	380	304	1.995	0.425	1.820	0.295
23X-3	0.75-0.80	212.45	28.33	367	266	1.644	0.165		
25X-1	0.76-0.81	228.76	30.70	455	329	1.908	-0.123	1.908	-0.123

Core & Section	Interval	Depth (mbsf)	Age (Ma)	Specimen size D (μm)	Specimen size T (μm)	$\delta^{18}O$	$\delta^{13}C$	$\delta^{18}O$ ave.	$\delta^{13}C$ ave.
Leg 121 Site 758 Hole A									
Gyroidina soldanii (Cont.)									
26X-1	0.75-0.80	238.45	31.20	380	304	2.144	0.117	2.144	0.117
26X-3	0.75-0.80	241.45	34.39	455	354	1.836	0.331	1.944	0.360
26X-3	0.75-0.80	241.45	34.39	367	304	1.920	0.424		
26X-3	0.75-0.80	241.45	34.39	380	278	2.075	0.324		
27X-1	0.75-0.80	248.05	41.42	468	367	2.027	0.445	2.060	0.629
27X-1	0.75-0.80	248.05	41.42	455	329	2.061	0.662		
27X-1	0.75-0.80	248.05	41.42	392	291	2.092	0.779		
Nuttallides truempyi									
28X-2	0.75-0.80	259.15	58.18	405	228	-0.165	1.611	-0.091	1.634
28X-2	0.75-0.80	259.15	58.18	405	228	-0.087	1.623		
28X-2	0.75-0.80	259.15	58.18	405	228	-0.022	1.669		
28X-6	0.75-0.80	265.15	59.27	443	253	-0.027	1.819	-0.027	1.819
29X-1	0.75-0.80	267.35	59.67	380	253	0.267	1.766	0.267	1.766
29X-3	0.75-0.80	270.35	60.22	531	316	0.259	1.481	0.274	1.665
29X-3	0.75-0.80	270.35	60.22	405	253	0.398	1.774		
29X-3	0.75-0.80	270.35	60.22	405	253	0.164	1.741		
30X-1	0.75-0.80	277.05	60.86	531	316	0.481	1.456	0.421	1.448
30X-1	0.75-0.80	277.05	60.86	443	253	0.477	1.470		
30X-1	0.75-0.80	277.05	60.86	582	329	0.304	1.418		
30X-3	0.75-0.80	280.05	61.11	506	304	0.228	1.159	0.117	1.102
30X-3	0.75-0.80	280.05	61.11	455	291	0.077	1.084		
30X-3	0.75-0.80	280.05	61.11	430	253	0.047	1.063		
31X-1	0.75-0.80	286.65	61.65	430	253	-0.048	0.770	-0.048	0.770
31X-5	0.75-0.80	292.65	63.62	430	278	0.152	0.918	0.116	0.909
31X-5	0.75-0.80	292.65	63.62	531	304	0.058	0.824		
31X-5	0.75-0.80	292.65	63.62	405	240	0.137	0.984		
Nuttallides truempyi (6 specimens)									
28X-2	0.75-0.80	259.15	58.18	278-329	177-202	-0.217	1.632		
28X-6	0.75-0.80	265.15	59.27	329	177-190	-0.624	1.726		
29X-1	0.75-0.80	267.35	59.67	329	177-202	0.208	2.105		
29X-3	0.75-0.80	270.35	60.22	291-342	164-228	0.044	1.702		
30X-1	0.75-0.80	277.05	60.86	278-354	164-215	0.117	1.669		
30X-3	0.75-0.80	280.05	61.11	278-329	177-202	0.058	1.222		
31X-1	0.75-0.80	286.65	61.65	291-342	152-190	-0.186	0.888		
31X-5	0.75-0.80	292.65	63.62	304-367	177-202	-0.209	0.945		
Oridorsalis umbonatus									
1H-1	0.75-0.80	0.75	0.05	557	354	3.686	-0.876	3.794	-0.887
1H-1	0.75-0.80	0.75	0.05	531	304	3.852	-0.870		
1H-1	0.75-0.80	0.75	0.05	531	304	3.843	-0.916		
1H-3	0.75-0.80	3.75	0.25	557	278	3.150	-1.349	3.438	-1.306
1H-3	0.75-0.80	3.75	0.25	506	278	3.396	-1.196		
1H-3	0.75-0.80	3.75	0.25	531	304	3.768	-1.372		
2H-1	0.75-0.80	6.75	0.45	759	430	3.653	-0.828	3.560	-0.981
2H-1	0.75-0.80	6.75	0.45	632	278	3.599	-0.959		
2H-1	0.75-0.80	6.75	0.45	531	354	3.428	-1.156		
2H-4	0.75-0.80	11.25	0.75	582	329	3.867	-1.337	3.979	-1.270
2H-4	0.75-0.80	11.25	0.75	632	329	4.106	-1.287		
2H-4	0.75-0.80	11.25	0.75	683	405	3.964	-1.186		
3H-1	0.75-0.80	16.35	1.07	531	329	3.955	-1.327	3.857	-1.405
3H-1	0.75-0.80	16.35	1.07	531	329	3.886	-1.458		
3H-1	0.75-0.80	16.35	1.07	506	253	3.730	-1.430		
3H-3	0.75-0.80	19.35	1.32	481	278	3.575	-1.138	3.476	-1.007
3H-3	0.75-0.80	19.35	1.32	455	329	3.365	-1.248		
3H-3	0.75-0.80	19.35	1.32	683	430	3.488	-0.636		
3H-5	0.75-0.80	22.35	1.57	430	278	3.010	-0.969	3.105	-0.905
3H-5	0.75-0.80	22.35	1.57	582	354	3.310	-0.837		
3H-5	0.75-0.80	22.35	1.57	481	304	2.996	-0.910		
4H-1	0.75-0.80	25.95	1.88	506	304	3.743	-1.024	3.526	-1.152
4H-1	0.75-0.80	25.95	1.88	557	354	3.364	-1.307		
4H-1	0.75-0.80	25.95	1.88	455	278	3.472	-1.125		
4H-4	0.75-0.80	30.45	2.20	557	329	3.388	-1.327	3.322	-1.316
4H-4	0.75-0.80	30.45	2.20	506	329	3.278	-1.273		
4H-4	0.75-0.80	30.45	2.20	531	329	3.301	-1.348		
5H-1	0.75-0.80	35.55	2.58	506	304	2.738	-1.209	2.731	-1.337
5H-1	0.75-0.80	35.55	2.58	481	329	2.879	-1.061		
5H-1	0.75-0.80	35.55	2.58	430	278	2.542	-1.373		

Appendix A-9. (continued).

Core & Section	Interval	Depth (mbsf)	Age (Ma)	Specimen size D (μm)	Specimen size T (μm)	$\delta^{18}O$	$\delta^{13}C$	$\delta^{18}O$ ave.	$\delta^{13}C$ ave.
Leg 121 Site 758 Hole A									
Oridorsalis umbonatus (Cont.)									
5H-1	0.75-0.80	35.55	2.58	531	329	2.766	-1.704		
5H-4	0.75-0.80	40.05	2.96	443	278	2.698	-1.253	2.848	-0.964
5H-4	0.75-0.80	40.05	2.96	632	329	2.795	-0.905		
5H-4	0.75-0.80	40.05	2.96	632	430	3.052	-0.734		
6H-1	0.75-0.80	45.15	3.34	557	304	2.571	-0.899	2.600	-0.844
6H-1	0.75-0.80	45.15	3.34	708	405	2.678	-0.645		
6H-1	0.75-0.80	45.15	3.34	607	329	2.551	-0.988		
6H-4	0.75-0.80	49.65	3.65	405	278	2.530	-1.146	2.692	-1.102
6H-4	0.75-0.80	49.65	3.65	582	354	2.811	-1.013		
6H-4	0.75-0.80	49.65	3.65	455	304	2.735	-1.146		
7H-1	0.75-0.80	54.75	4.00	430	266	2.657	-1.114	2.683	-1.029
7H-1	0.75-0.80	54.75	4.00	430	278	2.652	-1.076		
7H-1	0.75-0.80	54.75	4.00	430	278	2.739	-0.898		
7H-4	0.75-0.80	59.25	4.27	481	278	2.724	-1.171	2.784	-1.095
7H-4	0.75-0.80	59.25	4.27	632	329	2.852	-1.260		
7H-4	0.75-0.80	59.25	4.27	506	329	2.777	-0.853		
8H-1	0.75-0.80	64.45	4.60	506	304	3.026	-1.055	2.885	-1.158
8H-1	0.75-0.80	64.45	4.60	455	278	2.707	-1.065		
8H-1	0.75-0.80	64.45	4.60	430	278	2.922	-1.354		
8H-4	0.75-0.80	68.95	4.90	658	405	2.720	-0.857	2.724	-0.828
8H-4	0.75-0.80	68.95	4.90	531	342	2.707	-0.753		
8H-4	0.75-0.80	68.95	4.90	455	278	2.744	-0.873		
9H-1	0.75-0.80	74.15	5.22	531	329	2.813	-1.234	2.674	-1.362
9H-1	0.75-0.80	74.15	5.22	443	291	2.594	-1.447		
9H-1	0.75-0.80	74.15	5.22	430	253	2.616	-1.404		
9H-4	0.75-0.80	78.65	5.45	481	278	3.046	-1.242	2.850	-1.154
9H-4	0.75-0.80	78.65	5.45	405	253	2.622	-1.308		
9H-4	0.75-0.80	78.65	5.45	531	329	2.882	-0.911		
10H-1	0.75-0.80	83.85	5.83	582	380	2.754	-1.001	2.779	-1.114
10H-1	0.75-0.80	83.85	5.83	607	380	2.840	-1.188		
10H-1	0.75-0.80	83.85	5.83	468	329	2.742	-1.153		
10H-4	0.75-0.80	88.35	6.22	506	329	2.474	-0.643	2.638	-0.594
10H-4	0.75-0.80	88.35	6.22	582	380	2.782	-0.529		
10H-4	0.75-0.80	88.35	6.22	658	380	2.657	-0.609		
11H-1	0.75-0.80	93.55	6.63	557	329	2.669	-0.367	2.616	-0.247
11H-1	0.75-0.80	93.55	6.63	582	354	2.678	-0.020		
11H-1	0.75-0.80	93.55	6.63	455	304	2.502	-0.353		
11H-4	0.75-0.80	98.05	7.02	455	304	2.703	-0.295	2.759	-0.422
11H-4	0.75-0.80	98.05	7.02	405	278	2.861	-0.128		
11H-4	0.75-0.80	98.05	7.02	430	253	2.712	-0.844		
12X-1	0.75-0.80	103.15	7.46	430	278	2.596	0.096	2.726	-0.040
12X-1	0.75-0.80	103.15	7.46	405	253	2.863	0.027		
12X-1	0.75-0.80	103.15	7.46	430	253	2.720	-0.243		
12X-4	0.75-0.80	107.65	7.84	557	329	2.750	-0.167	2.804	-0.118
12X-4	0.75-0.80	107.65	7.84	506	329	2.815	-0.004		
12X-4	0.75-0.80	107.65	7.84	506	278	2.847	-0.183		
13X-1	0.75-0.80	112.85	8.29	557	304	2.949	-0.059	2.911	0.023
13X-1	0.75-0.80	112.85	8.29	455	304	2.938	0.026		
13X-1	0.75-0.80	112.85	8.29	405	278	2.846	0.102		
13X-4	0.75-0.80	117.35	8.67	531	278	2.661	-0.191	2.730	-0.457
13X-4	0.75-0.80	117.35	8.67	506	278	2.831	-0.452		
13X-4	0.75-0.80	117.35	8.67	405	253	2.698	-0.727		
14X-1	0.75-0.80	122.45	10.56	481	278	2.695	0.307	2.676	0.151
14X-1	0.75-0.80	122.45	10.56	455	278	2.517	0.077		
14X-1	0.75-0.80	122.45	10.56	557	380	2.815	0.069		
14X-3	0.75-0.80	125.45	11.66	557	354	2.277	-0.371	2.498	-0.255
14X-3	0.75-0.80	125.45	11.66	405	253	2.675	-0.177		
14X-3	0.75-0.80	125.45	11.66	455	253	2.542	-0.218		
15X-1	0.75-0.80	132.15	14.14	531	304	1.564	0.473	1.660	0.442
15X-1	0.75-0.80	132.15	14.14	430	278	1.894	0.445		
15X-1	0.75-0.80	132.15	14.14	455	304	1.521	0.409		
15X-3	0.75-0.80	135.15	15.25	506	304	1.582	0.415	1.669	0.569
15X-3	0.75-0.80	135.15	15.25	430	228	1.813	0.455		
15X-3	0.75-0.80	135.15	15.25	405	253	1.612	0.838		
16X-1	0.75-0.80	141.77	17.70	430	304	1.647	-0.157	1.848	0.014
16X-1	0.75-0.80	141.77	17.70	380	278	2.063	-0.091		

Core & Section	Interval	Depth (mbsf)	Age (Ma)	Specimen size D (μm)	Specimen size T (μm)	$\delta^{18}O$	$\delta^{13}C$	$\delta^{18}O$ ave.	$\delta^{13}C$ ave.
Leg 121 Site 758 Hole A									
Oridorsalis umbonatus (Cont.)									
16X-1	0.75-0.80	141.77	17.70	557	354	1.834	0.290		
16X-3	0.75-0.80	144.75	18.80	455	278	1.641	-0.453	1.836	-0.409
16X-3	0.75-0.80	144.75	18.80	430	278	2.003	-0.178		
16X-3	0.75-0.80	144.75	18.80	405	278	1.864	-0.595		
17X-1	0.75-0.80	151.45	19.44	506	304	2.011	0.012	2.056	-0.049
17X-1	0.75-0.80	151.45	19.44	506	253	1.979	-0.222		
17X-1	0.75-0.80	151.45	19.44	455	278	2.179	0.064		
17X-3	0.75-0.80	154.45	19.73	582	405	2.019	0.007	2.028	0.030
17X-3	0.75-0.80	154.45	19.73	557	329	2.069	0.126		
17X-3	0.75-0.80	154.45	19.73	481	304	1.995	-0.044		
18X-1	0.75-0.80	161.15	20.37	506	278	2.236	0.018	2.028	-0.016
18X-1	0.75-0.80	161.15	20.37	405	278	1.948	-0.012		
18X-1	0.75-0.80	161.15	20.37	405	278	1.899	-0.055		
18X-3	0.75-0.80	164.15	20.65	481	304	1.959	-0.142	1.959	-0.142
19X-1	0.75-0.80	170.75	21.28	455	304	1.698	-0.088	1.661	-0.097
19X-1	0.75-0.80	170.75	21.28	455	278	1.734	-0.107		
19X-1	0.75-0.80	170.75	21.28	430	253	1.550	-0.095		
20X-2	0.75-0.80	181.95	22.35	531	329	2.132	0.997	1.964	0.480
20X-2	0.75-0.80	181.95	22.35	455	304	2.005	0.489		
20X-2	0.75-0.80	181.95	22.35	380	228	1.754	-0.045		
21X-1	0.75-0.80	190.05	23.13	506	354	1.309	0.165	1.265	0.106
21X-1	0.75-0.80	190.05	23.13	506	304	1.161	0.086		
21X-1	0.75-0.80	190.05	23.13	430	253	1.325	0.066		
21X-3	0.75-0.80	193.05	23.41	455	354	1.633	0.285	1.633	0.285
22X-2	0.75-0.80	201.25	25.17	658	354	2.022	0.062	1.896	-0.040
22X-2	0.75-0.80	201.25	25.17	531	354	1.802	-0.026		
22X-2	0.75-0.80	201.25	25.17	557	329	1.863	-0.155		
23X-1	0.70-0.75	209.40	27.47	506	304	1.793	-0.046	1.871	-0.161
23X-1	0.70-0.75	209.40	27.47	506	304	1.765	-0.435		
23X-1	0.70-0.75	209.40	27.47	531	354	2.055	-0.003		
23X-3	0.75-0.80	212.45	28.33	506	304	1.632	-0.369	1.715	-0.288
23X-3	0.75-0.80	212.45	28.33	531	278	1.899	-0.109		
23X-3	0.75-0.80	212.45	28.33	430	278	1.613	-0.387		
24X-1	0.58-0.63	218.88	30.15	455	304	2.164	-0.630	2.027	-0.725
24X-1	0.58-0.63	218.88	30.15	455	278	1.889	-0.820		
24X-3	0.32-0.37	221.62	30.33	430	253	2.082	-0.463	1.922	-0.452
24X-3	0.32-0.37	221.62	30.33	430	278	1.917	-0.329		
24X-3	0.32-0.37	221.62	30.33	405	253	1.767	-0.564		
25X-1	0.76-0.81	228.76	30.70	683	354	1.597	-0.940	1.665	-1.196
25X-1	0.76-0.81	228.76	30.70	481	278	1.633	-1.083		
25X-1	0.76-0.81	228.76	30.70	430	278	1.764	-1.564		
26X-1	0.75-0.80	238.45	31.20	531	329	1.917	-0.574	1.919	-0.613
26X-1	0.75-0.80	238.45	31.20	493	304	1.809	-0.946		
26X-1	0.75-0.80	238.45	31.20	481	278	2.031	-0.318		
26X-3	0.75-0.80	241.45	34.39	455	304	1.731	-0.326	1.889	-0.445
26X-3	0.75-0.80	241.45	34.39	405	278	2.066	-0.695		
26X-3	0.75-0.80	241.45	34.39	405	278	1.871	-0.313		
27X-1	0.75-0.80	248.05	41.42	430	278	1.955	0.120	1.775	0.033
27X-1	0.75-0.80	248.05	41.42	405	278	1.871	0.028		
27X-1	0.75-0.80	248.05	41.42	392	240	1.499	-0.050		
Stensioina beccariiformis									
28X-2	0.75-0.80	259.15	58.18	392	228	0.102	1.912	0.102	1.912
28X-6	0.75-0.80	265.15	59.27	531	304	-0.221	1.835	-0.140	1.921
28X-6	0.75-0.80	265.15	59.27	405	228	-0.059	2.006		
29X-1	0.75-0.80	267.35	59.67	519	278	0.431	2.274	0.350	2.071
29X-1	0.75-0.80	267.35	59.67	493	228	0.283	1.965		
29X-1	0.75-0.80	267.35	59.67	468	278	0.335	1.973		
29X-3	0.75-0.80	270.35	60.22	506	304	0.288	1.662	0.198	1.659
29X-3	0.75-0.80	270.35	60.22	544	304	0.209	1.705		
29X-3	0.75-0.80	270.35	60.22	557	304	0.098	1.611		
30X-1	0.75-0.80	277.05	60.86	430	253	0.462	1.660	0.526	1.643
30X-1	0.75-0.80	277.05	60.86	468	278	0.463	1.558		
30X-1	0.75-0.80	277.05	60.86	405	202	0.652	1.712		
30X-3	0.75-0.80	280.05	61.11	443	240	0.215	1.275	0.116	1.207
30X-3	0.75-0.80	280.05	61.11	455	253	0.104	1.193		
30X-3	0.75-0.80	280.05	61.11	481	266	0.030	1.154		

Appendix A-10. (continued).

Core & Section	Interval	Depth (mbsf)	Age (Ma)	Specimen size D (μm)	Specimen size T (μm)	$\delta^{18}O$	$\delta^{13}C$	$\delta^{18}O$ ave.	$\delta^{13}C$ ave.
Leg 121 Site 758 Hole A									
Stensioina beccariiformis (Cont.)									
31X-1	0.75-0.80	286.65	61.65	455	228	0.108	1.116	0.108	1.116
31X-5	0.75-0.80	292.65	63.62	506	278	0.003	0.932	-0.128	0.834
31X-5	0.75-0.80	292.65	63.62	481	253	-0.311	0.739		
31X-5	0.75-0.80	292.65	63.62	455	253	-0.077	0.831		
Leg 122 Site 762 Hole C									
Anomalinoides danicus									
26X-1	0.70-0.73	398.70	56.91	443	278	-0.720	0.475	-0.720	0.475
26X-2	0.71-0.75	400.21	57.07	430	228	-0.793	0.120	-0.793	0.120
26X-3	0.76-0.81	401.76	57.24	380	228	-0.715	0.479	-0.715	0.479
26X-4	0.69-0.74	403.19	57.39	430	253	-0.760	0.456	-0.760	0.456
26X-5	0.70-0.75	404.70	57.55	455	266	-0.614	0.413	-0.583	0.392
26X-5	0.70-0.75	404.70	57.55	531	316	-0.552	0.371		
27X-4	0.70-0.75	407.70	57.87	506	278	-0.510	0.645	-0.510	0.645
28X-1	0.71-0.76	412.71	58.35	443	266	-0.237	1.498	-0.237	1.498
29X-3	0.69-0.73	425.19	59.55	405	278	-0.203	2.623	-0.203	2.623
30X-1	0.69-0.74	431.69	60.18	506	354	0.142	2.195	0.142	2.195
30X-2	0.69-0.74	433.19	60.32	430	278	0.209	2.325	0.234	2.329
30X-2	0.69-0.74	433.19	60.32	455	278	0.253	2.316		
30X-2	0.69-0.74	433.19	60.32	392	278	0.240	2.347		
30X-3	0.69-0.74	434.69	60.43	455	278	0.325	2.300	0.325	2.300
32X-1	0.65-0.69	450.65	61.18	443	278	0.120	1.816	0.094	1.809
32X-1	0.65-0.69	450.65	61.18	455	278	0.067	1.802		
Nuttallides truempyi									
26X-2	0.71-0.75	400.21	57.07	392	215	-1.189	-0.463	-1.189	-0.463
26X-3	0.76-0.81	401.76	57.24	392	228	-0.851	-0.086	-0.851	-0.086
29X-3	0.69-0.73	425.19	59.55	455	266	-0.079	1.874	-0.412	1.600
29X-3	0.69-0.73	425.19	59.55	380	202	-0.816	1.238		
29X-3	0.69-0.73	425.19	59.55	367	215	-0.340	1.688		
30X-1	0.69-0.74	431.69	60.18	392	215	-0.084	1.724	-0.084	1.724
31X-1	0.70-0.74	441.20	60.74	430	240	-0.410	1.568	-0.318	1.502
31X-1	0.70-0.74	441.20	60.74	392	215	-0.225	1.435		
31X-3	0.67-0.71	444.17	60.88	557	278	-0.076	1.618	-0.234	1.571
31X-3	0.67-0.71	444.17	60.88	405	228	-0.149	1.592		
31X-3	0.67-0.71	444.17	60.88	430	240	-0.476	1.502		
31X-5	0.68-0.72	447.18	61.02	417	228	-0.460	1.722	-0.167	1.748
31X-5	0.68-0.72	447.18	61.02	443	253	0.120	1.691		
31X-5	0.68-0.72	447.18	61.02	392	228	-0.161	1.830		
32X-1	0.65-0.69	450.65	61.18	493	253	-0.061	1.403	-0.021	1.420
32X-1	0.65-0.69	450.65	61.18	405	202	0.072	1.596		
32X-1	0.65-0.69	450.65	61.18	380	215	-0.073	1.260		
33X-1	0.71-0.75	460.21	61.61	455	266	-0.075	1.344	-0.106	1.295
33X-1	0.71-0.75	460.21	61.61	405	228	0.015	1.303		
33X-1	0.71-0.75	460.21	61.61	380	215	-0.258	1.238		
33X-3	0.69-0.73	463.19	61.67	481	253	-0.180	1.268	-0.160	1.294
33X-3	0.69-0.73	463.19	61.67	405	240	-0.234	1.236		
33X-3	0.69-0.73	463.19	61.67	380	215	-0.065	1.377		
33X-5	0.71-0.75	466.21	61.73	430	253	-0.323	1.412	-0.176	1.241
33X-5	0.71-0.75	466.21	61.73	443	240	-0.163	1.265		
33X-5	0.71-0.75	466.21	61.73	380	228	-0.042	1.046		
34X-1	0.61-0.65	469.61	61.80	405	228	-0.129	1.383	-0.129	1.383
34X-3	0.65-0.69	472.65	61.86	417	228	0.040	1.182	0.040	1.182
34X-5	0.65-0.70	475.65	61.92	405	190	-0.678	1.084	-0.404	1.108
34X-5	0.65-0.70	475.65	61.92	405	177	-0.430	1.080		
34X-5	0.65-0.70	475.65	61.92	405	215	-0.104	1.159		
Nuttallides truempyi (5 specimens)									
23X-1	0.69-0.74	370.19	55.33	253-329	164-190	-0.770	0.040		
24X-1	0.77-0.82	379.77	55.74	253-329	177-228	-1.055	-0.306		
25X-1	0.72-0.76	389.22	56.14	253-304	152-202	-0.999	-0.324		
25X-3	0.71-0.75	392.21	56.27	266-329	164-177	-0.768	0.064		
26X-1	0.70-0.73	398.70	56.91	278-342	164-215	-0.855	-0.073		
26X-2	0.71-0.75	400.21	57.07	278-342	177-215	-0.976	-0.489		
26X-3	0.76-0.81	401.76	57.24	253-304	152-202	-0.607	0.073		
26X-4	0.69-0.74	403.19	57.39	253-316	152-228	-0.839	-0.134		
27X-1	0.69-0.74	403.19	57.39	278-304	164-177	-0.847	-0.155		
27X-2	0.69-0.74	404.69	57.55	266-304	152-177	-0.803	-0.011		
26X-5	0.70-0.75	404.70	57.55	278-329	164-177	-0.567	-0.014		
Leg 121 Site 758 Hole A									
Nuttallides truempyi (5 specimens) (Cont.)									
27X-3	0.68-0.73	406.18	57.71	228-278	152-202	-0.701	-0.088		
27X-4	0.70-0.75	407.70	57.87	253-329	152-202	-0.592	0.189		
28X-1	0.71-0.76	412.71	58.35	228-342	152-215	-0.418	0.826		
29X-1	0.76-0.80	422.26	59.27	278-304	152-177	-0.464	1.312		
29X-2	0.69-0.74	423.69	59.41	304-329	164-202	-0.435	1.872		
29X-3	0.69-0.73	425.19	59.55	304-329	164-202	-0.524	1.554		
30X-1	0.69-0.74	431.69	60.18	266-304	152-177	-0.065	1.812		
31X-1	0.70-0.74	441.20	60.74	329-354	190-253	-0.248	1.490		
31X-3	0.67-0.71	444.17	60.88	278-342	164-177	-0.058	1.749		
31X-5	0.68-0.72	447.18	61.02	278-329	164-190	-0.299	1.713		
32X-1	0.65-0.69	450.65	61.18	278-329	164-190	-0.138	1.286		
33X-1	0.71-0.75	460.21	61.61	266-291	152-164	-0.286	1.222		
33X-3	0.69-0.73	463.19	61.67	278-342	164-215	-0.383	1.259		
33X-5	0.71-0.75	466.21	61.73	278-329	164-190	-0.260	1.059		
34X-1	0.61-0.65	469.61	61.80	278-316	164-190	-0.395	1.312		
34X-3	0.65-0.69	472.65	61.86	304-316	164-190	-0.258	0.873		
34X-5	0.65-0.70	475.65	61.92	291-329	164-190	-0.405	1.109		
35X-1	0.68-0.73	479.18	61.98	253-329	164-202	-0.972	0.856		
Oridorsalis umbonatus									
24X-1	0.77-0.82	379.77	55.74	481	278	-0.628	-0.547		
Stensioina beccariiformis									
29X-1	0.76-0.80	422.26	59.27	734	253	-0.236	1.605	-0.525	1.368
29X-1	0.76-0.80	422.26	59.27	392	202	-0.764	1.240		
29X-1	0.76-0.80	422.26	59.27	417	228	-0.576	1.258		
29X-2	0.69-0.74	423.69	59.41	493	266	-0.396	1.922	-0.397	1.946
29X-2	0.69-0.74	423.69	59.41	468	253	-0.281	1.996		
29X-2	0.69-0.74	423.69	59.41	430	266	-0.513	1.920		
29X-3	0.69-0.73	425.19	59.55	531	329	-0.602	1.583	-0.600	1.718
29X-3	0.69-0.73	425.19	59.55	455	215	-0.754	1.653		
29X-3	0.69-0.73	425.19	59.55	531	278	-0.444	1.919		
30X-1	0.69-0.74	431.69	60.18	481	278	0.083	1.824	-0.120	1.750
30X-1	0.69-0.74	431.69	60.18	493	354	-0.266	1.671		
30X-1	0.69-0.74	431.69	60.18	468	240	-0.178	1.756		
30X-2	0.69-0.74	433.19	60.32	557	278	-0.001	1.794	0.038	1.820
30X-2	0.69-0.74	433.19	60.32	380	177	0.128	1.880		
30X-2	0.69-0.74	433.19	60.32	380	202	-0.012	1.786		
30X-3	0.69-0.74	434.69	60.43	607	304	0.210	1.679	0.165	1.649
30X-3	0.69-0.74	434.69	60.43	468	253	0.120	1.618		
31X-1	0.70-0.74	441.20	60.74	380	202	-0.351	1.533	-0.351	1.533
31X-3	0.67-0.71	444.17	60.88	430	202	-0.068	1.820	-0.143	1.654
31X-3	0.67-0.71	444.17	60.88	405	228	-0.194	1.564		
31X-3	0.67-0.71	444.17	60.88	417	228	-0.166	1.577		
31X-5	0.68-0.72	447.18	61.02	380	202	-0.318	1.776	-0.278	1.781
31X-5	0.68-0.72	447.18	61.02	417	228	-0.238	1.785		
32X-1	0.65-0.69	450.65	61.18	380	240	-0.282	1.322	-0.345	1.319
32X-1	0.65-0.69	450.65	61.18	392	177	-0.408	1.316		
33X-1	0.71-0.75	460.21	61.61	544	278	-0.555	1.135	-0.470	1.239
33X-1	0.71-0.75	460.21	61.61	443	253	-0.255	1.290		
33X-1	0.71-0.75	460.21	61.61	455	266	-0.600	1.291		
33X-3	0.69-0.73	463.19	61.67	607	342	-0.135	1.111	-0.312	1.156
33X-3	0.69-0.73	463.19	61.67	569	304	-0.352	1.068		
33X-3	0.69-0.73	463.19	61.67	392	202	-0.450	1.288		
33X-5	0.71-0.75	466.21	61.73	493	304	-0.352	0.796	-0.311	0.926
33X-5	0.71-0.75	466.21	61.73	380	190	-0.269	1.056		
34X-1	0.61-0.65	469.61	61.80	506	253	-0.176	1.382	-0.183	1.399
34X-1	0.61-0.65	469.61	61.80	493	278	-0.322	1.431		
34X-1	0.61-0.65	469.61	61.80	430	240	-0.052	1.384		
34X-3	0.65-0.69	472.65	61.86	481	253	-0.314	0.820	-0.277	0.840
34X-3	0.65-0.69	472.65	61.86	493	266	-0.239	0.860		
34X-5	0.65-0.70	475.65	61.92	531	278	-0.386	0.984	-0.393	0.958
34X-5	0.65-0.70	475.65	61.92	481	228	-0.572	0.878		
34X-5	0.65-0.70	475.65	61.92	468	304	-0.221	1.012		
35X-1	0.68-0.73	479.18	61.98	417	228	-0.482	0.848	-0.482	0.848

Appendix A-11. (continued).

Core & Section	Interval	Depth (mbsf)	Age (Ma)	Specimen size D (μm)	Specimen size T (μm)	$\delta^{18}O$	$\delta^{13}C$	$\delta^{18}O$ ave.	$\delta^{13}C$ ave.
Planktonic Foraminifera									
Leg 121 Site 752 Hole A									
Acarinina primitiva(5 specimens)									
13X-1	0.70-0.75	113.60	55.27	329-380	278-304	-1.640	1.685		
13X-4	0.62-0.67	118.02	55.46	329-380	278-329	-1.410	1.074		
14X-1	0.70-0.75	123.30	55.70	342-380	291-304	-1.661	-0.101		
14X-3	0.70-0.75	126.30	55.83	329-380	304-329	-1.632	1.209		
15X-1	0.70-0.75	133.00	56.12	329-354	278-304	-1.510	0.592		
15X-5	0.70-0.75	139.00	55.75	329-380	278-304	-1.595	1.634		
16X-1	0.70-0.75	142.70	55.83	329-354	278-354	-1.547	1.371		
16X-5	0.25-0.30	148.25	55.95	329-405	304-329	-1.798	1.845		
17X-1	0.70-0.75	152.40	56.04	329-354	278-304	-2.160	0.377		
17X-3	0.70-0.75	155.40	56.11	329-405	278-329	-1.689	1.828		
Morozovella marginodentata (5 specimens)									
15X-1	0.70-0.75	133.00	56.12	316-392	164-202	-1.794	2.631		
16X-1	0.70-0.75	142.70	55.83	304-329	228	-1.662	1.751		
16X-5	0.25-0.30	148.25	55.95	304-354	177-202	-1.650	3.383		
17X-1	0.70-0.75	152.40	56.04	329-342	190-228	-2.291	2.047		
17X-3	0.70-0.75	155.40	56.11	278-380	177-228	-1.540	3.729		
18X-1	0.71-0.75	162.11	56.74	253-380	152-228	-1.724	2.744		
18X-2	0.67-0.70	163.57	56.91	278-380	177-215	-1.810	2.868		
19X-1	0.70-0.75	171.80	57.82	354-380	228-253	-1.677	3.225		
19X-3	0.75-0.79	174.85	57.91	291-329	202-228	-1.825	2.773		
20X-1	0.70-0.75	181.40	58.09	304-329	202-253	-1.520	3.618		
Subbotina spp. (5 specimens)									
17X-3	0.70-0.75	155.40	56.11	278-316	202-253	-1.409	0.716		
18X-1	0.71-0.75	162.11	56.74	240-291	177-215	-1.460	1.174		
18X-2	0.67-0.70	163.57	56.91	240-291	190-228	-1.324	1.123		
19X-3	0.75-0.79	174.85	57.91	253-304	177-228	-1.873	0.999		
20X-1	0.70-0.75	181.40	58.09	278-304	215-253	-1.622	1.777		
21X-1	0.70-0.75	191.10	58.36	253-304	202-253	-1.821	2.478		
21X-1	0.70-0.75	191.10	58.36	253	177-202	-1.736	2.477		
22X-1	0.70-0.75	200.80	58.63	253-329	202-253	-1.437	2.561		
22X-3	0.70-0.75	203.80	58.76	253-304	152-228	-1.554	2.556		
23X-1	0.54-0.56	210.34	59.04	253-291	202-228	-1.466	2.544		
24X-1	0.70-0.73	220.20	59.72	253-304	177-228	-1.259	2.917		
25X-1	0.79-0.84	229.89	60.53	278-329	202-253	-1.205	2.499		
25X-3	0.79-0.84	232.89	60.74	253-329	202-228	-1.453	2.520		
26X-1	0.97-1.00	239.77	60.96	178-329	177-253	-1.383	2.304		
26X-5	0.97-1.00	245.77	61.14	253-304	202-228	-1.342	1.923		
27X-1	0.70-0.75	249.10	61.24	253-329	190-228	-1.274	1.743		
27X-3	0.70-0.75	252.10	61.33	253	190-202	-1.501	1.837		
28X-1	0.70-0.75	258.80	61.53	253-304	190-228	-1.137	1.936		
28X-5	0.70-0.75	264.80	61.72	253-304	202-228	-1.189	2.226		
29X-1	0.70-0.73	268.40	61.83	253-267	177-202	-1.753	2.292		
29X-5	0.70-0.73	274.40	62.01	278-304	202-228	-1.870	2.046		
30X-1	0.73-0.76	278.13	62.12	278-304	190-228	-1.404	1.986		
31X-1	0.70-0.75	280.10	62.18	253-291	177-202	-1.598	2.026		
31X-5	0.70-0.75	286.10	62.36	278-316	177-228	-1.345	1.652		
32X-1	0.70-0.75	289.40	62.46	278	177-202	-1.419	1.713		
33X-1	0.68-0.71	299.08	62.76	266-278	190-202	-1.683	1.518		
33X-3	0.57-0.60	301.97	62.85	253-329	177-202	-1.752	1.640		
Leg 121 Site 752 Hole B									
Globorotalia pseudobulloides (8 specimens)									
10R-1	1.05-1.08	346.15	64.84	253-316	152-190	-2.020	2.150		
10R-2	1.00-1.02	347.60	65.06	228-291	139-202	-2.760	2.162		
10R-3	1.12-1.15	349.22	65.30	266-367	139-190	-2.303	2.306		
10R-4	0.79-0.81	350.39	65.48	228-342	127-202	-2.219	2.219		
10R-7	0.41-0.43	354.51	66.10	278-329	101-152	-2.377	1.595		
Rugoglobigerina pennyi (9 specimens)									
11R-3	1.12-1.14	358.92	66.42	266-304	177-202	-2.538	3.016		
12R-1	1.04-1.07	365.44	66.96	253-316	152-202	-2.718	2.280		
12R-3	0.10-0.13	367.50	67.10	253-304	177-228	-2.599	2.513		
12R-5	0.54-0.57	370.94	67.32	253-304	164-215	-2.988	2.759		
Leg 121 Site 757 Hole B									
Subbotina spp. (6 specimens)									
14H-1	0.70-0.75	120.80	35.34	304-342	202-253	1.012	1.517		
14H-5	0.70-0.75	126.80	37.28	266-354	177-240	1.040	1.493		
Leg 121 Site 757 Hole B									
Subbotina spp. (6 specimens) (Cont.)									
15H-1	0.70-0.75	130.50	38.55	253-329	202-253	0.807	1.595		
15H-5	0.70-0.75	136.50	40.98	253-329	177-228	0.927	1.571		
16H-1	0.70-0.75	140.20	41.89	253-329	190-278	0.792	1.581		
16H-5	0.70-0.75	146.20	43.38	253-329	177-228	0.616	1.759		
17H-5	0.70-0.75	155.80	45.88	266-304	202-304	0.451	1.540		
18H-1	0.70-0.75	159.50	47.09	215-278	177-202	0.379	1.362		
18H-5	0.70-0.75	165.50	48.67	253-278	190-228	0.440	1.563		
19H-1	0.70-0.75	169.20	49.24	266-329	202-253	0.222	1.273		
20X-1	0.70-0.75	175.40	49.90	278-329	215-253	-0.167	1.391		
20X-5	0.70-0.75	181.40	51.37	278-329	202-228	-0.125	1.432		
21X-1	0.70-0.75	183.40	51.85	278-304	202-228	-0.399	1.386		
21X-4	0.70-0.75	187.90	52.70	253-304	177-228	-0.505	1.452		
22X-1	0.70-0.75	193.10	53.05	228-278	177-202	-1.029	1.063		
22X-3	0.70-0.75	196.10	53.25	253-329	202-253	-0.616	1.424		
23X-3	0.70-0.75	205.70	54.19	253-329	202-253	-0.942	0.608		
24X-1	0.58-0.61	212.28	55.27	266-329	202-253	-1.026	0.545		
24X-4	0.58-0.61	216.78	56.01	278-304	177-228	-1.323	0.673		
Leg 121 Site 758 Hole A									
Acarinina praecursoria									
31X-5	0.75-0.80	292.65	63.62	557	291	-1.154	2.092	-1.201	2.023
31X-5	0.75-0.80	292.65	63.62	455	342	-0.777	1.614		
31X-5	0.75-0.80	292.65	63.62	557	405	-1.672	2.363		
Acarinina primitiva									
28X-2	0.75-0.80	259.15	58.18	430	329	-1.804	4.655	-1.596	4.519
28X-2	0.75-0.80	259.15	58.18	481	354	-1.226	4.481		
28X-2	0.75-0.80	259.15	58.18	455	329	-1.757	4.420		
Morozovella velascoensis									
28X-2	0.75-0.80	259.15	58.18	632	278	-1.463	4.968	-1.460	4.867
28X-2	0.75-0.80	259.15	58.18	607	304	-1.328	4.855		
28X-2	0.75-0.80	259.15	58.18	708	316	-1.590	4.778		
28X-6	0.75-0.80	265.15	59.27	620	329	-1.843	4.987	-1.853	4.829
28X-6	0.75-0.80	265.15	59.27	632	354	-2.126	5.017		
28X-6	0.75-0.80	265.15	59.27	531	278	-1.591	4.483		
29X-1	0.75-0.80	267.35	59.67	734	329	-1.693	5.445	-1.631	5.084
29X-1	0.75-0.80	267.35	59.67	607	304	-1.642	4.840		
29X-1	0.75-0.80	267.35	59.67	607	304	-1.558	4.968		
29X-3	0.75-0.80	270.35	60.22	683	304	-1.635	5.048	-1.492	4.799
29X-3	0.75-0.80	270.35	60.22	582	278	-1.399	4.851		
29X-3	0.75-0.80	270.35	60.22	557	278	-1.443	4.499		
30X-1	0.75-0.80	277.05	60.86	708	329	-1.501	5.093	-1.506	4.935
30X-1	0.75-0.80	277.05	60.86	708	380	-1.664	5.228		
30X-1	0.75-0.80	277.05	60.86	683	329	-1.353	4.484		
30X-3	0.75-0.80	280.05	61.11	632	304	-1.783	4.115	-1.587	4.015
30X-3	0.75-0.80	280.05	61.11	493	253	-1.551	4.168		
30X-3	0.75-0.80	280.05	61.11	531	354	-1.428	3.762		
31X-1	0.75-0.80	286.65	61.65	531	304	-1.362	3.763	-1.497	3.790
31X-1	0.75-0.80	286.65	61.65	582	380	-1.595	3.971		
31X-1	0.75-0.80	286.65	61.65	557	304	-1.535	3.635		
Subbotina pseudoeocaena									
28X-6	0.75-0.80	265.15	59.27	544	380	-1.240	2.761	-1.223	2.540
28X-6	0.75-0.80	265.15	59.27	481	354	-1.090	2.304		
28X-6	0.75-0.80	265.15	59.27	519	380	-1.340	2.555		
29X-3	0.75-0.80	270.35	60.22	506	392	-0.977	2.496	-0.901	2.568
29X-3	0.75-0.80	270.35	60.22	506	380	-0.978	2.784		
29X-3	0.75-0.80	270.35	60.22	493	380	-0.747	2.424		
30X-1	0.75-0.80	277.05	60.86	506	367	-0.603	1.892	-0.603	1.892
Subbotina eocaena									
30X-1	0.75-0.80	277.05	60.86	683	380	-0.660	2.026	-0.873	2.092
30X-1	0.75-0.80	277.05	60.86	632	380	-0.867	2.049		
30X-1	0.75-0.80	277.05	60.86	632	430	-1.093	2.202		
30X-3	0.75-0.80	280.05	61.11	721	481	-0.653	1.828	-0.799	1.696
30X-3	0.75-0.80	280.05	61.11	696	405	-1.022	1.721		
30X-3	0.75-0.80	280.05	61.11	670	380	-0.721	1.540		
31X-1	0.75-0.80	286.65	61.65	531	405	-0.756	1.437	-0.852	1.442
31X-1	0.75-0.80	286.65	61.65	506	329	-0.876	1.537		
31X-1	0.75-0.80	286.65	61.65	531	316	-0.925	1.351		

Appendix A. (continued).

Core & Section	Interval	Depth (mbsf)	Age (Ma)	Specimen size D (μm)	Specimen size T (μm)	$\delta^{18}O$	$\delta^{13}C$	$\delta^{18}O$ ave.	$\delta^{13}C$ ave.
Leg 121 Site 758 Hole A									
Subbotina sp.1									
29X-1	0.75-0.80	267.35	59.67	531	380	-0.455	2.642	-0.711	2.593
29X-1	0.75-0.80	267.35	59.67	519	329	-1.044	2.657		
29X-1	0.75-0.80	267.35	59.67	519	354	-0.635	2.480		
Subbotina spp. (5 specimens)									
28X-2	0.75-0.80	259.15	58.18	304-316	240-253	-0.773	2.389		
28X-6	0.75-0.80	265.15	59.27	304-354	240-354	-0.942	2.515		
29X-1	0.75-0.80	267.35	59.67	253-329	202-253	-0.517	2.529		
29X-3	0.75-0.80	270.35	60.22	316-367	228-266	-0.445	2.313		
30X-1	0.75-0.80	277.05	60.86	253-329	177-253	-0.409	2.251		
30X-3	0.75-0.80	280.05	61.11	266-329	202-228	-0.213	1.950		
31X-1	0.75-0.80	286.65	61.65	278-329	202-253	-0.411	1.567		
31X-5	0.75-0.80	292.65	63.62	278-329	190-228	-0.317	1.538		